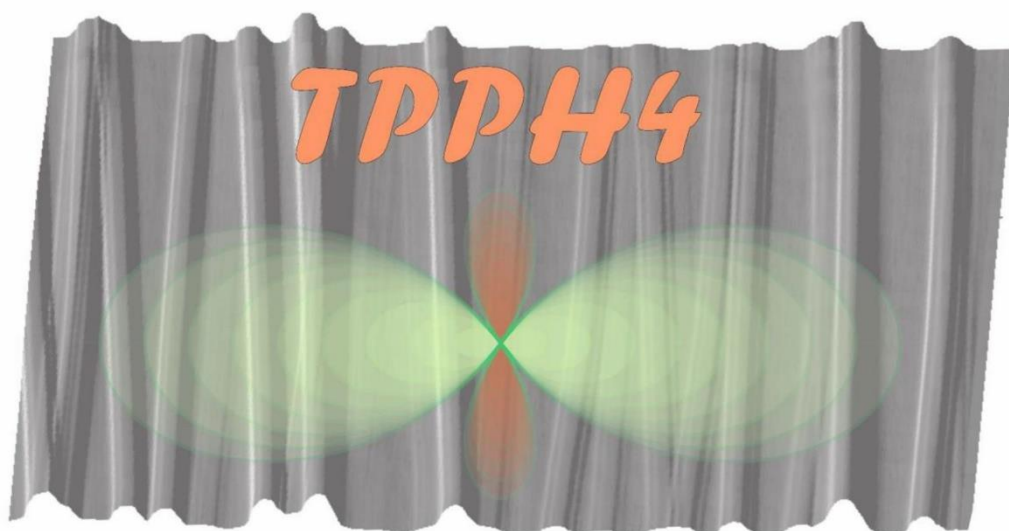


Санкт-Петербургский государственный университет  
Институт химии силикатов им. И.В. Гребенщикова РАН  
Институт металлургии УрО РАН  
Комиссия по кристаллохимии, рентгенографии и  
спектроскопии минералов  
Российского Минералогического Общества

**IV Конференция и Школа  
для молодых ученых  
Терморентгенография и рентгенография  
наноматериалов**



**СБОРНИК ТЕЗИСОВ**

19 – 21 октября 2020 г.  
Санкт-Петербург

**Saint Petersburg State University  
Grebenshchikov Institute of Silicate Chemistry Russ. Acad. Sci.  
Institute of Metallurgy Ural Branch Russ. Acad. Sci.  
Commission on Crystal Chemistry, X-ray Diffraction and Spectroscopy  
of Minerals of the Russian Mineralogical Society**

## **Book of Abstracts**

### **IV Conference and School for Young Scientists Non-Ambient Diffraction and Nanomaterials (NADM-4)**

October, 19 – 21, 2020  
St.-Petersburg

УДК 548.3, 536, 544.228  
ББК 22.37, 24.53, 26.31

Конференция и школа для молодых ученых Терморентгенография и Рентгенография  
Наноматериалов (ТРРН-4) (Сборник тезисов). С.-Петербург, 2020. 126 с.  
ISBN 978-5-9651-0559-5

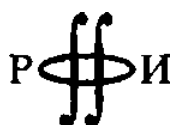
В сборнике представлены новые экспериментальные данные и методики по дифракционным исследованиям порошков, монокристаллов и наноматериалов. Особое внимание уделено исследованиям изменений кристаллической структуры при воздействии температур, давлений и структурных замещений.

Издание осуществлено при финансовой поддержке  
Российского фонда фундаментальных исследований  
проект № 20-03-22001

© Коллектив авторов

The book of abstracts presents new experimental data and methods for diffraction studies of powders, single crystals and nanomaterials. Particular attention is paid to studies of changes in the crystal structure under the conditions of temperature, pressure and structural substitutions.

The publication is financially supported by the Russian Foundation for Basic Research  
Project № 20-03-22001



© Group Authors



*Институт металлургии*

*Уральское отделение  
Российской Академии Наук*

## Committee

### *Chair:*

**S.K. Filatov** DSc, Prof. (SPBU, St. Petersburg)

### *Co-chairs:*

**E.V. Antipov** DSc, Prof., Cor. member of RAS (MSU, Moscow)

**R.S. Bubnova** DSc, Prof. (ISC RAS, St. Petersburg)

**S.V. Krivovichev** DSc, Prof., Cor. member of RAS (FRC KSC RAS, Apatity, SPBU, St. Petersburg)

**I.Yu. Kruchinina** DSc, Prof. (ISC RAS, St. Petersburg)

**A.A. Rempel** DSc, Prof., Academician (IMet UB RAS, Yekaterinburg)

### *Deputy Chair of the Organizing Committee:*

**M.G. Krzhizhanovskaya** PhD (SPBU, St. Petersburg)

### *Members of the Organizing Committee:*

**E.V. Boldyreva** DSc, Prof. (NSU, Novosibirsk)

**N.B. Bolotina** DSc (FRC Crystallography and photonics RAS, Moscow)

**O.S. Grunskiy** PhD (SPBU, St. Petersburg)

**A.A. Zolotarev** PhD (SPBU, St. Petersburg)

**N.N. Eremin** DSc, Cor. member of RAS (MSU, Moscow)

**A.V. Knyazev** DSc, Prof. (UNN, Nizhniy Novgorod)

**D.Yu. Pushcharovsky** DSc, Prof., Academician (MSU, Moscow)

**S.V. Tsybulya** DSc, Prof. (FRC IoC RAS; NSU, Novosibirsk)

**E.V. Chuprunov** DSc, Prof. (UNN, Nizhniy Novgorod)

**O.A. Shilova** DSc, Prof. (ISC RAS, St. Petersburg)

### *Chair of program committee:*

**S.G. Titova** DSc (IMet UB RAS, Yekaterinburg)

### *Co-chair of program committee:*

**O.V. Yakubovich** DSc, Prof. (MSU, Moscow)

### *Members of the Program Committee:*

**A.V. Egorysheva** DSc (IGIC RAS, Moscow)

**O.I. Siidra** DSc, Prof. (SPBU, St. Petersburg)

### *Scientific Secretariat:*

**S.N. Volkov** PhD (ISC RAS, St. Petersburg)

**V.A. Yukhno** (ISC RAS, St. Petersburg)

### *Chair of Interdisciplinary Committee:*

**S.K. Filatov** DSc, Prof. (SPBU, Saint Petersburg)

### *Interdisciplinary Committee (SPBU, St. Petersburg):*

**A.I. Brusnitsyn** DSc, Prof., Head of the Department of Mineralogy, Institute of Earth Sciences

**K.V. Chistyakov** DSc, Professor, Director, Institute of Earth Sciences

**M.G. Krzhizhanovskaya** PhD, Assoc. Prof. of the Dept. of Crystallography, Institute of Earth Sciences

**I.Ch. Mashek** DSc, Professor, Head of the Department of General Physics I, Faculty of Physics

**A.V. Povolotsky** DSc, Assoc. Prof. of the Department of Laser Chemistry and Laser Materials Science, Institute of Chemistry

**A.M. Toikka** DSc, Professor, Head of the Department of Chemical Thermodynamics and Kinetics, Institute of Chemistry

**D.Yu. Vlasov** DSc, Prof., Professor of the Department of Botany, Faculty of Biology

### *Local Committee:*

**Y.P. Biryukov** (ISC RAS, Saint Petersburg)

**V.A. Firsova** (ISC RAS, Saint Petersburg)

**A.P. Shablinsky** PhD (ISC RAS, Saint Petersburg)

**O.Yu. Shorets** (SPBU, ISC RAS, Saint Petersburg)

# Contents

PREFACE .....	10
<b>1. Plenary session .....</b>	<b>12</b>
Huppertz H. Extreme Conditions of Pressure and Temperature for the Synthesis of Crystalline Materials.....	13
Dubrovinsky L. Inorganic Synthesis and Crystal Chemistry at Multimegabar Pressures.....	14
Boldyreva E.V. Crystals of organic and coordination compounds – what can we learn about them from high-pressure experiments.....	15
Dubrovinskaia N. Materials synthesis and crystallography at extreme pressure-temperature conditions revealing remarkable materials properties.....	16
Rempel A.A. Phase transformations at moderated temperatures in nonstoichiometric compounds with high entropy .....	17
Антипов Е.В. Роль кристаллохимии в создании новых катодных материалов для металл-ионных аккумуляторов .....	18
Rempel A.A. Megascience facilities and russian-german travelling seminar of nanomaterials.....	19
Senyshyn A., Mühlbauer M.J., Baran V. Unusual thermal structural behaviour of lithiated graphite phases .....	20
Bolotina N.B. Aperiodic crystals.....	21
Steffan J., Totzauer L., Heck F., Hofmann K., Albert B. Investigating catalysts and luminescent materials by in situ powder diffractometry.....	22
Еремин Н.Н. Влияние эффектов порядка-беспорядка в кристаллических структурах на термодинамические функции смешения твердых растворов .....	23
Krivovichev S.V. Polymorphic transitions in feldspar structures.....	24
Чупрунов Е.В. Количественные измерения в теории симметрии кристаллов. Фазовые переходы второго рода .....	25
Dinnebier R.E. Fractional coordinates, symmetry modes, and rigid bodies: Three different ways for describing structural evolution during phase transitions.....	26
Bubnova R.S., Filatov S.K. Self-assembly and high anisotropy thermal expansion of crystal structures consisting of BO <sub>3</sub> triangular groups .....	27
Knyazev A.V., Shipilova A.S., Knyazeva S.S., Gusarova E.V., Amosov A.A., Kusutkina A.M. Low-temperature X-ray diffraction of biologically active substances .....	28
Krzhizhanovskaya M.G. Modern laboratory HTXRD for investigation of structure evolution with temperature or during phase transformations.....	29
Tsybulya S.V. Analysis of diffraction patterns of nanostructured powders .....	30
Titova S.G., Sterkhov E.V., Ryltsev R.E.. The origin of the first order structural phase transition for PrBaMn <sub>2</sub> O <sub>6</sub> double manganite .....	31
Titov A.N., Shkvarin A.S., Merentsov A.I., Avila J., Asensio M., Bushkova O.V., Sala A., Titov A.A., Kazantseva N.V., Postnikov M.S., Yarmoshenko Yu.M. Self-organization of the chalcogen sublattice in a solid solution Ti(S <sub>1-x</sub> Se <sub>x</sub> ) <sub>2</sub> .....	32
Siidra O.I. Fumarolic sulfate minerals: new data and possible applications .....	33
Yakubovich O.V. Phosphate-silicate epitaxial heterostructure: crystal chemistry and mechanism of formation.....	34
Федоров П.П. Трикритические точки на фазовых диаграммах солевых систем .....	35
<b>2. High-pressure crystal chemistry .....</b>	<b>36</b>
Golosova N.O., Kozlenko D.P., Belozeroва N.M., Nicheva D., Petkova T., Kichanov S.E., Lukin E.V., Avdeev G., Petkov P., Savenko B.N. A study of the crystal and magnetic structures of Co <sub>3</sub> O <sub>4</sub> at high pressure .....	37

Gavryushkin P.N., Sagatova D., Sagatov N., Banaev M.V. Silicate-like crystalchemistry for carbonates at high pressure. Reality or not? .....	38
Gavryushkin P.N., Banaev M.V., Sagatova D., Sagatov N. High-temperature structural changes of carbonates.....	39
Гайдамака А.А., Архипов С.Г., Захаров Б.А., Сереткин Ю.В., Болдырева Е.В. Сравнение кристаллических структур и сжимаемости гидратов натриевой и калиевой соли гуанина .....	40
Zakharov B.A. High-pressure experiments and X-ray diffraction data reduction: the difference from ambient pressure studies and factors influencing data quality .....	41
<b>3. Properties of materials and nano materials over a wide range of temperature and pressure .....</b>	<b>42</b>
Valeeva A.A., Rempel A.A. <i>In situ</i> behavior of titanium (III) oxideTi <sub>2</sub> O <sub>3</sub> structure at temperatures up to 1200 K .....	43
Drozhilkin P.D., Boldin M.S., Alekseeva L.S., Andreev P.V., Karazanov K.O., Smetanina K.E., Balabanov S.S. Structure and phase composition of silicon nitride ceramics and powders plated with yttrium-aluminum garnet .....	44
Еникеева М.О., Проскурина О.В. Полиморфные превращения и кристаллохимия наностержней La <sub>0.15</sub> Y <sub>0.85</sub> PO <sub>4</sub> .....	45
Kovalenko A.S., Nikolaev A.M., Khamova T.V., Kopitsa G.P., Shilova O.A. Influence of conditions for synthesis of iron oxide nanoparticles on their structure and phase composition .....	46
Komornikov V.A., Grebenev V.V., Timakov I.S., Makarova I.P., Selezneva E.V., Zainullin O.B. Proton-conducting composite materials based on superprotonic crystals .....	47
<b>4. Magnetic phase transitions .....</b>	<b>48</b>
Belskaya N.A., Kazak N.V., Knyazev Yu.V., Platunov M.S., Moshkina E.M., Bezmaternykh L.N., Solovyov L.A., Gavrilkin S.Yu., Veligzhanin A.A., Ovchinnikov S.G. Charge-ordering and magnetism of Mn <sub>2</sub> BO <sub>4</sub> oxyborate .....	49
Biryukov Y.P., Zinnatullin A.L., Bubnova R.S., Vagizov F.G., Filatov S.K. Investigation of thermal behavior of Fe(II,III)-containing borates .....	50
Житова Е.С., Кржижановская М.Г. Поведение эденита при повышенной температуре: окисление железа .....	51
Zinnatullin A.L., Biryukov Y.P., Vagizov F.G. Mössbauer effect study of iron borate Fe <sup>2+</sup> <sub>2</sub> Fe <sup>3+</sup> (BO <sub>3</sub> )O <sub>2</sub> with hulsite structure.....	52
Lis O.N., Kichanov S.E., Belozerova N.M., Lukin E.V., Savenko B.N., Balakumar S. Magnetic and structural properties of multiferroic Bi <sub>2-x</sub> Fe <sub>x</sub> WO <sub>6</sub> .....	53
Rutkauskas A.V., Kozlenko D.P., Kichanov S.E., Savenko B.N. The effect of doping with Sr <sup>2+</sup> ions on the magnetic properties of Ba <sub>1-x</sub> Sr <sub>x</sub> Fe <sub>12</sub> O <sub>19</sub> .....	54
Sterkhov E.V., Pryanichnikov S.V., Titova S.G. Crystal structure as a function of temperature for A-site substituted Nd <sub>1-x</sub> Pr <sub>x</sub> BaMn <sub>2</sub> O <sub>6</sub> double manganites .....	55
Shvanskaya L.V., Krikunova P.V. Ellenbergerite-like nickel phosphates: crystal chemistry and magnetic behavior .....	56
<b>5. HTXRD and high-temperature crystal chemistry .....</b>	<b>57</b>
Akramov D.F., Selezneva N.V., Baranov N.V. The effect of negative chemical pressure on phase stability, structure and physical properties in the Co <sub>7</sub> (Se <sub>1-y</sub> Te <sub>y</sub> ) <sub>8</sub> system.....	58
Borisov A., Siidra O., Depmeier W., Platonova N. Study of hydration and dehydration of sulfate exhalative minerals using powder X-ray diffraction.....	59
Демина С.В., Шаблинский А.П., Бубнова Р.С., Бирюков Я.П., Филатов С.К. Бораты Ba <sub>3</sub> Y <sub>2</sub> (BO <sub>3</sub> ) <sub>4</sub> :Er <sup>3+</sup> и Ba <sub>3</sub> Eu <sub>2</sub> (BO <sub>3</sub> ) <sub>4</sub> : синтез, термическое расширение .....	60
Bulanov E.N., Stasenko K.S. Investigation of isomorphism, polymorphism and morphotropic transitions in apatites using HTXRD .....	61

Gurzhiy V.V., Krivovichev S.V. X-ray diffraction analysis of natural and synthetic uranyl compounds at non-ambient temperatures: structure vs. stability .....	62
Zolotarev A.A. Jr., Avdontseva M.S., Krzhizhanovskaya M.G., Zhitova E.S., Krivovichev S.V. The high-temperature crystal chemistry of technogenic mineral phases from the burned dumps of the Chelyabinsk coal basin .....	63
Ismagilova R.M., Zhitova E.S., Zolotarev A.A., Krivovichev S.V., Shilovskih V.V. High-temperature crystal chemistry of copper trimolibdate $\text{CuMo}_3\text{O}_{10}\times\text{H}_2\text{O}$ .....	64
Panikorovskii T.L., Krivovichev S.V. Irreversible dehydration of murmanite .....	65
Charkin D.O., Gurianov K.E., Plokhikh I.V. Variable-temperature studies of $\text{Ni}_{3-x}\text{M}_x\text{Te}_2$ solid solutions (M = Co, Fe) .....	66
Shkvarina E.G., Titov A. A., Shkvarin A.S., Postnikov M.S., Radzivonchik D.I., Titov A.N. Thermal disorder in the $\text{Fe}_{0.5}\text{TiSe}_2$ .....	67
Shorets O.U., Filatov S.K., Bubnova R.S. Solid-phase synthesis of $\text{Na}_2\text{SO}_4\text{-K}_2\text{SO}_4$ sulfates on a thermo-x-ray equipment and the subsequent study of synthesis products during cooling .....	68
Yuriev A.A., Shablinskii A.P., Povolotskiy A.V., Bubnova R.S., Kolesnikov I.E., Filatov S.K. Novel red phosphor $\text{CaBi}_2\text{B}_4\text{O}_{10}:\text{Eu}^{3+}$ : synthesis, crystal structure, luminescence and thermal expansion .....	69
Yukhno V.A., Bubnova R.S., Krzhizhanovskaya M.G., Filatov S.K. Thermal expansion of calcium borates .....	70
<b>6. Structural analysis of modulated, disordered structures and nano-sized objects .....</b>	<b>71</b>
Volkov S.N., Bubnova R.S., Krzhizhanovskaya M.G., Galafutnik L.G. The first bismuth borate oxyiodide, $\text{Bi}_4\text{BO}_7\text{I}$ : commensurate or incommensurate? .....	72
Golovanova O.A. Synthesis and thermal stability of silicon-containing calcium phosphates .....	73
Izatulina A.R., Gurzhiy V.V., Krzhizhanovskaya M.G., Kuz'mina M.A., Frank-Kamenetskaya O.V. Evolution of crystal structures and thermal stability of calcium oxalates hydrates .....	74
Rotermel M.V., Pryanichnikov S.V., Sterkhov E.V., Sumnikov S.V., Titova S.G. Combined X-ray and neutron diffraction study of Zn/Mg substitution in $\text{Zn}_2\text{SiO}_4$ -based solid solutions .....	75
Filatov S.K., Shablinskii A.P., Krivovichev S.V., Vergasova L.P., Moskaleva S.V. Petrovite $\text{Na}_{10}\text{CaCu}_2(\text{SO}_4)_8$ , a new fumarolic mineral from the Tolbachik volcano, Kamchatka, Russia .....	76
Shablinskii A.P., Filatov S.K., Vergasova L.P., Krivovichev S.V., Moskaleva S.V., Avdontseva E.Yu., Bubnova R.S. Dobrovolskyite $\text{Na}_4\text{Ca}(\text{SO}_4)_3$ , a new fumarolic mineral with modular structure inherited from $\alpha\text{-Na}_2\text{SO}_4$ .....	77
Shefer K.I. Study of alumina-containing systems using X-ray diffraction methods .....	78
<b>7. Poster session .....</b>	<b>79</b>
Abdulina V.R., Siidra O.I. Crystal chemistry and high-temperature X-ray diffraction of hydrated iron sulfate minerals .....	80
Abramovich A.I., Bakaev S.E. Monocrystal $\text{Pr}_{0.65}(\text{Ca}_{0.8}\text{Sr}_{0.2})_{0.35}\text{MnO}_3$ : structure, magnetothermal and magnetoelectrical properties .....	81
Avdontseva M.S., Zolotarev A.A. Jr., Krzhizhanovskaya M.G., Krivovichev S.V. High-temperature crystal chemistry of fluorellestadite .....	82
Akkuratov V.I., Targonskiy A.V., Eliovich I.A., Protsenko A.I., Pisarevsky Yu.V., Blagov A.E. In-situ time-resolved X-ray diffraction studies of crystalline materials under static mechanical load .....	83
Bogdan T.V., Mishanin I.I., Koklin A.E., Smirnov A.V., Bogdan V.I. Transformation of Fe-Cr Catalytic Systems under Chemical Reactions by elevated temperature .....	84



Zakalyukin R.M., Levkevich E.A., Zimina G.V., Patrina Zh.G., Marchenko A.A., Busurin S.M. Interaction dynamics and phase formation in a ternary system $\text{Li}_2\text{O} - \text{B}_2\text{O}_3 - \text{MoO}_3$ during synthesis from the primary components.....	85
Fedorova O.M., Vedmid' L.B., Dimitrov V.M. Evolution of the structure $\text{Nd}_2\text{BaMn}_2\text{O}_7$ manganite in the temperature range of 20-400°C.....	86
Vinogradov V.Yu., Kalinkin A.M., Kalinkina E.V. Synthesis of nanocrystalline $\text{gd}_2\text{zr}_2\text{o}_7$ using mechanical activation.....	87
Vladimirova V.A., Siidra O.I. Thermal analysis and thermal expansion of volborthite $\text{Cu}_3\text{V}_2\text{O}_7(\text{OH})_2 \cdot 2\text{H}_2\text{O}$ .....	88
Golovanova O.A. Study of the effects of heat-treatment of hydroxyapatite synthesized in gelatine matrix.....	89
Губанова Н.Н., Матвеев В.А., Шилова О.А. Текстурирование в тонких кремнеземных пленках, допированных наночастицами Pt/Pd.....	90
Andreev P.V., Gudz D.A., Smetanina K.E. Local XRD analysis of the near $\alpha$ -titanium alloy PT3V modified by severe plastic deformation.....	91
Aksenov S.M., Yamnova N.A., Borovikova E.Yu., Stefanovich S.Yu., Volkov A.S., Deyneko D.V., Dimitrova O.V., Gurbanova O.A. Nixon A.E., Krivovichev S.V. Synthesis, crystal structure of the first lithium aluminum borophosphate $\text{Li}_3\{\text{Al}_2[\text{BP}_4\text{O}_{16}]\} \cdot 2\text{H}_2\text{O}$ , and conditions for Li-ion conductivity.....	92
Дихтяр Ю.Ю., Дейнеко Д.В., Болдырев К.Н. Фосфаты $\text{Ca}_{9-x}\text{Zn}_x\text{La}(\text{PO}_4)_7:\text{Ln}^{3+}$ , люминесцирующие в ближней ИК-области.....	93
Kozlenko D.P., Zel I.Yu., Dang T.N., Le Thao P.T. High pressure induced structural and magnetic phase transformations in $\text{BaYFeO}_4$ .....	94
Зельбст Э.А., Адамович С.Н., Оборина Е.Н., Моисеев А.А. От тетраэдрической координации атома кремния к тригонально-бипирамидальной.....	95
Kalashnikova S.A., Korniyakov I.V., Gurzhiy V.V. Synthesis, characterization and morphotropic transitions in a family of $\text{M}[(\text{UO}_2)(\text{CH}_3\text{COO})_3](\text{H}_2\text{O})_n$ ( $\text{M} = \text{Na}, \text{K}, \text{Rb}, \text{Cs}; n = 0-1.0$ ) compounds.....	96
Kiriukhina G.V., Yakubovich O.V., Dovgaliuk I.N., Simonov S.V. Novel complex copper phosphate chlorides: disordered structures and crystal chemistry.....	97
Kolobov A.Yu., Sycheva G.A. Features of crystallization of cristobalite in quartz glass obtained on plasmatrons of JSC.....	98
Kopylova Y.O., Krzhizhanovskaya M.G., Kolesnikov I.E., Shilovskih V.V. Thermal behavior and luminescence of natural rare-earth borosilicates stillwellite and tadjhikite.....	99
Korneev A.V., Frank-Kamenetskaya O.V., Kuz'mina M.A. Ti-bearing hydroxyapatite: synthesis, crystal chemistry, photocatalytic properties.....	100
Kuporev I.V., Gurzhiy V.V., Krivovichev S.V. Synthesis and structural study of the new modular uranyl selenite-selenate with melamine $[(\text{UO}_2)(\text{SeO}_4)(\text{H}_2\text{SeO}_3)][(\text{SeO}_4)(\text{C}_3\text{H}_8\text{N}_6)]$ .....	101
Кусуткина А.М., Князев А.В., Князева С.С., Гусарова Е.В. Амосов А.А., Шипилова А.С. Термические свойства D, L-аспарагиновой кислоты.....	102
Zakalyukin R.M., Levkevich E.A., Kumskov A.S. Ribbon structure of the wide-gap semiconductor $\text{Sb}_2\text{S}_3$ in the channels of SWCNT.....	103
Lomakin M.S., Proskurina O.V. Formation process of the Bi-Fe-W-O pyrochlore nanoparticles via microwave synthesis.....	104
Matveev V.A. The study of periodic multilayer systems NiMo/Ti and FeCo/TiZr by X-ray diffraction and reflectometry.....	105
Mikhailova A., Mikhailov B., Nikulin V., Silin P., Borovitskaya I. The effect of shock waves on the structure of Bi-2223 superconductors after plasma treatment.....	106

Perova E.R., Mayorov P.A. Thermal expansion of Cd- and Sr-containing NZP-related solid solutions .....	107
Popova E.F., Veselova V.O., Egorysheva A.V. Structure and thermal expansion of new high-temperature compounds $\text{Ln}_2\text{CrTaO}_7$ (Ln=Sm, Gd, Y).....	108
Sagatova D.N., Gavryushkin P.N. Theoretical study of magnesium and calcium orthocarbonate at <i>PT</i> conditions of the Earth's lower mantle .....	109
Sadovnichii R.V., Lorenz H., Kotelnikova E.N. Thermal deformations of the amino acid enantiomers L-serine and L-alanine.....	110
Smetanina K.E., Andreev P.V., Lantsev E.A., Vostokov M.M. Study of phase composition homogeneity of hard alloys based on WC – Co .....	111
Syrov E.V., Krashenninnikova O.V., Knyazev A.V., Tereshin A.I. High-temperature XRD studies of some new compounds of Dion – Jacobson series .....	112
Sycheva G.A., Kostyreva T.G. Nucleation of tin pyrophosphate crystals under the influence of x-ray radiation.....	113
Тимчук А.В. Влияние кислотности и поверхностно-активных веществ на фазообразование $\text{BiVO}_4$ при постоянной температуре.....	114
Торникова А.Р., Белоконева Е.Л., Димитрова О.В., Волков А.С., Зорина Л.В. $\text{KTm}[\text{B}_4\text{O}_6(\text{OH})_4]\cdot 3\text{H}_2\text{O}$ , a new member of the layered borate family with a high degree of disorder.....	115
Ushakov I.E., Goloveshkin A.S., Lenenko N.D., Korlyukov A.A., Golub A.S. Non-covalent interactions in layered compounds of $\text{MoS}_2$ with guanidinium cations .....	116
Chernyshova I.A., Frank-Kamenetskaya O.V., Vereshchagin O.S., Malyshkina O.V. The influence of temperature on crystal structure and pyroelectric properties of Ni- and Cu-bearing tourmalines .....	117
Шварева А.Г., Князев А.В., Кяшкин М.В., Жакупов Р.М. Терморентгенография соединений со структурой минерала пирохлора .....	118
Шипилова А.С., Князев А.В., Князева С.С., Гусарова Е.В., Амосов А.А., Кусуткина А.М. Низкотемпературная рентгенография азотистых оснований .....	119
Shkvarin A.S., Titov A.A., Postnikov M.S., Titov A.N., Shkvarina E.G. Thermal stability of the Cu-ZrTe <sub>2</sub> intercalation compounds .....	120

## PREFACE

A couple of decades ago, we were happy to find several reports on crystal chemistry of extreme or non-ambient conditions in the program of crystal chemical conferences. And today we are holding a full Conference-School for Young Scientists - HTXRD - and not the first, but the fourth one! Of course, this is the result of a rapid development and implementation into a practice of the initial main topic of the conference – diffraction studies of thermal expansion and phase transitions. This process has become possible due to the development of the equipment and software for processing large massifs of diffraction data.

This conference is aimed at providing young people with the approaches and methods of studying a behavior of a crystal structure under variable thermodynamic parameters, studying the structure and properties of crystals under extreme conditions, as well as studying of complex crystallographic objects - periodic and disordered crystals and nanomaterials.

For the first time in our program, the research of a behavior of a matter under pressure is so widely presented. These lectures will open the conference, although at the first school a lecture on the influence of pressure was presented only by Prof. Elena Boldyreva. Now lectures of the world's leading scientists on this hot topic are presented at the conference – Prof. Hubert Huppertz (University of Innsbruck, Austria), Professor Leonid Dubrovinsky (University of Bayreuth, Germany), Prof. Elena Boldyreva (Novosibirsk State University and Institute of Catalysis SB RAS), Prof. Natalia Dubrovinskaya (University of Bayreuth, Germany).

New topic of the school is research of various properties of materials; also under conditions of variable thermodynamic parameters - lectures will be presented by Prof. Barbara Albert (Technische Universität Darmstadt, Germany), Corr. Member RAS, Prof. Evgeny Antipov (Lomonosov Moscow State University), Prof. Anatoliy Senyshyn (Heinz Maier-Leibnitz Zentrum, Technische Universität München).

Several lectures cover phase transitions from various viewpoint of a thermodynamic, symmetrical and crystal-chemical-mineralogical aspects: academician, Prof. Andrey Rempel (Institute of Metallurgy, Ural Branch of the Russian Academy of Sciences, Yekaterinburg), Prof. Evgeny Chuprunov (Lobachevsky National Research Nizhny Novgorod State University), Corr. Member RAS, Prof. Nikolai Eremin, (Lomonosov Moscow State University), Corr. Member RAS, Prof. Sergey Krivovichev, Kola Science Center RAS, Apatity and Institute of Earth Sciences, Saint Petersburg State University.

Also academician, Prof. Andrey Rempel will present a report on Russian-German travel scientific seminars for young scientists.

HT X-ray diffraction and HT crystal chemistry are traditionally the main topics of these schools. However, new information awaits the listeners. For the first time Prof. Robert Dinnebier (Max Planck Institute for Solid State Research, Stuttgart, Germany) will give a lecture, also lectures by Prof. Rimma Bubnova (Institute of Silicate Chemistry RAS, St. Petersburg), Prof. Alexander Knyazev (Department of Chemistry, Lobachevsky National Research Nizhny Novgorod State University), Assoc. Prof. Maria Krzhizhanovskaya (Institute of Earth Sciences, St. Petersburg State University).

One of the main topics of crystal chemistry and traditional for these schools – aperiodic crystals and nanomaterials – also got a new vector for this time. This section will be opened by Prof. Nadezhda Bolotina (Federal Research Center "Crystallography and Photonics" RAS, Moscow), Prof. Svetlana Titova (Institute of Metallurgy, Ural Branch RAS, Yekaterinburg), Prof. Olga Yakubovich (Lomonosov Moscow State University), Prof. Alexander Titov (Institute of Metallurgy, Ural Branch RAS, Yekaterinburg), Prof. Sergey Tsybulya (Novosibirsk State University), Prof. Pavel Fedorov (**Prokhorov General Physics Institute** RAS, Moscow), Prof. Oleg Siidra (Institute of Earth Sciences, St. Petersburg State University).

We are grateful to these scientists – world's famous experts in their field – for their plenary lectures as offline (St. Petersburg) as well as online ones. It should be noted, that the geography of lecturers as well as participants is widely represented (more detailed information is on the HTXRD-4 website, [www.htxrd2020.ru](http://www.htxrd2020.ru)).

Workshops are an important component of all HTXRD schools, and we look forward for further cooperation with their initiators – Prof. Nadezhda Bolotina (Determination and analysis of complex non-standard structures, including modulated ones (Jana2006)), Prof. Rimma Bubnova,

Vera Firsova, Sergey Volkov, Andrey Shablinskii, Yaroslav Biryukov (Determination of thermal expansion tensor according to X-ray diffraction data (TTT and RTT)), Dmitry Yatsenko (Modeling of powder diffraction patterns of nanoscale systems (DIANNA software package)).

Of course, we are very grateful to our sponsors RFBR, ICDD, Bruker, Techninfo. Without their financial support, the organization of the Conference would have been practically impossible.

Special thanks to our local Organizing Committee from the Institute of Silicate Chemistry of the Russian Academy of Sciences, young scientific secretaries PhD Sergey Volkov and Valentina Yukhno, and local committee (Yaroslav Biryukov, Vera Firsova, Andrey Shablinskii, Olga Shorets).

For the first time, the Conference is held in an online format, but we are sure that this will not prevent the exchange of our young participants to present their new experimental results, creative ideas and methods, and start to apply the acquired knowledge and skills in their practice.

We invite everyone to the next offline conference-school which we hope hold in St. Petersburg!

Rimma Bubnova, Maria Krzhizhanovskaya, Stanislav Filatov

# **1. Plenary session**

## Extreme Conditions of Pressure and Temperature for the Synthesis of Crystalline Materials.

Huppertz H.

Institute of General, Inorganic and Theoretical Chemistry, University of Innsbruck, Innrain 80-82, A-6020 Innsbruck, Austria.

\*Correspondence email: Hubert.Huppertz@uibk.ac.at

In the field of solid state chemistry, high-pressure/high-temperature conditions realized *via* a 1000 ton press and a Walker-type module (Figure 1) can be used for the synthesis of new compounds [1]. The talk gives an introduction into the experimental challenges to realize such exotic conditions in the field of high-pressure research. Next to other examples from the field of basic fundamental research, a new HF-free synthesis route *via* a high-pressure/high-temperature experiment for the preparation of the novel hexafluorosilicate phosphor  $\text{Li}_2\text{SiF}_6:\text{Mn}^{4+}$  is presented (Figure 2);  $\text{Li}_2\text{SiF}_6:\text{Mn}^{4+}$  is a compound, which probably cannot be synthesized via a common wet-chemical etching process. Not many lithium-containing hexafluorosilicates are known so far, *e.g.*  $\text{LiNa}_2\text{AlF}_6:\text{Mn}^{4+}$  is one of them. However, the lithium ion is the lightest cation besides  $\text{H}^+$ , and therefore a blue shift of the emission is expected for lithium-rich phases in comparison to compounds of its heavier congeners. Because even a small blue-shift can lead to a higher luminous efficacy of radiation (LER), we expect good performance of  $\text{Li}_2\text{SiF}_6:\text{Mn}^{4+}$  in WLEDs [2]. So, this example demonstrates that not only basic fundamental research but also applied research can be performed under such exotic conditions.



Figure 1: 1000 t multianvil high-pressure device for the realization of extreme pressures and temperatures.

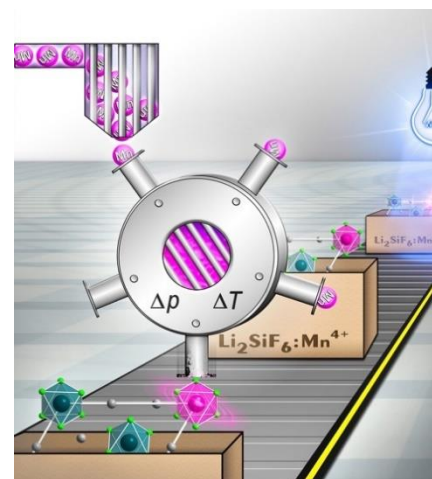


Figure 2: Schematic illustration of doping  $\text{Li}_2\text{SiF}_6$  with  $\text{Mn}^{4+}$ .

1. Huppertz H., Heymann G., Schwarz U., Schwarz M.R. Handbook of Solid State Chemistry, Editors: Dronskowski R., Kikkawa S., Stein A. Wiley-VCH Verlag GmbH & Co. KGaA. Weinheim. Germany. High-Pressure Methods in Solid State Chemistry. 2017. V. 2. P. 23-48.
2. Stoll C., Bandemehr J., Kraus F., Seibald M., Baumann D., Schmidberger M.J., Huppertz, H. HF-Free Synthesis of  $\text{Li}_2\text{SiF}_6:\text{Mn}^{4+}$ : A Red-Emitting Phosphor. Inorganic Chemistry. 2019. V. 58. P. 5518-5523.

## **Inorganic Synthesis and Crystal Chemistry at Multimegabar Pressures**

Dubrovinsky L.

BGI, University of Bayreuth, 95440 Bayreuth, Germany

\*Correspondence email: Leonid.Dubrovinsky@uni-bayreuth.de

The impact of high-pressure studies on fundamental physics and chemistry, and especially on the Earth and planetary sciences, has been enormous. Modern science and technology rely on the fundamental knowledge of matter that is provided by crystallographic studies. The most reliable information about crystal structures and their response to changes in pressure and temperature is obtained from single-crystal diffraction experiments. Advances in diamond anvil cell (DAC) techniques and double-stage DACs, as well as in modern X-ray facilities have increased the accessible pressure range for structural research up to multimegabar range. We have developed a methodology to perform single-crystal X-ray diffraction experiments in double-side laser-heated DACs. Our results demonstrated that the solution of crystal structures, their refinement, and accurate determination of thermal equations of state of elemental materials, oxides, carbides, borides, carbonates, and silicates from single-crystal diffraction data are possible well above 100 GPa at temperatures of thousands of degrees. These resulted in findings of novel compounds with unusual compositions, crystal chemistry, and physical properties. We illustrate application of new methodology for simultaneous high-pressure and high-temperature single crystal diffraction studies using examples of investigations of chemical and phase relations in the Fe-O system, transition metals carbonates, silicates, and hydrides.

## Crystals of organic and coordination compounds – what can we learn about them from high-pressure experiments

Boldyreva E.V.<sup>1,2</sup>

<sup>1</sup> Borekov Institute of Catalysis SB RAS, 630090, Novosibirsk, Lavrentieva ave. 5, Russia.

<sup>2</sup>Novosibirsk State University, 630090, Novosibirsk, Pirogova street, 2, Russia.

High-pressure research is becoming increasingly popular not only among mineralogists and geoscientists, inorganic chemists and physicists, but also among organic chemists. One does not need extremely high pressures, to induce various interesting transformations in coordination, organic and organometallic compounds, such as proton transfer, charge transfer, changes in the hydrogen bonds, halogen-halogen,  $\pi$ - $\pi$ , and other types of intermolecular interactions, conformational changes, rotation of molecules, as well as recrystallization from the pressure-transmitting fluids, to give new phases, which cannot be accessed at ambient pressure. These studies can be carried out using repeatedly, without replacing the diamonds after each experiment in the relatively modest budget diamond anvil cells and using laboratory sources of X-rays, not necessarily synchrotron radiation. The quality of data can be sufficiently high, not merely to follow reliably the changes in the intramolecular geometries (bond lengths and angles), but also to analyze the distribution of electron charge densities. This research is very important not only for improving the understanding of the nature of chemical bonds, intermolecular interactions, and factors that determine the crystallization and structural transformations of solids, but also for many practical applications, such as developing materials for organic electronics, optical materials, mechanically responsive materials, supramolecular devices, as well as new drug forms.

In my lecture I shall give an overview of the state-of-the-art of the experimental techniques, which are used for high-pressure diffraction experiments with coordination and organic materials. I shall also give examples of the studies of the anisotropy of the continuous structural distortion in relation to the intermolecular interactions and intramolecular bonds, of the mechanisms of crystallization, solid-state phase transitions, and chemical reactions. The role of seeding, of the protocol of increasing and increasing pressure, and of the pressure-transmitting fluids in pressure-induced transformations will be discussed. I shall also discuss the effect of pressure on photochemical and thermal transformations in the crystals of organic and coordination compounds.

The support from the Russian Ministry of Education and Science is acknowledged (project project AAAA-A19-119020890025-3).

1. Болдырева Е.В., Захаров Б.А., Ращенко С.В., Сереткин Ю.В., Туманов Н.А. Исследование твердофазных превращений при помощи рентгеновской дифракции в условиях высоких давлений *in situ*. 2016, Изд-во СО РАН, Новосибирск, ISBN 9785769215261. 256 стр.

2. Boldyreva E.V. High Pressure Crystallography, Elucidating the role of intermolecular interactions in the crystals of organic and coordination compounds, in: Understanding Inter-molecular Interactions in the Solid State – Approaches and Techniques, D. Chopra (Ed.), RSC, 2018., Print ISBN: 978-1-78801-079-5 (Серия Monographs in Supramolecular Chemistry), 339 pp.

3. Boldyreva E.V. Multi-component crystals and non-ambient conditions, in: Multi-Component Crystals. Synthesis, Concepts, Function. E. Tiekink, J. Zukerman-Schpector (Eds), De-Gruyter: Berlin, 2017, ISBN 3110463792, 9783110463798, 336 pp.

4. Zakharov B.A., Boldyreva E.V. High pressure: a complementary tool for probing solid state processes, *CrystEngComm*, 2019, 21, 10-22.

5. Gaydamaka A.A., Arkhipov S.G., Zakharov B.A., Seryotkin Y.V., Boldyreva E.V. Effect of Pressure on Slit Channels in Guaninine Sodium Salt Hydrate: A Link to Nucleobase Intermolecular Interactions, *CrystEngComm*. 2019, 21, 4484-4492.

6. Bogdanov N.E., Milašinović V., Zakharov B.A., Boldyreva E.V., Molčanov K. Pancake-Bonding of Semiquinone Radicals under Variable Temperature and Pressure Conditions, *Acta Crystallographica Section B: Structural Science, Crystal Engineering and Materials*. 2020, 76(2), 285-291. DOI: 10.1107/s2052520620002772.



## **Materials synthesis and crystallography at extreme pressure-temperature conditions revealing remarkable materials properties**

Dubrovinskaia N.

Material Physics and Technology at Extreme Conditions, Laboratory of Crystallography,  
University of Bayreuth, Universitaetstr. 30, 95440 Bayreuth, Germany

\*Correspondence email: natalia.dubrovinskaia@uni-bayreuth.de

Modern science and technology rely on the vital knowledge of matter which is provided by crystallographic investigations. The most reliable information about crystal structures of solids and their response to alterations of pressure and temperature is obtained from single-crystal diffraction experiments. We have developed a methodology for performing single-crystal X-ray diffraction experiments in double-side laser-heated DACs and demonstrated that it allows the crystal structure solution and refinement, as well as accurate determination of thermal equations of state above 200 GPa at temperatures of thousands of degrees. Application of this methodology resulted in discoveries of novel compounds with unusual chemical compositions and crystal structures, uncommon crystal chemistry and physical properties. It has been successful in investigations of various classes of solids - elemental materials, oxides, carbides, borides, carbonates, nitrides, and silicates.

In this contribution the results of our single-crystal diffraction studies of phase relations in various metal-nitrogen systems will be reported. The materials synthesis and crystallography at extreme pressure-temperature conditions revealing remarkable materials properties will be elucidated on example of one-step synthesis of metal-inorganic frameworks ( $\text{Hf}_4\text{N}_{20}\cdot\text{N}_2$ ,  $\text{WN}_8\cdot\text{N}_2$ , and  $\text{Os}_5\text{N}_{28}\cdot 3\text{N}_2$ ) and other types of nitrides and polynitrides. Perspectives of materials synthesis and crystallography at extreme conditions will be outlined.

## Phase transformations at moderated temperatures in nonstoichiometric compounds with high entropy

Rempel A.A.

Institute of metallurgy of the Ural Branch of the Russian Academy of Sciences,  
620016 Ekaterinburg, Amundsena str. 101, Russia.  
\*Correspondence email: rempel.imet@mail.ru

The results of performed experimental and theoretical studies, the prospects of the nonstoichiometric compounds for hard and tough materials, metallic and semiconductor materials, the materials which are photocatalytically active under visible light will be presented in the talk.

Nonstoichiometric compounds are best known among the carbides, nitrides, or oxides of the group IV and group V transition metals. The chemical formula of such nonstoichiometric compounds can be written as  $MX_y$  (where  $X = C, N, \text{ or } O$ ). The existence of nonstoichiometry is related to the presence of structural vacancies either on metal or on non-metal sublattices. The amount of vacancies can be very high that means that the nonstoichiometric compounds possess strongly extended homogeneity regions from  $y = 0.5$  up to  $y = 1.2$ . At high temperatures most of nonstoichiometric compounds have disordered cubic  $B1$  (NaCl) structure. The stability of this highly symmetric cubic phase at high temperature is provided by high configurational entropy due to *atom - structural vacancies* disordering on the same sublattice like it is case in high entropy alloys [1].

At moderated temperatures, lower than about 1000 K, the structural vacancies on metal and non-metal sublattices undergoing ordering and build low-symmetry superstructures of the  $M_2X$ ,  $M_3X_2$ ,  $M_6X_5$ ,  $M_8X_7$ , and  $M_5V_MX_5V_X$  types. This is supported by the use of diffraction analysis including neutron and synchrotron techniques and first principal calculations the structure of synthesized compounds with allowance of long range, short range and correlational orders of structural vacancies. Disorder-order phase transformations at moderated temperatures in the transition metal compounds have significant effects on the physical properties of the nonstoichiometric compounds and on their equilibrium phase diagrams [2].

Acknowledgements: This study was conducted under the state assignment for IMET UB RAS.

1. Rempel A.A., Gelchinsky B.R. Production, properties and practical application of high-entropy alloys. 2020. Steel in Translation, pp.243-247.
2. Rempel A.A., Gusev A.I. Nonstoichiometry in solids. 2018. Moscow: FIZMATLIT, 640 pages.

## **Роль кристаллохимии в создании новых катодных материалов для металл-ионных аккумуляторов**

Антипов Е.В.

Химический факультет, Московский государственный университет, Москва 119991,  
Россия

\*Correspondence email: [evgeny.antipov@gmail.com](mailto:evgeny.antipov@gmail.com)

Источником около 90% используемой в настоящее время энергии является ископаемое топливо, что имеет очень серьезные последствия: быстрое истощение природных ресурсов и существенный экологический ущерб. Поэтому актуальной задачей является развитие возобновляемых источников энергии и эффективных накопителей энергии, что позволит существенно уменьшить потребление природных ресурсов в будущем.

Li-ионные аккумуляторы, изначально разработанные для портативных переносных устройств, уже сейчас находят широкое применение в качестве стационарных накопителей энергии, в электромобилях и др. В настоящее время стремительно развиваются исследования в области Na и K-ионных аккумуляторов, которые обладают целым рядом преимуществ по сравнению с литий-ионными. Удельные энергетические характеристики металл-ионных аккумуляторов, в основном, определяются свойствами используемых электродных материалов. Для удовлетворения потребностей, существующих и, особенно, новых применений, электродные материалы металл-ионных аккумуляторов нуждаются в существенном улучшении их удельных энергетических параметров, безопасности и стоимости.

В докладе будут рассмотрены основные направления наших исследований в области новых катодных материалов для Li-, Na- и K-ионных аккумуляторов с особым акцентом на роль кристаллохимии в их создании и оптимизации важных для практического использования свойств.

Работа выполнена при поддержке Российского научного фонда (грант № 17-73-30006).

## **Megascience facilities and russian-german travelling seminar of nanomaterials**

Rempel A.A. \*

Institute of metallurgy of the Russian Academy of Sciences, 620016, Amundsena str. 101,  
Ekaterinburg, Russia.

\*Correspondence email: rempel.imet@mail.ru

Megascience facilities like synchrotron and neutron sources play an important role in the development of nanoscience. This is because of additional possibilities of these sources in giving precise information about atomic structure, particle size, particle size distribution, core-shell structure, etc. of the nanomaterials.

To make undergraduates and postgraduates from Russia and Germany to be familiar with possibilities of the synchrotron and neutron sources more than 10 years ago in 2006 a traveling school-seminar (TS) on physics and chemistry of nanomaterials (PCnano) had been started. To that time it was possible due to close collaboration between University of Erlangen-Nuremberg (Prof. Dr. Andreas Magerl), Ural Federal University and Ural Branch of the Russian Academy of Sciences.

Participants for the TS were selected from all over the country for academic excellence and interest in scientific and cultural exchange. Each of them will present a 15-minute research paper, which was usually their first presentation in English to an international audience. The group was accompanied by two Russian and two German professors who give extended lectures. The scientific part was also complemented by lectures by leading scientists at the visited institutes.

Since 2006 the participants of TS have visited most known and important synchrotron and neutron source facilities in Russia (Novosibirsk, Moscow) and Europe (Munich, Hamburg, Berlin, Karlsruhe, Grenoble). Since 2006 many participants of the TS have used synchrotron and neutron sources in their scientific work and have achieved important scientific results.

Recently, the project of the mobile Russian-German summer school-seminar TS for undergraduates and postgraduates was among the winners of the competition "Russia and Germany: scientific and educational bridges" [1].

Acknowledgements: Prof. Dr. Andreas Magerl, Ass.Prof. Dr. Maxim Vlasov, Prof. Dr. Mirijam Zobel and many many others.

See news at <https://urfu.ru/en/news/33203/>

## Unusual thermal structural behaviour of lithiated graphite phases

Senyshyn A.<sup>1</sup>, Mühlbauer M.J.<sup>2</sup>, Baran V.<sup>1</sup>

<sup>1</sup> Heinz Maier-Leibnitz Zentrum (MLZ), Technische Universität München, Lichtenbergstr. 1, 85748 Garching, Germany

<sup>2</sup> Institute for Applied Materials (IAM), Karlsruhe Institute of Technology (KIT), Hermann-von-Helmholtz-Platz 1, D-76344 Eggenstein-Leopoldshafen, Germany

Crystal structures of the phases in the Li-C system have vital importance for electrochemical energy storage, especially Li-ion battery technology. Due to difficulties with metallic lithium about 98 % of Li-ion batteries are utilizing graphite anode at the moment. Furthermore graphite additive is used to maintain electronic conductivity of weakly conducting cathodes, e.g. LiFePO<sub>4</sub>. Use of electrochemistry permits to intercalate one lithium per six carbon atoms, which is reflected in the formation of LiC<sub>6</sub> phase (stage I) – graphite sheets alternated by lithium layers along *c* axis. The phase has no homogeneity limits, i.e. upon lithium extraction stage II (LiC<sub>12</sub>) phase is formed, where every 2<sup>nd</sup> plane is occupied by lithium. Further lithium extraction leads to the formation of sequence of phases displaying solid-solution like behaviour reflecting the intermediate steps between stage II and electrochemically active graphite 2H [1].

Recent in operando structural studies of model cylinder-type Li-ion battery revealed a structural instability of certain low-lithiated graphites [2]. Furthermore anomalous structural behaviour of stage I and stage II had been noticed along with the considerable differences between in situ and ex situ modes of data collection [3]. In the current contribution a systematic temperature-resolved diffraction study of selected compositions from Li-C binary system will be presented and discussed in terms of battery performance at different temperatures.

1. Senyshyn, A., O. Dolotko, M. J. Mühlbauer, K. Nikolowski, H. Fuess and H. Ehrenberg (2013). "Lithium Intercalation into Graphitic Carbons Revisited: Experimental Evidence for Twisted Bilayer Behavior." *Journal of the Electrochemical Society* **160**(5): A3198-A3205.

2. Senyshyn, A., M. J. Mühlbauer, O. Dolotko and H. Ehrenberg (2015). "Low-temperature performance of Li-ion batteries: The behavior of lithiated graphite." *Journal of Power Sources* 282: 235-240.

3. Baran, V., O. Dolotko, M. J. Mühlbauer, A. Senyshyn and H. Ehrenberg (2018). "Thermal Structural Behavior of Electrodes in Li-Ion Battery Studied In Operando." *Journal of The Electrochemical Society* 165(9): A1975-A1982.

## Aperiodic crystals

Bolotina N.B.

Shubnikov Institute of Crystallography of Federal Scientific Research Centre “Crystallography and Photonics” of Russian Academy of Sciences, Leninskiy Prospekt 59, 119333, Moscow, Russia.  
Correspondence email: nb\_bolotina@mail.ru

Aperiodic crystals [1, 2] have a long-range order and give sharp diffraction patterns, like periodic crystals, but differ from the latter in the absence of three-dimensional translational periodicity of the atomic structure. There are three types (or families) of aperiodic crystals. Atoms of *incommensurately modulated* crystals are shifted from the points of the crystal lattice according to a periodic law, but the modulation period is incommensurate with one or more lattice periods. Two lattices with incommensurate periods are necessary to describe the structure of an *incommensurate composite*. *Quasicrystals* have symmetry that is unacceptable in crystals according to the laws of classical crystallography. The structures of aperiodic crystals are successfully studied in model spaces with more than three dimensions, but the principles for constructing the superspace models are different for the above three families. This lecture will focus on modulated and composite crystals. The methods for describing their structures in superspace have a common basis and are implemented in a single software package JANA [3]. Superspace modeling of quasicrystals is built on other principles and will not be considered here.

An idea will be formed on the methods for describing modulated and composite structures in the (3+d)D space. The capabilities of the JANA program for the structure solution and refinement will be discussed. A separate group is formed by crystals in which the period of structural modulation is commensurate with the period of a small basic lattice. In fact, these are 3D long-period structures, which are complicated or inaccessible for solution due to the huge number of strongly correlating structural parameters. The only way to solve this problem is to consider the long-period structure commensurately modulated with respect to the lattice with smaller cells and pass to the superspace model. The lecture contains examples of commensurately and incommensurately modulated crystals and incommensurate composites. The advantages of their description in (3+d)D are demonstrated.

This work was supported by Russian Foundation for Basic Research, grant No 18-29-12005.

1. T. Janssen, G. Chapuis, M. de Boissieu. Aperiodic Crystals. From Modulated Phases to Quasicrystals // IUCr Monographs on Crystallography, No 20, Oxford University Press, 2007.
2. S. van Smaalen. Incommensurate Crystallography. IUCr Monographs on Crystallography, No 21, Oxford University Press, 2007.
3. V. Petříček, M. Dušek, L. Palatinus, Crystallographic computing system JANA2006: General features, Z. Kristallogr. 229 (2014) 345–352.

## Investigating catalysts and luminescent materials by in situ powder diffractometry

Steffan J.<sup>1</sup>, Totzauer L.<sup>1</sup>, Heck F., Hofmann K., Albert B. <sup>\*1</sup>

<sup>1</sup> Eduard Zintl-Institute of Inorganic and Physical Chemistry, Technische Universität Darmstadt, 64285 Darmstadt, Germany.

\*Correspondence email: [barbara.albert@tu-darmstadt.de](mailto:barbara.albert@tu-darmstadt.de)

In-situ X-ray powder diffraction can be used to investigate the mechanisms of reactions between solids and gas phases.

The analysis of structural changes of a catalyst during a reaction is an important step towards a better understanding of the reaction mechanisms. Thus it may help to optimize both the catalyst and the process. Acrylic acid and methacrylic acid represent organic chemicals that are important technical products. Their industrial production relies on catalyzed reactions that are not fully optimized. We have designed an experimental set-up that allows it to detect and follow the changes of a crystalline catalyst during such oxidation reactions. As an example, we will present the following example in detail: cesium salts of vanadium-substituted heteropolyacids with Keggin anions used as heterogeneous catalysts to partially oxidize acrolein. Acrolein vapour was led through a reaction chamber at the diffractometer. A catalyst of the nominal composition  $Cs_2H_2[VPMo_{11}O_{40}]$  was investigated at varying conditions (temperature, water pressure, reaction time). The in-situ/operando experiments revealed how the occupation of the different atomic sites reversibly changed during the reaction. The oxygen content of the catalyst was monitored and new conclusions concerning the reaction mechanism were drawn.

As a second example the investigation of a luminescent material in the context of thermographic measurements will be discussed.

## Влияние эффектов порядка-беспорядка в кристаллических структурах на термодинамические функции смешения твердых растворов

Еремин Н.Н.

МГУ им. М.В.Ломоносова, Геологический факультет, 119991, Москва, Ленинские горы, 1А  
neremin@geol.msu.ru

В настоящее время математический аппарат теоретической кристаллохимии позволяет во многих случаях заменять физический эксперимент математическим. Качественный скачок повышения быстродействия компьютеров в первые два десятилетия XXI-ого века позволил перейти к предсказанию кристаллических структур не только соединений с фиксированной стехиометрией, но и протяженных твердых растворов, которыми являются все природные минералы без исключения, причем как методами «из первых принципов», так и полуэмпирическими методами межатомных потенциалов.

В реальном кристалле распределение различных сортов атомов по структурно-эквивалентным позициям в общем случае подчиняется законам математической статистики. Как было показано в обзоре [1] использование небольшого числа элементарных ячеек приводит к изучению не твердых растворов, а упорядоченных промежуточных соединений, обладающими радикально отличными от неупорядоченных твердых растворов термодинамическими свойствами. В связи с этим, интерес к моделированию твердых растворов, сталкивается с проблемой распределения атомов в расчетной ячейке ограниченных размеров для наилучшей имитации неупорядоченности. Эта проблема с той или иной степенью успеха решается различными методическими приемами. Оригинальный авторский подход, изложенный в [2] позволяет в рамках ячейки разумных конечных размеров максимально приблизиться к статистически неупорядоченному распределению в макроскопическом кристалле произвольного состава.

Помимо изложения методических особенностей авторского подхода в докладе на следующих конкретных примерах демонстрируется результативность и предсказательные возможности методики:

- 1) влияние эффектов упорядочения на кристаллографические параметры и энергетические характеристики твердого раствора объем ячейки в системе скиагит - Fe-мейджорит;
- 2) предсказание термодинамических функций смешения, фазовой стабильности и отклонения от правила Вегарда в твердых растворах гибридных перовскитов  $\text{CH}_3\text{NH}_3\text{Pb}(\text{I}_{1-x}\text{Br}_x)_3$  [3];
- 3) создание термодинамической базы данных [4] для твердых растворов редкоземельных фосфатов, допированными радиоактивными актиноидами.

1. Urusov V.S. Comparison of semi-empirical and ab-initio calculations of the mixing properties of MO-M'O solid solutions. *J. Solid State Chemistry*. V. 153. P. 357-364.

2. Еремин Н.Н., Деянов Р.З, Урусов В.С. Выбор сверхячейки с оптимальной атомной конфигурацией при моделировании неупорядоченных твердых растворов. *Физика и химия стекла*. 2008. Т. 34, № 1, С. 9-18.

3. Marchenko E.I. et al. Transferable approach of semi-empirical modeling of disordered mixed halide hybrid perovskites  $\text{CH}_3\text{NH}_3\text{Pb}(\text{I}_{1-x}\text{Br}_x)_3$ : prediction of thermodynamic properties, phase stability and deviations from Vegard's law. *J. Phys. Chem. C*. 2019. V. 123, № 42, P. 26036-26040.

4. Eremin N.N. et al. Solid solutions of monazites and xenotimes of lanthanides and plutonium: atomistic model of crystal structures, point defects and mixing properties. *Comp. Mat. Sci*. 2019. Vol. 157, P. 43-50



## Polymorphic transitions in feldspar structures

Krivovichev S.V.<sup>1,2</sup>

<sup>1</sup> Nanomaterials Research Centre, Kola Science Centre RAS, Fersman st., 14, Apatity, 184209 Russia

<sup>2</sup> Saint Petersburg State University, University Emb., 7/9, Saint Petersburg, 199034 Russia  
Correspondence email: s.krivovichev@ksc.ru

The various aspects of polymorphism in the feldspar family of minerals are considered with special emphasis upon their structural diversity and complexity [1]. The feldspar family is defined as consisting of valid minerals and unnamed or conditionally named mineral phases with the general formula  $M^{n+}[T_4^{k+}O_8]$ , where  $n$  is the average charge of the  $M^{n+}$  cation ( $n = 1-2$ ;  $M^{n+} = Na^+, K^+, Rb^+, (NH_4)^+, Ca^{2+}, Sr^{2+}, Ba^{2+}$ ),  $k$  is the average charge of the  $T^{k+}$  cation ( $k = 4 - n/4$ ;  $T^{k+} = Be^{2+}, Zn^{2+}, Al^{3+}, B^{3+}, Fe^{3+}, Si^{4+}, As^{5+}, P^{5+}$ ). There are twenty-nine valid mineral species known to date that can be assigned to the feldspar family. Maskelynite is the natural X-ray amorphous feldspar polymorph (glass) with the plagioclase composition. All feldspar polymorphs can be classified into two groups: those containing T atoms in tetrahedral coordination only and those containing T atoms in non-tetrahedral coordination. There are four basic topologies of the feldspar-family tetrahedral networks: **fsp** (3D; feldspar *sensu stricto*; eleven mineral species), **pcl** (3D; paracelsian; seven mineral species), **bet** (3D, svyatoslavite; two mineral species), and **dms** (2D; dmisteinbergite; six mineral species). There are three minerals that contain T atoms in exclusively octahedral (sixfold) coordination and crystallize in the hollandite structure type. The high-pressure polymorphism for the structures with the **fsp** and **pcl** topologies is controlled by the distinction of these topologies as flexible and inflexible, respectively. The analysis of structural complexity by means of the Shannon information theory indicates the following general trends: (i) structural complexity decreases with the increasing temperature; (ii) kinetically stabilized metastable feldspar polymorphs are topologically simpler than the thermodynamically stable phases; (iii) the high-pressure behavior of feldspar-family structures does not show any obvious trends in the evolution of structural complexity. The feldspar polymorphism includes a number of structural phenomena: (i) coordination changes of intra- and extraframework cations; (ii) topological reconstructions, including changes in dimensionality; (iii) cation ordering, including Al/Si and M-cation ordering in solid solutions, resulting in the chemical stabilization of particular structure types and the formation of incommensurately modulated structures (in plagioclases); (iv) displacive distortions involving tilting of tetrahedra and rotations of crankshaft chains; (v) amorphization. The observed structural phenomena are controlled by temperature, pressure (including shock-induced transformations) and crystallization kinetics that may stabilize metastable phases with unique crystal structures.

The study was funded by RFBR, project number 19-15-50064.

Krivovichev S.V. Feldspar polymorphs: diversity, complexity, stability. Zapiski Ross. Mineral. Ob-va. 2020. CXLIX. P. 16–66.

## Количественные измерения в теории симметрии кристаллов. Фазовые переходы второго рода

Чупрунов Е.В.

Национальный исследовательский Нижегородский государственный университет им. Н.И. Лобачевского"

Привычное понятие симметрии как двухуровневое «симметрично-несимметрично» давно расширено до определения «почти симметрично», «частично симметрично» и т.д. Такие частично симметричные системы известны в различных разделах физики, химии, кристаллографии. Специалисты по рентгеноструктурному анализу называют атомные структуры с приближительной симметрией псевдосимметричными.

Пусть функция электронной плотности кристалла инвариантна относительно пространственной группы  $G$ . Если часть электронной плотности кристалла инвариантна также относительно федоровской надгруппы  $T \supset G$ , то будем говорить, что для кристалла характерна федоровская псевдосимметрия.

Для количественной оценки степени инвариантности кристаллической структуры относительно изометрической операции используется функционал, который принимает значения от  $-1$  до  $+1$ , показывая тем самым степень инвариантности исследуемой системы от точной антисимметрии ( $-1$ ) до точной симметрии ( $+1$ ). Для кристаллов оценивается степень инвариантности функции электронной плотности.

Для функций вводится понятие псевдосимметричной функции и приводятся соответствующие примеры. В кристаллохимии вводится понятие псевдосимметричный структурный тип и описываются специальные диаграммы для количественного описания принадлежащим этим структурным типам кристаллов.

Обсуждаются диаграммы для всех кристаллов, описанных в Кембриджском банке структурных данных.

В физике кристаллов количественное описание приближенной симметрии (псевдосимметрии) может быть полезно при описании кристаллических структур в низкотемпературной фазе, которые образуются в ходе фазовых переходов второго рода. Введенный функционал количественно описывает величину параметра порядка Ландау для кристаллов в низкосимметричной фазе.

**Fractional coordinates, symmetry modes, and rigid bodies:  
Three different ways for describing structural evolution during phase transitions**

Dinnebier R.E.

Max Planck Institute for Solid State Research, Heisenbergstraße 1, 70569 Stuttgart, Germany  
Correspondence email: r.dinnebier@fkf.mpg.de

If a direct subgroup relation exists between the two phases undergoing a displazive phase transition, it is often advantageous to describe the crystal structures not in form of individual fractional coordinates but using symmetry/distortion modes starting from an existing (or virtual) parent phase. Usually only very few modes are active, thus reducing the number of parameters considerably. Often, these modes or combinations of these modes define polyhedral tilts allowing the use of (more complex) rigid body modes.

Freely available user-friendly group-theoretical pograms like ISODISPLACE<sup>1</sup> or AMPLIMODES<sup>2</sup> can be used to derive the required irreducible representations. In a second step, the active modes can be determined and parameterized, allowing the direct determination of physical quantities like order parameter, lattice strain etc.

The evaluation of the crystal structure during the high temperature phase transition of the double salt  $\text{Mg}(\text{H}_2\text{O})_6\text{RbBr}_3$  is analyzed in four different ways during this presentation<sup>3</sup>.

1 B. J. Campbell, H. T. Stokes, D. E. Tanner, and D. M. Hatch, "ISODISPLACE: a web-based tool for exploring structural distortions," *J. Appl. Cryst.* 39, 607-614 (2006).

2 D. Orobengoa, C. Capillas, M. I. Aroyo and J. M. Perez-Mato, AMPLIMODES: symmetry-mode analysis on the Bilbao Crystallographic Server, *J. Appl. Cryst.* (2009). 42, 820-833

3 R E. Dinnebier, A. Leineweber, J.S.O. Evans, Rietveld Refinement: Practical Powder Diffraction Pattern Analysis using TOPAS, De Gruyter STEM, 347 pages, 2018, ISBN-13: 978-3110456219.

## Self-assembly and high anisotropy thermal expansion of crystal structures consisting of $\text{BO}_3$ triangular groups

Bubnova R.S.<sup>1</sup>, Filatov S.K.<sup>2</sup>

<sup>1</sup> Institute of the Silicate Chemistry RAS, Makarov Nab., 2, 199034 St. Petersburg, Russia

<sup>2</sup> Saint Petersburg State University, University Emb., 7/9, Saint Petersburg, 199034 Russia

Correspondence email: rimma\_bubnova@mail.ru

Nowadays, self-assembly of building blocks into ordered structures is of increased interest at atomic, meso-, nano-, micro-length scales. Self-assembly of building blocks is defined as the spontaneous organization of building blocks into ordered structures that ubiquitously occur in materials science and nature.

In present time borates represent one of the most investigated class of chemical compounds in the area of high-temperature chemistry and they can contribute to the development of this branch of science in the other classes of chemical compounds, for example, carbonates and nitrates. Specific features of borate crystal structures can be used for formulation of the following principles of formation process of borates and particular carbonates, nitrates etc. The practical parallel alignment of thermal vibration ellipsoids of  $T$  and  $O$  atoms in the crystalline phases evidences a collective character of the thermal atomic motion and motion of the rigid  $B-O$  groups, with the ensuing preferable orientation of the rigid  $T-O$  groups in many crystalline phases with  $\text{TO}_3$  groups. This allows formulating the following principles of self-organization of  $\text{TO}_3$  and rigid  $B-O$  groups, of preferably parallel mutual orientation in the crystal structures of these compounds:

Thermal motion is the inherent driving force of crystal substances formation. In borates, borates carbonates and nitrates such an organizing force is the strong anisotropy of thermal vibrations of atoms in the  $\text{TO}_3$  triangles ( $T = B, C, N$ ), flat triborate and other  $B-O$  rigid groups containing  $\text{TO}_3$  triangles and its rigid groups.

During the crystallization of borates, carbonates and nitrates from  $\text{TO}_3$  triangles, their rigid groups and  $M$  metals, the long axes of thermal ellipsoids of the  $T$  and  $O$  atoms tend to be realized for the parallel (or preferable) orientation by taking electrostatic interaction into account.

These principles of self-assembly allow us to better understand the process of formation of crystalline substance. The principles can be generalized for other flat atomic-molecular groups. In particular, the steric similarity of borates and organic compounds allows us to expect that the principles of high-temperature crystal chemistry, and self-assembly in borates will motivate the development of the high-temperature structural chemistry for some groups of organic compounds.

The examples of the self-organization of atoms,  $\text{TO}_3$  triangles ( $T = B, C, N$ ) and rigid  $B-O$  groups are given in [1, refs therein].

The study was funded by the Russian Foundation for Basic Research, project number 18-29-12106.

1. Bubnova R.S., Filatov S.K. Self-assembly and high anisotropy thermal expansion of compounds consisting of  $\text{TO}_3$  triangular radicals. *Struct. Chem.* 2016, 27, 1647–1662. DOI 10.1007/s11224-016-0807-9

## Low-temperature X-ray diffraction of biologically active substances

Knyazev A.V.<sup>1</sup>, Shipilova A.S.<sup>1</sup>, Knyazeva S.S.<sup>1</sup>, Gusarova E.V.<sup>1</sup>, Amosov A.A.<sup>1</sup>, Kusutkina A.M.<sup>1</sup>

<sup>1</sup> Lobachevsky State University of Nizhni Nogrrod, 603950, Gagarin av. 23, Nizhni Nogrrod, Russia.

Amino acids, hormones, vitamins and proteins - one of the most important representatives of biologically active substances. However, for most compounds there is no information on their behavior in a wide temperature range, polymorphism, and thermophysical parameters. We conducted a study of a significant amount of biologically active substances over the past seven years. The most used methods are low-temperature X-ray diffraction, vacuum adiabatic calorimetry, and differential scanning calorimetry. Recently, we have actively begun to use X-ray diffraction analysis for a detailed understanding of structural rearrangements in polymorphic transitions.

We carry out systematic X-ray studies in the temperature range 100-350 K in increments of 25 K. This is the most typical temperature range, but in the case of stable compounds the temperature range can be extended, and in the presence of phase transitions the step can be reduced. X-ray studies allowed us to calculate the coefficients of thermal expansion in a wide temperature range. Thermal expansion coefficient is the quantitative characteristic of thermal expansion. Value of the thermal expansion coefficient in given direction corresponds to length of radius-vector, which is traced from origin of coordinates to edge of figure of expansion. We have built figures of thermal expansion for more than 30 biologically active substances. Almost all the compounds studied have a pronounced anisotropy of thermal expansion. This behavior of the structure is in good agreement with the direction of intermolecular interactions and hydrogen bonds.

The authors are grateful to the Ministry of Science and Higher Education of the Russian Federation for financial support through grant 0729-2020-0039.

1. Knyazev A.V., Ishmayana S., Soedjanaatmadja U.M.S., Lelet M.I., Shipilova A.S., Knyazeva S.S., Amosov A.A., Shushunov A.N. Comprehensive thermodynamic and structural study of hevein. *Journal of Chemical Thermodynamics*. 2019. V.131. P. 168-174.

2. Knyazev A.V., Emel'yanenko V.N., Smirnova N.N., Shipilova A.S., Zaitsau D.H., Knyazeva S.S., Gulenova M.V. Thermodynamic investigation of L-carnitine. *Journal of Chemical Thermodynamics*. 2019. V.131. P.495-502.

3. Knyazev A.V., Emel'yanenko V.N., Shipilova A.S., Zaitsau D.H., Lelet M.I., Knyazeva S.S., Gusarova E.V., Varfolomeev M.A. Thermodynamic properties of myo-inositol. *Journal of Chemical Thermodynamics*. 2018. V. 116. P. 76-84.

## Modern laboratory HTXRD for investigation of structure evolution with temperature or during phase transformations

Krzhizhanovskaya M.G.

Department of Crystallography, Saint-Petersburg State University 199034, University Emb. 7/9, St.Petersburg, Russia.

\*Correspondence email: mariya.krzhizhanovskaya@spbu.ru

Nowadays high-temperature X-ray diffraction (HTXRD) studies are not uncommon. Many research labs are equipped with modern high-end XRD technique meanwhile others prefer “mega-science” facilities. Recent studies of complex and/or unusual thermal transformations by laboratory XRD under non ambient condition are reported for a number of oxygen compounds with the crystal structures based on oxygen tetrahedra or octahedra.

Among tetrahedral crystal structures new data on phase transition of natural REE borosilicates, stillwellite and tazhikite are presented. The temperature region of highly anisotropic thermal behavior for stillwellite and even negative thermal expansion for tazhikite were revealed. Both anomalies of thermal behavior correspond presumably to the regions of structure reconstruction before phase transition. A special attention is paid to the phase transitions with lowering symmetry on heating. Two cases of this type transformation are presented for  $\text{KBSi}_2\text{O}_6$  [1] and  $\text{Ca}_2\text{B}_2\text{SiO}_7$  [2].

Complex consequences of high-temperature phase transitions of octahedrally based structures are described using the example of  $\text{BiRO}_4$  ( $\text{R} = \text{Nb}, \text{Ta}$ ) [3, 4]. The strong anisotropy of triclinic  $\text{BiTaO}_4$  structure, manifested by a radical change in the direction of the thermal expansion tensor, was studied by Rietveld method at elevated temperatures [5].

The possibilities, advantages and disadvantages of laboratory HTXRD are discussed.

The authors acknowledge the Resource Center of X-ray diffraction Studies, Center for Optical and Laser Materials Research and “Geomodel” Resource Centre of Saint Petersburg State University for instrumental and computational resources. This work was partially supported by the Russian Foundation for Basic Research (18-29-12106).

1. Krzhizhanovskaya M.G., Bubnova R.S., Derkacheva E.S., Depmeier W., Filatov S.K. Thermally induced reversible phase transformations of boroleucite,  $\text{KBSi}_2\text{O}_6$ . *Eur. J. Mineral.* 2016, 28, 15-21.

2. Krzhizhanovskaya M.G., Gorelova L.A., Bubnova R.S., Pekov I.V., Krivovichev S. V. High-temperature crystal chemistry of layered calcium borosilicates:  $\text{CaBSiO}_4(\text{OH})$  (datolite),  $\text{Ca}_4\text{B}_5\text{Si}_3\text{O}_{15}(\text{OH})_5$  (‘bakerite’) and  $\text{Ca}_2\text{B}_2\text{SiO}_7$  (synthetic analogue of okayamalite). *Phys. Chem. Mineral.* 2018, 45, 463-473.

3. Zhuk N.A., Krzhizhanovskaya M.G., Belyy V.A., Makeev B.A. High-temperature crystal chemistry of  $\alpha$ -,  $\beta$ -, and  $\gamma$ - $\text{BiNbO}_4$  polymorphs. *Inorg. Chem.* 2019. 58. 1518-1526.

4. Zhuk N.A., Krzhizhanovskaya M.G., Belyy V.A., Sekushin N.A., Chichineva A.I. The bismuth orthotantalate with high anisotropic thermal expansion. *Scripta Mater.* 2019. 173. 6-10.

5. Zhuk N.A., Krzhizhanovskaya M.G., Belyy V.A., Kharton V.V., Chichineva A.I. Phase Transformations and Thermal Expansion of  $\alpha$ - and  $\beta$ - $\text{BiTaO}_4$  and the High-Temperature Modification  $\gamma$ - $\text{BiTaO}_4$ . *Chem. Mater.* 2020. 32. 13. 5493–5501.

## **Analysis of diffraction patterns of nanostructured powders.**

Tsybulya S.V. <sup>1,2</sup>

<sup>1</sup> Federal Research Center Boreskov Institute of Catalysis, 630090, Lavrentieva pr. 5,  
Novosibirsk, Russia

<sup>2</sup> Novosibirsk National Research State University, 630090, Pirogova str. 1, Novosibirsk, Russia  
Correspondence email: tsybulya@catalysis.ru

Nanostructured materials are specific objects of study for X-ray structural analysis due to the presence of diffraction effects associated with the size, shape, and means of joining primary nanoparticles with each other. Not only the broadening of diffraction peaks, but also their shift or complete disappearance can be a consequence of the size factor. During the growth of crystallites, stacking faults or layer displacement faults often occur. In the case of a large concentration of planar defects and their ordering the diffuse scattering effects arise in both the neighborhood of the Bragg maxima and the regions outside coherent scattering. The nanostructures of coherent type also characterize their diffraction features. Additional factors, such as dislocations and related microstrains of the crystal structure, complicate the diffraction pattern and make it difficult to correctly interpret it.

Various examples of the influence of the real structure of polycrystalline samples on their diffraction patterns will be given in the report. Several methods of analysis, including modeling of diffraction patterns based on models of various types of nanostructures, will also be presented. The method for calculating of diffraction patterns using the Debye formula is currently the most promising and widely used for the analysis of diffraction patterns from powder nanomaterials [1].

1. Yatsenko D., Tsybulya S. DIANNA (Diffraction Analysis of Nanopowders) – A Software for Structural Analysis of Nanosized Powders. *Zeitschrift für Kristallographie - Crystalline Materials*. 2018. V.233. N1. P.61-66.

# The origin of the first order structural phase transition for PrBaMn<sub>2</sub>O<sub>6</sub> double manganite

Titova S.G., Sterkhov E.V., Ryltsev R.E.

Institute of Metallurgy of Ural Branch of Russian Academy of Sciences, 620016, Amundsen St. 101, Ekaterinburg, Russia.

\*Correspondence email: sgitova@mail.ru

Double manganites  $RBaMn_2O_6$  ( $R$  – rare earth element) have the crystal structure which can be represented as alternating of cubic perovskite elementary cells  $RMnO_3$  and  $BaMnO_3$  along  $c$ -direction. Due to difference in size of  $R$  and Ba atoms  $a$  slightly bigger than  $c/2$ , also other structure distortions may appear. Double manganites with  $R = Nd, Pr$  demonstrate a number of magnetic and structural phase transitions close to room temperature being perspective magnetocaloric and magnetoresistive materials, the temperature of magnetic phase transitions drop rapidly when the material becomes disordered  $(R,Ba)MnO_3$ .

Earlier we have studied magnetic and structural phase transitions in solid solutions of double manganites  $Nd_{1-x}Pr_xBaMn_2O_6$  by magnetometry and X-ray powder diffraction [1]. It has been shown that the structural phase transition is not related neither to magnetic nor to metal-insulator phase transition (Fig. 1).

We perform LDA+DMFT calculations for two unit cells, using the structure data obtained experimentally at temperatures 215 K and 185 K, which are slightly above and slightly below the structural transition temperature  $T_{str} = 200$  K, respectively. Both these temperatures are far below the temperature of metal-insulator phase transition  $T_{MI} \sim 270$  K. The structural transition leads to the increase in the distortion of Mn-O octahedra.

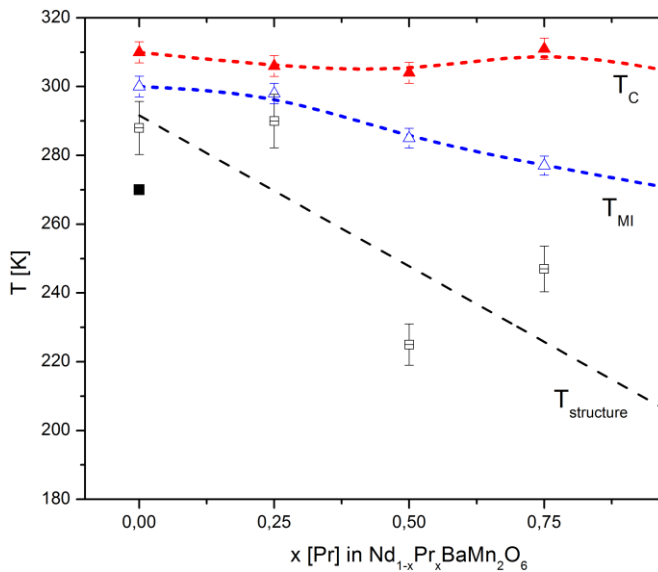


Fig. 1. Temperatures of ferromagnetic order  $T_c$ , metal-insulator phase transition  $T_{MI}$  and structure phase transition  $T_{str}$  for  $Nd_{1-x}Pr_xBaMn_2O_6$  solid solutions. The data from [1].

In general, the results of LDA+DMFT calculations suggest that structural transition at  $T_{str}$  in  $PrBaMn_2O_6$  compound, and so, in  $Nd_{1-x}Pr_xBaMn_2O_6$  solid solutions, are caused by partial orbital ordering of  $e_g$  states of Mn.

The work is supported by RFBR, project No 19-29-12013.

1. Titova S.G., Sterkhov E.V., Uporov S.A. Crystal structure and Magnetic Properties of A-Site Substituted  $Nd_{1-x}Pr_xBaMn_2O_6$  Double Manganite. Journal of Superconductivity and Novel Magnetism. 2020. Doi: 10.1007/s10948-020-05445-x.



## Self-organization of the chalcogen sublattice in a solid solution $\text{Ti}(\text{S}_{1-x}\text{Se}_x)_2$

Titov A.N.<sup>1,2</sup>, Shkvarin A.S.<sup>2</sup>, Merentsov A.I.<sup>1</sup>, Avila J.<sup>3</sup>, Asensio M.<sup>3</sup>, Bushkova O.V.<sup>4</sup>, Sala A.<sup>5</sup>,  
Titov A.A.<sup>2</sup>, Kazantseva N.V.<sup>2</sup>, Postnikov M.S.<sup>2</sup>, Yarmoshenko Yu.M.<sup>2</sup>

<sup>1</sup>Ural Federal University, Condensed Matter Dept. 620026 Kuybishev str. 48a, Yekaterinburg,  
Russia

<sup>2</sup>M.N.Miheev Institute of Metal Physics UrB RAS, 620108 S.Kovalevskaya str. 18,  
Yekaterinburg, Russia

<sup>3</sup>Synchrotron SOLEIL, ANTARES beamline, L'Orme des Merisiers Saint-Aubin BP 48 91192  
Gif-sur-Yvette Cedex, France

<sup>4</sup>Institute of Solid State Chemistry UrB RAS, 620990, Pervomaiskaya str. 91 Yekaterinburg,  
Russia

<sup>5</sup>Sincrotrone ELETTRA, BUCH beamline, 34149 Bazovizza, Trieste S.C.p.A., Italy

\*Correspondence email: antitov@mail.ru

The layered transition metal dichalcogenides form an extensive group of isostructural materials within which it is natural to expect the possibility of the formation of solid solutions. The most studied system of solid solutions is  $\text{TiS}_2$  -  $\text{TiSe}_2$ . This system is traditionally treated as an example of a uniform substitution inside the chalcogen sublattice. Our careful analysis of the  $\text{Ti}(\text{S}_{1-x}\text{Se}_x)_2$  system showed that there is a transition from "true" solid solution in the range of  $0 < x < 0.25$  and  $0.75 < x < 1$  to the formation region with nano- heterogeneity in the chalcogen sublattice.

The experimental study included a set of methods, such as electrochemical research, HREM and STM examination, and a set of spectral techniques: ResPES, ARPES, including those with resonant  $\text{Ti}2p$ - $3d$  and  $\text{S}2p$ - $3d$  excitation. The sum of the experimental results made it possible to conclude that the nature of nano-inhomogeneities is associated with the formation of Janus layers S-Ti-Se. The chirality of the Janus layers makes it possible to observe boundaries between homogeneous regions as stacking faults. The characteristic size of the homogeneous region is 100 Å. The formation of Janus layers should have a strong effect on the structure and properties of intercalate derivatives of solid solutions of transition metal dichalcogenides.

## **Fumarolic sulfate minerals: new data and possible applications**

Siidra O.I.

Dept. Crystallography, Saint-Petersburg State University, University emb. 7/9, St.Petersburg,  
199034, Russia

\*Correspondence email: siidra@mail.ru

Minerals with sulfate anions are one of the most diverse classes. More than 400 minerals containing sulfate anion are known to date. Most of known anhydrous sulfates have relatively simple chemical composition and structural architecture. In contrast, hydrated sulfate minerals have more complex compositions and structures. Most of the anhydrous sulfates are highly soluble compounds and unstable in humid atmosphere, namely, sulfates of alkali and alkaline earth metals. Under terrestrial conditions, hydrated sulfate minerals are common in various geological environments. Whereas the anhydrous sulfate minerals of alkali, alkaline earth and transition metals form almost exclusively in active fumaroles.

The fumaroles of Tolbachik volcano are a unique mineralogical locality with a large number of endemic mineral species. The variety of sulfate minerals observed in Tolbachik fumaroles is impressive. Since 2014, we have discovered 11 new mineral species with sulfate anions of fumarolic origin. Many of the fumarolic minerals demonstrate unique structure types with unprecedented and complex architectures and have no synthetic analogues. Several examples of the recently obtained synthetic sulfate materials inspired by Nature will be discussed.

This work was financially supported by the Russian Science Foundation through the grant 16-17-10085.

## Phosphate-silicate epitaxial heterostructure: crystal chemistry and mechanism of formation

Yakubovich O.V.

M.V. Lomonosov Moscow State University, 119191, Leninskie Gory, 1, Moscow, Russia.

\*Correspondence email: yakubol@geol.msu.ru

A novel phase of phosphate-silicate composition was obtained under soft hydrothermal conditions (so-called “chemie douce”). The crystal structure of  $K(Al_{1.5}Zn_{0.5})(P_{1.5}Si_{0.5})O_8$  is a three-dimensional network of two types of tetrahedra, statistically populated by two different atoms (Yakubovich *et al.*, 2020). In the first case, these are Al and Zn metal atoms, in the second - P atoms (non-metal, typical acid-forming agent) and Si (metalloid). A mixed type anionic framework built from sharing vertices alternating  $(Al,Zn)O_4$  and  $(P,Si)O_4$  tetrahedra, is stabilized by large  $K^+$  in the cavities. In the same structure type minerals celsian,  $BaAl_2Si_2O_8$  (Griffen & Ribbe, 1976) and filatovite,  $K(Al,Zn)_2(As,Si)_2O_4$  (Filatov *et al.*, 2004) crystallize, as well as a large group of phosphates with first row transition metals and Al (Yakubovich *et al.*, 2019). The structural feature of the isotopic natural and synthetic compounds of this family is the close topology of their cationic substructures to that of feldspars with the characteristic design of “crosslinked Jacob’s ladder” (Taylor, 1933).

A study of the sample using a scanning electron microscope demonstrated an obvious separation of the crystals in two zones with sharply defined regions of white and gray colours. A microprobe analysis of polished crystals of  $K(Al,Zn)_2(P,Si)_2O_4$  revealed a clear correlation between the colour of the studied areas and their chemical composition. Thus, P and Zn atoms on one hand and Si atoms on the other hand occur distributed between sectors with different colour. The average chemical composition of the light part of the sample was found to be “phosphate”, while the averaged chemical composition of the dark part is essentially “silicate”; their idealized formulae are  $KZnAlP_2O_8$  and  $KAlSi_3O_8$ .

In accordance with experimental data and detailed crystal chemical analysis we came to the conclusion that composite  $K(Al,Zn)_2(P,Si)_2O_4$  crystals present the product of an epitaxial intergrowth of the silicate  $KAlSi[SiO_4]_2$  and phosphate  $KAlZn[PO_4]_2$  phases with identical topology of their cationic substructures and close similar crystal structures (that of minerals orthoclase and celsian, accordingly). In our opinion, the two-phase crystal studied using X-ray diffraction was the assembly of phosphate and silicate “coherent intergrowth” with epitaxial “heterostructure”, which could be described in the framework of a single diffraction pattern due to phase matching of scattered waves.

The proposed scenario is supported by rare cases of isomorphic distribution of P and Si atoms in oxygen tetrahedra in crystal structures of mineral and synthetic solids. Most often, if these elements together are part of one crystal, they occupy different structural positions.

The Russian Foundation for Basic Research (grant No. 18-29-12076) is acknowledged.

Griffen, D.T. & Ribbe, P.H. (1976). *Amer. Mineral.* 61, 414-418.

Filatov, S.K., Krivovichev, S.V., Burns, P.C. & Vergasova, L.P. (2004). *Eur. J. Mineral.* 16, 537-543.

Taylor, W.H. (1933). *Z. Kristallogr.* 85, 425-442.

Yakubovich, O., Kiriukhina, G., Volkov, A., Dimitrova, O. (2019). *Acta Cryst.* C75, 514-522.

Yakubovich, O., Kiriukhina, G., Shvanskaya, L., Volkov, A., Dimitrova, O. (2020). *Acta Cryst.* B76, <https://doi.org/10.1107/S2052520620005715>.

## Три критические точки на фазовых диаграммах солевых систем

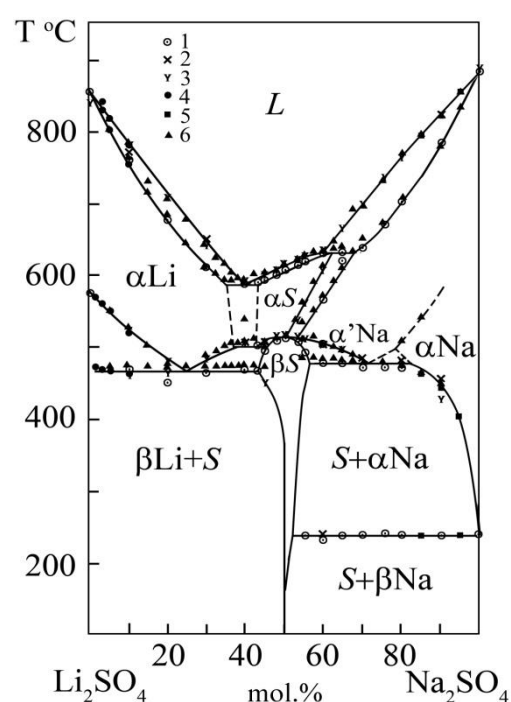
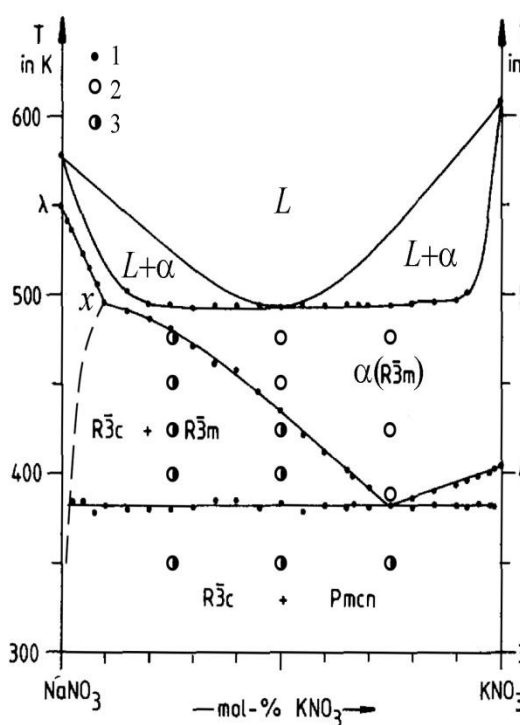
Федоров П.П.

Институт общей физики им. А.М. Прохорова РАН, Москва

\*Correspondence email: ppfedorov@yandex.ru

В теории фазовых переходов известны так называемые три критические точки, соответствующие превращению в бинарных системах фазовых переходов второго рода в фазовые переходы первого рода с порождением области расслаивания раствора [1]. Такая три критическая точка хорошо известна для системы из изотопов гелия [2], а также реализуется, например, в расплаве системы сера-дифенил.

Недавние исследования, проведенные с использованием высокотемпературного РФА, выявили наличие таких три критических точек в твердом состоянии в системе  $\text{NaNO}_3\text{-KNO}_3$  (точка X на рисунке) [3], и, по-видимому, в системе  $\text{Li}_2\text{SO}_4\text{-Na}_2\text{SO}_4$  [4].



1. Федоров П.П. Этюды по физико-химическому анализу. / Сб. статей М.: Наука, 2019. 191 с. ISBN 978-5-02-040205-8

2. Есельсон Б.Н., Григорьев В.Н., Иванцов В.Г. и др. Растворы квантовых жидкостей  $\text{He}^3\text{-He}^4$ . М.: Наука, 1973.

3. Fedorov P.P., Alexandrov A.A., Kuznetsov S.V., Voronov V.V. // J. Chem. Therm., in press.

4. Fedorov P.P., Proydakova V.Yu., Kuznetsov S.V., Voronov V.V., Pynenkov A.A., Nishchev K.N. // J. Amer. Ceram. Soc. 2020. DOI:10.1111/jace.16996.

## **2. High-pressure crystal chemistry**

## A study of the crystal and magnetic structures of $\text{Co}_3\text{O}_4$ at high pressure

Goloseva N.O.<sup>1</sup>, Kozlenko D.P.<sup>1</sup>, Belozeroва N.M.<sup>1</sup>, Nicheva D.<sup>2</sup>, Petkova T.<sup>2</sup>, Kichanov S.E.<sup>1</sup>, Lukin E.V.<sup>1</sup>, Avdeev G.<sup>3</sup>, Petkov P.<sup>4</sup> and Savenko B.N.<sup>1</sup>

<sup>1</sup> Frank Laboratory of Neutron Physics, JINR, 141980 Dubna Moscow Reg., Russia.

<sup>2</sup> Institute of Electrochemistry and Energy Systems, Bulgarian Academy of Sciences, 1113 Sofia, Bulgaria.

<sup>3</sup> Institute of Physical Chemistry, Bulgarian Academy of Sciences, 1113 Sofia, Bulgaria.

<sup>4</sup> University of Chemical Technology and Metallurgy, 1756 Sofia, Bulgaria.

\*Correspondence email: nmbelozeroва@jinr.ru

The internal structure of  $\text{Co}_3\text{O}_4$ , and its magnetic behavior has been the subject of many investigations. Because of the unique magnetic properties of  $\text{Co}_3\text{O}_4$  spinel, as well as their potential use in technological applications, the study of the magnetic structure of such compounds have been drawing much attention [1,2]. The magnetism of antiferromagnetic particles has attracted interest because it exhibits superparamagnetism and ferrimagnetism. Néel suggested that antiferromagnetic fine particles induce permanent magnetic moments, which he attributed to uncompensated spins in two sublattices [2].

As an important magnetic p-type semiconductor, the spinel cobalt oxide  $\text{Co}_3\text{O}_4$  is of special interest in a variety of technological applications and heterogeneous catalysts due to its surface redox reactivity properties [3]. The  $\text{Co}_3\text{O}_4$  as solid-state sensor is reported to be sensitive to the isobutene,  $\text{CH}_4$ ,  $\text{H}_2$ ,  $\text{NH}_3$ ,  $\text{CO}$  and  $\text{NO}_2$  gases at low temperature.  $\text{Co}_3\text{O}_4$  shows high-catalytic activity for the oxidation of  $\text{CO}$ ,  $\text{N}_2\text{O}$  catalytic decomposition.  $\text{Co}_3\text{O}_4$  nano-materials have been used as lithium batteries and gas sensors [3].

Further understanding of the properties of  $\text{Co}_3\text{O}_4$  bulk and its surface is crucial to potential development of the technological performance and efficiency of  $\text{Co}_3\text{O}_4$ -based materials applications.  $\text{Co}_3\text{O}_4$  is readily accessible and is the thermodynamically stable form of cobalt oxide under ambient room temperature and oxygen partial pressure. Although, it is well-known that at room temperature  $\text{Co}_3\text{O}_4$  has the spinel structure, there is still uncertainty about the distribution and valence of the ions in the tetrahedral and octahedral interstices of the oxygen lattice. Moreover, during a study of cobalt oxides it was found that the interionic distances in  $\text{Co}_3\text{O}_4$  were not well established. In addition, high-pressure effect on the crystal and magnetic structure of such compounds remain poorly explored.

Therefore, the crystal and magnetic structures of the  $\text{Co}_3\text{O}_4$  spinel oxide have been studied by means of neutron diffraction on the diffractometer DN-12 of pulse high-flux reactor IBR-2 (Dubna, Moscow region) at high pressures up to 8.7 GPa in the temperature range 5 – 300K. At ambient pressure, the long-range ordered antiferromagnetic (AFM) phase is formed below  $T_N = 33\text{K}$ . An additional magnetically disordered phase was also found at low temperatures. At high pressure, the Néel temperature of the AFM phase increases drastically in 1.5 times from 33K (0 GPa) to 51K (8.7 GPa) with a pressure coefficient  $dT_N/dP = 2.1 \text{ K/GPa}$ . The disordered phase is suppressed for  $P > 2\text{GPa}$ . The microscopic mechanisms of the observed phenomena are discussed in terms of competing magnetic interactions.

The work was supported by the Russian Foundation for Basic Research, grant RFBR 18-02-00359-a.

1. Cossee P. Structure and magnetic properties of  $\text{Co}_3\text{O}_4$  and  $\text{ZnCo}_2\text{O}_4$ . Recueil des Travaux Chimiques des Pays-Bas. 1956. V. 75(9). P. 1089-1096.

2. Ichiyangi Y., Kimishima Y., Yamada S. Magnetic study on  $\text{Co}_3\text{O}_4$  nanoparticles. Journal of Magnetism and Magnetic Materials. 2004. V. 272-276. P. e1245–e1246.

3. Xu, X. L., Chen, Z. H., Li, Y. et al. Bulk and surface properties of spinel  $\text{Co}_3\text{O}_4$  by density functional calculations. Surface Science. 2009. V. 603(4). P. 653-658.

## Silicate-like crystalchemistry for carbonates at high pressure. *Reality or not?*

Gavryushkin P.N.<sup>1,2</sup>, Sagatova D.<sup>1,2</sup>, Sagatov N.<sup>1,2</sup>, Banaev M.V.<sup>1,2</sup>

<sup>1</sup> Sobolev Institute of Geology and Mineralogy, Siberian Branch of Russian Academy of Sciences, prosp. acad. Koptuyuga 3, 630090 Novosibirsk, Russia

<sup>2</sup> Novosibirsk State University, Pirogova 2, Novosibirsk, 630090, Russia

\*Correspondence email: gavryushkin@igm.nsc.ru, p.gavryushkin@g.nsu.ru

Theoretical and experimental findings of the last decade have revolutionarily changed our vision of carbonates crystalchemistry at extreme pressures. The most radical structural change of carbonates at high pressure is the transition from  $sp^2$  to  $sp^3$  hybridisation of carbon, which results in transition from CO<sub>3</sub> triangle to CO<sub>4</sub> tetrahedron.

Since the first theoretical prediction of CaCO<sub>3</sub> with pyroxene-like chains of tetrahedrons the question about possibility of silicate-like crystalchemistry for carbonates was stated [1]. Due to more rigid character of C–O bond in comparison with Si–O, this scenario was considered as unlikely. However, the further experiments reveal the bunch of structures, which state this question again. There were synthesised orthocarbonates or island carbonates of four different types: 1) with isolated CO<sub>4</sub> tetrahedrons in Fe<sub>4</sub>C<sub>3</sub>O<sub>12</sub> [2], 2) with tetrads of CO<sub>4</sub> tetrahedrons linked by vertices in Fe<sub>2</sub>Fe<sub>2</sub>C<sub>4</sub>O<sub>13</sub> [2], 3) with threefold C<sub>3</sub>O<sub>9</sub> carbonate rings in MgCO<sub>3</sub>-II [3] and dolomite-IV [4]. Carbonates with chains of CO<sub>4</sub> tetrahedrons, which by analogy with silicates can be called in-carbonates, were predicted and synthesised for both CaCO<sub>3</sub> and MgCO<sub>3</sub> [5]. Fylosilicates with sheets of CO<sub>4</sub> tetrahedrons have not been revealed theoretically or experimentally. However, carbonate CaC<sub>2</sub>O<sub>5</sub> with framework of CO<sub>4</sub> tetrahedrons was predicted theoretically by Yao and Oganov [5]. Thus, all the structural types of silicates, except of phyllosilicates, is also typical for carbonates at high pressure.

However, whether the class of tetrahedrally coordinated carbonates is comparable in number of representatives with silicates, or the found structure are only some exotic cases. To answer this question, the systematic experimental investigation of different compositions at pressure 50-100 GPa and temperatures above 2000 K with the use of single crystal X-ray diffraction technique is necessary. Due to extreme laboriousness of such experiments and limited availability of experimental technique the systematic theoretical investigation is completely necessary first step on the way of solution of this complex problem.

In the present work we present the result of such an investigation with the use of evolutionary (USPEX) and random (AIRSS) crystal structure predictions techniques. With this techniques we performed the search of  $sp^3$ -hybridised structures in M<sub>2</sub>O-CO<sub>2</sub> and M'O-CO<sub>2</sub> systems, where M=Li, Na, K, M'=Mg, Ca, Sr, Ba. As the result the  $sp^3$  hybridised carbonates M<sub>2</sub>CO<sub>3</sub> are found for all the alkaline metals except of Li. As well as in the case of alkaline-earth carbonates, found  $sp^3$ -hybridised structures MCO<sub>3</sub> became stable above 100 GPa. The difference, is that in case of alkaline carbonates transition is not reconstructive. Steady deformation of CO<sub>3</sub> triangles produces chains of CO<sub>4</sub> tetrahedrons. M<sub>4</sub>CO<sub>4</sub> and M'<sub>2</sub>CO<sub>4</sub> orthocarbonates were found for all alkaline and alkaline-earth metals (M=Li, Na, K; M'=Mg, Sr, Ba). The structures became more energetically favourable then the mixture of corresponding carbonate and oxide at pressures above 15-30 GPa. This is sufficiently lower than the pressure of 75-100 GPa, at which  $sp^3$ -hybridised structures was observed before.

For the investigation of more complex compositions we used the so-called data-mining approach. The initial structures were constructed based on the analogy with silicates, phosphates and borates. The systematic search of appropriate structures in ICSD database was performed with TOPOSPro package.

As the result, new stable structures, which will be discussed on conference were, revealed.

The investigation was financially supported by the project of RFBR 20-03-00774.

1. Oganov, A. R., Glass, C. W., and Ono, S. 2006. EPSL, 241(1-2). P. 95–103.
2. Cerantola, V., Bykova, E., Kuppenko, I., et al. Stability of iron-bearing carbonates in the deep earth's interior. 2017. Nature Communications. 8. P. 15960.
3. Chariton, S., Bykov, M., Bykova, E., et al. 2020 Act. Cryst. E. 76(5). P. 715–719.
4. Merlini, M., Cerantola, V., Gatta, et al.. Dolomite-I. 2017. P.1763-1766.
5. Yao, X., Xie, C., Dong, X., et al. Novel high-pressure calcium carbonates. 2018. Phys. Review B, 98(1):014108.

## High-temperature structural changes of carbonates

Gavryushkin P.N.<sup>1,2</sup>, Banaev M.V.<sup>1,2</sup>, Sagatova D.<sup>1,2</sup>, Sagatov N.<sup>1,2</sup>

<sup>1</sup> Sobolev Institute of Geology and Mineralogy, Siberian Branch of Russian Academy of Sciences, prosp. acad. Koptyuga 3, 630090 Novosibirsk, Russia

<sup>2</sup> Novosibirsk State University, Pirogova 2, Novosibirsk, 630090, Russia

\*Correspondence email: gavryushkin@igm.nsc.ru, p.gavryushkin@g.nsu.ru

In the present work with the use of *ab initio* molecular dynamic (MD) simulation, we investigate the rotation disordering of CO<sub>3</sub> groups in crystal structures of calcite-like (MgCO<sub>3</sub>, CaCO<sub>3</sub>, FeCO<sub>3</sub>) and aragonite-like (CaCO<sub>3</sub>, SrCO<sub>3</sub>, BaCO<sub>3</sub>) carbonates. Up to now, this poorly investigated phenomena occurs at pre-melting or pre-decomposition temperatures, is known only for calcite. At 1000 K, the CO<sub>3</sub> triangles start to flip 30°, and on further heating start to undulate in umbrella-like manner around threefold axis [1]. As this transition takes place at a temperature sufficiently higher than the temperature of calcite decomposition the dense CO<sub>2</sub> atmosphere of nearly 0.4 Mpa is necessary. Due to the experimental difficulties in permanence of such an experiments, around a century was necessary to completely elucidate this sort of disordering in calcite. Thus, the absence of findings of similar phenomena on other carbonates with calcite structure can be attributed to the lack of experimental data. The similar investigations of aragonite-like carbonates are absent at all. In the last case, the situation is complicated by the necessity to apply pressure, as at ambient pressure aragonite (CaCO<sub>3</sub>), strontianite (SrCO<sub>3</sub>), and witherite (BaCO<sub>3</sub>) transforms to calcite-like structures. This is still an open question whether dynamically disordered aragonite can be formed in subducting slab within transition zone or lower mantle. The same is true about high-pressure phase of alkaline-earth carbonates post-aragonite, which high-temperature structural changes have not been investigated at all. This was the motivation for us to determine the PT boundaries between normal and disordered phases for aragonite and post-aragonite phases of CaCO<sub>3</sub>, SrCO<sub>3</sub>, and BaCO<sub>3</sub> and analyse the possibility of their appearance in the Earth's interiors.

With MD simulations (VASP package) and evolutionary metadynamic calculations (USPEX package), we also predict the intermediate phases, realised during aragonite to calcite transformation. These are structures with different numbers of close packed (cp) Ca-layers. Their enthalpy is lower than that of aragonite but higher than that of calcite (Fig.1). For the structures with number of cp layers higher than three, the enthalpy per formula unit remains the same (Fig.1). Our transition electron microscopy (TEM) experiments confirm the formation of 8-layered polytype during mechanical grinding of aragonite, in consistence with theoretical predictions. The realisation of predicted hexagonal 2-layered structure (called *hexarag*) during aragonite heating is disputable. Performed high-temperature XRD experiment does not give any arguments for its formation.

Microstructure is one of the main factors, determining the temperatures and even mechanism of phase transition. The effect of microstructure on aragonite to calcite transformation has not been analysed before. In our work, we present the result of microstructural investigations with TEM of aragonite crystals

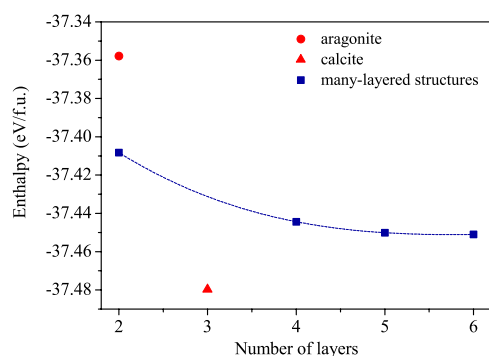


Fig.1. The dependency of enthalpy on number of cp layers (N) for CaCO<sub>3</sub>

from different localities and show their inherent twinning by {001}. With differential thermal analysis we show the dependence of transition temperature on the density of twinning, varying in the range of 50 °C. Untwinned aragonite transforms to calcite at lower temperatures, which means that twinning planes act as a barrier on the way of transformation of the 2-layered close-packed structure of aragonite to 3-layered of calcite. With MD simulations we also analyse the effect of twinning by {110} on high-temperature structural changes of aragonite.

The investigation was financially supported by the project of RFBR 18-35-20047.



## Сравнение кристаллических структур и сжимаемости гидратов натриевой и калиевой соли гуанина

Гайдамака А.А.<sup>1,2</sup>, Архипов С.Г.<sup>1,2</sup>, Захаров Б.А.<sup>1,2</sup>, Сереткин Ю.В.<sup>3,2</sup>, Болдырева Е.В.<sup>1,2</sup>

<sup>1</sup> ФИЦ «Институт катализа им. Г.К. Борескова СО РАН», Новосибирск, Россия

<sup>2</sup> Новосибирский государственный университет

<sup>3</sup> Институт геологии и минералогии им. В.С. Соболева, Новосибирск, Россия

\*Correspondence email: a.gaidamaka@g.nsu.ru

Биологические объекты и биомиметики интересны как с точки зрения фундаментальных исследований, так и для создания новых лекарств и материалов. Гуанин – азотистое основание, входящее в состав ДНК и РНК. Особую биологическую важность представляют соединения с фрагментами «гуанин – катион щелочного металла», (особенно с калием). Из-за низкой растворимости в большинстве растворителей, известно ограниченное количество соединений гуанина, отдельную проблему представляет получение монокристаллов.

Нами методами монокристаллической рентгеновской дифракции и КР-спектроскопии, в том числе при переменных температурах (от комнатной до 100 К) и высоких давлениях проведено сравнительное исследование монокристаллов гидратов натриевой и калиевой соли гуанина, вторая из которых получена нами впервые. Сопоставлены сами кристаллические структуры, анизотропия их сжатия, области фазовых переходов и характер структурных изменений в ходе этих переходов.

Работа выполнена в рамках государственного задания ИК СО РАН (проект АААА-А19-119020890025-3).

1. A.Gaydamaka *et al.*, CrystEngComm, 2019, **21**, 4484-92.

## High-pressure experiments and X-ray diffraction data reduction: the difference from ambient pressure studies and factors influencing data quality

Zakharov B.A.<sup>1,2</sup>

<sup>1</sup> Borekov Institute of Catalysis SB RAS, 630090, Lavrentiev Ave. 5, Novosibirsk, Russia.

<sup>2</sup> Novosibirsk State University, 630090, Pirogova Str. 2, Novosibirsk, Russia.

\*Correspondence email: b.zakharov@yahoo.com

High pressures can influence the structure of different materials leading to a number of interesting phenomena like phase transitions, changes in conductivity, amorphisation, metallisation *etc.* Pressures can also be used for chemical synthesis and often lead to formation of previously unknown solvates and clathrates. In order to understand all these phenomena one needs to know exact structure changes caused by high pressures. X-ray diffraction with diamond anvil cells (DACs) is widely used to determine crystal structures for most organic, inorganic and biological crystalline samples. The quality of diffraction data is critically important for obtaining reliable information on atomic coordinates and intermolecular distances. The recent improvements in high-pressure X-ray diffraction were related not only to technical aspects of diffraction experiment (new DAC designs, fast and sensitive detectors, brilliant X-ray sources), but also to development of a new software for sample centering, absorption correction, recognizing and excluding unwanted reflections that do not belong to the sample, data reduction, finding the orientation matrices for several crystallites in the same diamond anvil cell. The recent developments in instrumentation and software allowed even determination of electron charge density distribution for such a samples.

All types of high-pressure studies require rigorous experimental planning and special methods of X-ray diffraction data treatment since the crystal is not “free” but located in confined environment in hydrostatic liquid inside DAC with certain construction with limited opening windows for X-ray probe. A lot of questions can arise on planning the experiment: which pressure transmitting media to choose? how fast the pressure should be increased? Is not it better to perform all the experiments at synchrotron rather than at lab source if I have this opportunity? which factors should be taken into account on data collection and reduction? This list of issues is quite far from being complete. *The aim* of my contribution is to give a brief overview of the most interesting and useful generally arising questions and try to answer them. I would also like to highlight the importance of considering some “hidden” factors like choice of pressure transmitting media, pressure variation protocol and diffraction equipment while planning and performing the diffraction measurements to obtain the most reliable results of high-pressure experiment.

The work was supported by a grant from RFBR (19-29-12026 mk).

### **3. Properties of materials and nano materials over a wide range of temperature and pressure**

## ***In situ* behavior of titanium (III) oxide $\text{Ti}_2\text{O}_3$ structure at temperatures up to 1200 K**

Valeeva A.A.<sup>1</sup>, Rempel A.A.<sup>1,2</sup>

<sup>1</sup> Institute of Solid State Chemistry of the Ural Branch of the Russian Academy of Sciences, 620990, Pervomaiskaya Str. 91, Ekaterinburg, Russia.

<sup>2</sup> Institute of Metallurgy of the Ural Branch of the Russian Academy of Sciences, 620016, Amundsen Str. 101, Ekaterinburg, Russia

\*Correspondence email: anibla\_v@mail.ru

Titanium-oxygen (Ti-O) system is an important object from both fundamental and applied viewpoints since titania compounds, depending on nonstoichiometry, possess properties which show much promise for the application in metallurgy, nanoelectronics, data and energy storage, photocatalysis. The crystal structure, microstructure, morphology and the electronic structure in the Ti-O system strongly correlate with stoichiometry, which enables compounds with desired functional properties to be produced [1, 2]. The aim of this work is to study the thermal stability and chemical transitions in  $\text{Ti}_2\text{O}_3$  micro- and nanocrystals in the temperature interval from 300 to 1200 K using magnetic susceptibility method.

*In situ* studies of the thermal stability and transformations in titanium (III) oxide  $\text{Ti}_2\text{O}_3$  with corundum structure by using magnetic susceptibility method in the temperature range from 300 to 1200 K revealed that the crystal size had a large effect on the magnetic susceptibility value, structure and transformations in  $\text{Ti}_2\text{O}_3$ . Analysis of the experimental data showed that  $\text{Ti}_2\text{O}_3$  microcrystals and nanocrystals is weak paramagnets. In addition, the *in situ* temperature dependences of magnetic susceptibility showed that the crystal size greatly affects the value of magnetic susceptibility; the magnetic susceptibility value of nanocrystals is twice as small in absolute magnitude as that of microcrystals.

The structure of  $\text{Ti}_2\text{O}_3$  microcrystals is stable during long-term annealing in vacuum, according to the analysis of X-ray diffraction patterns, the crystal structure of  $\text{Ti}_2\text{O}_3$  microcrystals with corundum structure (sp. gr.  $R\bar{3}c$ ) remains trigonal, the intensity of diffraction reflections of  $\text{Ti}_2\text{O}_3$  phase increases in the X-ray diffraction patterns. Analysis of reflection intensity variation revealed that the structural-phase state, namely the degree of  $\text{Ti}_2\text{O}_3$  crystallinity, changed during long-term annealing in vacuum.

Vacuum annealing of  $\text{Ti}_2\text{O}_3$  nanocrystals in the temperature range from 300 to 1200 K demonstrated that the system was not stable. In the temperature region from 300 to 400 K, the structure of initial  $\text{Ti}_2\text{O}_3$  nanocrystal remains trigonal; annealing of  $\text{Ti}_2\text{O}_3$  nanocrystals at temperature above 400 K leads to phase transformations and, as a result, to magnetic susceptibility enhancement. X-ray diffraction analysis shows that after annealing to 673 K the powder contains additional phases of  $\text{Ti}_9\text{O}_{10}$  (sp. gr. *Immm*),  $\text{Ti}_9\text{O}_{17}$  sp. gr.  $\bar{1}$ ),  $\text{Ti}_2\text{O}_3$  phase (sp. gr.  $R\bar{3}c$ ). In the temperature interval of 673-873 K, an insignificant increase in the magnetic susceptibility value is observed. According to XRD data, upon annealing to 873 K the  $\text{Ti}_9\text{O}_{10}$  (sp. gr. *Immm*),  $\text{Ti}_2\text{O}_3$  (sp. gr.  $R\bar{3}c$ ) and  $\text{Ti}_4\text{O}_7$  (sp. gr.  $A\bar{1}$ ) phases are observed. When the temperature rises above 873 K up to 1200 K, stable oxide  $\text{Ti}_3\text{O}_5$  (sp. gr. *I2/c*) is formed. Thus, the experimental results show that the phase stability and phase transitions in  $\text{Ti}_2\text{O}_3$  are greatly affected above all by the crystal sizes.

The reported study was funded by RFBR according to the research project No. 19-03-00051a.

Andersson S., Collen B., Kuylenstierna U., Magneli A. Phase-analysis studies on the titanium-oxygen system. Acta Chem. Scand. 1957. Vol. 11. P. 1641-1652.

Valeeva A.A., Rempel S.V., Schroettner H., Rempel A.A. Influence of the degree of order and nonstoichiometry on the microstructure and microhardness of titanium monoxide. Inorg. Mater. 2017. V. 53. P. 1174-1179.

## Structure and phase composition of silicon nitride ceramics and powders plated with yttrium-aluminum garnet

Drozhilkin P.D.<sup>1</sup>, Boldin M.S.<sup>1</sup>, Alekseeva L.S.<sup>1</sup>, Andreev P.V.<sup>1,2</sup>, Karazanov K.O.<sup>1</sup>, Smetanina K.E.<sup>1</sup>, Balabanov S.S.<sup>2</sup>

<sup>1</sup>N.I. Lobachevsky State University of Nizhny Novgorod, Nizhny Novgorod

<sup>2</sup>Institute of Chemistry of High-Purity Substances RAS, Nizhny Novgorod

Correspondence e-mail: pddrozhilkin@yandex.ru

One of the modern methods of creating refractory ceramic nanocomposites based on Si<sub>3</sub>N<sub>4</sub> is application of ultra-thin coatings of oxides on silicon nitride powder particles of various dispersity and their subsequent compaction by spark plasma sintering (SPS) method.

The development of the plating technology of nanopowders with ultra-thin layers of oxides requires optimization of deposition modes, including the solution of the Si<sub>3</sub>N<sub>4</sub> pre-agglomeration problem.

Powder compositions were obtained in three ways: (1) Pechini method (with the addition of citric acid) and (2) deposition in gelatin matrix, and also (3) the vacuum dispersal method. The intermediate products obtained from the syntheses were annealed in stages for 2–8 hours at 300, 500, 800, 1000°C with grinding in the agate mortar between stages.

Powder samples annealed to 1000°C and their intermediates, which annealed for 3 hours at 300°C, were compacted by spark plasma sintering method.

Sintering was carried out on the “Dr. Sinter model SPS-625” (SPS Syntex, Japan) in vacuum in a graphite mold with an inner diameter of 12 mm. The heating speed was 50°C/min, pressure was 70 MPa, the sintering temperature varied between 1200–1680°C.

Control of phase composition of powders and ceramics was carried out on X-ray diffractometer “Shimadzu XRD-7000” (CuK $\alpha$ ,  $\lambda=1.54$  Å). The microstructure of the powders and ceramics was studied by scanning electron microscopy technique on the JEOL JSM-6490.

The reported study was funded by RFBR, project number №19-33-60084.

## Полиморфные превращения и кристаллохимия наностержней $\text{La}_{0.15}\text{Y}_{0.85}\text{PO}_4$

Еникеева М.О.<sup>1,2</sup>, Проскурина О.В.<sup>1,2</sup>

<sup>1</sup> Физико-технический институт им. А.Ф. Иоффе РАН, 194021, Политехническая ул, 26, Санкт-Петербург, Россия.

<sup>2</sup> Санкт-Петербургский государственный технологический институт (технический университет), 190013, Московский пр-т, 26, Санкт-Петербург, Россия.

\*Correspondence email: odin2tri45678@gmail.com

Редкоземельные фосфаты можно отнести к трем различным природным минералам: монацит, рабдофан и ксенотим [1]. Материалы на их основе применяются в качестве люминофоров, термобарьерных покрытий, керамики. При нагревании структура рабдофана теряет воду, переходя в метастабильное состояние с последующим необратимым структурным превращением в монацит или ксенотим в зависимости от исходного катиона [2]. Цель работы – получение с использованием гидротермально-микроволновой обработки [3] наноразмерного  $\text{La}_{0.15}\text{Y}_{0.85}\text{PO}_4$ , изучение его кристаллической структуры и термического поведения.

Синтез наночастиц производили методом соосаждения из водных растворов  $\text{La}(\text{NO}_3)_3 \cdot 6\text{H}_2\text{O}$ ,  $\text{Y}(\text{NO}_3)_3 \cdot 5\text{H}_2\text{O}$  и  $\text{NH}_4\text{H}_2\text{PO}_4$  при комнатной температуре и  $\text{pH}=1$ . Гидротермальная обработка (ГТО) с микроволновым нагревом осуществлялась в реакторе Monowave 400 (Anton Paar) при  $T=180^\circ\text{C}$  и времени изотермической выдержки  $\tau=120$  минут, после чего образец промывался дистиллированной водой, высушивался и растирался в ступке.

Съемка дифрактограмм осуществлялась на дифрактометре Shimadzu XRD7000, оснащенный термоприставкой Anton Paar НТК 1200 N, в диапазоне температур  $100 - 1000^\circ\text{C}$  с шагом  $100^\circ\text{C}$ . Поведение образца также изучали методом ДТА, ДСК и ТГ на приборе синхронного термического анализа NETZSCH 449 F3 Jupiter в платиновом тигле в атмосфере воздуха со скоростью нагрева  $10^\circ/\text{мин}$ .

По данным РФА осажденный ортофосфат РЗЭ до ГТО представляет собой рентгеноаморфный осадок. После ГТО или спекания на воздухе до  $800^\circ\text{C}$  осадок кристаллизуется в гексагональной сингонии, соответствующей минералу рабдофан. На ДТА кривой регистрируется эндотермический пик при  $772^\circ\text{C}$ , соответствующий кристаллизации монацита из анализа дифрактограмм спеченных порошков. Размер кристаллитов рабдофана после ГТО около 60 нм, дальнейшее повышение температуры приводит к частичной трансформации в моноклинную и тетрагональную структуры. Для спеченного при  $T=1000^\circ\text{C}$  порошка метод Ритвельда показал содержание моноклинной и тетрагональной структуры – 40% и 60%, соответственно. На дифрактограммах можно отметить приоритетное направление  $h00$  роста частиц. Морфология частиц рабдофана, исследованная на СЭМ, – шестиугольные призмы, которые трансформируются с ростом температуры в иглоподобные частицы монацита. По

Из твердого раствора на основе монацита могут быть получены двухфазные керамические материалы. Рабдофан, содержащий 85%  $\text{Y}^{3+}$  (от общего числа катионов) является общим прекурсором для керамических ортофосфатных материалов. Терморентгенографией и ДСК показано, что соединение  $\text{La}_{0.15}\text{Y}_{0.85}\text{PO}_4$  кристаллизуется в монацит-ксенотим при  $T \geq 800^\circ\text{C}$ . Керамические материалы на основе монацита-ксенотима обладают высокой температурой плавления, ударопрочностью, работоспособны при длительных температурных воздействиях.

Работа выполнена при поддержке гранта РФФИ № 18-29-12119.

1. Ondrejka, M., Vačík, P., Sobocký, T., Uher, P., Škoda, R., Mikuš, T. et al. Minerals of the rhabdophane group and the alunite supergroup in microgranite: products of low-temperature alteration in a highly acidic environment from the Velence Mountains, Hungary. *Mineralogical Magazine*. 2018. V. 82(6). P. 1–46.

2. Shelyug A., Mesbah A. Szenknect S., Clavier N., Dacheux, N., Navrotsky A. Thermodynamics and Stability of Rhabdophanes, Hydrated Rare Earth Phosphates  $\text{REPO}_4 \cdot n\text{H}_2\text{O}$ . *Frontiers in Chemistry*. 2018. V.6. P. 604.

3. Еникеева М.О., Кенес К.М., Проскурина О.В., Данилович Д.П., Гусаров В.В. Влияние условий гидротермальной обработки на формирование ортофосфата лантана со структурой монацита // ЖПХ. 2020. Т.93. Вып. 4. С. 529–539.

## **Influence of conditions for synthesis of iron oxide nanoparticles on their structure and phase composition**

Kovalenko A.S.<sup>1</sup>, Nikolaev A.M.<sup>1</sup>, Khamova T.V.<sup>1</sup>, Kopitsa G.P.<sup>1,2</sup>, Shilova O.A.<sup>1</sup>

<sup>1</sup> Grebenshchikov Institute of Silicate Chemistry, Russian Academy of Sciences, 199053, Makarov Emb. 2, St.Petersburg, Russia.

<sup>2</sup> Petersburg Institute of nuclear physic of National research centre "Kurchatov institute", 188300, MD Orlova grove 1, Gatchina, Leningrad region, Russia.

\*Correspondence email: anastasiya.bychk@mail.ru

In recent years, iron oxide nanoparticles are very popular materials in many fields of science, medicine, industry and agriculture, due to their unique properties such as biocompatibility, magnetic properties, and environmental safety [1]. Applications in a specific field of research require that nanoparticles have certain properties, structure, morphology, and phase composition. It is known that these characteristics are significantly influenced by the choice of the synthesis method, and, in addition, the conditions for its implementation. Currently, there are many works devoted to the study of the effect of synthesis conditions on certain characteristics of the obtained iron oxide nanoparticles separately (for example, only on the phase composition or shape), but there are still no works describing the complex study of the effect of synthesis conditions on various characteristics and properties of the obtained iron oxide nanoparticles.

Therefore, the aim of this work is to study the effects of conditions for the synthesis of iron oxide nanoparticles on their structure, morphology, phase composition and surface properties.

Iron oxide nanoparticles were obtained by co-precipitation from aqueous solutions of iron salts. During the synthesis process, such synthesis conditions as the synthesis time (17 and 32 min), the method for separating the sediment from the mother solution (filtration, decantation), the drying method (drying cabinet, rotary evaporator), the presence or absence of a surfactant (oleic acid) were changed. The phase composition, morphology, structure, and surface properties of synthesized iron oxide nanoparticles were studied using x-ray phase analysis, SAXS, scanning and transmission electron microscopy, low-temperature nitrogen adsorption, infrared spectroscopy and Raman spectroscopy.

The results of a comprehensive study showed that the conditions for the synthesis of iron oxide nanoparticles have a significant impact on the phase composition, structure, size and shape of the resulting iron oxide nanoparticles, as well as on their specific surface area, pore shape and size.

The study was funded by a grant from the Russian Science Foundation (Project No. 19-13-00442).

1. Cornell R.M., Schwertmann U. The Iron Oxides. 2003, 694. Wiley-VCH Verlag GmbH & Co. KGaA.

## Proton-conducting composite materials based on superprotonic crystals

Komornikov V.A., Grebenev V.V., Timakov I.S., Makarova I.P., Selezneva E.V., Zainullin O.B.

Shubnikov Institute of Crystallography, Federal Scientific Research Centre “Crystallography and Photonics,” Russian Academy of Sciences, 119333, Leninskiy, 59, Moscow, Russia.

Perspective materials for the development of hydrogen fuel cells (hydrogen energy) are compounds of the family with the general formula  $M_mH_n(XO_4)_{(m+n)/2} \cdot yH_2O$  ( $M = K, Rb, Cs, NH_4$ ;  $XO_4 = SO_4, SeO_4, HPO_4$ ). Unique properties of crystals of this family (called superprotonics), is the abnormally high proton conductivity at a relatively low temperature, which manifests itself as a result of a phase transition. Moreover, the superprotonic conductivity in them is associated only with the structural features of these compounds and does not depend on humidity, defects in the real structure, or the influence of dopants.

One of the most promising crystals in this family is superprotonic crystals  $Cs_4(HSO_4)_3(H_2PO_4)$  and  $Cs_6H(HSO_4)_3(H_2PO_4)_4$ . These compounds exhibit increased proton conductivity at temperatures of 414 and 390 K, respectively. Moreover, a non-trivial technical problem is the use of these superprotonic crystals in the form of a thin membrane suitable for a hydrogen-air fuel cell. The solution to this problem was achieved by using special techniques for the preparative synthesis of composite materials. Two groups of composite materials were synthesized using inorganic and organosilicon components.

With an inorganic reinforcing component over a wide range of compositions, composite materials  $xCs_4(HSO_4)_3(H_2PO_4) + (1-x)AlPO_4$  and  $xCs_6H(HSO_4)_3(H_2PO_4)_4 + (1-x)AlPO_4$  were obtained. A feature of the approach used in the synthesis is the formation of a proton-conducting phase and a reinforcing polyaluminophosphate additive in one volume. The application of this technique at the macro level allows one to obtain the mentioned materials in the form of relatively thin transparent films with a given geometry and adjustable mechanical properties (strength, elasticity, transparency, etc.).

As the organosilicon reinforcing component, we used a two-component silicone compound for the synthesis of composite materials  $xCs_4(HSO_4)_3(H_2PO_4) + (1-x)[R_2SiO]_n$  and  $xCs_6H(HSO_4)_3(H_2PO_4)_4 + (1-x)[R_2SiO]_n$  in a wide range of compositions.

A comparative study of the main properties of the obtained materials was carried out by methods of x-ray phase analysis, DSC/TGA, impedance spectroscopy and scanning electron microscopy.

The reported study was funded by RFBR according to the research project № 18-32-20050.

The experiments were performed using the equipment of the Shared Research Center of the Institute of Crystallography, Russian Academy of Sciences.



## **4. Magnetic phase transitions**

## Charge-ordering and magnetism of Mn<sub>2</sub>BO<sub>4</sub> oxyborate

Belskaya N.A.<sup>1</sup>, Kazak N.V.<sup>2</sup>, Knyazev Yu.V.<sup>2</sup>, Platunov M.S.<sup>2</sup>, Moshkina E.M.<sup>2</sup>,  
Bezmaternykh L.N.<sup>2</sup>, Solovyov L.A.<sup>3</sup>, Gavrilkin S.Yu.<sup>4</sup>, Veligzhanin A.A.<sup>5</sup>, Ovchinnikov S.G.<sup>2,6</sup>

<sup>1</sup>Reshetnev Siberian State University of Science and Technology, 660037, Krasnoyarsky  
Rabochy Ave. 31, Krasnoyarsk, Russia

<sup>2</sup>Kirensky Institute of Physics, FRC KSC SB RAS, 660036, Akademgorodok 50/38, Krasnoyarsk,  
Russia

<sup>3</sup>Institute of Chemistry and Chemical Technology, FRC KSC SB RAS, 660036, Akademgorodok  
50/24, Krasnoyarsk, Russia

<sup>4</sup>P.N. Lebedev Physical Institute of RAS, 119991 Moscow, Russia

<sup>5</sup>National Research Centre “Kurchatov Institute”, 123182, Moscow, Russia

<sup>6</sup>Siberian Federal University, 660041, Svobodny pr. 79, Krasnoyarsk, Russia

Oxyborates with general formula  $M^{2+}M^{3+}BO_4$ , which are isostructural to the mineral “warwickite”, contain equal amounts of divalent and trivalent metal ions, and in a similar manner to magnetite Fe<sub>3</sub>O<sub>4</sub> [1] it might undergo a charge ordering (CO). Three known mixed-valence warwickites Mn<sub>2</sub>BO<sub>4</sub> [2], Fe<sub>2</sub>BO<sub>4</sub> [3] and V<sub>2</sub>BO<sub>4</sub> [4] demonstrate a temperature-induced CO transitions, which is accompanied by the orthorhombic → monoclinic symmetry lowering. The Fe<sub>2</sub>BO<sub>4</sub> shows a rich electronic phase diagram with commensurately and incommensurately modulated charge ordered states at  $T < T_{CO} = 340$  K and the valence fluctuating state above  $T_{CO}$ . The CO in iron warwickite is supposed to be driven by electrostatic repulsion between the charges (Wigner crystallization), while the CO in manganese warwickite Mn<sub>2</sub>BO<sub>4</sub> is associated with the orbital ordering in the presence of a  $x^2-y^2$  hole localized at Mn<sup>3+</sup>. The nature of CO in warwickites is the subject of hot discussions for two decades.

In this work we studied the long-range crystal structure, valence states and local structure around Mn atoms in Mn<sub>2</sub>BO<sub>4</sub> through the temperature dependent X-ray powder diffraction (XRPD), Mn K-edge X-ray absorption (XAFS) spectroscopy, and heat capacity (HC) measurements. The XRPD, XAS and HC measurements were carried out in temperature ranges 298-973 K, 9-500 K, and 2-773 K, respectively.

The monoclinic symmetry (P21/n) was found to persist up to highest temperature measured. The *a*-lattice parameter shows negative thermal expansion in the T range 300-500 K. The BVS calculations were revealed large valence difference between two manganese sites that strongly supports the presence of CO up to high temperatures. The above estimations suggest that the Mn1 site is filled exclusively by Mn<sup>3+</sup> ions, whereas the Mn2 site is occupied by Mn<sup>2+</sup> ions. The pronounced temperature dependence of the Debye-Waller (DW) factor corresponding to the Mn-O coordination shell was found from the extended x-ray absorption fine structure (EXAFS) analysis and was associated with variations in the local distortions in MnO<sub>6</sub> octahedra and emergence of short-range magnetic correlations at low temperatures. Magnetization and heat capacity measurements establish the formation of an antiferromagnetic order at Neel temperature  $T_N = 26$  K. No any other anomalous were observed in the temperature dependence of HC, which could indicate structural phase transitions. In conclusion we discuss possible mechanisms of CO in Mn<sub>2</sub>BO<sub>4</sub> and compare it with the CO observed in Fe<sub>2</sub>BO<sub>4</sub>.

The reported study was funded by RFBR, project number 20-02-00559.

1. Verwey, E.J.W. Electronic conduction of magnetite (Fe<sub>3</sub>O<sub>4</sub>) and its transition point at low temperatures. Nature 144, 327–328 (1939), <https://doi.org/10.1038/144327b0>

2. N.V. Kazak, M.S. Platunov, Y.V. Knyazev, *et al.*, Uniaxial anisotropy and low-temperature anti-ferromagnetism of Mn<sub>2</sub>BO<sub>4</sub> single crystal, J. Magn. Magn Mater. 393, 316–324 (2015), <https://doi.org/10.1016/j.jmmm.2015.05.081>

3. J.P. Attfield, A.M.T. Bell, L.M. Rodriguez-Martinez, *et al.*, Electrostatically driven charge-ordering in Fe<sub>2</sub>OBO<sub>3</sub>, Nature 396, 655–658 (1998).

4. E.M. Carnicom, K. Górnicka, T. Klimczuk, R.J. Cava, The homometallic warwickite V<sub>2</sub>OBO<sub>3</sub>, J. Solid State Chem. 265, 319–325 (2018), <https://doi.org/10.1016/j.jssc.2018.06.021>

## Investigation of thermal behavior of Fe(II,III)-containing borates.

Biryukov Y.P.<sup>1</sup>, Zinnatullin A.L.<sup>2</sup>, Bubnova R.S.<sup>1\*</sup>, Vagizov F.G.<sup>2</sup>, Filatov S.K.<sup>3</sup>

<sup>1</sup> Institute of silicate chemistry of Russian Academy of Sciences, 199034, Makarova Emb. 2, St.Petersburg, Russia.

<sup>2</sup> Kazan Federal University, 420008, Kremlyovskaya Str., 18, Kazan, Russia.

<sup>3</sup> Institute of Earth Sciences, Dep. of Crystallography, Saint Petersburg State University, 199034, Universitetskaya Emb., 7/9, Saint Petersburg, Russia.

\*Correspondence email: rimma\_bubnova@mail.ru

Fe(II,III)-containing borates exhibit a number of useful properties such as magnetic, magnetoacoustics, resonance and other. However, there is a lack of high-temperature crystal chemical investigations of iron borates in general. There are a few works known devoted to such investigations (Shimomura *et al.*, 2007; Biryukov *et al.*, 2016; Biryukov *et al.*, 2018).

This work reports on the investigation of thermal behavior of Fe(II,III)-containing borates by *in situ* low- and high-temperature X-ray diffraction methods, Mössbauer spectroscopy and thermal analysis. A combination of the methods in the revealing of magnetic phase transitions, investigation of the Fe<sup>2+</sup> to Fe<sup>3+</sup> oxidation occur with an increase in temperature using data of these methods showed a good compatibility between each other. Thermal expansion of the borates is described from a viewpoint of crystal chemistry of compounds containing cation- and oxocentred polyhedra.

The following funding is acknowledged: Russian Foundation for Basic Research (grant No. 18-29-12106).

1. Shimomura S., Nakamura S., Ikeda N., Kaneko E., Kato K. & Kohne K. *Journal of Magnetism and Magnetic Materials*. 2007. V. 310. P. 793–795.

2. Biryukov Ya. P., Bubnova R. S., Filatov S. K. & Goncharov A.G. *Glass Phys. Chem.* 2016. V. 42. P. 202–206.

3. Biryukov Y. P., Filatov S. K., Vagizov F. G., Zinnatullin A. L. & Bubnova R. S. *J. of Struct. Chem.* 2018. V. 59. P. 1980–1988.

## Поведение эденита при повышенной температуре: окисление железа

Житова Е.С.<sup>1,2</sup>, Кржижановская М.Г.<sup>2</sup>

<sup>1</sup> Институт вулканологии и сейсмологии ДВО РАН, 683004, бул. Пийпа 9, Петропавловск-Камчатский, Россия.

<sup>2</sup> Санкт-Петербургский государственный университет, 199034, Университетская набережная 7/9, Санкт-Петербург, Россия.

\*Correspondence email: zhitova\_es@mail.ru

Эденит – минерал, относящийся к кальциевым разновидностям надгруппы амфибола с общей формулой  $AB_2C_5T_8O_{22}W_2$ , где основными компонентами являются Na в позиции А, Са – В, Mg – С, Т =  $Si_7Al$ , W = OH. Минерал был обнаружен при проходке скважины в толще глин (на глубине около 2.5 метра), покрывающих поверхность Восточно-Паужетского термального поля (п. Паужетка, южная Камчатка, Россия). Согласно данным электронно-зондового анализа для минерала характерно высокое содержание  $Fe^{2+}$ , химическая формула следующая  $(Na_{0.47}K_{0.04})(Ca_{1.70}Fe^{2+}_{0.21}Mn_{0.05})(Mg_{3.09}Fe^{2+}_{1.09}Fe^{3+}_{0.46}Ti_{0.21}Al_{0.15})(Si_{6.88}Al_{1.12})O_{22}(OH_{1.66}O_{0.34})$ .

Высокотемпературная съемка эденита проводилась на порошковом дифрактометре Rigaku Ultima IV (излучение  $CoK\alpha$ ), оснащенного высокотемпературной камерой, в диапазоне температур от 25 до 1000 °С. Согласно проведенному исследованию, дифракционная картина немного изменяется с нагревом, прослеживаются 3 этапа: 1) 25-500 °С – эденит, 2) 500-700 °С – высокотемпературная модификация I, 3) 700-1000 °С – высокотемпературная модификация II.

Для исследования происходящих с ростом температуры структурных изменений кристаллы эденита прокаливались при температуре 670 и 800 °С (обозначены далее как ed670, ed800) в муфельной печи. Затем кристаллы исходного эденита, ed670 и ed800 изучались с помощью монокристалльного рентгеновского дифрактометра Bruker SMART APEX (излучение  $CoK\alpha$ ), обработка данных включала введение необходимых поправок и уточнение кристаллической структуры. Исследование с помощью рентгеноструктурного анализа показало сокращение параметров элементарной ячейки эденита в результате прогрева. Позиция С химической формулы представлена тремя позициями кристаллической структуры M1, M2, M3, характеризующихся, как показано выше, смешанной заселенностью (Mg,  $Fe^{2+}$ ,  $Fe^{3+}$ , Ti, Al). Основные изменения, контролирующие сокращение параметров элементарной ячейки, относятся к изменению длин связей M1-O и M3-O с ростом температуры, так они составляют 2.086 и 2.080 Å для эденита; 2.074 и 2.069 Å для высокотемпературной модификации I; 2.060 и 2.052 Å для высокотемпературной модификации II. Зарегистрированные структурные изменения позволяют полагать, что для изученного эденита характерен процесс окисления железа при сохранении структурного типа, происходящего с ростом температуры

Исследование выполнено при финансовой поддержке РФФИ в рамках научного проекта № 20-35-70008.

## Mössbauer effect study of iron borate $\text{Fe}^{2+}_2\text{Fe}^{3+}(\text{BO}_3)\text{O}_2$ with hulsite structure

Zinnatullin A.L.<sup>1\*</sup>, Biryukov Y.P.<sup>2</sup>, Vagizov F.G.<sup>1</sup>

<sup>1</sup> Institute of Physics, Kazan Federal University, 18 Kremlyovskaya str, Kazan, 420008, Russian Federation

<sup>2</sup> Institute of Silicate Chemistry of the Russian Academy of Sciences, 2, Makarova emb., Saint Petersburg, 199034, Russian Federation

\*Correspondence email: almaz.zinnatullin@gmail.com

Mixed valence oxoborates have attracted much attention of scientists recently. This is due to the fact that rather unusual magnetic properties are realized in them. The reason for this is the structural features of these compounds, which determine magnetic ordering of reduced dimension. For example, for a structure like ludwigite, quasi-one-dimensional ordering is observed, and for a structural type of pinakiolite, to which the hulsite refers, quasi-planar magnetic ordering is characteristic. Meanwhile, researchers note that oxoborates with a pinakiolite structure have been studied much less than others. In mineral deposits hulsite is found, as a rule, in the form of an iron-based mineral with tin impurity [1].

Mössbauer spectroscopy allows obtaining important information about the local environment, the valence state of resonant nuclei in a solid, and also about the magnetic ordering in it. This makes it possible to study the microscopic properties of solids in the vicinity of resonant atoms even when they are distributed in several crystallographic positions [2].

In this work we report the results of  $^{57}\text{Fe}$  and  $^{119}\text{Sn}$  Mössbauer effect studies of natural hulsite with idealized formula  $\text{Fe}^{2+}_2\text{Fe}^{3+}(\text{BO}_3)\text{O}_2$ . The mineral was collected from the Titovskoe boron deposit, Tas-Khayakhtakh Range, Polar part of Sakha (Yakutia) Republic, Russia. Mössbauer experiments were performed in transmission geometry using a conventional spectrometer (WissEl, Germany) operating in constant acceleration mode equipped with a Mössbauer Furnace MBF-1100 and temperature controller TR55. Measurements were provided within the temperature range of 295–745 K in air atmosphere. The  $^{57}\text{Co}$  (Rh) with an activity of about 50 mCi and the  $^{119\text{m}}\text{Sn}$  ( $\text{CaSnO}_3$ ) with an activity of about 15 mCi (both RITVERC GmbH, Russia) were used as a source of resonance radiation. The spectrometer velocity scale was calibrated using thin metallic iron foil (at room temperature). SpectrRelax software [3] was used for experimental data processing. Isomer shifts were measured relative to  $\alpha\text{-Fe}$  at room temperature for  $^{57}\text{Fe}$  Mössbauer spectra and  $\text{SnO}_2$  at room temperature for  $^{119}\text{Sn}$  Mössbauer spectra.

The room temperature  $^{57}\text{Fe}$  Mössbauer spectrum of hulsite was processed by sum of three components, namely, one magnetically splitted component and two paramagnetic doublets. This fact means a partial magnetic ordering of iron atoms in the hulsite. It should be caused by two-dimensional character of magnetic interaction. Hyperfine parameters of magnetically splitted component are characteristic for ferric ions, while the parameters of other components – for ferrous ions. With an increasing of temperature, hyperfine field of magnetically splitted component decreases, and magnetic splitting disappears at about 383 K. At the temperatures above 600 K, new magnetically splitted component appears. This component is related with hematite ( $\alpha\text{-Fe}_2\text{O}_3$ ), and its appearance is connected with the start of oxidation of the hulsite.

The room temperature  $^{119}\text{Sn}$  Mössbauer spectrum is doublet with hyperfine parameters characteristic for  $\text{Sn}^{4+}$  ions. The absence of magnetic splitting shows that exchange interaction of ferric ions is not transferred through tin ions in hulsite structure.

The reported study was funded by RFBR according to the research project № 18-33-00644.

1. Medrano C. P. C., Freitas D. C., Passamani E. C., Resende J. A. L. C., Alzamora M., Granado E., Galdino C. W., Baggio-Saitovitch E., Continentino M. A., Sanchez D. R. Magnetic frustration in low-dimensional substructures of hulsite  $\text{Ni}_{1.15}\text{Sn}_{0.85}(\text{O}_2\text{BO}_3)_2$ . *Phys Rev B*. 2018. V.98. N 054435.

2. Wertheim G.K. Mössbauer Effect: Principles and Applications, 2<sup>nd</sup> ed. Academic Press. 1964. 116 pp.

3. Matsnev M.E., Rusakov V.S. SpectrRelax: an application for Mössbauer spectra modeling and fitting. *AIP Conference Proceedings*. 2012. V1489. N10. P. 178-185.

## Magnetic and structural properties of multiferroic $\text{Bi}_{2-x}\text{Fe}_x\text{WO}_6$

Lis O.N.<sup>1,2</sup>, Kichanov S.E.<sup>1</sup>, Belozerova N.M.<sup>1</sup>, Lukin E.V.<sup>1</sup>, Savenko B.N.<sup>1</sup>, Balakumar S.<sup>3</sup>

<sup>1</sup>Frank Laboratory of Neutron Physics, Joint Institute for Nuclear Research, 141980, Joliot-Curie str. 6, Dubna, Russia.

<sup>2</sup>Kazan Federal University, 420008, Kremlevskaya str. 16, Kazan, Russia.

<sup>3</sup>University of Madras, Gandhi Mandapam Rd, Anna University, Kotturpuram, 600085, Chennai, Tamil Nadu, India.

\*Correspondence email: lisa\_9477@mail.ru

The discovery of unusual dielectric properties (ferroelectricity) led to the study of a large number of ferroelectric oxides of various structural families to identify new materials and/or compositions for use in devices. Among all these materials, serious attention has been attended on various lead-free multiferroics (exhibiting ferroelectric/antiferroelectric and ferromagnetic/antiferromagnetic properties in the same phase) with unique properties can be applied for a wide range of applications.

$\text{BiFeO}_3$  Bismuth ferrite (BFO) modified with  $\text{WO}_3$  is one of such magnetoelectric material, exhibiting antiferromagnetic and ferroelectric properties in the same crystal structure. As  $\text{WO}_3$  has ferroelectric properties at low temperature, it is expected that addition of a small amount of this compound to BFO will result in some interesting multiferroic properties, including a shift of their transition temperature. The  $\text{Fe}^{3+}$  ions in BFO like multiferroics provide an effective approach in creating a weakly ferromagnetic state in ferroelectric phase. Therefore, for the most complete understanding of the effects occurring in this compound, detailed studies of the structural and magnetic properties of  $\text{Bi}_{2-x}\text{Fe}_x\text{WO}_6$  are necessary. Exposure of high pressure is directly method of controlled changing the magnetic interactions by the variation of the interatomic distances and angles, in comparison with other experimental methods.

The present work focuses on detailed studies of the crystal and magnetic structure of  $\text{Bi}_{2-x}\text{Fe}_x\text{WO}_6$  by means of neutron diffraction on a DN-6 diffractometer of a pulsed high-flux IBR-2 reactor (FLNP, JINR, Dubna, Russia) using a high-pressure cell with sapphire anvils in the wide pressure and temperature range. The pressure and temperature dependences of the unit cell parameters, the volume and the interatomic bond lengths of the  $\text{Bi}_{2-x}\text{Fe}_x\text{WO}_6$  compound were obtained. The calculated compressibility coefficients indicate anomalies in the behavior of interatomic lengths.

The work was supported by the Russian Foundation for Basic Research, grant RFBR N19-52-45009 IND\_a.

## The effect of doping with $\text{Sr}^{2+}$ ions on the magnetic properties of $\text{Ba}_{1-x}\text{Sr}_x\text{Fe}_{12}\text{O}_{19}$

Rutkauskas A.V. \*, Kozlenko D.P., Kichanov S.E., Savenko B.N.

Frank Laboratory of Neutron Physics, Joint Institute for Nuclear Research, 141980, Joliot-Curie St. 6, Dubna, Russia.

\*Correspondence email: ranton@nf.jinr.ru

Multiferroics have been intensively studied in recent decades. These compounds have a close relationship between magnetic and electrical properties. It makes them promising materials for wide technological application: permanent magnets, microwave devices, spintronics and etc. M-type barium hexaferrites ( $\text{Ba}_{1-x}\text{Sr}_x\text{Fe}_{12}\text{O}_{19}$ ) are ones of these compounds. They have remarkable physical properties: high coercive force, large magnetocrystalline anisotropy, high Curie temperature, relatively large magnetization, as well as excellent chemical stability and corrosion resistance.

A significant improvement of the intrinsic magnetic properties of hexaferrites can be obtained by the partial substitution of  $\text{Sr}^{2+}$  ions. Thus, the concentration of  $\text{Sr}^{2+}$  ions in  $\text{Ba}_{1-x}\text{Sr}_x\text{Fe}_{12}\text{O}_{19}$  compounds determines the magnetic properties of the material such as magnetization, Curie temperature and the magnetocrystalline anisotropy.

The neutron diffraction method allows to study simultaneously crystal and magnetic structure of compounds. Also, this method allows to determine light elements or elements with close atomic numbers. The former is especially important when studying complex oxides, where the formation of magnetic ordering is carried out through oxygen ions.

Our work presents the results of study of hexaferrites  $\text{Ba}_{1-x}\text{Sr}_x\text{Fe}_{12}\text{O}_{19}$  ( $x = 0, 0.25, 0.5, 0.75$ ) by means of neutron diffraction method at room temperature. The structural parameters and magnetic moments of Fe ions were calculated. Their dependences on concentration of  $\text{Sr}^{2+}$  ions were also obtained. The lattice parameters and bond distances have an anisotropic behavior with increasing of  $\text{Sr}^{2+}$  concentration. Doping of  $\text{Sr}^{2+}$  ions have not changed the type of the magnetic structure among the studied samples.

This work was supported by the Russian Foundation for Basic Research (project no. 20-02-00550-«a»).

# Crystal structure as a function of temperature for A-site substituted $\text{Nd}_{1-x}\text{Pr}_x\text{BaMn}_2\text{O}_6$ double manganites

Sterkhov E.V., Pryanichnikov S.V., Titova S.G.

Institute of Metallurgy of Ural Branch of Russian Academy of Sciences, 620016, Amundsen St. 101, Ekaterinburg, Russia.

\*Correspondence email: altximik@mail.ru

Double manganites  $R\text{BaMn}_2\text{O}_6$  ( $R = \text{Nd}, \text{Pr}$ ) demonstrate magnetic phase transitions near room temperature being perspective magnetocaloric materials. Except magnetic phase transitions they also demonstrate a change of  $a/c$  ratio of tetragonal unit cell constants (Fig. 1a). We established that this change of crystal structure is not connected with magnetic phase transitions [1], the origin of crystal structure change is not clear up to now.

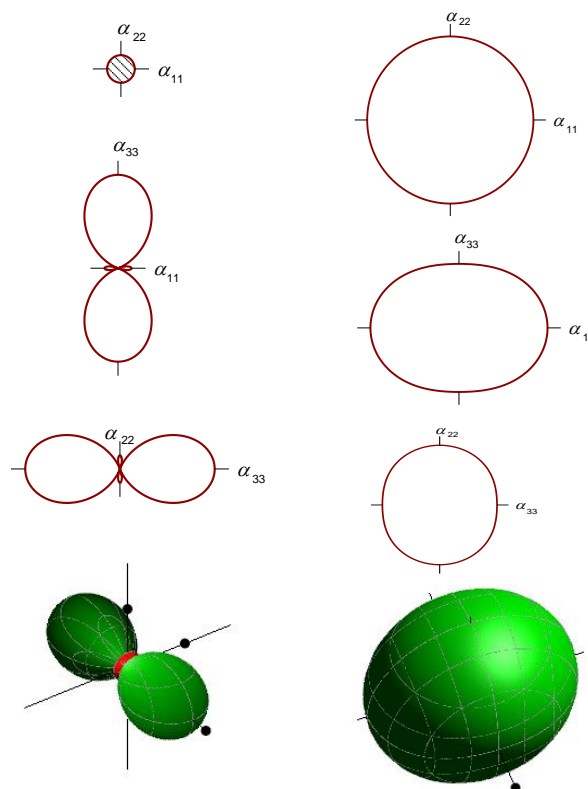
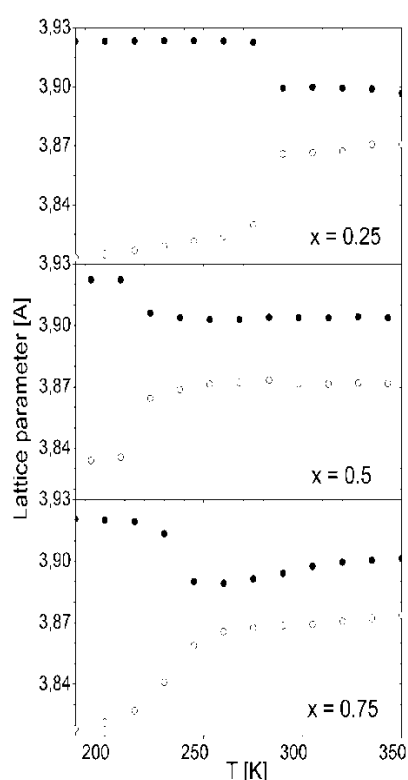


Fig. 1. Temperature dependence of lattice parameters  $a$  (black) and  $c/2$  (white) for  $\text{Nd}_{1-x}\text{Pr}_x\text{BaMn}_2\text{O}_6$  solid solutions with  $x = 0.25; 0.5; 0.75$ .

Fig. 2. The components of the tensor of thermal expansion below structural transition (left) and above the transition (right) for  $\text{Nd}_{0.25}\text{Pr}_{0.75}\text{BaMn}_2\text{O}_6$ .

The components of the tensor of thermal expansion were calculated using Rietveld to Tensor program [2] and are shown in Fig. 2 for  $\text{Nd}_{0.25}\text{Pr}_{0.75}\text{BaMn}_2\text{O}_6$ . For other compounds the results are similar. At high temperature the tensor has almost isotropic shape while below the transition the components along  $ab$ -plane become either very small or even negative.

The work is supported by RFBR, grant No 19-29-12013.

1. Titova S.G., Sterkhov E.V., Uporov S.A. Crystal structure and Magnetic Properties of A-Site Substituted  $\text{Nd}_{1-x}\text{Pr}_x\text{BaMn}_2\text{O}_6$  Double Manganite. Journal of Superconductivity and Novel Magnetism. 2020. Doi: 10.1007/s10948-020-05445-x.

2. R.S. Bubnova, V.A. Firsova, S.K. Filatov, S.N. Volkov. Rietveld To Tensor: Program for Processing Powder X-Ray Diffraction Data under Variable Conditions. Glass Physics and Chemistry. 2018, 44(1), 33–40.



## Ellenbergerite-like nickel phosphates: crystal chemistry and magnetic behavior

Shvanskaya L.V., Krikunova P.V.

M. V. Lomonosov Moscow State University, 119991, Leninskie Gory, GSP-1, Moscow, Russia

\*Correspondence email: lshvanskaya@mail.ru

Among the mineral phases, there are those that have flexible crystal structures showing the ability to broad isomorphous substitutions. This flexibility may be the key to creating new materials with technologically important properties. One of the attractive structural motifs for chemical modifications is the type of ellenbergerite,  $(\text{Mg,Ti})\text{Mg}_3(\text{Mg,Al})_3(\text{OH})_3[\text{HSiO}_4][\text{H}_{0.33}\text{SiO}_4]_3$  [1]. The incorporation of transition metals in ellenbergerite-like crystal structures allows the synthesis of analogs with non-trivial magnetic behavior, such as metamagnetic [2], canted antiferromagnetic [3], multiferroic [4].

The novel phase  $(\text{Na,Ni})_{1-x}\text{Ni}_6(\text{OH})_3[\text{HPO}_4][\text{H}_{x/3}\text{PO}_4]_3$  was prepared under hydrothermal conditions. A mixture of chemically pure  $\text{Ni}(\text{NO}_3)_2 \cdot 6\text{H}_2\text{O}$ ,  $\text{Na}_2\text{CO}_3$  was grounded and directly loaded into a 25 mL Teflon-lined stainless steel autoclave with adding 85%  $\text{H}_3\text{PO}_4$  to achieve molar ratios of  $\text{Ni}:\text{Na}:\text{P}=7:1:4$ . Finally, the autoclave was filled with distilled water up to 83% of the volume and heated at  $220^\circ\text{C}$  for 7 days. Green powder was washed and dried. The powder XRD (ADP diffractometer,  $\text{CoK}\alpha 1$  radiation,  $\lambda = 1.7890 \text{ \AA}$ ) shows that ellenbergerite type compound was formed. Its crystal structure was refined with the Rietveld method using the JANA2006 software [5]. The refined cell constants for  $(\text{Ni,Na})_{1-x}\text{Ni}_6(\text{OH})_3[\text{HPO}_4][\text{H}_{x/3}\text{PO}_4]_3$  ( $a = 12.4710(2) \text{ \AA}$ ,  $c = 4.9436(1) \text{ \AA}$ ,  $V=665.84(2) \text{ \AA}^3$ ,  $Z=1$ , space group  $P6_3mc$ ) were found close to the data reported by A. Le Bail [Crystallography Open Database, #350056] for nickel phosphate. Both structures are based on a 3D framework built from  $\text{NiO}_6$  octahedra and  $\text{PO}_4$  tetrahedra and differ by a composition of octahedra, (Ni) or (Ni, Na), in the hexagonal channels.

Magnetic susceptibility measurements of  $(\text{Na,Ni})_{1-x}\text{Ni}_6(\text{OH})_3[\text{HPO}_4][\text{H}_{x/3}\text{PO}_4]_3$  revealed a strong antiferromagnetic interaction and magnetic transition to low temperature spin-canted phase at  $T_N = 67 \text{ K}$ .

The reported study was funded by RFBR according to the research project № 18-03-00908.

1. Chopin C., Klaska R., Medenbach O. and Dron D. Ellenbergerite, a new high-pressure Mg-Al-(Ti, Zr)-silicate with a novel structure based on face-sharing octahedra. *Contrib. Mineral. Petrol.* 1986. V. 92. P. 316-321.

2. Zhang S.Y., Guo W.-B., Yang M., Tang Y.-Y., Wang N.-N., Huang R.-R., Cui M.-Y., He Z.-Z. Synthesis, crystal structure and magnetic property of a new cobalt (II) vanadate. *Journal of Solid State Chemistry.* 2015. V. 225. P. 78–82.

3. Yakubovich O.V., Kiriukhina G.V., Dimitrova O.V., Shvanskaya L.V., Volkova O.S. and Vasiliev A.N. A novel cobalt sodium phosphate hydroxide with the ellenbergerite topology: crystal structure and physical properties. *Dalton Trans.* 2015. V. 44. P. 11827-11834.

4. Poienar M., Maignan A, Sfirloaga P., Malo B., Vlazan P., Guesdon A., Lainé F., Rouquette G., Martin C. Polar space group and complex magnetism in  $\text{Ni}_{11}\square(\text{HPO}_3)_8(\text{OH})_6$ : towards a new multiferroic material? *Solid State Sciences.* 2015. V. 39. P. 92-96.

5. Petříček V., Dušek M., and Palatinus, L., Jana2006. Structure Determination Software Programs, Praha: Instit. Phys., 2006.

## **5. HTXRD and high-temperature crystal chemistry**

## The effect of negative chemical pressure on phase stability, structure and physical properties in the $\text{Co}_7(\text{Se}_{1-y}\text{Te}_y)_8$ system

Akramov D.F.<sup>1\*</sup>, Selezneva N.V.<sup>1</sup>, Baranov N.V.<sup>2</sup>

<sup>1</sup> Ural Federal University, Institute of Natural Sciences and Mathematics, 620026, Kuibyshev str 48, Ekaterinburg, Russia.

<sup>2</sup> M.N. Miheev Institute of Metal Physics, Ural Branch of Russian Academy of Sciences, 620108, Sofia Kovalevskaya str 18, Ekaterinburg, Russia.

\*Correspondence email: dmaster96@mail.ru

Cation-deficient transition metal (M) chalcogenides  $\text{M}_7\text{X}_8$  (X – chalcogen) with a layered crystal structure of the NiAs type have a wide variety of physical properties. The presence of cation vacancies and their ordering leads to the appearance of various superstructures, which substantially affects the physical properties of the compounds. Another feature of the  $\text{M}_7\text{X}_8$  compounds is the possibility of the formation of solid solutions upon substitution in both anionic and cationic sublattices. Thus, continuous substitutional solid solutions were observed in the  $(\text{Co}_{1-x}\text{Fe}_x)_7\text{Se}_8$  system at the replacement of cobalt by iron [1] and in  $\text{Co}_7(\text{S}_{1-y}\text{Se}_y)_8$  [2] when sulfur was replaced by selenium. Because of the difference in ionic radii such substitutions result in the expansion of the crystal lattice. In  $(\text{Co}_{1-x}\text{Fe}_x)_7\text{Se}_8$ , the negative chemical pressure arising with increasing iron concentration leads to an increase in the average interlayer distance  $c$  (up to  $\sim 10\%$  at  $x = 7$ ) and a slight change in the parameter  $a$ . While  $\text{Co}_7\text{Se}_8$  ( $x = 0$ ) exhibits Pauli paramagnetic properties, an increase in the Fe concentration up to  $x = 4$  leads to the appearance of the long-range ferrimagnetic ordering in  $(\text{Co}_{1-x}\text{Fe}_x)_7\text{Se}_8$ . In the  $\text{Co}_7(\text{S}_{1-y}\text{Se}_y)_8$  system, the substitution leads to an increase in the lattice parameter  $c$  by 2 %, however, it does not lead to significant changes in the properties. It is of interest to create a significant negative chemical pressure in the  $\text{Co}_7\text{Se}_8$  compound by substituting selenium with tellurium.

Polycrystalline  $\text{Co}_7(\text{Se}_{1-y}\text{Te}_y)_8$  samples were obtained by solid-phase synthesis in evacuated ampoules at  $T = 1000\text{ }^\circ\text{C}$ . The X-ray diffraction analysis was carried out using a Bruker D8 ADVANCE diffractometer equipped with an NTK-16 Anton Paar thermal camera for studies in the temperature range of 25 – 500  $^\circ\text{C}$ . The thermal expansion of the samples was measured on a DL-1500 RHP dilatometer (ULVAC-SINKU RIKO) in the same temperature range.

It was found that the continuous solid solution with hexagonal symmetry is formed upon substitution in the anion sublattice of the  $\text{Co}_7(\text{Se}_{1-y}\text{Te}_y)_8$  compounds. X-ray diffraction analysis showed that even insignificant substitution of selenium by tellurium ( $y \geq 0.2$ ) leads to disordering of vacancies in the cation sublattice, which is accompanied by a transition from the 3C superstructure to the 1C structure. Substitution is also accompanied by changes in space groups.

Contrary to expectations, an anisotropic increase in the lattice parameters with an increase in tellurium concentration is observed, since the complete replacement of selenium with tellurium leads to an increase in the lattice parameter  $a$  by 8.3%, while the lattice parameter  $c$  increases by 2% only. Due to a small change in the lattice parameter  $c$ , no significant changes in the properties were detected, although a decrease in electrical resistivity, i. e. an increase in metallicity, was observed with increasing Te concentration in  $\text{Co}_7(\text{Se}_{1-y}\text{Te}_y)_8$ . The analysis of X-ray diffraction patterns measured at different temperatures has shown that phase separation occurs in samples with high tellurium contents ( $y > 0.5$ ) at temperatures of about 450  $^\circ\text{C}$ . The phase separation was confirmed by the thermal expansion measurements, since dilatometric data have shown a pronounced anomaly in the tellurium-rich compositions ( $y \geq 0.55$ ). In the compounds with a low tellurium content ( $y \leq 0.2$ ) was also observed an anomalous behavior of thermal expansion associated a phase transition of the «order-disorder» type upon heating.

This work was financially supported by the Ministry of Education and Science of the Russian Federation (project № FEUZ-2020-0054

1. Baranov N.V., Ibrahim P.N.G., Selezneva N.V., Gubkin A.F., Volegov A.S., Shishkin D.A., Keller L., Sheptyakov D., Sherstobitova E.A. Layer-preferential substitutions and magnetic properties of pyrrhotite-type  $\text{Fe}_{7-y}\text{M}_y\text{X}_8$  chalcogenides (X = S, Se; M = Ti, Co). Journal of Physics: Condensed Matter. 2015. V.27. P. 286003 (12pp).

2. Miller V.L., Lee W.L., Lawes G., Ong N.P., Cava R.J. Synthesis and properties of the  $\text{Co}_7\text{Se}_{8-x}\text{S}_x$  and  $\text{Ni}_7\text{Se}_{8-x}\text{S}_x$  solid solutions. Journal of Solid State Chemistry. 2005. V. 178. P. 1508-1512.

## Study of hydration and dehydration of sulfate exhalative minerals using powder X-ray diffraction

Borisov A.<sup>1\*</sup>, Siidra O.<sup>1,2</sup>, Depmeier W.<sup>3</sup>, Platonova N.<sup>4</sup>

<sup>1</sup> Department of Crystallography, St. Petersburg State University, University Emb. 7/9, 199034 St. Petersburg, Russia

<sup>2</sup> Kola Science Center, Russian Academy of Sciences, Apatity 184200, Murmansk Region, Russia

<sup>3</sup> Institut für Geowissenschaften der Universität Kiel, Olshausenstr. 40, D-24098 Kiel, Germany

<sup>4</sup> X-ray Diffraction Resource Center, St. Petersburg State University, University Emb. 7/9, 199034 St. Petersburg, Russia

\*Correspondence email: as\_borisov@inbox.ru

Anhydrous copper sulfate minerals with additional alkali cations are the most abundant species in the - famous for its mineral diversity - Second Scoria Cone (SSC hereafter) of the Great Tolbachik Fissure Eruption (1975-1976), and likewise in the Naboko scoria cone of the 2012-2013 Tolbachik Fissure eruption (FTE) of the Tolbachik volcano on Kamchatka peninsula, Far East region, Russian Federation. When exposed to humid atmosphere, let alone wet environment, these minerals react rapidly and convert to a wide range of hydrated sulfate minerals. The extent and the exact nature of these transformations depend on a combination of many, partly interrelated, parameters, e.g. the seasonal changes of atmospheric conditions and precipitations (temperature, relative humidity, rain, snow, fog). Due to the high temperature of the exhausting gases from the fumaroles some of the hydration processes of the minerals are reversed.

Hydration/dehydration experiments combined with powder X-ray diffraction reveal a complex behavior of studied minerals: euchlorine  $\text{KNaCu}_3(\text{SO}_4)_3\text{O}$ , chalcocyanite  $\text{CuSO}_4$ , dolerophanite  $\text{Cu}_2(\text{SO}_4)\text{O}$ , alumoklyuchevskite  $\text{K}_3\text{Cu}_3(\text{Al,Fe}^{3+})(\text{SO}_4)_4\text{O}_2$  and itelmenite  $\text{Na}_4\text{Mg}_3\text{Cu}_3(\text{SO}_4)_8$ . Remarkably, upon heating stepwise dehydration occurs whereby the complex mixture of hydrated sulfates gradually reverses and becomes again essentially either single-phase or in rare cases changes to the phase structurally unrelated to the initial mineral.

The current study is also interesting in terms of methodology as it has demonstrated the possibility of studying the phase formation in the highly moisture-sensitive sulfate systems during hydration using conventional in house X-ray powder diffractometers, without being obliged to wait a long time for short experimental shifts at high-end instruments of synchrotron sources.

This work was financially supported by the RSF grant №16-17-10085.

Siidra O.I., Borisov A.S., Lukina E.A., Depmeier W., Platonova N.V., Colmont M., Nekrasova D.O.

Reversible hydration/dehydration and thermal expansion of euchlorine, ideally  $\text{KNaCu}_3\text{O}(\text{SO}_4)_3$  // *Physics and Chemistry of Minerals*. 2019. Vol. 46 P. 403-416.

## Бораты $\text{Ba}_3\text{Y}_2(\text{BO}_3)_4:\text{Er}^{3+}$ и $\text{Ba}_3\text{Eu}_2(\text{BO}_3)_4$ : синтез, термическое расширение

Демина С.В.<sup>1,2</sup>, Шаблинский А.П.<sup>1</sup>, Бубнова Р.С.<sup>1</sup>, Бирюков Я.П.<sup>1</sup>, Филатов С.К.<sup>2</sup>

<sup>1</sup> Институт химии силикатов им. И.В. Гребенщикова РАН, 199053, Набережная Макарова 2, Санкт-Петербург, Россия.

<sup>2</sup> Санкт-Петербургский государственный университет, 199034, Университетская набережная 7 – 9, Санкт-Петербург, Россия.

\*Correspondence email: rimma\_bubnova@mail.ru

Поиск новых высокоэффективных люминофоров в системе  $\text{REE}_2\text{O}_3\text{--BaO--B}_2\text{O}_3$  на сегодняшний день является актуальной задачей. Допированные бораты этой системы являются хорошими люминофорами для применения в LED и PDP дисплеях [1].

При медленном охлаждении от температуры 1350 °С были получены монокристаллы боратов  $\text{Ba}_3\text{Eu}_2\text{B}_4\text{O}_{12}$  и  $\text{Ba}_3\text{Y}_2\text{B}_4\text{O}_{12}$ , относящиеся к семейству  $A_3\text{REE}_2(\text{BO}_3)_4$ , где  $A = \text{Ca}, \text{Sr}, \text{Ba}$  [1–4]. Также было проведено допирование бората  $\text{Ba}_3\text{Y}_2\text{B}_4\text{O}_{12}$  по формуле:  $\text{Ba}_3\text{Y}_{2-x}\text{Er}_x(\text{BO}_3)_4$  ( $x = 0.01, 0.05, 0.1, 0.15, 0.2, 0.25, 0.3$ ), и получены гомогенные образцы.

Монокристаллическая дифрактометрия проводилась на дифрактометре Bruker Smart APEX II. Рентгенофазовый анализ и терморентгенографические эксперименты – на дифрактометре Rigaku Ultima IV. Кристаллическая структура  $\text{Ba}_3\text{Y}_2\text{B}_4\text{O}_{12}$  впервые уточнена в анизотропном приближении методом рентгеноструктурного анализа до значения  $R$ -фактора  $R = 0.037$ . Оба бората кристаллизуются в ромб. синг., пр. гр.  $Pnma$ . Параметры элементарной ячейки бората  $\text{Ba}_3\text{Y}_2\text{B}_4\text{O}_{12}$ :  $a = 7.7013(22)$ ,  $b = 16.5172(51)$ ,  $c = 8.9853(30)$  Å,  $V = 1142.97(40)$  Å<sup>3</sup>,  $Z = 4$ .

Кристаллические структуры данных боратов содержат плоские треугольные радикалы  $\text{BO}_3$ , предпочтительно ориентированные в плоскости  $bc$ . В структуре есть три независимые кристаллографические позиции для катионов, две из которых общие, а одна частная. Позиции катионов координированы восемью атомами кислорода, а катионы разупорядочены по трем позициям.

Расчитаны коэффициенты термического расширения в широком интервале температур для  $\text{Ba}_3\text{Y}_2\text{B}_4\text{O}_{12}$  и  $\text{Ba}_3\text{Eu}_2\text{B}_4\text{O}_{12}$ . Коэффициенты термического расширения бората  $\text{Ba}_3\text{Y}_2\text{B}_4\text{O}_{12}$  при температуре 25 °С:  $\alpha_a = 10.5(9)$ ,  $\alpha_b = 13.0(1)$ ,  $\alpha_c = 12.9(5)$ ,  $\alpha_V = 36.4(5) \times 10^{-6} \text{ °C}^{-1}$ . При температуре приблизительно 700 °С происходит изгиб на зависимости параметров элементарной ячейки от температуры. Коэффициенты термического расширения бората  $\text{Ba}_3\text{Eu}_2\text{B}_4\text{O}_{12}$  при температуре 25 °С:  $\alpha_a = 14.1(2)$ ,  $\alpha_b = 6.0(7)$ ,  $\alpha_c = 12.4(1)$ ,  $\alpha_V = 32.5(3) \times 10^{-6} \text{ °C}^{-1}$ . При температуре приблизительно 800 °С также происходит изгиб на зависимости параметров элементарной ячейки от температуры.

Исследование люминесцентных свойств находится в процессе.

Работа выполнена при поддержке РФФИ (проект № 18-03-00679). Терморентгенография выполнена в Ресурсном центре СПбГУ «Рентгенодифракционные методы исследования».

1. Хамаганова Т. Н. Особенности структур и свойства боратов щелочноземельных и редкоземельных металлов. Известия Академии Наук. 2017. С. 187-200.

2. Палкина К. К., Кузнецов В. Г., Джурицкий Б. Ф. и др. Результаты рентгеновской дифракции и пространственная группа смешанных боратов  $\text{Pr}_2\text{Sr}_3(\text{BO}_3)_4$ ,  $\text{Gd}_2\text{Sr}_3(\text{BO}_3)_4$ ,  $\text{La}_2\text{Ba}_3(\text{BO}_3)_4$  и  $\text{La}_2\text{Sr}_3(\text{BO}_3)_4$  // Журнал неорганической химии. 1972. Т. 17. С. 341-343.

3. Палкина К. К., Кузнецов В. Г., Моруга Л. Г. Кристаллическая структура  $\text{Pr}_2\text{Sr}_3(\text{BO}_3)_4$  // Журнал неорганической химии. 1973. Т. 14. С. 988-992.

4. Reuther C., Möc I R., Gö z J. al. Synthesis and optical characterization of Gd-neso-borate single crystals // Chemie der Erde. 2015. V.75. P. 317-322.

## Investigation of isomorphism, polymorphism and morphotropic transitions in apatites using HTXRD

Bulanov E.N., Stasenko K.S.

Lobachevsky State University of Nizhny Novgorod, 603950, Gagarin av. 23, Nizhny Novgorod, Russia.

Apatites are one of the broadest mineral family. This fact is made possible by different isomorphous substitutions in the chemical composition of the apatites. In the common case, the general formula of the apatites may be represented as follows:  $M_5(AO_4)_3L$ , where M – mono-, di-, tris- and tetravalent cations and their combinations; A – atoms, which can form tetrahedra as coordination polyhedra (Si, Ge; P, V; S; etc); L – is the position for halogen and different groups of atoms such as OH,  $CO_3$  and others. Moreover, in all of the positions various types of defects can be observed.

Thermal expansion of apatites with pentavalent atoms in tetrahedral positions has several features. First of all, thermal dependence of unit cell parameters of such apatites can be approximated primarily by the second-low polynomial. This situation is typical for close-packed structure in comparison to structures with lower density layout of polyhedra in a unit-cell. Thermal expansion of s-element-containing phases is more isotropic in comparison with Cd- and Pb-apatites. Another conclusion is that for phosphates and vanadates crystallographic axis  $c$  is the primary direction of the thermal deformations whereas for Mn and Cr-containing apatites it is the  $a$  axis. It can be explained by the different ratio of bonds energy between layers formed by  $AO_4$  tetrahedrons and within them.

Also, we have shown for the first time that there is a polymorphic transition in some apatites which is accompanied by the lowering of unit-cell symmetry from hexagonal  $P6_3/m$  to monoclinic  $P2_1/b$  ( $Pb_5(PO_4)_3F$ ,  $Pb_5(PO_4)_3Cl$ ,  $Pb_5(VO_4)_3Cl$ ). Further studies have shown that there is a group of apatites ( $Ca_5(PO_4)_3Cl$ ,  $Ca_5(VO_4)_3Cl$ ,  $Ca_5(CrO_4)_3Cl$ , etc) which also has transitions, but the high-temperature modification may be called pseudohexagonal. In this case crystallographic axis  $a$  of hexagonal modification almost matches with axis  $b$  of monoclinic modification,  $b^2 = 2a^2$ ,  $\gamma \approx 120^\circ$ . In some apatites ( $Ca_5(PO_4)_3Cl$ ,  $Sr_5(CrO_4)_3Cl$ ,  $Na_3Cd_2(SO_4)_3Cl$ , etc) negative volumes of thermal expansion coefficients were observed. Apatites have high isomorphous capacity, which causes necessity of investigation not only individual compounds, but various binary systems. In case of  $Pb_5(PO_4)_3F_xCl_{1-x}$  in the range of  $0 < x < 0.5$  volume thermal expansion coefficient doesn't depend on the composition for all temperatures, while in the range of compositions  $0.5 < x < 1$  we observed an increased thermal sensitivity of the structure. Thus, position 2b of apatite structure is more tolerant to the content of the larger atoms. In the case of  $Pb_5(P_xV_{1-x}O_4)_3Cl$  we found that there is the independence of  $\alpha_v(T)$  at  $x=0.5$ . We assume that this phenomenon is connected with the formation of superstructure in the solid solution due to the ordering of the P- and V-atoms in the 6h position. Also, we used HTXRD for investigating  $Ca_{8-2x}Pb_{2x}Bi_2(PO_4)_6O_2$  ( $x = 0, 1, 2, 3, 4$ ) solid solution series. The main feature of such system is that  $Pb_8Bi_2(PO_4)_6O_2$ , despite its isoformality, crystallizes in the Pnma space group of orthorhombic system, which is not characteristic of the structural type of apatite. Thus, the phenomenon of morphotropy was observed (a sharp change in the crystal structure in a regular series of chemical compounds while maintaining a quantitative ratio of structural units). The crystal structure of  $Pb_8Bi_2(PO_4)_6O_2$  is framework, with independent positions for Bi and Pb atoms. Moreover, in this structure coordination numbers are smaller for both cations in comparison with apatite structure.

The absolute values of thermal expansion coefficients for apatites in  $Ca_{8-2x}Pb_{2x}Bi_2(PO_4)_6O_2$  range ( $x = 0-3$ ) are agree well with previously founded for substances with the same structural type: thus, all of them can be described as highly-expanded. Moreover, we have shown, that Ca-apatites have relatively isotropic expansion, while Pb-apatites have pronounced predominance of expansion along one  $c$ -axis over expansion along the  $a$ -axis. This fact is also a good reason to call apatite structure quasi-layered, not framework: during the heating layers formed by  $AO_4$  tetrahedrons and  $M^{6h}$  polyhedra moves from each other along  $c$ -axis.

Addition of  $p$ -elements (Bi and then Pb) into structure of pure calcium-apatite ( $Ca_{10}(PO_4)_6O$ ) leads to an increase in the rate of growth of parameter  $c$  during heating compared to changes in parameter  $a$ . And the more lead in the composition, the greater this difference.

It also should be noted that for  $Pb_8Bi_2(PO_4)_6O_2$  as for framework compound changes in anisotropy during heating is not so critical, and its expansion stays relatively isotropic in spite of absence of calcium.

The research was financially supported by the Scholarship Program of the Grants Council under the President of the Russian Federation.

## X-ray diffraction analysis of natural and synthetic uranyl compounds at non-ambient temperatures: structure vs. stability

Gurzhiy V.V.<sup>1\*</sup>, Krivovichev S.V.<sup>1,2</sup>

<sup>1</sup>Department of Crystallography, St. Petersburg State University, University Emb. 7/9, St. Petersburg, 199034, Russia

<sup>2</sup>Kola Science Centre, Fersmana Str. 14, 184209 Apatity, Murmansk Region, Russia

\*Correspondence email: vladgeo17@mail.ru

Within the last few years, uranium mineralogy and crystal chemistry has witnessed a true Renaissance, due to the discoveries of exceptional suites of new uranium minerals in Jáchymov, Czech Republic and San Juan County, Utah, U.S. The diversity of new natural species is of particular interest since most of them do not have direct synthetic analogues and therefore are new to the synthetic inorganic chemistry as well. Most of the new uranium minerals are the products of secondary low-temperature hydrothermal processes, which are often associated with crystallization of very complex mineral species such as ewingite,  $\text{Mg}_8\text{Ca}_8(\text{UO}_2)_{24}(\text{CO}_3)_{30}\text{O}_4(\text{OH})_{12}(\text{H}_2\text{O})_{138}$ , the most structurally complex mineral known today. The structural architectures of novel natural phases, for instance, uranyl sulfates, show many similarities to synthetic uranyl sulfates, chromates, molybdates and selenates. In most of them, uranyl ions are interlinked via tetrahedral  $\text{TO}_4$  groups ( $T = \text{S}, \text{Cr}, \text{Se}, \text{Mo}$ ) into finite clusters, chains or layers, in which interaction between adjacent uranyl groups is mediated by the hexavalent  $T^{6+}$  cations.

A family of actinyl-bearing isotopic compounds  $\text{Cs}_2[(\text{AnO}_2)_2(\text{TO}_4)_3]$  (where  $\text{An} = \text{U}, \text{Np}$  and  $T = \text{S}, \text{Se}, \text{Cr}, \text{Mo}$ ) is the only known to date example of structural type preservation with such a large diversity in chemical composition [1]. Vertex-sharing way of the polyhedral linkage leaves great opportunity for the structure to reflect the substitution in the oxyanion or actinyl-ion parts. However, the conservation of the structural motif doesn't mean the maintaining of chemical and physical properties. In the absence of definite dependencies between the angles at the bridged O atoms or volume of  $\text{An}$  and  $T$  polyhedra, which are usually regarded as the most sensitive structural fragments, the coordination of cesium atoms remains the only significant factor. Alteration in the oxyanion composition of the  $\text{An}$ -bearing layers results in change of the  $\text{Cs}^+$  cations local environment, which in turn leads to the increase of its influence on the layered substructural units and on the stability of the structure itself. Such substitution mechanisms could be regarded as an interesting and valuable example of the chemical composition selection for the preparation of compounds with the desired properties.

This work was supported by St. Petersburg State University and Russian Science Foundation (grant 18-17-00018). X-ray studies were carried out at the Research Center for X-ray structural studies of St. Petersburg State University.

1. Gurzhiy V.V., Korniyakov I.V., Szymanowski J.E.S., Felton D., Tyumentseva O.S., Krzhizhanovskaya M.G., Krivovichev S.V., Burns P.C. Chemically-induced structural variations of a family of  $\text{Cs}_2[(\text{AnO}_2)_2(\text{TO}_4)_3]$  ( $\text{An} = \text{U}, \text{Np}$ ;  $T = \text{S}, \text{Se}, \text{Cr}, \text{Mo}$ ) compounds: thermal behavior, calorimetry studies and spectroscopy characterization of Cs uranyl sulfate and selenate. *Journal of Solid State Chemistry*. 2020. V. 282. P. 121077.

## The high-temperature crystal chemistry of technogenic mineral phases from the burned dumps of the Chelyabinsk coal basin

Zolotarev A.A. Jr.<sup>1</sup>, Avdontseva M.S.<sup>1</sup>, Krzhizhanovskaya M.G.<sup>1</sup>, Zhitova E.S.<sup>1,2</sup>,  
Krivovichev S.V.<sup>1,3</sup>

<sup>1</sup> Department of Crystallography, Institute of Earth Sciences, St. Petersburg State University, University Emb. 7/9, 199034, Saint-Petersburg, Russia

<sup>2</sup> Institute of Volcanology and Seismology FEB RAS, Piip Blvd 9, 683006 Petropavlovsk-Kamchatsky, Russia

<sup>3</sup> Federal Research Center, Kola Science Center, RAS, Fersmana Str. 14, 184209 Apatity, Russia

\*Correspondence email: a.zolotarev@spbu.ru

Burned dump formations of Chelyabinsk coal basin continue to attract significant attention due to a large variety of mineral species and their immediate connection to the processes of technogenesis [1-3 and references within]. Herein we report on the results of HT-XRD studies of number technogenic mineral phases from the burned dumps of the Chelyabinsk coal basin.

The mineral phases “redikortsevite”  $\text{NH}_4\text{MgCl}_3 \cdot 6\text{H}_2\text{O}$  and  $(\text{NH}_4)_2\text{Fe}^{3+}\text{Cl}_5 \cdot \text{H}_2\text{O}$  [1, 3] are isostructural with natural minerals novograbenovite [4] and kremersite [5], respectively.  $\text{NH}_4\text{MgCl}_3 \cdot 6\text{H}_2\text{O}$  is stable up to 90 °C and then transforms to the less hydrated phase isotypic to  $\beta\text{-Rb}(\text{MnCl}_3)(\text{H}_2\text{O})_2$  (i.e.,  $\text{NH}_4\text{MgCl}_3 \cdot 2\text{H}_2\text{O}$ ) [6], the latter phase being stable up to 150 °C.  $(\text{NH}_4)_2\text{Fe}^{3+}\text{Cl}_5 \cdot \text{H}_2\text{O}$  is stable up to 120 °C and then transforms to an X-ray amorphous phase. Hydrogen bonds provide an important linkage between the main structural units and play the key role in determining structural stability and physical properties of the studied phases. Fluorellestadite  $\text{Ca}_5(\text{SiO}_4)_{1.5}(\text{SO}_4)_{1.5}\text{F}$  is sulphato-silicate mineral which belongs to ellestadite group of apatite supergroup [7]. The thermal expansion of fluorellestadite is almost isotropic in the temperature range 25-800 °C. The similar thermal behavior had been observed for fluorapatite [8]. The technogenic mineral phases “korkinoite” is close to mineral rapidcreekite  $\text{Ca}_2(\text{SO}_4)(\text{CO}_3) \cdot 4\text{H}_2\text{O}$  [9]. The “korkinoite” phase is characterized by rather strong anisotropy of thermal expansion. Under heating phase is stable up to 200 °C.

Acknowledgments: this research was funded by the Russian Foundation for Basic Research (grant No. 19-05-00628). The X-ray diffraction studies were performed in the X-ray Diffraction Resource Centre of St. Petersburg State University.

1. Chesnokov B.V., Shcherbakova E.P., Nishanbaev T.P. Minerals of burnt dumps of the Chelyabinsk coal basin. Ural branch of RAS: Miass. 2008. 139 p.

2. Zolotarev A.A., Krivovichev S.V., Panikorovskii T.L., Gurzhiy V.V., Bocharov V.N., Rassomakhin M.A. Dmisteinbergite,  $\text{CaAl}_2\text{Si}_2\text{O}_8$ , a metastable polymorph of anorthite: Crystal-structure and Raman spectroscopic study of the holotype specimen. Minerals. 2019. V. 9. 570.

3. Zolotarev A.A., Zhitova E.S., Krzhizhanovskaya M.G., Rassomakhin M.A., Shilovskikh V.V., Krivovichev S.V. Crystal chemistry and high-temperature behaviour of ammonium phases  $\text{NH}_4\text{MgCl}_3 \cdot 6\text{H}_2\text{O}$  and  $(\text{NH}_4)_2\text{Fe}^{3+}\text{Cl}_5 \cdot \text{H}_2\text{O}$  from the burned dumps of the Chelyabinsk coal basin. Minerals. 2019. V. 9. 486.

4. Okrugin V.M., Kudaeva S.S., Karimova O.V., Yakubovich O.V., Belakovskiy D.I., Chukanov N.V., Zolotarev A.A., Gurzhiy V.V., Zinovieva N.G., Shiryayev A.A., Kartashovet P.M. The new mineral novograbenovite,  $(\text{NH}_4, \text{K})\text{MgCl}_3 \cdot 6\text{H}_2\text{O}$  from the Tolbachik volcano, Kamchatka, Russia: mineral information and crystal structure. Miner. Mag. 2019. V. 83. P. 223–231.

5. Kremers P. Ueber die aschenbestandtheile und die producte der trocknen destillation bei Braun und Steinkohlen. Ann. der Phys. und Chem. 1851. V. 84. P. 67–80.

6. Jensen S.J., Lehmann M.S. Neutron diffraction study of  $\beta\text{-RbMnCl}_3 \cdot 2\text{H}_2\text{O}$ . Acta Chem. Scand. 1970. V. 24. P. 3422–3424.

7. Pasero M., Kampf A., Ferraris C., Pekov I., Rakovan J., White T. Nomenclature of the apatite supergroup minerals. Eur. J. Mineral. 2010. V. 22. P. 163-179.

8. Chernorukov N.G., Knyazev A.V., Bulanov E.N. Phase transition and thermal expansion of apatite-structured compounds. Inorganic materials. 2011. V. 47. P. 172-177.

9. Roberts A.C., Ansell H.G., Jonasson I.R., Grice J.D., Ramik R.A. Rapidcreekite, a new hydrated calcium sulfate-carbonate from the Rapid Creek area, Yukon Territory. Can. Mineral. 1986. V. 24. P. 51-54.



## High-temperature crystal chemistry of copper trimolibdate $\text{CuMo}_3\text{O}_{10}\times\text{H}_2\text{O}$

Ismagilova R.M.<sup>1</sup>, Zhitova E.S.<sup>2</sup>, Zolotarev A.A.<sup>1</sup>, Krivovichev S.V.<sup>1,3</sup>, Shilovskih V.V.<sup>1</sup>

<sup>1</sup> Institute of Earth Sciences, St.Petersburg State University, 199155, Per. Dekabristov 16, St.Petersburg, Russia.

<sup>2</sup> Institute of Volcanology and Seismology, the Russian Academy of Sciences, 683006, Piip Boulevard 9, Petropavlovsk-Kamchatsky, Russia.

<sup>3</sup> Nanomaterials Research Centre, Kola Science Centre, the Russian Academy of Sciences, 184209, ul. Fersmana 14, Apatity, Russia.

\*Correspondence email: rezeda\_marsovna@inbox.ru

Copper trimolybdate  $\text{CuMo}_3\text{O}_{10}\times\text{H}_2\text{O}$  crystals were obtained by hydrothermal synthesis as a result of the reaction of  $(\text{NH}_4)_6\text{Mo}_7\text{O}_{24}\times 4\text{H}_2\text{O}$  and  $\text{Cu}(\text{CH}_3\text{COO})_2$  for 7 days at  $T = 220$  °C. The crystal structure of  $\text{CuMo}_3\text{O}_{10}\times\text{H}_2\text{O}$  contains ribbons of edge-sharing  $\text{MoO}_6$  octahedra parallel to the  $b$  axis [1]. The ribbons are connected by  $\text{CuO}_6$  octahedra to form three-dimensional framework. The high-temperature crystal chemistry of the compound has been studied by high- and low-temperature X-ray powder diffraction in the temperature range of  $-100 - 900$  °C and single crystal X-Ray diffraction in the temperature range  $-180 - 27$  °C.

$\text{CuMo}_3\text{O}_{10}\times\text{H}_2\text{O}$  is stable up to  $300$  °C and decomposes to  $\text{MoO}_3$  and  $\alpha\text{-CuMoO}_4$  at  $T > 300$  °C by the reaction scheme:



The nature of thermal behavior changes smoothly at the temperature range  $-100 - -50$  °C. A slight compression of the crystal structure occurs at low temperatures up to  $-100$  °C according to the single crystal X-Ray diffraction results. Thermal expansion is anisotropic and positive at  $T > -100$  °C up to dehydration. Thermal expansion coefficients  $\alpha_{11}$ ,  $\alpha_{22}$ ,  $\alpha_{33}$  at  $T = 100$  °C are  $28.5$ ,  $6.1$ ,  $13.3$  °C<sup>-1</sup>  $\times 10^{-6}$ , respectively.

The low-temperature compression along the  $a$  axis occurs due to the most intense shortening of the Mo-O bond lengths in this direction up to  $-100$  °C. The high-temperature anisotropy is determined by the changes in the interatomic angles in the  $\text{CuO}_6$  octahedra leading to elongation or reduction of the lengths of its edges.

Thus, trimolybdate units are rigid structural units in the high-temperature range  $> -100$  °C, and thermal behavior of the structure of  $\text{CuMo}_3\text{O}_{10}\times\text{H}_2\text{O}$  is determined by  $\text{CuO}_6$  octahedron geometry alignment. Nevertheless,  $\text{MoO}_6$  octahedra are more flexible units than  $\text{CuO}_6$  for the low-temperature range  $-180 - -100$  °C.

The reported study was funded by the research grant of the president of the Russian Federation for leading scientific schools (Nsh-2526.2020.5). This research was carried out using the facilities of the XRD Resource Centre of St. Petersburg State University and the Russian Foundation for Basic Research (20-35-90007).

1. Tian C., Wang E., Li Y., Xu L., Hu C., Peng J. A novel three-dimensional inorganic framework: hydrothermal synthesis and crystal structure of  $\text{CuMo}_3\text{O}_{10}\cdot\text{H}_2\text{O}$ . *Journal of Solid State Chemistry*. 2004. V. 177. P. 839–843.

## Irreversible dehydration of murmanite

Panikorovskii T.L.<sup>1,2\*</sup>, Krivovichev S.V.<sup>1,2</sup>

<sup>1</sup> Kola Science Centre of RAS, Fersman Str. 14, Apatity, Murmansk Region, 184209 Russia.

<sup>2</sup> Department of Crystallography, St. Petersburg State University, 7–9 University Emb, St. Petersburg 199034, Russia.

\*Correspondence email: t.panikorovskii@ksc.ru

Murmanite is widespread in the Lovozero massif both in pegmatite bodies and in rocks [1]. It was first found by Wilhelm Ramsay in 1890. In the reports of the expedition by A.E. Fersman in 1923, this mineral was referred as "viophyllite", and after a detailed description of N.N. Gutkova was named for the area - Murmanite [2]. It was noted that upon heating of murmanite has three endothermic peaks observed at 165, 315, and 730 °C, the first one corresponds to loss molecular water from the structure [3].

The first description of murmanite crystal structure was given by A.D. Khalilov et al. (1965) in space group *P1*.  $a = 5.50$ ,  $b = 7.00$ ,  $c = 11.94$  Å,  $\alpha = 96^\circ 00'$ ,  $\beta = 100^\circ 26'$ ,  $\gamma = 88^\circ 55'$ , the mineral formula was defined as  $\text{Na}_2\text{Mn}[\text{Ti}_2(\text{OH})_4(\text{Si}_2\text{O}_7)_2](\text{H}_2\text{O})_4$ . Later, the general formula of the mineral was refined as  $\text{Na}_4\text{Ti}_4(\text{Si}_2\text{O}_7)_2\text{O}_4(\text{H}_2\text{O})_4$ , in which the overestimated role of manganese was noted earlier [4]. Recently the murmanite structure refined by F. Camara et al. [5] in the space group *P-1* and the mineral formula proposed by Khalilov [4] was confirmed.

The crystal structure of murmanite at the room conditions were refined at the *P-1* space group with  $R_1 = 0.077$  for 1660 independent reflections  $a = 5.3822(6)$ ,  $b = 7.0538(8)$ ,  $c = 11.6477(15)$  Å,  $\alpha = 86.385(9)^\circ$ ,  $\beta = 81.967(10)^\circ$ ,  $\gamma = 89.970(9)^\circ$ ,  $V = 436.98(9)$  Å<sup>3</sup>. Generally, the modular structure of murmanite based on *TS* block consist of two types of layers parallel to (001) called *HOH* modules. The *HOH* modules have a three-layered structure consisting of a central sheet of octahedra (O sheet) and two adjacent heteropolyhedral sheets (H sheets). Each Ti-octahedra has one long bond, which correspond to H<sub>2</sub>O molecule. The formula according refinement can be written as  $\text{Na}_4(\text{Ti}_{3.60}\text{Nb}_{0.40})_{\Sigma 4}(\text{Si}_2\text{O}_7)_2\text{O}_4 \cdot 4\text{H}_2\text{O}$ .

The structure of the dehydrated phase at 150 °C was refined in the *P-1* space group with an  $R_1 = 0.096$  for 1643 independent reflections  $a = 5.3089(9)$ ,  $b = 7.0373(13)$ ,  $c = 9.822(4)$  Å,  $\alpha = 81.74(2)^\circ$ ,  $\beta = 80.60(2)^\circ$ ,  $\gamma = 89.862(14)^\circ$ ,  $V = 358.18(17)$  Å<sup>3</sup>. The dehydration causes a change in the coordination of titanium in the H layer from the octahedral to the five-coordinated. The collapse of *HOH* modules with simultaneously migration of sodium cations into the interlayer space exists without loss of material crystallinity. The dehydrated murmanite formula can be written as  $\text{Na}_4\text{Ti}_4(\text{Si}_2\text{O}_7)_2\text{O}_4$ .

The research is supported by the Kola Science Center of Russian Academy of Sciences (0226-2019-0011) (study of the chemical composition and spectroscopic characteristics) and by grants of the Russian Science Foundation (19-17-00038) and the Russian Foundation for Basic Research (18-29-12039) (X-ray structural studies).

1. Gutkova N.N. The new titanosilicate is Murmanite from the Lovozersky tundra. - Reports of the Academy of Sciences, series A, 1930. P. 731-736

2. Gerasimovsky V.I. Murmanite of the Lovozero Tundra. Rare Metals. 1936, 4, P. 37-39

3. Vlasov K.A., Kuzmenko M.V., Yeskova E.M. Lovozero alkaline massif. IMGRE AN USSR. M.: USSR Academy of Sciences. 1959. 618 pp.

4. Khalilov A.D. Refinement of the crystal structure of murmanite and new data on its crystal-chemical features. Mineral. Journal. 1989. V. 11. P. 19-27

5. Cámara F, Sokolova E, Hawthorne F. C., Abdu Y. From structure topology to chemical composition. IX. Titanium silicates: revision of the crystal chemistry of lomonosovite and murmanite, Group-IV minerals, Mineralogical Magazine, 2008. V. 72. P. 1207-1228.

## Variable-temperature studies of $\text{Ni}_{3-x}\text{M}_x\text{Te}_2$ solid solutions (M = Co, Fe)

Charkin D.O.<sup>1\*</sup>, Gurianov K.E.<sup>1</sup>, Plokhikh I.V.<sup>2</sup>

<sup>1</sup> Chemistry Department, Moscow State University, 119991 Leninskie Gory 1, Moscow, Russia.

<sup>2</sup> Institute of Inorganic chemistry, University of Regensburg, 93053, Regensburg, Germany

\*Correspondence email: d.o.charkin@gmail.com

Recent studies have shown that nickel subtellurides, known from the beginning of 1960s [1], may find application in electrocatalysis and sensing of biological molecules [2, 3]. Yet, their crystal and thermochemistry remain contradictory. Complex phase relationships between several compounds of similar  $\text{Ni}_{3\pm x}\text{Te}_2$  composition ( $x \leq 0.1$ ) and slightly different  $\text{Cu}_2\text{Sb}$ -related structures have been reported which are yet not fully clear. Some of high-temperature polymorphs are known to be selectively stabilized by Fe doping, yet nothing is known about possible doping by Co, the nearest neighbor of Ni, and other  $3d$  transition metals.

Low-temperature studies of undoped  $\text{Ni}_{3\pm x}\text{Te}_2$  confirmed existence of two individual compounds, monoclinic  $\text{Ni}_{3+x}\text{Te}_2$  ( $P2_1/m$ ) and tetragonal  $\text{Ni}_{3-x}\text{Te}_2$  ( $P\bar{4}m2$ ), the latter structure determined from single-crystal data. Both structures correspond to slightly different motifs of Ni/vacancy ordering in the Ni-deficient  $\text{Cu}_2\text{Sb}$  lattice. On heating to 130 – 150°C, both compounds convert into a single, relatively broad solid solution with a mean orthorhombic symmetry ( $Pm\bar{m}n(0b0)00s$ ) which is stable until 350°C. Above, a disordered tetragonal  $\text{Cu}_2\text{Sb}$  structure ( $P4/nmm$ ) is stable which in its turn converts to a disordered FCC structure above 800°C.

The Co doping of  $\text{Ni}_3\text{Te}_2$ , which is observed for the first time, stabilizes the orthorhombic polymorph in the entire  $\text{Ni}_{3-y}\text{Co}_y\text{Te}_2$  compositional range ( $y \leq 1$ ) at room temperature. Surprisingly, the transition temperature to the  $P4/nmm$  form remains insensitive to the Co content ( $325 \pm 10^\circ\text{C}$ ). The phase sequence changes for the Co-richest composition where a new rhombohedral ( $R\bar{3}m$ ) phase exists in a very narrow range between  $P4/nmm$  and  $Fm\bar{3}m$ . The dependence of lattice parameters vs. temperature is complex suggesting several subtle transitions within the same symmetry.

The  $\text{Ni}_{3-y}\text{Fe}_y\text{Te}_2$  exists in a more narrow compositional range of  $y \leq 0.8$ . At low Fe content, also the orthorhombic  $Pm\bar{m}n$  form is stabilized, with transition temperature to  $P4/nmm$  being slightly lower ( $\approx 275^\circ\text{C}$ ). At highest Fe content, the  $P4/nmm$  form is stabilized at room temperature. Thermal studies also indicate intermediate formation of  $R\bar{3}m$  phase which is stable in a wider temperature range. Hence, both Co and Fe doping is equivalent to increasing temperature, yet the effect is sensitive to the nature of dopant and not to doping level.

1. Kok R.B., Wiegers G.A., Jellinek F. The system nickel-tellurium I. Structure and some superstructure of the  $\text{Ni}_{3\pm x}\text{Te}_2$ . Recl. Trav. Chim. Pay-B. 1965. V. 84. P. 1585-1588.

2. De Silva U., Masud J., Zhang N., Hong Y., Liyanage W.P.R., Zaeem M.A., Nath M. Nickel telluride as a bifunctional electrocatalyst for efficient water splitting in alkaline medium. J. Mater. Chem. A 2018 V. 6. id. 7608.

3. Amin B.G., De Silva U., Masud J., Nath M. Ultrasensitive and highly selective  $\text{Ni}_3\text{Te}_2$  as a non-enzymatic glucose sensor at extremely low working potential. ACS Omega 2019 V. 4. id. 11152.

## Thermal disorder in the $\text{Fe}_{0.5}\text{TiSe}_2$

Shkvarina E.G., Titov A. A., Shkvarin A.S.\*, Postnikov M.S., Radzivonchik D.I., Titov A.N.

<sup>1</sup>M.N. Miheev Institute of Metal Physics of Ural Branch of Russian Academy of Sciences,  
620990 Ekaterinburg, Russia

\*Correspondence email: shkvarin@imp.uran.ru

Quasi-two-dimensional transition-metals dichalcogenides have gained growing interest in the last decades [1]. The structural type of such materials is widely known in literature as "1T" (s.g.  $P-3m1$ ). Iron atoms introduced into the interlayer space between sandwiches occupy the sites octahedrally-coordinated by chalcogen atoms, similar to the titanium sites inside the sandwich [2]. Increasing Fe concentration up to 50% lead to change space group to  $I2/m$  with  $(a_0 \times \sqrt{3}a_0 \times 2c_0)$  superstructure formation. Existence of a region of retrograde solubility, observed in the phase diagram of the Fe –  $\text{TiSe}_2$  system [3] are introduce additional uncertainty. It can be expected that heating would lead to the disintegration of any ordered superstructure and to the increase of the symmetry class. This may be due to a simple increase in the kinetic energy of iron atoms, similar to a melting process, or it might be a consequence of the possible iron precipitation [3], which lowers the iron concentration below that required to form the superstructure. To address this question, we carried out an extended in-situ investigation of the crystal structure of  $\text{Fe}_{0.5}\text{TiSe}_2$  in the temperature range of 25 – 1000 °C by means of synchrotron powder diffraction.

Polycrystalline  $\text{Fe}_{0.5}\text{TiSe}_2$  was synthesized by iron intercalation into preliminary synthesized  $\text{TiSe}_2$ . The in-situ synchrotron radiation X-ray powder diffraction SR-XRPD experiments were performed *in-situ* ( $\lambda = 1.0332 \text{ \AA}$ ) at the MCX beamline at the Elettra Synchrotron, Trieste (Italy) [4]. The crystal structure refinement was performed using GSAS (General Structure Analysis System) [5].

The disordering of the intercalated iron has been ascribed to a second-order phase-transition associated with a change in the symmetry-class from monoclinic to trigonal and it is not caused by the extraction of iron. The critical temperature of the order – disorder phase transition in the two-dimensional ferromagnetic Ising model is 422 °C and the critical exponent (in the scaling law  $\eta = |T - T_c|^{-\beta_c}$ ) for our experimental data is  $\beta_c = 0.169$ .

The transition is related only to the iron sublattice and does not affect the  $\text{TiSe}_2$  lattice. This ultimately indicates that the  $\text{Fe}_x\text{TiSe}_2$  system can be considered as intercalation system rather than a triple chalcogenide. The monoclinic-to-trigonal phase-transition manifests itself mainly as 2D disorder associated with the destruction of chains of intercalated atoms within the van der Waals gap. However, the 2D iron-chain sublattices appear to be not completely independent due to weak out-of-plane interactions, thus suggesting a non-negligible 3D character.

The research was carried out with partial financial support of the RFBR (project 18-32-20141).

1. Wilson J.A., Yoffe A.D. The transition metal dichalcogenides discussion and interpretation of the observed optical, electrical and structural properties // *Adv. Phys.* 1969. Vol. 18, № 73. P. 193–335.
2. Arnaud Y. et al. Etude structurale des composés  $\text{MxTiSe}_2$  (M = Fe, Co, Ni) // *J. Solid State Chem.* 1976. Vol. 18, № 1. P. 9–15.
3. Shkvarina E.G. et al. Phase diagram and thermodynamic equilibrium in the Fe x  $\text{TiSe}_2$  system // *Phys. Solid State.* 2012. Vol. 54, № 3. P. 626–629.
4. Rebuffi L. et al. MCX: a Synchrotron Radiation Beamline for X-ray Diffraction Line Profile Analysis // *Zeitschrift für Anorg. und Allg. Chemie.* 2014. Vol. 640, № 15. P. 3100–3106.
5. Larson A.C., Von Dreele R.B. GSAS: generalized structure analysis system // *Doc. LAUR.* 1994. P. 86–748.

# Solid-phase synthesis of $\text{Na}_2\text{SO}_4\text{-K}_2\text{SO}_4$ sulfates on a thermo-x-ray equipment and the subsequent study of synthesis products during cooling.

Shorets O.U.<sup>1,2</sup>, Filatov S.K.<sup>2\*</sup>, Bubnova R.S.<sup>1</sup>

<sup>1</sup> Grebenshchikov Institute of Silicate Chemistry, Russian Academy of Sciences, 199053, Makarov Emb. 2, St.Petersburg, Russia.

<sup>2</sup> Department of Crystallography, Institute of Earth Sciences, Saint Petersburg State University, University Emb. 7/9, 199034, Saint Petersburg, Russia.

\*Correspondence email: filatov.stanislav@gmail.com

The object of the study was a mechanical equimolar mixture of  $\text{Na}_2\text{SO}_4$  – *Fddd* phase [1, 2] and  $\text{K}_2\text{SO}_4$  – *Pmcn* phase [3] in the ratios 1:3, 1:1 and 3:1. All samples were heated from room temperature to 800 °C with subsequent cooling, the temperature step – 20 °C.

The research was carried out using a Rigaku Ultima IV diffractometer ( $\text{CuK}\alpha_{1+2}$ , 40 kV, 30 mA, geometry for reflection, high-speed energy-dispersive detector DTEX/ULTRA) with a high-temperature camera "SHT-1500". The range of  $2\theta$  diffraction angles was 10-80°. The preparation was prepared on a substrate by precipitation from a heptane suspension.

An example of the study is shown in figure 1. The experiment was performed by heated from 30 °C to 800 °C and then cooled to room temperature (from bottom to top in figure 1). Horizontal solid lines indicate the temperatures of phase transitions. The unit cell parameters of various phases, including in heterogeneous mixtures, were refined at different temperatures by the Rietveld method, the temperature dependences of these parameters were approximated by 2nd-degree polynomials, and the coefficients of thermal expansion were calculated using the RietTensor [4] and ThetaToTensor-TTT [5] software complexes. The investigations were performed using the equipment of the Saint-Petersburg State University Resource Center «X-ray diffraction studies».

The authors appreciate the financial support provided by the Russian Fund for Basic Research (project 19-35-90094).

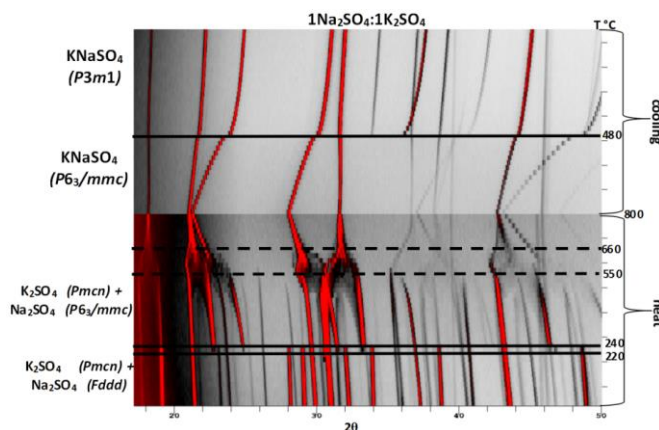


Fig. 1. Thermal phase transformation upon cooling in a belomarinaite. The horizontal line indicates the phase transition temperature.

1. Nord A.G. Refinement of the Crystal Structure of Thenardite // Acta Chemica Scandinavica. 1973. P. 814-822.

2. Rasmussen S. E., Jørgensen J. E. and Lundtoft B. Structures and Phase Transitions of  $\text{Na}_2\text{SO}_4$  // J. Appl. Cryst., 1996. Vol. 29, p. 42-47.

3. Ojima K., Nishihata Y. and Sawada A. Structure of potassium sodium sulphate at temperatures from 296 K down to 15 K // Acta Crystallographica. 1995. V. B51. P. 287–293.

4. Bubnova R.S., Firsova V.A., Volkov S.N., Filatov S.K. Rietveld To Tensor: Program for Processing Powder X-Ray Diffraction Data under Variable Conditions // Glass Physics and Chemistry. 2018. V. 44. P. 33–40.

5. Bubnova R.S., Firsova V.A., Filatov S.K. Software for Determining the Termal Expansion Tensor and the Graphic Representation of Its Characteristic Surface (ThetaToTensor-TTT) // Glass Physics and Chemistry. 2013. V. 39. P. 347–350.

## Novel red phosphor $\text{CaBi}_2\text{B}_4\text{O}_{10}:\text{Eu}^{3+}$ : synthesis, crystal structure, luminescence and thermal expansion

Yuriev A.A.<sup>1,3\*</sup>, Shablinskii A.P.<sup>1</sup>, Povolotskiy A.V.<sup>2</sup>, Bubnova R.S.<sup>1</sup>, Kolesnikov I.E.<sup>4</sup>, Filatov S.K.<sup>3</sup>

<sup>1</sup>Institute of Silicate Chemistry, Russian Academy of Sciences, Makarov Emb. 2, St. Petersburg 199034, Russia

<sup>2</sup>Institute of Chemistry, St. Petersburg State University, University Emb. 7/9, St. Petersburg 199034, Russia

<sup>3</sup>Department of Crystallography, Institute of Earth Sciences, St. Petersburg State University, University Emb. 7/9, St. Petersburg 199034, Russia

<sup>4</sup>Center for Optical and Laser Materials Research, Research Park, St. Petersburg State University, University Emb. 7/9, St. Petersburg 199034, Russia

\*Correspondence email: artem.yurev@gmail.com

In recent years, phosphors converted white LED have replaced traditional fluorescent light sources due to high efficiency, long serving time, chemical stability and environmental friendliness. As it was found [1], Bi-containing compounds have some advantages as a host matrix for  $\text{Eu}^{3+}$  ions, especially when the crystal structure contains a few crystallographically independent sites for alkali earth metals and  $\text{Bi}^{3+}$  ions. For the first time  $\text{CaBi}_2\text{B}_4\text{O}_{10}$  was obtained and studied by the DSC method in the  $\text{CaO}-\text{Bi}_2\text{O}_3-\text{B}_2\text{O}_3$  system [2]. In our work, The  $\text{CaBi}_{2-x}\text{Eu}_x\text{B}_4\text{O}_{10}$  ( $x = 0; 0.01; 0.05; 0.1; 0.15; 0.2; 0.25; 0.3$ ) solid solutions were synthesized by solid state reactions. Then the pressed mixture were placed in a Pt crucible and heated at 630 °C for 20 h in air, and the pellets of  $\text{CaBi}_{2-x}\text{Eu}_x\text{B}_4\text{O}_{10}$  were heated at 650 °C for 25 h in air. Single crystals of  $\text{CaBi}_2\text{B}_4\text{O}_{10}$  were obtained at 700 °C for 0.5 h. The  $\text{CaBi}_2\text{B}_4\text{O}_{10}$  crystal structure was solved and refined from single crystal X-ray diffraction data to  $R_1 = 0.029$ . The compound is isotypical to the borate of  $\text{SrBi}_2\text{B}_4\text{O}_{10}$  [3].  $\text{CaBi}_2\text{B}_4\text{O}_{10}$  crystallizes in triclinic space group,  $P-1$  ( $a = 6.6704$  (1),  $b = 6.8317$  (1),  $c = 9.5775$  (1) Å,  $\alpha = 94.33$ ,  $\beta = 108.48$ ,  $\gamma = 101.34$  °,  $V = 401.37$  Å<sup>3</sup>,  $Z = 2$ ) [4]. Crystal structure contains  $[\text{B}_4\text{O}_9]^{6-}$  isolated tetraborate groups ( $4\text{B}:3\Delta\Box: <2\Delta\Box>\Delta$ ), Bi–O chains and interstitial Sr atoms. Tetraborate group consists of the triborate ring  $[\text{B}_3\text{O}_7]^{5-}$  and branched  $\text{BO}_3$  triangle.  $\text{CaBi}_2\text{B}_4\text{O}_{10}$  was studied using Rigaku “Ultima IV” powder diffractometer (CoK $\alpha$  radiation,  $2\theta = 10\text{--}70^\circ$ , temperature range 25–700 °C, step 25 °C). Thermal expansion is sharply anisotropic. The coefficients and parameters of the thermal expansion tensor at 25 °C:  $\alpha_{11} = 3 \times 10^{-6}$ ,  $\alpha_{22} = 15 \times 10^{-6}$ ,  $\alpha_{33} = 7 \times 10^{-6}$ ,  $\alpha_a = -3 \times 10^{-6}$ ,  $\alpha_b = 5 \times 10^{-6}$ ,  $\alpha_c = 3 \times 10^{-6}$ ,  $\alpha_V = 25 \times 10^{-6}$  °C<sup>-1</sup>. The temperature dependencies of triclinic unit-cell parameters demonstrate that the thermal expansion of the structure along  $a$  and  $c$  crystallographic directions is greater than along  $b$  direction. We observed the increase of  $\gamma$  (from 101.3 to 101.8) angle, decrease of  $\beta$  (from 108.65 to 108.25) angle and insignificant increase of  $\alpha$  (from 94.2 to 94.4) angle.

The emission spectra of  $\text{CaBi}_2\text{B}_4\text{O}_{10}:\text{Eu}^{3+}$  spectra include characteristic narrow intra-configurational 4f-4f transitions from  $^5\text{D}_0$  level to  $^7\text{F}_J$  ( $J = 0, 1, \dots, 4$ ) levels. The most prominent band centered at 612 nm corresponds to the forced electric dipole transition  $^5\text{D}_0\text{--}^7\text{F}_2$ . Prevalence of this transition over magnetic dipole one ( $^5\text{D}_0\text{--}^7\text{F}_1$ ) displays that  $\text{Eu}^{3+}$  ions occupy site without inversion symmetry in the  $\text{CaBi}_2\text{B}_4\text{O}_{10}$  crystal structure. The concentration dependence of integrated emission intensity data presents linear increase of emission intensity along with growth of doping concentration in studied range. No evidence of concentration quenching was observed. The CIE chromaticity coordinates of  $\text{CaBi}_{1.8}\text{Eu}_{0.2}\text{B}_4\text{O}_{10}$  phosphor were calculated from emission spectrum and were found to be (0.63, 0.35).

X-ray studies were performed at the St. Petersburg State University Resource Center “X-ray diffraction methods of research”. The study was supported by RFBR (Project No. 18-03-00679 ).

A.P. Shablinskii, R.S. Bubnova, I.E. Kolesnikov, M.G. Krzhizhanovskaya, A. V. Povolotskiy, V.L. Ugolkov, S.K. Filatov, Novel  $\text{Sr}_3\text{Bi}_2(\text{BO}_3)_4:\text{Eu}^{3+}$  red phosphor: synthesis, crystal structure, luminescent and thermal properties, *Solid State Sci.* 70 (2017) 93–100.

Egorysheva A.V., Volodin V.D., Skorikov V.M. Calcium-bismuth borates in the  $\text{CaO}-\text{Bi}_2\text{O}_3-\text{B}_2\text{O}_3$  system // *Neorgan. materials.* 2008. V. 44, No. 1. P. 76–81.

Krzhizhanovskaya, M.G.; Bubnova, R.S.; Egorysheva, A.V.; Kozin, M.S.; Volodin, V.D.; Filatov, S.K. Synthesis, crystal structure and thermal behavior of a novel oxoborate  $\text{SrBi}_2\text{B}_4\text{O}_{10}$  // *J. Solid State Chem.* 2009. Vol. 182. P. 1260–1264.

Shablinskii A.P., Povolotskiy A.V., Yuriev A.A., Bubnova R.S., Kolesnikov I.E., Filatov S.K. Novel  $\text{CaBi}_2\text{B}_4\text{O}_{10}:\text{Eu}^{3+}$  red phosphor: synthesis, crystal structure, luminescence and thermal expansion // *Solid State Sciences.* 2020. V. 106. 106280.

## Thermal expansion of calcium borates

Yukhno V.A.<sup>1</sup>, Bubnova R.S.<sup>1,2</sup>, Krzhizhanovskaya M.G.<sup>2</sup>, Filatov S.K.<sup>2</sup>

<sup>1</sup> Grebenshchikov Institute of Silicate Chemistry, Russian Academy of Sciences, 199053, Makarov Emb. 2, St.Petersburg, Russia.

<sup>2</sup> St. Petersburg State University, 199034, Universitetskaya emb., 7–9, St. Petersburg, \*Correspondence email: yukhno.valentina@gmail.com

The high-temperature behaviour of four calcium borates ( $\text{Ca}_3\text{B}_2\text{O}_6$ ,  $\text{Ca}_2\text{B}_2\text{O}_5$ ,  $\text{CaB}_2\text{O}_4$ ,  $\text{CaB}_4\text{O}_7$ ) has been studied by *in situ* high-temperature powder X-ray diffraction (HTXRD), differential scanning calorimetry and thermogravimetry.

The tendency of decrease in the volume expansion is observed with an increase in the  $\text{B}_2\text{O}_3$  content in the  $\text{CaO-B}_2\text{O}_3$  system as a result of the degree of polymerization increase. High anisotropy of the expansion is observed for  $\text{Ca}_3\text{B}_2\text{O}_6$ ,  $\text{Ca}_2\text{B}_2\text{O}_5$  (0D) and  $\text{CaB}_2\text{O}_4$  (1D) based on the  $\text{BO}_3$  triangles only: the structure highly expands perpendicular to the  $\text{BO}_3$  planes, i. e. along the direction of the weaker bonds in the crystal structure.

$\text{Ca}_3\text{B}_2\text{O}_6$  (0D). In the trigonal structure, isolated triangles  $\text{BO}_3$  are arranged perpendicular to the  $c$  axis. Oxygen and boron atoms oscillate perpendicularly to strong B–O bonds. Therefore, the maximum amplitude of vibration is perpendicular to the plane of the triangle.

$\text{Ca}_2\text{B}_2\text{O}_5$  (0D) undergoes two reversible polymorphic transitions at about 500 and 516 °C. The structure expands intensively along the  $a$  axis, in a direction perpendicular to the plane of borate triangles. Minimal expansion occurs along the boron-oxygen chains parallel to the  $c$  axis since the strongest bonds are realized in the chains.

$\text{CaB}_2\text{O}_4$  (1D). The structure contains the chains of  $\text{BO}_3$  triangles that are located along the  $c$  axis. Planes of the triangles are approximately parallel to the (001) plane. The structure expands intensively along the  $a$  axis, in a direction perpendicular to the plane of borate triangles. Minimal expansion occurs along the boron-oxygen chains parallel to the  $c$  axis since the strongest bonds are realized in the chains.

$\alpha\text{-CaB}_4\text{O}_7$  (3D). The crystal structure is characterized by a boron-oxygen polyanion consisting of four crystallographically independent  $\text{BO}_3$  triangles and four  $\text{BO}_4$  tetrahedra linked via common vertices. The eight triangles and tetrahedra form a  $[\text{B}_8\text{O}_{14}]^{4-}$ -unit, which is repeated throughout the structure. The maximal direction of thermal expansion in the structure coincides with an acute angle bisector of the  $ac$  parallelogram and the minimum expansion occurs along the other diagonal. The structure expands along the monoclinic axis less intensively. Such sharply anisotropic behavior could be explained using shear deformation of the monoclinic plane.

High-temperature powder X-ray diffraction experiments were performed in Saint-Petersburg State University Research Centre for XRD Studies.

The study was supported by the Russian Foundation for Basic Research (No. 18-03-00679).

## **6. Structural analysis of modulated, disordered structures and nano-sized objects**



## The first bismuth borate oxyiodide, $\text{Bi}_4\text{BO}_7\text{I}$ : commensurate or incommensurate?

Volkov S.N.<sup>1</sup>, Bubnova R.S.<sup>1</sup>, Krzhizhanovskaya M.G.<sup>2</sup>, Galafutnik L.G.<sup>1</sup>

<sup>1</sup> Grebenshchikov Institute of Silicate Chemistry, Russian Academy of Sciences, 199053, Makarov Emb. 2, St.Petersburg, Russia.

<sup>2</sup> Crystallography, Saint Petersburg State University, University Emb., 7/9, Saint Petersburg, 199034, Russian Federation

The first bismuth borate oxyiodide,  $\text{Bi}_4\text{BO}_7\text{I}$ , has been prepared by solid-state reaction in evacuated silica ampoules. Its crystal structure (s.g.  $Immm(00\gamma)000$ ) is comprised of litharge-related layers of edge-sharing  $\text{OBi}_4$  tetrahedra; the interlayer space is filled by  $\Gamma^-$  and  $[\text{BO}_3]^{3-}$ . These anions are ordered in a complex sequence along  $[001]$ ,  $-\langle-\text{BO}_3-\text{BO}_3-\text{I}-\rangle_n =_{28}-\text{I}-\text{I}-\text{I}-\langle-\text{BO}_3-\text{BO}_3-\text{I}-\rangle_n =_{28}-\text{BO}_3-\text{BO}_3-\text{BO}_3-$  leading to a structural modulation. The wave vector,  $\mathbf{q} = 0.242(3)\mathbf{c}^*$ , is very close to the rational value of  $\mathbf{c}^*/4$ , yet refinement based on commensurate modulation faces essential problems indicating the incommensurate nature of the modulation. The latter's principal feature is the presence of  $-\text{I}-\text{I}-\text{I}-$  and  $-\text{BO}_3-\text{BO}_3-\text{BO}_3-$  sequences that cannot be accounted for in the  $a \times b \times 4c$  supercell (Fig. 1). Two  $\text{Bi}_4\text{BO}_7\text{X}$  ( $X = \text{Cl}, \text{Br}$ ) halide borates were briefly mentioned in a preprint (Egorova, 2011), yet their crystal structures remain unknown. The new compound,  $\text{Bi}_4\text{BO}_7\text{I}$ , was found to be structurally close to a commensurately modulated rare-earth oxyantimonide,  $\text{Pr}_2\text{SbO}_2$  (Magdysyuk *et al.*, 2013) which can be described within an  $a \simeq 13.58$ ,  $b \simeq 15.93$ ,  $c \simeq 4.00$  Å supercell in a  $Pmmm$  space group. The thermal expansion of  $\text{Bi}_4\text{BO}_7\text{I}$  is weakly anisotropic ( $\alpha_a = 8$ ,  $\alpha_b = 15$ ,  $\alpha_c = 17 \times 10^{-6} \text{K}^{-1}$  at 500 K) which is caused by preferential orientation of the borate groups.

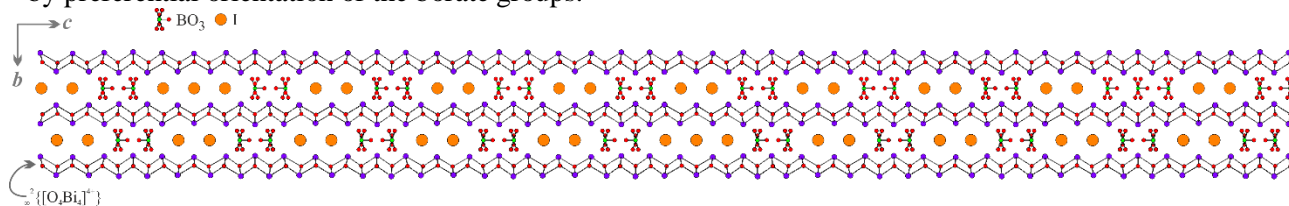


Fig. 1.  $\text{Bi}_4\text{BO}_7\text{I}$  crystal structure projected along the  $a$ -axis. The shown supercell has a size of  $a \times b \times 42c$ , where  $a$ ,  $b$  and  $c$  are the unit-cell parameters of  $\text{Bi}_4\text{BO}_7\text{I}$ . It is seen that after every 28 “normal” cells come the  $(\text{I}-\text{I}-\text{I})$  or  $(\text{BO}_3)-(\text{BO}_3)-(\text{BO}_3)$  “inclusion”, while the “normal” sequence is  $\langle-\text{I}-\text{I}-(\text{BO}_3)-(\text{BO}_3)-\rangle$ . The abundance of the iodide and borate “inclusions” is assumed to be equal to maintain the overall electroneutrality.

This work was supported by the Russian Foundation for Basic Research (18-29-12106)

1. Egorova B.V. (2011). Sintez, poisk i diagnostika slozhnykh borat galogenidov Pb(II), Sn(II), Bi(III) [abstract]. In: Proceedings of the Lomonosov-2011 conference; 2011, Moscow, 49.

2. Magdysyuk, O. V., Jürgen, N. Jansen, M. Modulated crystal structure of  $\text{Pr}_2\text{SbO}_2$ . Acta Cryst. 2013. B69, P. 547–555.

## Synthesis and thermal stability of silicon-containing calcium phosphates

Golovanova O.A.

Department of Inorganic Chemistry Omsk F. M. Dostoevsky State University, Russia, Prospekt Mira, 55-A

Correspondence email: golovanoa2000@mail.ru

The development of biomaterials necessary for the restoration and replacement of bone tissue is an important area of medical materials science. Biogenic material for bone replacement based on carbonate-containing non-stoichiometric hydroxylapatite (HA) and collagen protein is unique in its properties and composition. It is characterized by high mineralization of the intercellular matrix and contains 50 wt. % inorganic compounds, 25 wt. % organic and 25 wt. % water.

Minerals give it hardness, organic - elasticity and resilience. The results of clinical studies showed that, along with the advantages of HA-based materials, they have such disadvantages as a low bioresorption rate and a weak stimulating effect on the growth of new bone tissue. Modification of GA by various biologically active ions due to isomorphic substitutions makes it possible to purposefully change the properties of GA and to obtain materials based on it with an elemental composition close to human bone tissue. One of these dopant ions is silicon - a vital trace element for bone formation and maintenance of its structure is normal. It has been established that the composition of human interstitial fluid includes silicic acids. When bone tissue is damaged, silicon is localized in the area of formation of a new bone framework and is spent on the formation of the main substance of bone and cartilage.

Synthetic calcium-phosphate biomaterials, the structure of which includes silicon, have increased biological activity compared to unsubstituted HA, promote the growth of extracellular matrix and accelerate bone mineralization. Si-HA is a biocompatible material and does not cause rejection when introduced into the tissues of a living organism. Thus, silicate ions are very promising for improving the biological activity of HA. The synthesis of HA was carried out by precipitation when draining solutions of calcium nitrate  $\text{Ca}(\text{NO}_3)_2 \cdot 4\text{H}_2\text{O}$ , disubstituted ammonium phosphate  $(\text{NH}_4)_2\text{HPO}_4$  and an aqueous solution of ammonia  $\text{NH}_4\text{OH}$ . Silicate ions were introduced as  $\text{Na}_2\text{SiO}_3 \cdot 9\text{H}_2\text{O}$ . The concentrations of the starting reagents were calculated so that  $\text{Ca}(\text{NO}_3)_2 / (\text{NH}_4)_2\text{HPO}_4 = 1.70$ . The concentration of silicate ions was varied in the range from 1 to 30%. The synthesis time was 24 and 48 hours.

For thermogravimetric analysis, samples weighing  $0.1000 \pm 0.0002$  g were heated in an LF-7/13-G1 LOIPLF muffle furnace at a temperature of 600 to 1000°C with an interval of 100 ° C for 1 h (after the furnace entered operating mode). After calcination, the samples were cooled in air to room temperature, weighed on an analytical balance and transferred to labeled containers. The mass difference before and after calcination was used to calculate the mass loss of the substance as a result of heat treatment. Three experiments were performed for each sample.

Bioceramics, in the production of which HA is used, is widely used in medicine for the treatment of dental and bone defects. Ceramics is also used in conjunction with polymers in order to fill bone cavities during restoration. Therefore, an attempt was made to create ceramics by exposing the synthesized silicon-containing samples to temperatures in the range of 600–1000°C. After heat treatment, an increase in the total mass loss with an increase in the calcination temperature was observed for all samples. In the temperature range 25–230°C, unbound and adsorption water is removed from the composition of the samples. At  $t > 600$  ° C, CO leave the KHA structure. Modestration begins at a temperature of about 800°C. As a result of the release of CO from the structure, KHA decomposition and the formation of two phases occur:  $\beta$ -TCP (tricalcium phosphate) and Si-HA. The XRD results confirm the presence of two phases in the precipitation after calcination. As the initial concentration of silicate ions increases, the intensity of the diffraction peaks increases, and their width decreases, which indicates a greater degree of crystallization of the solid phase in comparison with the pure sample. X-ray powder diffraction data are consistent with IR spectroscopy data. The spectra of samples obtained after calcination at  $t = 800$  ° C exhibit absorption bands characteristic of the vibration of the P – O bond in the PO tetrahedron. Absorption bands at 450–550  $\text{cm}^{-1}$  indicate the presence of silicate ions in the structure of synthesized calcium phosphates. After heat treatment, the peaks at 1383 and 873–880  $\text{cm}^{-1}$  disappear, which corresponds to stretching and deformation vibrations of the C = O bond. With an increase in the concentration of silicate ions in the samples, the intensity increases and the peak expands at 1096  $\text{cm}^{-1}$ , which is characteristic of P – O bond vibrations and Si – O stretching vibrations.

## Evolution of crystal structures and thermal stability of calcium oxalates hydrates

Izatulina A.R. , Gurzhiy V.V., Krzhizhanovskaya M.G., Kuz'mina M.A., Frank-Kamenetskaya O.V.

<sup>1</sup> Department of Crystallography, St. Petersburg State University, University Emb. 7/9, 199034 St. Petersburg, Russia

\*Correspondence email: alina.izatulina@mail.ru

Calcium oxalates are represented in nature by three hydrated forms: whewellite ( $\text{CaC}_2\text{O}_4 \cdot \text{H}_2\text{O}$ ; COM), weddellite ( $\text{CaC}_2\text{O}_4 \cdot (2.5-x)\text{H}_2\text{O}$ ; COD) and caoxite ( $\text{CaC}_2\text{O}_4 \cdot 3\text{H}_2\text{O}$ ; COT). Calcium oxalates are notably common biominerals and can be found, e.g., in coal basins, bituminous shale, bottom sediments, on the contact of rocks with guano, lichens, fungi, or some higher plants, and even on a surface of monuments. Thermal stability, structural evolution pathways and phase transition mechanisms of the calcium oxalates whewellite, weddellite and caoxite have been analyzed using single crystal and powder X-ray diffraction (XRD) [Izatulina et al., 2018]. The reduction of H<sub>2</sub>O content in the structures increases dimensionality from dimers and chains to the layered structural units and from rarefied to denser sheets within the compounds whose structures are based on the 2D units. While studying the phase transitions pathways within the calcium oxalate family, two crystalline compounds have been structurally characterized for the first time ( $\alpha\text{-CaC}_2\text{O}_4$  and  $\text{CaC}_2\text{O}_4 \cdot \text{H}_2\text{O}$ ), among which the novel COM modification has been obtained for the first time as well. The highest thermal expansion of these compounds is observed along the direction of the hydrogen bonds, whereas the lowest expansion and even contraction of the structures occur due to the displacement of neighbor layered complexes towards each other and to an orthogonalization of the monoclinic angles. Within the calcium oxalate family, whewellite should be regarded as the most stable crystalline phase at ambient conditions. Weddellite and caoxite transform to whewellite during dehydration-driven phase transition promoted by time and/or heating.

This work was supported by the Russian Science Foundation (no. 19-17-00141). The XRD measurements have been performed at the X-ray Diffraction Centre of St. Petersburg State University.

1. Izatulina A.R., Gurzhiy V.V., Krzhizhanovskaya M.G., Kuz'mina M.A., Leoni M., Frank-Kamenetskaya O.V. Hydrated Calcium Oxalates: Crystal Structures, Thermal Stability and Phase Evolution. *Cryst. Growth Des.*, 2018, 18, 5465–5478.

## Combined X-ray and neutron diffraction study of Zn/Mg substitution in Zn<sub>2</sub>SiO<sub>4</sub>-based solid solutions

Rotermel M.V.<sup>1</sup>, Pryanichnikov S.V.<sup>\*2</sup>, Sterkhov E.V.<sup>2</sup>, Sumnikov S.V.<sup>3</sup>, Titova S.G.<sup>2</sup>

<sup>1</sup>Institute of Solid State Chemistry Ural Branch of Russian Academy of Sciences, 620990 str. Pervomayskaya, 91, Ekaterinburg, Sverdlovskaya reg, Russia.

<sup>2</sup>Institute of Metallurgy Ural Branch of Russian Academy of Sciences, 620016, str. Amundsena, 101, Ekaterinburg, Russia

<sup>3</sup>Frank Laboratory of Neutron Physics, Joint Institute for Nuclear Research, 141980 Dubna, Moscow region, Russia

\*Correspondence email: stepian@mail.ru

Due to the thermal and chemical stability, Zn<sub>2</sub>SiO<sub>4</sub> zinc silicate has found technical application as a special-purpose pigment, and the introduction of dopant ions into its structure significantly expanded the scope of its use. Currently, Zn<sub>2-x</sub>Mg<sub>x</sub>SiO<sub>4</sub> solid solutions are most actively studied, which are promising as crystalline phosphors of green luminescence.

There are two different crystallographic positions of Zn in Zn<sub>2</sub>SiO<sub>4</sub>-structure. It is difficult enough to define occupancies each of Zn/Mg position from Rietveld-analysis of X-ray diffraction only. We performed high-resolution TOF-neutron diffraction experiment on Zn<sub>2-x</sub>Mg<sub>x</sub>SiO<sub>4</sub> with x= 0.1, 0.2, 0.28, 0.36 at HRFD, Dubna. Then we treated the results of both X-ray and neutron-diffraction using FullProf [1]. Crystallography data [2] were used as started, atoms of Mg were equally distributed between Zn1 and Zn2 positions. In the Figure 1 experimental, calculated and difference curves for Zn<sub>1.64</sub>Mg<sub>0.36</sub>SiO<sub>4</sub> and occupation of Zn/Mg-1 position are shown as result of the calculations.

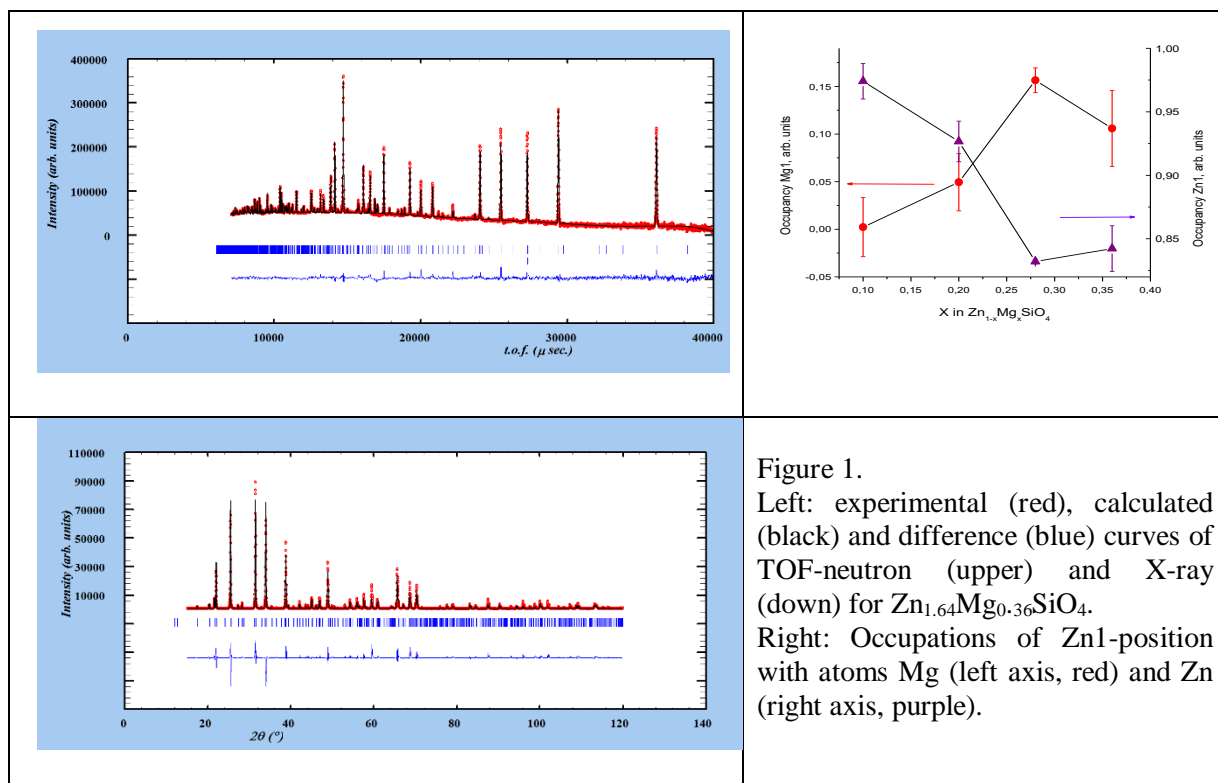


Figure 1.

Left: experimental (red), calculated (black) and difference (blue) curves of TOF-neutron (upper) and X-ray (down) for Zn<sub>1.64</sub>Mg<sub>0.36</sub>SiO<sub>4</sub>.

Right: Occupancies of Zn1-position with atoms Mg (left axis, red) and Zn (right axis, purple).

We have found that magnesium is distributed mainly in the Zn2-position.

The work was supported by RFBR, grant No 19-03-00189.

1. Rodriguez-Carvajal, J Physica B.(1993), 192, 55

2. K.-H. Klaska, J. C. Eck and D. Pohl. New investigation of willemite. Acta Cryst. (1978). B34, 3324-3325.

## Petrovite $\text{Na}_{10}\text{CaCu}_2(\text{SO}_4)_8$ , a new fumarolic mineral from the Tolbachik volcano, Kamchatka, Russia

Filatov S.K.<sup>1</sup>, Shablinskii A.P.<sup>2</sup>, Krivovichev S.V.<sup>1,3</sup>, Vergasova L.P.<sup>4</sup>, Moskaleva S.V.<sup>4</sup>

<sup>1</sup>St. Petersburg State University, 199034, University Emb. 7/9, St. Petersburg, Russia

<sup>2</sup>Grebenshchikov Institute of Silicate Chemistry, Russian Academy of Sciences, 199053, Makarov Emb. 2, St. Petersburg, Russia.

<sup>3</sup>Nanomaterials Research Centre, Kola Science Centre, Russian Academy of Sciences, 199034, Fersmana str. 14., Apatity, Russia

<sup>4</sup>Institute of Volcanology and Seismology, Far Eastern Branch of the Russian Academy of Sciences, 683006, Piip Boulevard 9, Petropavlovsk-Kamchatsky, Russia

\*Correspondence email: filatov.stanislav@gmail.com

The petrovite holotype was collected in the fumarole located on the west side of the micrograben of the Second scoria cone of the Northern Breakthrough of the Great Tolbachik fissure eruption that occurred in 1975–1976 on the Tolbachik volcano, Kamchatka, Far-Eastern Region, Russia. The specimen was found in 2000. The temperature of the surface of the fumarole was  $\sim 200^\circ\text{C}$ . The mineral is a product of exhalative fumarolic activity. The mineral is named in honour of Prof. Dr. Tomas Georgievich Petrov (b. 1931), a former chairman of the Crystallogenes Laboratory of the Department of Crystallography, St. Petersburg State University. The scientific activities of Tomas Petrov were devoted to the modelling of crystal growth of minerals. He was the first to develop the industrial technology of fabrication of jewellery malachite back in 1977. Tomas Petrov is the author of the two-parameter Alphabet for the Coding of Structural–Chemical Information and RHAT-catalogue of modal mineral compositions of magmatic rocks [1].

The mineral occurs as blue and green globular aggregates of tabular crystals up to 0.2 mm in maximal dimension, generally with gaseous inclusions. The streak is white and the lustre is vitreous. Fracture is conchoidal. No cleavage or parting was observed. The Mohs' hardness is 4. The calculated density based on the empirical formula and single-crystal unit-cell parameters is  $2.80 \text{ g/cm}^3$ . The mineral is optically biaxial (+), with  $\alpha = 1.498(3)$ ,  $\beta_{\text{calc}} = 1.500$ ,  $\gamma = 1.516(3)$  and  $2V = 20(10)$  ( $\lambda = 589 \text{ nm}$ ). No dispersion or pleochroism was observed. Petrovite is monoclinic, space group  $P2_1/c$ ,  $a = 12.6346(8)$ ,  $b = 9.0760(6)$ ,  $c = 12.7560(8) \text{ \AA}$ ,  $\beta = 108.75(9)^\circ$ ,  $V = 1385.1(3) \text{ \AA}^3$ ,  $Z = 2$ . The chemical composition of petrovite was studied using a TESCAN "Vega3" electron microprobe, operated at 20 kV and 700 pA, with a beam size of 220 nm –  $\text{Na}_2\text{O}$  25.03,  $\text{K}_2\text{O}$  0.80,  $\text{CaO}$  3.91,  $\text{CuO}$  12.64,  $\text{MgO}$  0.59,  $\text{SO}_3$  55.98, total 98.97 % (wt.%). The crystal structure of petrovite belongs to a new structure type. It contains four symmetrically independent  $\text{SO}_4$  tetrahedra with the average  $\langle \text{S–O} \rangle$  bond lengths in the range 1.45–1.47  $\text{Å}$ , in general agreement with the average value of 1.475  $\text{Å}$  given for sulfate minerals [2]. The short S–O bonds in several tetrahedra can be explained by libration effects, typical for the crystal structures with statistical or dynamical disorder. There are six Na and one Cu sites with different occupancies. The Cu atom forms five Cu–O bonds in the range 1.980–2.180  $\text{Å}$  and two long bonds  $\approx 2.9 \text{ Å}$  resulting in the formation of the  $\text{CuO}_7$  polyhedra with [5+2] coordination of Cu. The  $\text{CuO}_7$  polyhedra share corners with  $\text{SO}_4$  tetrahedra to form isolated  $[\text{Cu}_2(\text{SO}_4)_8]^{12-}$  anionic clusters, which are the fundamental building blocks for the structure of petrovite. The four Na sites, Na2, Na3, Na4 and Na5, are fully occupied by Na. In the Na1 site, the essential amount of Ca is present (ca. 47%). The Na6 site is only partially occupied (53%). The petrovite structure can also be described as a three-dimensional framework, taking into account the essential occupancy of the Na1 site by  $\text{Ca}^{2+}$  cations. In this description, the  $[\text{Cu}_2(\text{SO}_4)_8]^{12-}$  clusters are linked by  $\text{NaIO}_6$  octahedra, forming a porous three-dimensional framework with cavities occupied by  $\text{Na}^+$  cations [3].

This work was financially supported by the Russian Found of Basic Research, grant no. 18-29-12106. Technical support by the SPbSU X-ray Diffraction Centre is gratefully acknowledged.

1. Petrov T.G. Separation-Mixing as a Model of composition Evolution of any Nature. Journal on Systemics, Cybernetics and Informatics. 2014. V.12. P. 76–81.

2. Hawthorne F.C., Krivovichev S.V., Burns P.C. The crystal chemistry of sulfate minerals. Reviews in Mineralogy & Geochemistry. 2000. V.40. P. 1–112.

3. Filatov S.K., Shablinskii A.P., Krivovichev S.V., Vergasova L.P., Moskaleva S.V. Petrovite,  $\text{Na}_{10}\text{CaCu}_2(\text{SO}_4)_8$ , a new fumarolic sulfate from the Great Tolbachik fissure eruption, Kamchatka Peninsula, Russia. Mineralogical Magazine. 2020. 1–8

## Dobrovolskyite $\text{Na}_4\text{Ca}(\text{SO}_4)_3$ , a new fumarolic mineral with modular structure inherited from $\alpha\text{-Na}_2\text{SO}_4$

Shablinskii A.P.<sup>1</sup>, Filatov S.K.<sup>2</sup>, Vergasova L.P.<sup>3</sup>, Krivovichev S.V.<sup>1,2,4</sup>, Moskaleva S.V.<sup>3</sup>,  
Avdontseva E.Yu.<sup>2</sup>, Bubnova R.S.<sup>1</sup>

<sup>1</sup> Grebenshchikov Institute of Silicate Chemistry, Russian Academy of Sciences, 199053,  
Makarov Emb. 2, St.Petersburg, Russia

<sup>2</sup> St. Petersburg State University, 199034, University Emb. 7/9, St. Petersburg, Russia

<sup>3</sup> Institute of Volcanology and Seismology, Far Eastern Branch of the Russian Academy of  
Sciences, 683006, Piip Boulevard 9, Petropavlovsk-Kamchatsky, Russia

<sup>4</sup> Nanomaterials Research Centre, Kola Science Centre, Russian Academy of Sciences, 199034,  
Fersmana str. 14., Apatity, Russia

\*Correspondence email: shablinskii.andrey@mail.ru

Dobrovolskyite,  $\text{Na}_4\text{Ca}(\text{SO}_4)_3$  [1], is a new sulfate mineral from the Great Tolbachik fissure eruption. It occurs as aggregates of tabular crystals up to 1-2 mm in maximal dimension, with the abundant gas inclusions. Dobrovolskyite was found in close paragenesis with petrovite  $\text{Na}_{10}\text{CaCu}_2(\text{SO}_4)_8$  [1]. Single finds of grains of euchlorine  $\text{NaKC}_3\text{O}(\text{SO}_4)_3$ , tenorite  $\text{CuO}$ , anhydrite  $\text{CaSO}_4$ , and anglesite  $\text{PbSO}_4$  were established by electron microscopy data in pyroclastic material of magnesian basalt scoria. The empirical formula calculated on the basis of  $\text{O} = 12$  is  $(\text{Na}_{3.90}\text{K}_{0.10})_{\Sigma 4}(\text{Ca}_{0.45}\text{Mg}_{0.16}\text{Cu}_{0.12}\text{Na}_{0.10})_{\Sigma 0.83}\text{S}_{3.08}\text{O}_{12}$ . The crystal structure of dobrovolskyite was determined using single-crystal X-ray diffraction data; the space group is  $R\bar{3}$ ,  $a = 15.7223(2)$  Å,  $c = 22.0160(5)$  Å,  $V = 4713.1(2)$  Å<sup>3</sup>,  $Z = 18$  and  $R_1 = 0.072$ . The Mohs' hardness is 3.5. The mineral is uniaxial (+), with  $\omega = 1.489(2)$  and  $\varepsilon = 1.491(2)$  ( $\lambda = 589$  nm). The seven strongest lines of the powder X-ray diffraction pattern [ $d$ , Å (I, %) ( $hkl$ )] are: 11.58(40)(101); 5.79(22)(202); 4.54(18)(030); 3.86(88)(033); 3.67(32)(006); 2.855(50)(306); 2.682(100)(330). The mineral is named in honor of Prof. Dr. Vladimir Vitalievich Dolivo-Dobrovolsky (1927–2009), who was one of the leading Russian scientists in the field of petrology, crystal optics and crystal chemistry. The main results of these studies are presented in more than 100 articles, including fundamental work “The crystallography of the Earth's shells”, where he gave a numerical characterization of the symmetry of various Earth shells [2]. The dobrovolskyite crystal structure is composed of three symmetrically independent rods elongated along the  $c$  axis. The rods consist of six octahedral–tetrahedral  $[\text{Na}(\text{SO}_4)_6]^{11-}$  or  $[\text{Ca}(\text{SO}_4)_6]^{10-}$  clusters composed of  $\text{NaO}_6$  octahedron which share corners with six  $\text{SO}_4$  tetrahedra. Crystal structure of metathénardite contains parent FBB for these octahedral–tetrahedral clusters. The parent FBB consists of octahedron surrounded by six disordered tetrahedra. Minerals similar to dobrovolskyite were formed upon cooling of the high-temperature phase containing the parent FBB. The cluster that will be inherited from the parent FBB is determined primarily by the ionic radius and charge of the cations in the mineral.

This work was financially supported by the Russian Found of Basic Research, grant no. 18-29-12106. Technical support by the SPbSU X-ray Diffraction Centre is gratefully acknowledged.

1. Shablinskii A.P., Filatov S.K., Vergasova L.P., Moskaleva S.V., Avdontseva E.Yu., Bubnova R.S. Dobrovolskyite, IMA 2019-106. European Journal Of Mineralogy, 2020. V. 32. doi.org/10.5194/ejm-32-275-2020

2. Filatov S.K., Shablinskii A.P., Krivovichev S.V., Vergasova L.P., Moskaleva S.V. Petrovite,  $\text{Na}_{10}\text{CaCu}_2(\text{SO}_4)_8$ , a new fumarolic sulfate from Tolbachik fissure eruption, Kamchatka Peninsula, Russia. Mineralogical Magazine, 2020. P. 1–8. doi:10.1180/mgm.2020.53

3. Dolivo-Dobrovolskiy V.V. The crystallography of the Earth's shells. Proceedings of the Russian Mineralogical Society, 1984. V. 113(5). P. 586–590.

## Study of alumina-containing systems using X-ray diffraction methods

Shefer K.I. <sup>1,2</sup>

<sup>1</sup> Borskov Institute of Catalysis, Siberian Branch of Russian Academy of Sciences, Novosibirsk, Russia, 630090, Lavrentiev Ave. 5, Novosibirsk, Russia.

<sup>2</sup> Novosibirsk State University, 630090, Pirogova str. 2, Novosibirsk, Russia.

\*Correspondence email: shefer@catalysis.ru

This work is devoted to the characterization of several systems containing alumina using X-ray diffraction methods. Such systems are extensively applied in catalysis as adsorbents, catalysts, and catalyst support. Alumina properties, as well as properties of obtained from them catalysts, depend on various factors, including synthesis conditions. The appearance of novel methods of alumina synthesis requires research on their structure and properties. In the case of supported catalysts, the investigation often starts from the consideration of precursors of catalyst support and active component and ends with the study of prepared and tested in reaction catalysts. Such materials as alumina and based on them catalysts exist often in nanoscale view. Therefore, they are interesting objects for research and require special methods for their investigation, including structure investigation. We can extract the most reliable structural information from direct structural diffraction methods. In the case of disperse alumina containing materials the use of special methods that take into account the specific features of X-ray scattering from small objects is required.

The catalyst's composition may include various modifications of alumina. In this work, we considered aluminas obtained in different ways and having different compositions. Structural features of alumina-containing systems are examined using the complex of diffraction methods: XRD phase analysis, full profile analysis, modeling of diffraction patterns, pair distribution function (PDF) analysis.

The work was supported by the Russian Foundation for Basic Research (project #19-03-00595) and by the Ministry of Science and Higher Education of the Russian Federation (project # AAAA-A17-117041710079-8).

## **7. Poster session**



## Crystal chemistry and high-temperature X-ray diffraction of hydrated iron sulfate minerals.

Abdulina V.R.<sup>1,\*</sup>, Siidra O.I.<sup>1,2,3</sup>

<sup>1</sup> Department of Crystallography, St. Petersburg State University, 199034, University Emb. 7/9, St. Petersburg, Russia.

<sup>2</sup> Kola Science Center, Russian Academy of Sciences, 184200, ul. Fersmana 14, Apatity, Russia.

<sup>3</sup> Grebenshchikov Institute of Silicate Chemistry, Russian Academy of Sciences, 199053, Makarov Emb. 2, St. Petersburg, Russia.

\* Correspondence author email: abdnik@yandex.ru

Hydrated iron sulphate minerals, coquimbite  $\text{Fe}^{3+}_2(\text{SO}_4)_3 \cdot 9\text{H}_2\text{O}$ , römerite  $\text{Fe}^{2+}\text{Fe}^{3+}_2(\text{SO}_4)_4 \cdot 14\text{H}_2\text{O}$  and copiapite  $\text{Fe}^{2+}\text{Fe}^{3+}_4(\text{SO}_4)_6(\text{OH})_2 \cdot 20\text{H}_2\text{O}$  are found as secondary minerals in the oxidation zones of iron sulfide deposits in arid regions of the Earth. Noteworthy, the experimental mineralogy of sulfates has intensified in the last decade due to the new data obtained via satellites and rovers on Mars surface. The sulfate content reaches up to 30% at some sampling points on Mars surface. Many of the sulfate minerals are hydrated, which indicates the existence of water on Mars in the past [1].

Thermal behavior of the coquimbite, römerite and copiapite samples from Alcaparossa mine (Chile) has been studied in air by means of a Rigaku Ultima X-ray diffractometer ( $\text{CoK}\alpha$  radiation). The samples were prepared from heptane's suspension on a Pt-Rh plate. Unit-cell parameters at different temperatures were refined by least-square methods. Main coefficients of the thermal expansion tensor were determined using linear approximation of temperature dependences by the *ThetaToTensor* program.

The diffraction maxima of coquimbite gradually disappear at approximately 175°C. The structure of römerite is stable up to 85°C. Copiapite is the most unstable mineral and decays at 14°C. All three minerals become amorphous after dehydration. At 275°C mikasaite  $\text{Fe}_2(\text{SO}_4)_3$  starts to crystallize. Thermal expansion features for all three minerals will be discussed.

This work was financially supported by the Russian Science Foundation through the grant 16-17-10085. Technical support by the SPbSU X-ray Diffraction and Geomodel Resource Centers is gratefully acknowledged.

1. Vaniman D.T., Bish D.L., Chipera S.J., Fialips C.I., Carey J.W., Feldman W.G. Magnesium sulphate salts and the history of water on Mars. *Nature*. 2004. 431. 663-665.

## Monocrystal $\text{Pr}_{0.65}(\text{Ca}_{0.8}\text{Sr}_{0.2})_{0.35}\text{MnO}_3$ : structure, magnetothermal and magnetoelectrical properties

Abramovich A.I. , Bakaev S.E.

Department of Chemistry, M.V. Lomonosov Moscow State University, Moscow, Russia  
E-mail: a-abramovich@yandex.ru

Modern technology companies strive to improve devices - make them compact and energy-saving. For this it is necessary that the same element in the microcircuit simultaneously performs several functions. Magnetic semiconductors, in particular, manganites with a perovskite-like structure ( $\text{R}_{1-x}\text{A}_x\text{MnO}_3$ , where R = La, Pr, Nd, Sm, etc., A =  $\text{Sr}^{2+}$ ,  $\text{Ca}^{2+}$ ,  $\text{Ba}^{2+}$  etc.) can claim this role. Manganites are characterized by a strong interconnection between the crystal lattice with electronic and magnetic subsystems, which leads to a number of unusual properties. In the temperature region of the magnetic phase transition giant values of magnetoresistance, magnetostriction, thermopower, magnetothermopower, magnetocaloric effect etc. are observed.

The aim of this work is to establish the relationship between the structure and physical properties (resistance, magnetoresistance, thermopower and magnetothermopower) of the  $\text{Pr}_{0.65}(\text{Ca}_{0.8}\text{Sr}_{0.2})_{0.35}\text{MnO}_3$  monocrystal.

The electrical resistance and magnetoresistance, thermopower and magnetothermopower of the studied monocrystal were measured in the temperature range 90–300 K in magnetic fields of 1–15 kOe. The temperature and field dependences of these parameters are analyzed. It was found that the resistivity of the sample increases with decreasing temperature. Starting from a temperature of 120 K it sharply increases and at 104 K it passes through a maximum. Influence of a magnetic field leads to a decrease in resistivity. Negative magnetoresistance passes through a maximum at 104 K and reaches a value of 45% in a magnetic field of 15 kOe. We emphasize that the maximum of resistance and magnetoresistance are observed at the temperature exceeding the temperature of the magnetic phase transition (85 K) by about 20 K.

When approaching the temperature of the magnetic phase transition from the high temperature side, a sharp increase in the thermopower was found. So, at the temperature of 98 K, the thermopower reaches 250  $\mu\text{V}/\text{K}$ , which is comparable with the thermopower of widely used thermoelectric materials based on bismuth telluride. When a magnetic field is applied, the thermopower decreases, and the magnetothermopower reaches 50% in a magnetic field of 15 kOe at 98 K.

A feature of this compound is its magnetic and structural heterogeneity. The charge-ordered antiferromagnetic phase coexists with the ferromagnetic phase, and these phases have a different crystalline structure. It is assumed that the detected large values of thermopower and magnetothermopower are caused by these inhomogeneities.

## High-temperature crystal chemistry of fluorellestadite

Avdontseva M.S.<sup>1\*</sup>, Zolotarev A.A. Jr.<sup>1</sup>, Krzhizhanovskaya M.G.<sup>1</sup>, Krivovichev S.V.<sup>1,2</sup>

<sup>1</sup>Institute of Earth Sciences, St.Petersburg State University, 199034, University Emb. 7/9, St. Petersburg, Russia.

<sup>2</sup>Federal Research Center, Kola Science Center, Russian Academy of Sciences, 184209, Fersmana str., Apatity, Russia

\*Correspondence email: m.avdontceva@spbu.ru

Fluorellestadite,  $\text{Ca}_5(\text{SiO}_4)_{1.5}(\text{SO}_4)_{1.5}\text{F}$ , is a sulfate-silicate, which belongs to the ellestadite group along with chlorellestadite,  $\text{Ca}_5(\text{SiO}_4)_{1.5}(\text{SO}_4)_{1.5}\text{Cl}$ , hydroxyllelestadite,  $\text{Ca}_5(\text{SiO}_4)_{1.5}(\text{SO}_4)_{1.5}\text{OH}$ , and mattheddleite,  $\text{Pb}_5(\text{SiO}_4)_{1.5}(\text{SO}_4)_{1.5}\text{OH}$ . All these minerals are members of the apatite supergroup with the general chemical formula  $^{\text{IX}}\text{M}_1^{\text{VII}}\text{M}_2^{\text{IV}}\text{M}_3^{\text{IV}}(\text{TO}_4)_3\text{X}$ , where  $\text{M} = \text{Ca}^{2+}, \text{Pb}^{2+}, \text{Mn}^{2+}, \text{Ba}^{2+}, \text{Sr}^{2+}, \text{Na}^+, \text{Ce}^{3+}, \text{La}^{3+}, \text{Y}^{3+}, \text{Bi}^{3+}$ ;  $\text{T} = \text{P}^{5+}, \text{As}^{5+}, \text{V}^{5+}, \text{Si}^{4+}, \text{S}^{6+}, \text{B}^{3+}$ ;  $\text{X} = \text{F}^-, \text{Cl}^-, \text{OH}^-$  [1]. Fluorellestadite was first described in burned coal dumps of the Chelyabinsk coal basin by Chesnokov et al.[2]. Later fluorellestadite was found in a number of natural localities associated with the ultrahigh-temperature – low-pressure pyrometamorphic and combustion metamorphic metacarbonate rocks such as Hatrurim Formation (Israel), Mottled Zone (Jordan), Shadil-Khokh volcano (South Ossetia), Bellerberg volcano (Germany), etc. [3-4].

Thermal behavior of fluorellestadite was studied in air by the high-temperature powder X-ray diffraction (HTXRD) method using a Rigaku Ultima IV ( $\text{CoK}\alpha_{1+2}$  radiation, 40 kV/30 mA, Bragg-Brentano geometry, PSD D-Tex Ultra) diffractometer with a high-temperature attachment. The temperature range of the measurement was 20 - 800 °C with temperature steps of 20 °C. Thin powder sample was deposited on a Pt sample holder (20x12x2 mm<sup>3</sup>) using an ethanol suspension. Silicon was used as an external standard. The calculated thermal expansion coefficients indicate that fluorellestadite,  $\text{Ca}_5(\text{SiO}_4)_{1.5}(\text{SO}_4)_{1.5}\text{F}$ , expands almost isotropically in the temperature range 25-800 °C with the  $\alpha_a/\alpha_c$  ratio changing from 0.98 to 1.00. The observed almost isotropic thermal expansion of fluorellestadite is very similar to that observed for fluorapatite,  $\text{Ca}_5(\text{PO}_4)_3\text{F}$ . This could be explained by the similar chemical composition, which differs only in the occupancy of the tetrahedral sites. According to Chernorukov et al. [5] the thermal expansion anisotropy in hexagonal apatite-structured compounds directly depends on the s-element content with the anisotropy increasing in the row  $\text{Ca} < \text{Sr} < \text{Ba} < \text{Pb} < \text{Cd}$ .

The study was supported by the Russian Foundation for Basic Research (grant № 19-05-00628).

1. Pasero M., Kampf A.R., Ferraris C., Pekov I.V. Rakovan J., White T.J. Nomenclature of the apatite supergroup minerals. *European Journal of Mineralogy*. 2010. V. 22. P. 163-179.

2. Chesnokov B.V., Bazhenova L.F., Bushmakina A.F. Fluorellestadite  $\text{Ca}_{10}[(\text{SO}_4),(\text{SiO}_4)]_6\text{F}_2$  – a new mineral. *Zapiski Rossiiskogo Mineralogicheskogo Obshchestva*. 1987c. V. 116. P. 743-746.

3. Galuskina I.O., Vapnik Y., Lazic B., Armbruster T., Murashko M. and Galuskin E.V. Harmunite  $\text{CaFe}_2\text{O}_4$ : A new mineral from the Jabel Harmun, West Bank, Palestinian Autonomy, Israel. *American Mineralogist*. 2014. V. 99. P. 965-975.

4. Sokol E.V., Kokh S.N., Sharygin V.V., Danilovsky V.A., Seryotkin Y.V., Liferovich R., Deviatiiarova A.S., Nigmatulina E.N. and Karmanov N.S. Mineralogical diversity of  $\text{Ca}_2\text{SiO}_4$ -bearing combustion metamorphic rocks in the Hatrurim Basin: Implications for storage and partitioning of elements in oil shale clinkering. *Minerals*. 2019. V. 9(8). P. 465

5. Chernorukov N.G., Knyazev A.V., Bulanov E.N. Phase transition and thermal expansion of apatite-structured compounds. *Inorganic Materials*. 2011. V. 47. P. 172-177

## **In-situ time-resolved X-ray diffraction studies of crystalline materials under static mechanical load**

Akkuratov V.I.<sup>1,2\*</sup>, Targonskiy A.V.<sup>1,2</sup>, Eliovich I.A.<sup>1,2</sup>, Protsenko A.I.<sup>1,2</sup>, Pisarevsky Yu.V.<sup>1,2</sup>, Blagov A.E.<sup>1,2</sup>

<sup>1</sup> Federal Scientific Research Center «Crystallography and photonics», Russian Academy of Science, 119333, Leninsky pr. 59, Moscow, Russia.

<sup>2</sup> National Research Center «Kurchatov Institute», 123182, Akademika Kurchatova pl. 1, Moscow, Russia.

\*Correspondence email: akkuratov.val@gmail.com

A new approach to time-resolved X-Ray experiments implementation at both laboratory X-Ray sources and synchrotron facilities is presented. Proposed X-Ray diffraction method is based on adaptive X-ray optics and applied for investigation of irreversible deformation processes in crystalline materials under external loading with time resolution. This method allows receiving information about changes in atomic structure recording rocking curves (dependence of X-ray radiation intensity in the vicinity of Bragg angle) and reciprocal space maps (RSM) by fast tunable X-Ray optical element. This element consists of a piezoelectric monolithic bimorph lithium niobate (LiNbO<sub>3</sub>) single crystal and a silicon plate attached to its face. When electrical signal is applied to the lithium niobate, it is possible to control the spatial position of the diffracted X-ray beam [1]. Time resolution of proposed method scales up to milliseconds for rocking curve record and up to hundreds of milliseconds in RSM case, and mainly depending on brilliance of X-ray.

The presented approach makes it possible to obtain information about changes in crystal structure with a lower time delay compared to existing methods [2].

The evolution of the defective structure of crystalline materials subjected to controllable and measured uniaxial mechanical compression (load up to MPa range) was investigated using the proposed method. The essence of such evolution is defect multiplication, displacement and shifting of atomic planes, which can be easily determined by changes in rocking curve and RSM parameters. This structural process is of great interest, as it is possible to observe defects behavior in a crystal during elastic deformation with time resolution.

The reported study was funded by RFBR and DFG 19-52-12029 and by RFBR according to the research project №18-32-20108.

1. Blagov A. E. et al. 2017. Bimorph Actuator: a New Instrument for Time-Resolved X-ray Diffraction and Spectroscopy. *Experimental Techniques*. V. 41. P. 517–523.

2. Eliovich Y. A. et al. Rocking Curve Measurement for Deformed Crystals Using an Adaptive X-Ray Optical Bending Monochromator *Experimental Techniques*. *Crystallography Reports*. 2018. V. 63. P. 708-712.

## Transformation of Fe-Cr Catalytic Systems under Chemical Reactions by elevated temperature

Bogdan T.V.<sup>1</sup>, Mishanin I.I.<sup>2</sup>, Koklin A.E.<sup>2</sup>, Smirnov A.V.<sup>1</sup>, Bogdan V.I.<sup>1,2</sup>

<sup>1</sup> M.V. Lomonosov Moscow State University, Department of Chemistry, 19991, Leninskyie Gory, 1-3, Moscow, Russia.

<sup>2</sup> N.D. Zelinsky Institute of Organic Chemistry, the Russian Academy of Sciences, 119991, Leninsky Prospekt, 47, Moscow, Russia.

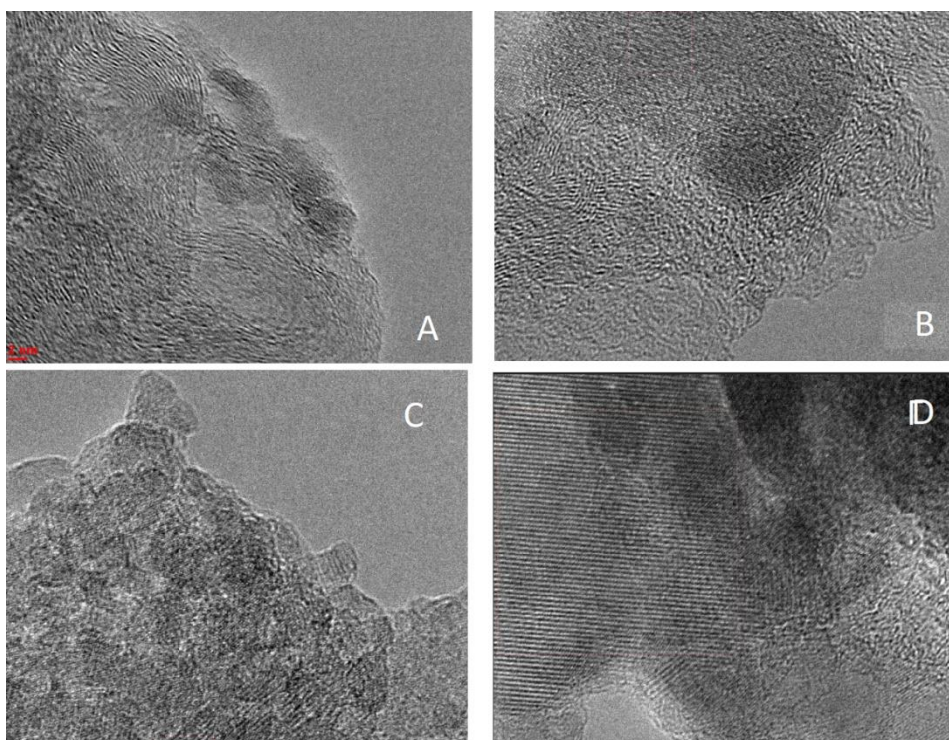
\*Correspondence email: chemist2014@yandex.ru

The results of studying the structure of Fe – Cr oxide catalysts supported on carbon-carrier “Sibunit” and  $\text{MgAl}_x\text{O}_y$  (“Puralox MG 30 Spinel” from Sasol) are presented before and after the chemical oxidative dehydrogenation reaction of ethylene at 650° C and normal pressure. Data on the structure of the systems were obtained by TEM, XRD, and thermomagnetometry.

Catalyst samples with concentrations of 5 wt.% Fe and 5 wt.% Cr were prepared by the method of single impregnation of the carrier with water by solutions of  $\text{Fe}(\text{NO}_3)_3 \cdot 9 \text{H}_2\text{O}$  and  $\text{Cr}(\text{NO}_3)_3 \cdot 9 \text{H}_2\text{O}$  salts. After impregnation, the samples were dried in air for 12 hours. To decompose the deposited metal nitrates, the samples were calcined in a helium flow ( $= 60 \text{ ml / min}$ ) for four hours at 450 ° C.

The following phase transformations can occur on the surface of Fe-containing catalysts in a reducing medium:  $\text{Fe}_2\text{O}_3 \rightarrow \text{Fe}_3\text{O}_4 \rightarrow \text{FeO} \rightarrow \text{Fe}$ . Sibunit exhibits reducing properties. It was found that the initial catalyst on sibunit (system Fe-Cr/C, Fig. A) is a polyphase sample in which, along with metal (III) oxides  $\text{Fe}_2\text{O}_3$ ,  $\text{Cr}_2\text{O}_3$ ,  $\text{FeCrO}_3$ , also FeO and metal phases are detected. The catalyst particles are in a finely divided state. Under the reaction conditions, an inhomogeneous multiphase catalytic system is formed: the magnetometry method indicates the existence of a metal phase, carbides and iron oxides. The catalyst supported on Puralox (Fe-Cr/ $\text{MgAl}_x\text{O}_y$ , Fig. B) is also polyphase, however, it is characterized by a higher degree of crystallinity of the supported particles. During the reaction, there is an increase in the degree of crystallinity of the catalysts and particle size (Fe-Cr / C Fig. C, Fe-Cr /  $\text{MgAl}_x\text{O}_y$  Fig. D), while in the Fe-Cr /  $\text{MgAl}_x\text{O}_y$  system, the predominant formation of phases with spinel structure occurs, while carbide phases were detected on Fe-Cr / C.

The principal difference in the catalytic effect of two polycrystalline Fe-Cr /  $\text{MgAl}_x\text{O}_y$  and Fe-Cr / C samples is a significant methane emission in the case of the last sample. The results of our work show that this is due to the formation of a catalytically active carbide phase (Hägg carbide).



## Interaction dynamics and phase formation in a ternary system $\text{Li}_2\text{O} - \text{B}_2\text{O}_3 - \text{MoO}_3$ during synthesis from the primary components

Zakalyukin R.M.<sup>1</sup>, Levkevich E.A.<sup>1</sup>, Zimina G.V.<sup>1</sup>, Patrina Zh.G.<sup>2</sup>, Marchenko A.A.<sup>2</sup>,  
Busurin S.M.<sup>2\*</sup>

<sup>1</sup> MIREA - Russian Technological University, 119454, Vernadskogo ave., 78, Moscow, Russia.

<sup>2</sup> OOO "NTO "IRE-Polus", 141190, Vvedenskogo sq, 1, buld. 3, Fryazino, Moscow region, Russia.

\*Correspondence email: sbusurin@ntoire-polus.ru

The lithium borate system is widely used in crystal growth technique and glasses production [1]. Glassy lithium borates are used as gamma and neutron scintillators, at the same time crystalline lithium borates are used as piezoelectric and nonlinear optical materials. Phase formation in the system  $\text{Li}_2\text{O} - \text{B}_2\text{O}_3$  is completely unexplored and there are a number of unsolved problems. Particularly, phase formation near lithium triborate  $\text{Li}_2\text{B}_6\text{O}_{10}$  ( $\text{LiB}_3\text{O}_5$ ) is of great practical importance.

Lithium triborate, which is also known as LBO crystal, has unique optical properties and it is widely known as one of the most attractive materials of nonlinear optics. One of the difficulties is that  $\text{Li}_2\text{B}_6\text{O}_{10}$  compound melts incongruently and can be grown only by the flux method. Therefore, investigation of binary and ternary systems, containing the lithium triborate, is an important practical task. A large number of works on the study of the ternary system  $\text{Li}_2\text{O} - \text{B}_2\text{O}_3 - \text{MoO}_3$  have been published, however, to date, the compositions of the forming phases and the temperatures of their phase transitions have not been determined.

A ternary system  $\text{Li}_2\text{O} - \text{B}_2\text{O}_3 - \text{MoO}_3$  was studied, namely, dynamics of interaction and phase formation along  $\text{LiB}_3\text{O}_5 - \text{Li}_4\text{Mo}_5\text{O}_{17}$  and  $\text{LiB}_3\text{O}_5 - \text{Li}_4\text{Mo}_5\text{O}_{17}$  system sections.

This work was carried out by methods of solid-phase synthesis and X-Ray phase analysis. To study the interaction of the components of the cross sections, samples of components mixtures were prepared with boric acid  $\text{H}_3\text{BO}_3$  (chemically pure), lithium carbonate  $\text{Li}_2\text{CO}_3$  (chemically pure) and ammonium molybdate tetrahydrate  $(\text{NH}_4)_6\text{Mo}_7\text{O}_{24} \cdot 4\text{H}_2\text{O}$  (analytical grade).

Synthesis technique: samples of substances were prepared based on the calculation of the components of quasi-binary sections  $\text{LiB}_3\text{O}_5 - \text{Li}_4\text{Mo}_5\text{O}_{17}$  and  $\text{LiB}_3\text{O}_5 - \text{Li}_4\text{Mo}_5\text{O}_{17}$ . The test-charges were carefully ground in an agate mortar and placed in a muffle furnace at a temperature range 350-575°C for hardening. The samples tempered were investigated with X-Ray phase analysis.

The synthesis of lithium borate samples showed that, depending on the composition of the sample, the reaction proceeds differently: the larger the composition of boron, the earlier the reaction begins to proceed.

The reaction in the mixture of the starting components proceeds sequentially: first, boric anhydride is consumed in the reaction with lithium carbonate, then molybdenum oxide reacts with the formed borates. The composition of the reaction products – a mixture of intermediate lithium borates – reacting with molybdenum oxide to form molybdates, moves along the connode in the direction of the  $\text{MoO}_3$  peak of the  $\text{Li}_2\text{O} - \text{B}_2\text{O}_3 - \text{MoO}_3$  concentration triangle, crossing several crystallization fields of different phases, which can affect the formation of structural fragments of boron-oxygen frame in the composition.

Along both  $\text{LiB}_3\text{O}_5 - \text{Li}_4\text{Mo}_5\text{O}_{17}$  and  $\text{LiB}_3\text{O}_5 - \text{Li}_4\text{Mo}_5\text{O}_{17}$  system sections at a temperature range 500-575°C two unidentified phases are formed, perhaps real composition of the first phase is located away from the section in the direction of the apex of the  $\text{Li}_2\text{O}$  concentration triangle  $\text{Li}_2\text{O} - \text{B}_2\text{O}_3 - \text{MoO}_3$ . The second phase is found in small quantities and can be characterized as a low-temperature phase or as an intermediate product of solid-phase synthesis.

The study made it possible to determine the nature and sequence of interaction of components in systems, that is, the sequence of reactions, which is of great interest, as it helps with further decoding and interpretation of diffraction patterns.

1. Rousse G., Baptiste B., Lelong G. Crystal Structures of  $\text{Li}_6\text{B}_4\text{O}_9$  and  $\text{Li}_3\text{B}_{11}\text{O}_{18}$  and Application of the Dimensional Reduction Formalism to Lithium Borates. 2014. V. 53. P. 6034-6041.

## Evolution of the structure $\text{Nd}_2\text{BaMn}_2\text{O}_7$ manganite in the temperature range of 20-400°C

Fedorova O.M.<sup>1</sup>, Vedmid' L.B.<sup>1\*</sup>, Dimitrov V.M.<sup>1</sup>

<sup>1</sup>Institute of Metallurgy of the Ural Branch of the Russian Academy of Science, 620016, Amundsen str. 101, Yekaterinburg, Russia.

\*Correspondence email: elarisa100@mail.ru

Perovskites of rare earth elements  $\text{Ln}_2\text{BaMn}_2\text{O}_7$  ( $\text{Ln}=\text{Rare Earth}$ ) with the homological series  $\text{AO}(\text{ABO}_3)_2$  and structural type  $\text{Sr}_3\text{Ti}_2\text{O}_7$  have a number of unique properties, one of which is the manifestation of the effect of colossal magnetoresistance (CMR) [1-2]. The synthesis of single-phase oxides is much complex, due to a number of phase structural transformations are observed in them during heating, which depend on the partial pressure of oxygen in the gas atmosphere during heating, the cooling rate of samples, and the other factors. Changes in the crystal structure may affect to the functional properties of manganites. Therefore, it is important to design conditions for the synthesis of  $\text{Ln}_2\text{BaMn}_2\text{O}_7$  manganites and study their stability when changing external parameters. Synthesized at  $T=1300^\circ\text{C}$  and partial pressure of oxygen  $P_{\text{O}_2} = 10^{-5}\text{atm}$  homogeneous  $\text{Nd}_2\text{BaMn}_2\text{O}_7$  has an orthorhombic crystal structure (np.rp. Fmmm) at room temperature. When the sample is heated, its crystal structure changes. The temperature region of the phase transition were determined by high-temperature radiography (HFA): Fmmm  $\rightarrow$  I4/mmm in the  $\text{Nd}_2\text{BaMn}_2\text{O}_7$  manganite. The transition starts at a temperature of 250°C, and when it reaches 300°C, the cell parameters are fixed, which are typical for the tetragonal crystal structure (of the I4/mmm type). The obtained data were confirmed by differential scanning calorimetry (DSC). The refinement of the structure by the Rietveld method using the GSAS software package revealed the main difference between the two structures: in the orthorhombic four planar oxygen atoms in the  $\text{MnO}_6$  bipyramid form a rectangle with a manganese atom in the center, and in a tetragonal one, a square.

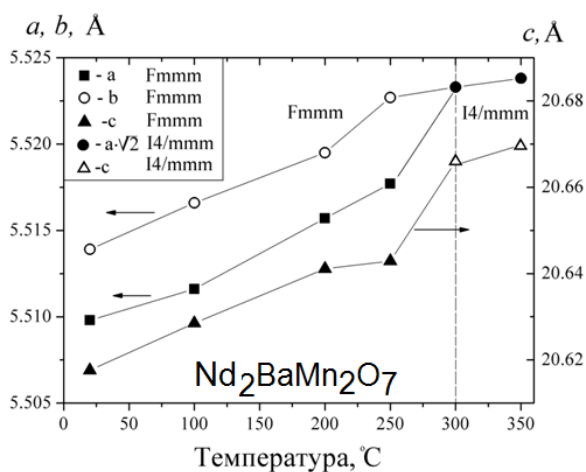


Fig. The temperature dependence of the unit cell parameters  $\text{Nd}_2\text{BaMn}_2\text{O}_7$

This work was carried out as part of the implementation of the RFBR project № 19-29-12013

1. Liu R.S., Jang L.Y., Chen J.M., WU J.B., Liu R.G., Lin J.G. and Huang C.Y. X-ray absorption near edge structure studies of colossal magnetoresistance ferromagnet  $(\text{La}_{1.4}\text{Sr}_{1.6})\text{Mn}_2\text{O}_7$ . Solid State Communications. 1998. Vol. 105. No. 9. P. 605-608.

2. Missyul, A. B., Zvereva, I. A., Palstra, T. T. M. The formation of the complex manganites  $\text{LnSr}_2\text{Mn}_2\text{O}_7$  ( $\text{Ln}=\text{La, Nd, Gd}$ ). Materials Research Bulletin. 2012. V. 47(12). P.4156-4160.

## Synthesis of nanocrystalline $Gd_2Zr_2O_7$ using mechanical activation

Vinogradov V. Yu.<sup>1</sup>, Kalinkin A.M.<sup>1</sup>, Kalinkina E.V.<sup>1</sup>

<sup>1</sup> Tananaev Institute of Chemistry, Subdivision of the Federal Research Centre “Kola Science Centre of the Russian Academy of Sciences”, Akademgorodok 26a, Apatity, Murmansk Region 184209, Russia

\*Correspondence email: vinogradov-vu@yandex.ru

Rare earth zircoates  $Ln_2Zr_2O_7$  (where Ln is rare earth element) have been intensively investigated over the last decade as promising candidates for various applications such as thermal barrier coatings, catalysts, solid oxide fuel cells, host material for radioactive nuclear waste storage, etc [1].

It has been well known that ceramics prepared from nanocrystalline  $Ln_2Zr_2O_7$  powders offers major advantages over the coarser-grained ceramics due to unique thermal, mechanical, electrical, and other characteristics [2].

For preparation of nanocrystalline  $Ln_2Zr_2O_7$  apply a number of approaches such as sol–gel, hydrothermal, Pechini method, hydroxide coprecipitation–calcination and solid-phase synthesis. The last two methods are recognized as the most effective. The main advantages of the hydroxide coprecipitation–calcination are the simplicity, reproducibility of the results, and the absence of the need to use organic reagents. It is necessary note that this method is sensitive to changes in external conditions (mixing speed, pH value), as a result of which, upon further calcination, single-phase products are not always obtained [3]. But at the same time, one of the most common methods for producing  $Gd_2Zr_2O_7$  is the solid-phase synthesis due to a number of primary factors, such as the absence of liquid phases, which significantly reduces the possibility of contamination and loss of the reaction mixture. Also, the absence of liquid phases eliminates the need to dispose of liquid effluents and chemical synthesis products. But despite the advantages, this method also has a number of disadvantages, such as: synthesis from oxides requires much more stringent synthesis conditions (an increase in sintering temperatures, sintering pressure, the use of mechanical activation of the reacting components, which increases any costs, and therefore the cost received material.

The mechanical activation of the reaction mixture significantly accelerates the formation of  $Gd_2Zr_2O_7$  during subsequent calcination.

Compared with ceramics with a microcrystalline structure, nanosized ceramics based on rare-earth zirconates have increased radiation resistance, reduced thermal conductivity, and higher oxygen-ion conductivity [4].

1. Popov V.V., Petrunin V.F., Korovin S.A., Menushenkov A.P., Kashurnikova O.V., Chernikov R.V., Yaroslavtsev A.A., Zubavichus Y.V. Formation of nanocrystalline structures in the  $Ln_2O_3$ - $MO_2$  systems (Ln = Gd, Dy; M = Zr, Hf). Russian Journal of Inorganic Chemistry. 2011. V. 56. P.1538–1544.

2. Mandal B.P., Dutta A., Deshpande S.K., Basu R.N., Tyagi A.K. Nanocrystalline  $Nd_{2-y}Gd_yZr_2O_7$  pyrochlore: facile synthesis and electrical characterization. Journal of Materials Research. 2009. V. 24 P.2855–2862.

3. Zhou L., Huang Z., Qi J., Feng Z., Wu D., Zhang W., Yu X., Guan Y., Chen X., Xie L., Sun K., Lu T. Thermal-driven fluorite–pyrochlore–fluorite phase transitions of  $Gd_2Zr_2O_7$  ceramics probed in large range of sintering temperature. Metallurgical and Materials Transactions A. 2016. V. 47 P.623–630.

4. Zhang J.M., Lian J., Fuentes A.F., Zhang F.X., Lang M., Lu F.Y., Ewing R.C. Enhanced radiation resistance of nanocrystalline pyrochlore  $Gd_2(Ti_{0.65}Zr_{0.35})_2O_7$ . Applied Physics Letters. 2009. V. 94. P. 243110.



## Thermal analysis and thermal expansion of volborthite $\text{Cu}_3\text{V}_2\text{O}_7(\text{OH})_2 \cdot 2\text{H}_2\text{O}$

Vladimirova V.A.<sup>1</sup>, Siidra O.I.<sup>1,2,3</sup>

<sup>1</sup> St. Petersburg State University, 199155, Dekabristov Lane 16, St. Petersburg, Russia.

<sup>2</sup> Center for Nanomaterial Science, Kola Science Center, 189209, Fersman street, Apatity, Russia.

<sup>3</sup> Grebenshchikov Institute of Silicate Chemistry, Russian Academy of Sciences, 199053, Makarov Emb. 2, St. Petersburg, Russia.

Volborthite [tricopper(II) divanadium(V) heptaoxide dihydroxide dihydrate] is an uncommon secondary mineral formed in the oxidized zone of vanadium-bearing mineral deposits. The studied sample of volborthite originated from the occurrence at Tyuya-Muyun Cu-V-U deposit (Radium Mine), Kyrgyzstan.

Single crystal of studied volborthite  $\text{Cu}_3\text{V}_2\text{O}_7(\text{OH})_2 \cdot 2\text{H}_2\text{O}$  selected for X-ray diffraction (XRD) data collection was tested on a Bruker APEX II DUO X-ray diffractometer with a Mo- $\text{I}\mu\text{S}$  microfocus X-ray tube ( $\lambda = 0.71073 \text{ \AA}$ ). The refined unit cell parameters of the studied volborthite for monoclinic space group, C2/m,  $a = 10.617(3)$ ,  $b = 5.8842(15)$ ,  $c = 7.2042(18) \text{ \AA}$ ,  $\beta = 94.559(5)^\circ$ ,  $R_1 = 0.0542$  are comparable with the data published for this phase. The results of chemical analyses lead to empirical formula  $(\text{Cu}_{2.84}, \text{Zn}_{0.2}, \text{Ni}_{0.06})_{\Sigma 3.1} \text{V}_{1.9} \text{O}_7(\text{OH})_{1.7} \cdot 2\text{H}_2\text{O}$  on the basis of  $(\text{Cu} + \text{Zn} + \text{Ni} + \text{V}) = 5 \text{ apfu}$ .

The crystal structure of volborthite consists of corrugated layers located in the (001) plane, formed by Cu-centered octahedra. The layers are combined with each other by pyrovanadate groups  $[\text{V}_2\text{O}_7]^{4-}$ . Water molecules are located in the interlayer space. The volborthite layers are arranged in a symmetrical kagome lattice. This feature affects the manifestation of interesting magnetic properties.

A selected sample of volborthite  $\text{Cu}_3\text{V}_2\text{O}_7(\text{OH})_2 \cdot 2\text{H}_2\text{O}$  was examined on a Rigaku "Ultima IV" diffractometer with a low-temperature attachment "R-300". The temperature range was set from  $-180 \text{ }^\circ\text{C}$  to  $300 \text{ }^\circ\text{C}$ . The temperature step was  $20 \text{ }^\circ\text{C}$ . Thermal X-ray data were processed using the Topas software. Generally volborthite  $\text{Cu}_3\text{V}_2\text{O}_7(\text{OH})_2 \cdot 2\text{H}_2\text{O}$  exhibits weakly anisotropic thermal expansion with increasing temperature. Features of the thermal behavior of volborthite will be reported.

This work was financially supported by the Russian Science Foundation, grant №16-17-10085. Technical support by the SPbSU X-ray Diffraction and Geomodel Resource Centers is gratefully acknowledged.

1. Anthony J.W., Bideaux R. A., Bladh K. W., Nichols M. C., Handbook of Mineralogy. V. 4. Arsenates, Phosphates, Vanadates. Mineral Data Publishing: Tuscon, AZ, USA. 2000.
2. Lafontaine M. A., Le Bail A., F'erey G. The synthetic homolog of volborthite; Crystal structure determination from X-ray and neutron data; Structural correlation. Journal of Solid State Chemistry. 1990. V. 85. P. 220-227.
3. Kashaev A. A., Rozhdestvenskaya I. V., Bannova I. I., Sapozhnikov A. N. & Glebova O. D. Balance, uniformity, and asymmetry of the structure of volborthite  $\text{Cu}_3(\text{OH})_2(\text{V}_2\text{O}_7) \cdot 2\text{H}_2\text{O}$ . Journal of Structural Chemistry. 2008. V. 49. P. 708–711.

## Study of the effects of heat-treatment of hydroxyapatite synthesized in gelatine matrix

Golovanova O.A.

Department of Inorganic Chemistry Omsk F. M. Dostoevsky State University, Russia, Prospekt Mira, 55-A

Correspondence email: golovanoa2000@mail.ru

The global bioceramics demand on the market currently reaches ~40 billion euros per year, the estimated annual growth rate is of 7–12% and the required amount of the material to meet the demand is estimated at tens of tons. The number of patients in need of surgery to restore the integrity of the bone is increasing every year: in the US, the annual number of patients exceeds more than 1 million people (of which over 300 thousand people need hip and knee prosthetics, the same holds true for dental implants).

Materials based on hydroxyapatite  $\text{Ca}_{10}(\text{PO}_4)_6(\text{OH})_2$  are analogs of the mineral component of bone, and they are considered the most promising biocomposites to be used as substitutes for bone defect repair due to their high bioactivity.

It is known that the main components of bone are type I collagen (~ 20%), a mineral phase (~ 60%), water (~ 9%) and non-collagenous proteins (~ 3%), the rest being polysaccharides and lipids. The organic part of bone is composed of collagen fibers and proteins, such as osteocalcin, osteonectin and fibronectin. Gelatin is a natural polymer formed through hydrolysis of collagen. In contrast to the latter, it is more stable and exhibits less antigenicity, thereby can be effectively used as a calcium phosphate based organic matrix biomaterial. Gelatin contains biologically active functional amino acid groups, and it is an advanced material for bone regeneration, including its combination with hydroxyapatite. Since gelatin is a denatured form of collagen and it contains significant amounts of biologically functional amino acid groups, the investigation of properties of hydroxyapatite synthesized in the gelatin matrix (HAG) under near-physiological conditions is a challenging and relevant physicochemical problem.

The SBF was used as a model solution of extracellular fluid. A solid phase was prepared by precipitation from aqueous solutions; the starting components of the system were  $\text{CaCl}_2$ ,  $\text{MgCl}_2$ ,  $\text{K}_2\text{HPO}_4$ ,  $\text{NaHCO}_3$ ,  $\text{Na}_2\text{SO}_4$ ,  $\text{NaCl}$  [15] solutions and 3 wt.% gelatin.

Thermal effects were studied by isothermal thermogravimetric analysis. Hydroxyapatite samples synthesized in the presence of gelatin were placed in dry ceramic crucibles. Then the samples were placed in a muffle furnace and kept for 2 h. The calcination temperature was varied from 200 to 800°C by increment of 200°C. After that, the crucibles were allowed to cool to room temperature, and then weighed on an analytical balance. The solid precipitates were analyzed by FT-IR spectroscopy and X-ray diffraction (XRD) – qualitative and quantitative phase analysis, measurement of the crystallite sizes (coherent scattering regions – CSR). The IR spectra were recorded using a FT-801 spectrometer (the samples were prepared in the form of KBr pallets). The XRD of the powder samples was performed with the Bruker D8 Advance X-ray diffractometer, and the diffraction patterns were identified using the software package EVA (developed by Bruker AXS).

The TGA diagram demonstrates the highest weight loss at 200°C and 400°C that can be attributed to adsorption and removal of the chemically bound water from the HAG samples. An increased weight loss at 400°C can be caused by burn out of the organic phase (gelatin) in the HA samples. At 600°C, the weight decreases insignificantly, while at 800°C, the weight loss increases by 2 times (compared to that at 600°C), which indicates the removal of the carbonate groups from the HA structure. These data is consistent with the results obtained by FT-IR spectroscopy.

The X-ray diffraction patterns of the HAG samples subjected to heat treatment show peak splitting at 400°C. In our opinion, this is caused by degradation of the gelatin components (amino acids), and thereby release of the carbonate component that has been partially released in the form of carbon dioxide, and partially entered the calcium phosphate structure.

At 600°C and 800°C, the intensity of peak splitting did not increase and remained at the same level. This is most likely due to the fact that no orbitals are left vacant to bind carbonate ions in calcium phosphate as compared to that in case of unsubstituted hydroxyapatite.

The isothermal thermogravimetric analysis revealed four stages of thermal decomposition of composite materials: 1) removal of water and easily volatile impurities ( $t=25^\circ\text{C}-280^\circ\text{C}$ ); 2) gelatin pyrolysis ( $t=280^\circ\text{C}-400^\circ\text{C}$ ); 3) calcium pyrophosphate phase formation ( $t=400^\circ\text{C}-600^\circ\text{C}$ ); 4) removal of carbonate ions from the HA structure and its decomposition ( $t > 600^\circ\text{C}$ ).

## Текстурирование в тонких кремнеземных пленках, допированных наночастицами Pt/Pd.

Губанова Н.Н.<sup>1,2</sup>, Матвеев В.А.<sup>2</sup>, Шилова О.А.<sup>1</sup>

<sup>1</sup> ФГБУН Ордена Трудового Красного Знамени Институт химии силикатов им. И.В. Гребенщикова Российской академии наук (ИХС РАН), 199034, наб. Макарова 2, Санкт-Петербург, Россия.

<sup>2</sup> Федеральное государственное бюджетное учреждение «Петербургский институт ядерной физики им. Б. П. Константинова» Национального исследовательского центра «Курчатовский институт», 188300, мкр. Орлова роща 1, Гатчина, Ленинградская область, Россия.

\*Correspondence email: gubanova\_nn@npfi.nrcki.ru

Исследование кремнеземных пленок, допированных наночастицами Pt/Pd, вызывает большой интерес в связи с их возможным применением в качестве каталитических слоев. Каталитические свойства биметаллических наночастиц в пленках определяются их размерами, структурой, и преимущественной ориентацией, которые в свою очередь зависят от метода их получения. Одним из наиболее технологически простых и мало затратных методов получения таких пленок является нанесение золь с помощью центрифугирования (spin-coating method).

В наших предыдущих исследованиях были изучены тонкие кремнеземные пленки толщиной ~30 нм, допированные наночастицами Pt/Pd [1, 2]. Для формирования кремнеземной матрицы в качестве прекурсора использовали ТЭОС, для синтеза легирующих компонентов – неорганические соединения платины и палладия ( $H_2[PtCl_6] \cdot 6H_2O$  и  $PdCl_2$ ). Пленки получали из золь методом центрифугирования с последующей термофиксацией. В результате исследований было установлено, что наночастицы Pt/Pd имеют общую кристаллическую решетку по типу твердого раствора замещения, с характерным размером кристаллитов 3-8 нм [2].

В настоящей работе представлены результаты исследования текстурирования в тонких кремнеземных пленках, допированных наночастицами Pt/Pd, путем измерения полюсных фигур. Результаты измерений показали наличие преимущественной ориентации кристаллитов Pt/Pd относительно поверхности пленки.

1. Shilova O.A., Gubanova N.N., Matveev V.A., Ivanova A.G., Arsentiev M.Y., Pugachev K.E., Ivankova E.M., Kruchinina I.Yu. Processes of film-formation and crystallization in catalytically active 'spin-on glass' silica films containing Pt and Pd nanoparticles. *Journal of Molecular Liquids*, 2019, 288, P. 110996.

2. Gubanova N.N., Matveev V.A., Shilova O.A. Bimetallic Pt/Pd nanoparticles in sol-gel-derived silica films and xerogels. *Journal of Sol-Gel Science and Technology*. 2019, P. 1-9.

## Local XRD analysis of the near $\alpha$ -titanium alloy PT3V modified by severe plastic deformation.

Andreev P.V.<sup>1,2</sup>, Gudz D.A.<sup>2</sup>, Smetanina K.E.<sup>2</sup>

<sup>1</sup> Institute of Chemistry of High-Purity Substances of the Russian Academy of Sciences, Nizhny Novgorod, Russia

<sup>2</sup> National Research Lobachevsky State University of Nizhny Novgorod, Nizhny Novgorod, Russia

\*Correspondence email: andreev@phys.unn.ru

In the current study, an ultrafine-grained (UFG) structure of the PT3V titanium alloy was formed by Rotary Swaging.

Phase composition study requires locality due to the microstructure heterogeneity (the grain size gradient in the cross section of the swaged rod after annealing). Traditional polycrystal research methods – the method of X-ray diffraction in Bragg-Brentano geometry cannot meet this requirement.

Obviously, areas with different grain sizes can differ in phase composition both qualitatively and quantitatively and therefore have different physical properties: electrical conductivity, thermal stability, magnetic properties [1].

It is supposed to solve the problem of local analysis using X-ray technology with a narrow primary beam technique. One option is to use an Oxford Diffraction single crystal diffractometer equipped with an X-ray tube with a copper anode, a graphite monochromator and collimator that generates a primary beam with a diameter of 0.3 mm and a CCD detector.

This work was supported by the Russian Science Foundation (Grant №19-73-00295).

1. Faraji G., Kim H. S., Kashi H. T. Severe plastic deformation: methods, processing and properties. – Elsevier, 2018.

**Synthesis, crystal structure of the first lithium aluminum borophosphate  $\text{Li}_3\{\text{Al}_2[\text{BP}_4\text{O}_{16}]\}\cdot 2\text{H}_2\text{O}$ , and conditions for Li-ion conductivity.**

Aksenov S.M.<sup>1,2</sup>, Yamnova N.A.<sup>3</sup>, Borovikova E.Yu.<sup>3</sup>, Stefanovich S.Yu.<sup>3</sup>, Volkov A.S.<sup>3,4</sup>, Deyneko D.V.<sup>3</sup>, Dimitrova O.V.<sup>3</sup>, Gurbanova O.A.<sup>3</sup>, Hixon A.E.<sup>2</sup>, Krivovichev S.V.<sup>1,5</sup>

<sup>1</sup>Kola Science Center, Russian Academy of Sciences, 184209 Murmansk region, Apatity, Fersman st., 14

<sup>2</sup>Department of Civil and Environmental Engineering and Earth, Sciences, University of Notre Dame, 156 Fitzpatrick Hall Notre Dame, IN 46556

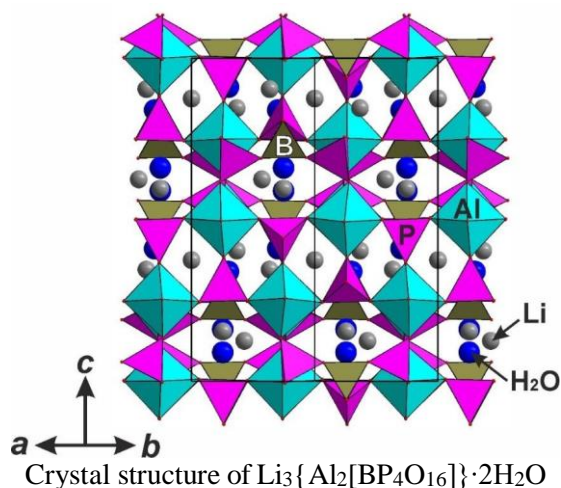
<sup>3</sup>Lomonosov Moscow State University, 119991 Moscow, Leninskie Gory, 1, Russia

<sup>4</sup>Institute of Experimental Mineralogy RAS, 142432, Academica Osypyna ul., 4, Chernogolovka, Moscow region, Russian Federation

<sup>5</sup>Saint-Peterburg State University, 7/9Universitetskaya Emb, St-Peterburg, 119034, Russia

\*Correspondence email: gur\_o@mail.ru

A new water-containing borophosphate of aluminum and lithium obtained by hydrothermal synthesis in a borophosphate system, has been studied by X-ray diffraction analysis. Tetragonal cell parameters are as follows:  $a = 8.7549(4)$ ,  $c = 16.256(2)\text{\AA}$ ,  $V = 1951.2(4)\text{\AA}^3$ , sp.gr.  $P4_122$ . The investigated borophosphate is characterized by the crystal chemical formula ( $Z = 4$ )  $\text{Li}_3\{\text{Al}_2[\text{BP}_4\text{O}_{16}]\}\cdot 2\text{H}_2\text{O}$ , where the composition of the borophosphate anion is shown in square brackets, and the composition of the heteropolyhedral framework is shown in the curly ones. The framework is formed by  $\text{AlO}_6$  octahedra and  $\text{PO}_4$  and  $\text{BO}_4$  tetrahedra, while  $\text{Li}^+$  cations and  $\text{H}_2\text{O}$  molecules are located in the framework channels. The presence of channels creates the preconditions for high mobility of lithium ions, which can be used in the development of new Li-conducting materials. Due to the performed topological analysis of mixed tetrahedral (TTT) and heteropolyhedral (MTT and TrTTT) frameworks in the structures of borophosphates, a number of structural features have been established, which allows us to take a fresh look at the crystal chemistry of borophosphates.



## Фосфаты $\text{Ca}_{9-x}\text{Zn}_x\text{La}(\text{PO}_4)_7:\text{Ln}^{3+}$ , люминесцирующие в ближней ИК-области

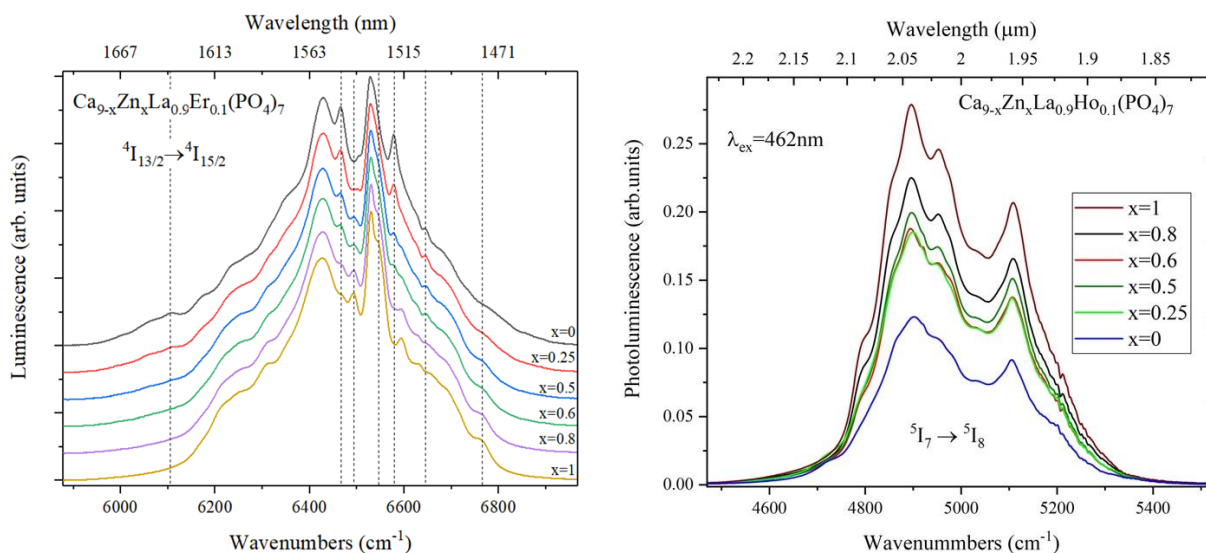
Дихтяр Ю.Ю.<sup>1</sup>, Дейнеко Д.В.<sup>1</sup>, Болдырев К.Н.<sup>2</sup>

<sup>1</sup> Московский государственный университет имени М.В. Ломоносова, г. Москва, Россия,  
<sup>2</sup> Институт спектроскопии РАН, г. Троицк, Россия

Несмотря на то, что молекулярные механизмы перерождения обычных клеток организма в раковые до сих пор остаются не совсем ясны, в настоящее время проводится поиск эффективных лекарств и средств диагностики от данного заболевания. Тераностические агенты – вещества, которые можно использовать как для визуализации, так и для терапевтических целей представляют интерес для решения данной проблемы.

Ионы  $\text{Er}^{3+}$ ,  $\text{Ho}^{3+}$  в определенной матрице являются перспективными активаторами в качестве биологической метки. Интересной кристаллической матрицей для допирования ионами РЗЭ являются фосфаты со структурой минерала витлокита. Фосфаты состава  $\text{Ca}_{9-x}\text{Zn}_x\text{La}(\text{PO}_4)_7:\text{Ln}^{3+}$  ( $\text{Ln} = \text{Ho}, \text{Er}$ ) изоструктурны минералу витлокиту и кристаллизуются в полярной ( $R3c$ ) или centrosymmetric ( $R\bar{3}c$ ) федоровских группах, в зависимости от содержания катионов  $\text{Zn}^{2+}$ . Данные соединения рассматриваются как перспективные материалы для дизайна материалов, способных люминесцировать в ближнем ИК-диапазоне, что позволит в дальнейшем их использовать для тераностических целей.

В настоящей работе исследовали влияние катионов  $\text{Zn}^{2+}$  и  $\text{Sr}^{2+}$  на люминесцентные свойства витлокитоподобных твердых растворов, допированных катионами  $\text{Er}^{3+}$ ,  $\text{Ho}^{3+}$ . Полученные образцы охарактеризованы методом РФА, ГВГ и люминесценции. Исследованы диэлектрические свойства составов с  $\text{Er}^{3+}$  для более детального установления пространственной группы симметрии – нецентросимметричной  $R3c$ , или centrosymmetric  $R\bar{3}c$ , так как рентгенографически данные группы симметрии неразличимы в условиях лабораторного рентгенографического эксперимента.



На представленных рисунках видно изменение формы спектра в зависимости от концентрации ионов  $\text{Zn}^{2+}$ . Видны множественные пики для основных переходов, что связано со Штарковской структурой основного и возбужденного состояния каждого из центров люминесценции (3 в случае группы  $R3c$  и 2 в случае группы  $R\bar{3}c$ ). Монотонное перераспределение расщеплений переходов связано с различным влиянием кристаллического поля, которое также меняется в зависимости от концентрации ионов  $\text{Zn}^{2+}$ .

Работа выполнена при финансовой поддержке РФФИ, проект 20-03-00929.

## High pressure induced structural and magnetic phase transformations in BaYFeO<sub>4</sub>

Kozlenko D.P.<sup>1</sup>, Zel I.Yu.<sup>1\*</sup>, Dang T.N.<sup>2,3</sup>, Le Thao P.T.<sup>4,5</sup>

<sup>1</sup> Frank Laboratory of Neutron Physics, Joint Institute for Nuclear Research, 141980, 6 Joliot-Curie St., Dubna, Russia.

<sup>2</sup>Institute of Research and Development, Duy Tan University, 550000 Da Nang, Viet Nam

<sup>3</sup>Faculty of Natural Sciences, Duy Tan University, 550000 Da Nang, Viet Nam

<sup>4</sup>University of Education, The University of Da Nang, 550000 Da Nang, Viet Nam

<sup>5</sup> Department of Physics, University of Sciences, Hue University, 530000 Hue, Viet Nam

\*Correspondence email: ivangreat2009@gmail.com

Multiferroic materials exhibiting the magnetism-driven ferroelectricity, where ferroelectricity is induced by magnetic ordering, have been attracting continuous attentions in scientific research due to their application potential as well as from the fundamental science angle. It is worth to note that the magnetism-induced ferroelectricity is commonly observed in magnetically frustrated systems such as BaYFeO<sub>4</sub>, since spin frustration induces spatial variation in magnetization, which leads to the loss of the lattice inversion symmetry, thereby resulting in the occurrence of ferroelectricity. The geometric magnetic frustration due to its structural complexity gives rise to their peculiar physical properties, raising from the complex interplay among magnetic frustration due to competing superexchange interactions and spin, lattice, charge and orbital degrees of freedom. To better understanding the nature of magnetoelectric phenomena in the sample, we have performed high pressure effect on the crystal and magnetic structure of BaYFeO<sub>4</sub> by using a combination of neutron diffraction and Raman spectroscopy up to 5.2 and 18 GPa, respectively. It has been established that BaYFeO<sub>4</sub> possess two long-range magnetic transitions: one at 55 K corresponding to a formation of the spin density wave antiferromagnetic (AFM) order (SDW), which then transforms to the cycloid AFM order at 36 K. The latter one is supposed to be the origin of ferroelectricity of the sample. It has been observed that application of pressure,  $P > 2$  GPa, tends to convert the lower-temperature cycloid order to the SPW one, pointing a pressure-induced suppression of ferroelectricity. The Neel temperature  $T_N$  of the SPW order almost linearly decreases upon compression with pressure coefficient of -1.4 K/GPa. Moreover, at  $P \sim 5$  GPa a structural phase transformation accompanied by anomalies in pressure behavior of vibrational modes was observed. The observed phenomena have been discussed using the DFT calculations.

The work has been supported by the Russian Foundation for Basic Research, grant 20-52-54002  
Вьет\_a

## От тетраэдрической координации атома кремния к тригонально-бипирамидальной

Зельбст Э.А.<sup>1</sup>, Адамович С.Н.<sup>2</sup>, Оборина Е.Н.<sup>2</sup>, Моисеев А.А.<sup>1</sup>

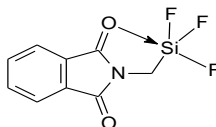
<sup>1</sup>Педагогический институт Иркутского государственного университета

<sup>2</sup>Иркутский институт химии им. А.Е. Фаворского СО РАН

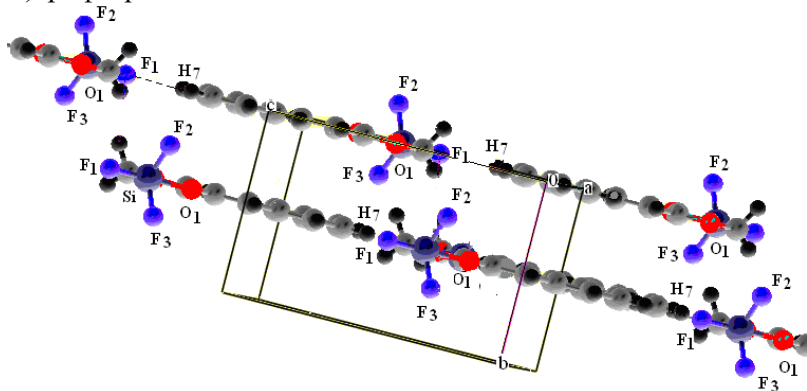
\*Correspondence email: zelbst@rambler.ru

Кремнийорганические соединения, содержащие гетероцикл и гипервалентный атом кремния, представляют большой теоретический интерес. Знание их молекулярной структуры позволяет расширить представления о строении таких соединений и также установить специфическое влияние Si-органических заместителей на реакционную способность гетероцикла. Кроме того, такие соединения часто обладают высокой биологической активностью и являются перспективными в качестве лекарственных препаратов и средств химизации сельского хозяйства. О расширении координационной сферы атома кремния в силатранах известно давно, но строение таких молекул все еще вызывает большой интерес [1].

Другой класс соединений пентакоординированного кремния - (гетерил)алкилтрифторсиланы – как и силатраны широко исследован физико-химическими методами.



Установлено, что длина координационной связи O→Si, входящей в пятичленный гетероцикл, зависит от того, насколько этот гетероцикл плоский. На предлагаемом стенде мы описываем вероятную причину перехода атома кремния в (органил)трифторсиланах в пентакоординированное состояние, а также слоистый характер упаковки молекул в одном из них - (циннамоилоксиметил)трифторсилане - C<sub>6</sub>H<sub>4</sub>CH=CHCOOCH<sub>2</sub>SiF<sub>3</sub>.



Толщина слоя – она же примерно удвоенная сумма ковалентных радиусов атома кремния и фтора – очень мала по сравнению с его длиной и шириной. Расстояние между слоями составляет 3,42 Å. Облик такой упаковки можно назвать «графено-подобной».

Таким кристаллам присущи самые неожиданные свойства, наиболее замечательной их особенностью является анизотропия. Это позволяет рекомендовать их как полигон для самых разнообразных физических исследований.

Исследование выполнено при финансовой поддержке РФФИ и Правительства Иркутской области в рамках научного проекта № 20-43-380001.

1. G.Singh, G.Kaur, J.Singh // Inorganic Chemistry Communication. 2018.- V.88. – P.11-22.



**Synthesis, characterization and morphotropic transitions in a family of  $M[(\text{UO}_2)(\text{CH}_3\text{COO})_3](\text{H}_2\text{O})_n$  ( $M = \text{Na, K, Rb, Cs}$ ;  $n = 0-1.0$ ) compounds.**

Kalashnikova S.A.<sup>1\*</sup>, Korniyakov I.V.<sup>1,2</sup>, Gurzhiy V.V.<sup>1</sup>

<sup>1</sup> Saint Petersburg State University, 199034, Universitetskaya nab., 7-9, St.Petersburg, Russia.

<sup>2</sup> Kola Science Center, the Russian Academy of Sciences, 189209, Fersmana str., 14, Apatity, Russia.

\*Correspondence email: kalashnikova.soff@gmail.com

Single crystals of  $\text{Na}[\text{UO}_2(\text{CH}_3\text{COO})_3]$  (**I**),  $\text{K}[\text{UO}_2(\text{CH}_3\text{COO})_3](\text{H}_2\text{O})_{0.5}$  (**2**),  $\text{Rb}[\text{UO}_2(\text{CH}_3\text{COO})_3]$  (**3**) and  $\text{Cs}[\text{UO}_2(\text{CH}_3\text{COO})_3](\text{H}_2\text{O})_{0.5}$  (**4**) have been prepared by evaporation from 3 ml aqueous solution of uranyl acetate dihydrate, ammonium carbonate, and sodium chloride, potassium chloride, rubidium chloride or cesium chloride for **I**, **II**, **III** and **IV**, respectively. Single crystal X-Ray Diffraction data had been collected at 100 K for **II**, **III**, **IV** and 296 K for **I** using Bruker Kappa Apex II Duo diffractometer.

The unit cell parameters were determined and refined by least squares method [0]. The crystal structures were solved by direct methods and refined using the Shelx programs incorporated in Olex2 program package. **I**:  $P2_13$ ,  $a = 10.721(6)$  Å,  $V = 1232.4(19)$  Å<sup>3</sup>,  $Z = 4$ ,  $R_1 = 0.041$ . **II**:  $I4_1/a$ ,  $a = 14.222(5)$ ,  $c = 25.715(8)$  Å,  $V = 5201(4)$  Å<sup>3</sup>,  $Z = 16$ ,  $R_1 = 0.037$ . **III**:  $I4_1/a$ ,  $a = 13.787(3)$ ,  $c = 27.511(7)$  Å,  $V = 5230(3)$  Å<sup>3</sup>,  $Z = 16$ ,  $R_1 = 0.037$ . **IV**:  $P\bar{1}$ ,  $a = 8.353(4)$ ,  $b = 11.008(5)$ ,  $c = 15.354(7)$  Å,  $\alpha = 108.409(11)$ ,  $\beta = 100.140(9)$ ,  $\gamma = 96.370(9)^\circ$ ,  $V = 1297.5(10)$  Å<sup>3</sup>,  $Z = 4$ ,  $R_1 = 0.036$ .

Structures **I**, **II** and **III** contain one symmetrically nonequivalent uranium atom each. The structure of **IV** contains two independent uranium atoms. Each uranyl ion is coordinated by six oxygen atoms in the equatorial plane, which belong to three acetate groups. Resulting hexagonal bipyramids (coordination polyhedrons of  $\text{U}^{6+}$  atoms) share three common edges with  $(\text{CH}_3\text{COO})$  groups, forming uranyl-three-carbonate clusters, which are a core unit of structures **I-IV**.

The amount of symmetrically nonequivalent acetate groups increases from one in the structure of **I** to three in the structures of **II** и **III** and six in the structure of **IV**. The number of nonequivalent uranium atoms also increases with the decreasing of symmetry (from cubic in **I** to triclinic in **IV**).

The main structural differences within morphotropic transitions in family of  $M[(\text{UO}_2)(\text{CH}_3\text{COO})_3](\text{H}_2\text{O})_n$  ( $M = \text{Na, K, Rb, Cs}$ ;  $n = 0-1.0$ ) compounds are associated with changes in the ionic radii of alkali metal cations. The first structural transformation is induced by the Na-to-K substitution and results in the symmetry decrease from cubic  $P2_13$  to tetragonal  $I4_1/a$ . It happens due to the significant difference in the ionic radii of Na и K (~0.44 Å). The K-to-Rb substitution does not lead to any significant structural changes, because of the less significant difference in the ionic radii (~0.06 Å). The Rb-to-Cs substitution again causes structural changes due to large difference in the ionic radii (~0.17 Å), resulting in the symmetry decrease to triclinic.

The research was supported by SPBU and Russian Scientific Foundation grant № 18-17-00018. XRD studies have been performed at the X-ray Diffraction Resource Centre of St Petersburg State University.

1. Korniyakov I.V. Synthesis, characterization and morphotropic transitions in a family of  $M[(\text{UO}_2)(\text{CH}_3\text{COO})_3](\text{H}_2\text{O})_n$  ( $M = \text{Na, K, Rb, Cs}$ ;  $n = 0-1.0$ ) compounds. Zeitschrift für kristallographie. 2020. V. 235(3). P. 95-103.

## Novel complex copper phosphate chlorides: disordered structures and crystal chemistry

Kiriukhina G.V.<sup>1,2</sup>, Yakubovich O.V.<sup>1</sup>, Dovgaliuk I.N.<sup>3</sup>, Simonov S.V.<sup>4</sup>

<sup>1</sup> Lomonosov Moscow State University, GSP-1, Leninskie Gory, Moscow, 119991, Russia.

<sup>2</sup> Institute of Experimental Mineralogy, Russian Academy of Science, Akademika Osip'yana st. 4, Chernogolovka, Moscow Region 142432, Russia.

<sup>3</sup> Swiss-Norwegian Beamlines, European Synchrotron Radiation Facility, 71 Avenue des Martyrs, F-38000 Grenoble, France.

<sup>4</sup> Institute of Solid State Physics, Russian Academy of Science, Akademika Osip'yana st. 2, Chernogolovka, Moscow Region 142432, Russia.

\*Correspondence email: g-biral@yandex.ru

Two novel copper phosphate chlorides, deep-green small isometric crystals (I) and turquoise-colored thin plates (II), have been obtained under the middle-temperature hydrothermal conditions. Their complex and disordered crystal structures have been established based on the low-temperature X-ray diffraction and crystal chemical analysis: (I)  $(\text{Na,Cs,K})_3[\text{Cu}_5(\text{PO}_4)_4\text{Cl}] \cdot 3.5\text{H}_2\text{O}$ , sp. gr.  $C2/m$ ,  $a = 19.3951(8)\text{\AA}$ ,  $b = 9.7627(3)\text{\AA}$ ,  $c = 9.7383(4)\text{\AA}$ ,  $T = 150\text{K}$ ,  $\lambda = 0.71073$ ; (II)  $(\text{NH}_4)_9\text{Cu}_{5.5}(\text{VO})_{0.5}[\text{P}_2\text{O}_7]_4\text{Cl}_3(\text{PO}_4)_{0.5}\text{Ca}_{0.4}(\text{H}_2\text{O},\text{OH})_5$ , sp. gr.  $I4/mcm$ ,  $a = 17.9007(3)\text{\AA}$ ,  $c = 13.5442(5)\text{\AA}$ ,  $T = 100\text{K}$ , synchrotron radiation,  $\lambda = 0.64066$ .

Both crystal structures include similar tetrameric Cu-centered clusters,  $(\text{CuO}_3)_4\text{Cl}$  or  $(\text{CuO}_4)_4\text{Cl}$ , as the main building blocks (Fig. 1). In these units four copper pyramids share apical Cl vertices. These clusters are combined through phosphate groups and additional copper-centered polyhedra to form a 2D layer (I) or 3D open framework (II) structures, both mostly ordered. Between the 2D blocks and inside the 3D framework channels, alkaline and ammonium ions,  $\text{H}_2\text{O}$  molecules or OH groups are statistically distributed. Crystals (I) present a novel synthetic modification of mineral sampleite, a member of the lavendulan mineral group of copper phosphates and arsenates [1]. In previous work [2], we have published the crystal structure of another synthetic analogue of mahnertite, a member of this group. The modular approach was used to describe the structures of natural and synthetic compounds as various polysomes, all containing two-dimensional  $[\text{Cu}_4\text{X}(\text{TO}_4)_4]_\infty$  modules ( $T = \text{As}, \text{P}$ ;  $X = \text{Cl}, \text{O}$ ). Inside the 3D framework (II) small amounts of  $[\text{PO}_4]^{3-}$  complexes and  $\text{Ca}^{2+}$  ions are trapped by large, flexible, one-dimensional channels of  $5.5\text{\AA}$  in diameter. Similar complex ionic inclusions were found in homeotype crystal structures of copper diphosphates, i.e.  $\text{Rb}_9\text{Cu}_6[\text{P}_2\text{O}_7]_4\text{Cl}_3 \cdot \text{CuCl}_4$  [3].

This study was supported by the Russian Science Foundation, project no. 19-77-00081.

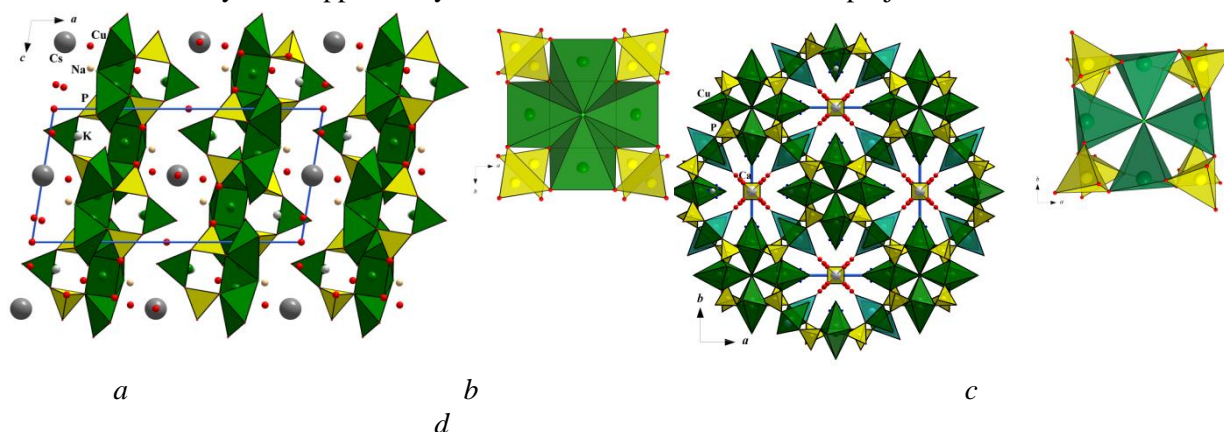


Figure 1. Crystal structures of two novel complex phosphates chlorides:

$(\text{Na,Cs,K})_3[\text{Cu}_5(\text{PO}_4)_4\text{Cl}] \cdot 3.5\text{H}_2\text{O}$  (I) (a) built of  $(\text{CuO}_3)_4\text{Cl}$  tetrameric clusters (b), and  $(\text{NH}_4)_9\text{Cu}_{5.5}(\text{VO})_{0.5}[\text{P}_2\text{O}_7]_4\text{Cl}_3(\text{PO}_4)_{0.5}\text{Ca}_{0.4}(\text{H}_2\text{O},\text{OH})_5$  (II) (c) with  $(\text{CuO}_4)_4\text{Cl}$  units (d).

1. Giester, G., Kolitsch, U., Leverett, P., Turner, P. & Williams, P. A. The crystal structures of lavendulan, sampleite, and a new polymorph of sampleite. *Eur. J. Mineral.* 2007. V. 19. P. 75-93.

2. Yakubovich, O.V., Steele, I.M., Kiriukhina, G.V. & Dimitrova, O.V. A microporous potassium vanadyl phosphate analogue of mahnertite: hydrothermal synthesis and crystal structure. *Z. Kristallogr.* 2015. V. 230(5). P. 337-344.

3. Williams, E.R., Leithall, R.M., Rajab, R. & Weller, M.T. Complex anion inclusion compounds: flexible anion-exchange materials. *Chem. Commun.* 2013. V. 49. P. 249-251.

## Features of crystallization of cristobalite in quartz glass obtained on plasmatrons of JSC "DINUR" from quartz sand of the Ramenskoye Deposit

Kolobov A.Yu.<sup>1,2</sup>, Sycheva G.A.<sup>2</sup>

<sup>1</sup>JSC "DINUR", 623103, city of Pervouralsk, Sverdlovsk region, Ilyich street, 1

<sup>2</sup>Grebenshchikov Institute of Silicate Chemistry, Russian Academy of Sciences, 199034, St.

Petersburg, nab. Makarova 2

art.kolobov@yandex.ru

At the present stage of its development, humanity is faced with global problems: the lack of energy resources, the need for rational use of minerals using energy-saving technologies. Currently, special attention is focused on obtaining materials from domestic raw materials (import substitution). JSC DINUR specializes in production of quartz glass from quartz sand of the Ramenskoye Deposit (Russia, Moscow region). It is known from the literature that quartz glass can be obtained in various ways: electro thermal, gas-flame, plasma, steam-phase, each of which has many options and modifications, advantages and disadvantages. At JSC DINUR, sand melting is performed in plasmatrons. The operating current of the reactor arc is about 1300 A at a voltage of 300-400 V. The Current-Voltage characteristics of the melting process depend on the specific reactor and the quality of the Sands (the content of impurity components, such as aluminum and iron oxides). The resulting ingot is a rod several meters long, about half a meter in diameter and weighing more than 600 kg.

In this paper, we studied the features of obtaining, crystallization, and properties of quartz glass synthesized by the plasma method. Complex studies (chemical analysis, RFA, dilatometry, thermal analysis) of the properties of quartz glass and its products were carried out in the Central factory laboratory of DINUR. The main crystalline phases found in quartz glass are cristobalite and quartz ("non-melt"). For quantitative determination of cristobalite, x-ray phase analysis was used based on changes in the intensity of diffraction reflection depending on the content of cristobalite. In General, the problem of quantitative determination of cristobalite in the resulting quartz glass is the simplest problem of x-ray phase analysis. The basic equation for this case is:  $C=(I_c/I_o)\times 100\%$ , where C is the concentration of cristobalite in the material;  $I_c$ ,  $I_o$ -intensity of the selected cristobalite reflex in the sample under study and in pure cristobalite (quartz glass firing at 1600 °C with an exposure time of at least 4 hours), respectively. The most intense cristobalite reflex 101 ( $d=4.04\times 10^{-10}$  m) was chosen as the analytical reflex.

It was found that the product of melting quartz sand has a reduced resistance to crystallization. The chemical ( $Al_2O_3$  content 0.25 Fe  $Fe_2O_3$  less than 0.05%) and x-ray phase composition of the ingot from the center to the periphery were found to be constant. The proportion of cristobalite in the samples under study increases with increasing temperature and holding time and is maximum 23% for isothermal exposure for 5 hours at 1400 degrees and 35.5%, respectively, after 10 "heating-cooling" cycles up to 1400 degrees with a heating rate of 2.5 degrees per minute. In a dense crust on the surface of the ingot (coat), 10 to 12% of quartz was found, and the content of cristobalite in the crust did not exceed 2.0%. At the same time, the mineralogical composition of most of the studied samples of quartz glass, purified from the surface crystal crust, is represented by pure quartz glass. Quartz and cristobalite were not detected by RFA and microscopy in most samples. In those samples where the presence of cristobalite was established by the RFA method, petrographic research confirmed the origin of crystals on foreign impurities.

1. Kolobov A. Yu., Sycheva G. A. // *Physics of the Solid State*. 2019. V. 61. N 12. R. 2359.

2. Kolobov A. Yu., Sycheva G. A. // *Glass Physics and Chemistry*. 2020 (In print).

## Thermal behavior and luminescence of natural rare-earth borosilicates stillwellite and tadzhikite

Kopylova Y.O.<sup>1</sup>, Krzhizhanovskaya M.G.<sup>1</sup>, Kolesnikov I.E.<sup>2</sup>, Shilovskih V.V.<sup>3</sup>

<sup>1</sup>Institute of Earth Sciences, St. Petersburg State University, University Emb. 7/9, 199034, St. Petersburg, Russia

<sup>2</sup>Institute of Chemistry, Saint-Petersburg State University, University Emb. 7/9, 199034, St. Petersburg, Russia

<sup>3</sup>Centre for Geo-Environmental Research and Modelling, Saint-Petersburg State University, Ulyanovskaya str. 1, 198504, St. Petersburg, Russia.

\*Correspondence email: yuliua.kopylova@gmail.com

Crystalline inorganic borates and borosilicates are promising and interesting objects of study as they possess a variety of different structural and therefore physical properties. Their special features such as transparency for a wide range of radiation, a large forbidden electron band, chemical and thermal stability, optical stability and laser damage resistance determine their value for use as optical materials. In particular boron containing compounds activated by rare-earth ions are effective converters of high-energy radiation into visible light. In this work attention is paid to such REE borosilicate minerals as tadzhikite and stillwellite, quite rare and poorly studied minerals. The paper presents the results of studies of chemical composition, high-temperature crystal chemistry, and luminescent properties.

The chemical composition was determined in energy-dispersive mode by means of a Hitachi S-3400N scanning electron microscope equipped with AzTec Energy X-Max 20 energy dispersive spectrometer. According to microprobe stillwellite (general formula REEBSiO<sub>5</sub>) contains Ce, La, Nd, Pr, Sm and tadzhikite (Ca<sub>4</sub>REE<sup>3+</sup><sub>2</sub>(Ti,Fe,Al)(B<sub>4</sub>Si<sub>4</sub>O<sub>22</sub>)(OH)<sub>2</sub>) has Y, Ce, Nd, La as rare earth cations and no Al in the composition. Photoluminescence properties were studied at modular fluorescence spectrometer Horiba Fluorolog-3 equipped with 450 W Xe lamp as an excitation source. At room temperature powder samples have been measured with a Rigaku Ultima IV diffractometer (CuK $\alpha$  radiation, 40 kV/30 mA, PSD detector DtexUltra). PDF-2 database (2016) and PDXL program package have been used for the phase analysis.

The high-temperature powder X-ray diffraction (HTPXRD) has been carried out in air in the temperature range of 25–1100°C with a Rigaku Ultima IV (CoK $\alpha$  radiation, 40 kV, 30 mA, temperature step 30°C) equipped by a high-temperature attachment. Stillwellite as its synthetic analogue [1] undergoes polymorphic transformation at 600°C and decomposes at 990°C with the formation of new phases. Presumably tadzhikite undergoes a similar polymorphic transformation in the same temperature region and decomposes earlier at about 870°C.

Emission spectra were recorded in 400-800 nm range with 10 nm slits and increment of 1 nm. The measurements were carried out at room temperature. A low-intense luminescence was observed for stillwellite and tadzhikite in the blue and red light regions, respectively.

The authors acknowledge the Resource Center of X-ray diffraction Studies, Center for Optical and Laser Materials Research and “Geomodel” Resource Centre of Saint Petersburg State University for instrumental and computational resources. The authors are grateful to Professor I.V. Pekov for mineral samples.

This work was supported by the Russian Foundation for Basic Research (18-29-12106).

1. E L Belokoneva *et al* 1998 *J. Phys.: Condens. Matter* **10** 9975

## Ti-bearing hydroxyapatite: synthesis, crystal chemistry, photocatalytic properties

Korneev A.V.<sup>1\*</sup>, Frank-Kamenetskaya O.V.<sup>1</sup>, Kuz'mina M.A.<sup>1</sup>

<sup>1</sup> St. Petersburg State University, Department of Crystallography, 199034, Universitetskaya Emb. 7-9, St.Petersburg, Russia.

\*Correspondence email: a\_v\_korneev@list.ru

According to a number of researchers, Ti-bearing hydroxyapatite yields photocatalytic activity, comparable to activity of anatase TiO<sub>2</sub>, main component of several commercial photocatalysts [1,2]. This modification significantly improves bactericidal properties of hydroxyapatite, which makes it perspective material for biomedical applications.

The regularities of the incorporation of Ti-ions into apatite are not well-studied yet, as well as origin of photocatalytic activity of apatite. According to Ribeiro [3], titanium can incorporate in hydroxyapatite, replacing Ca or P ions resulted in decreasing or increasing a parameter, respectively. Synthesis of monophasic samples of hydroxyapatite is problematic due to one-time formation of anatase, which is possible in wide range of pH and concentrations.

Three series of syntheses were carried out in presence of Ti-ions in solutions (T=90-95 °C, pH=8-11) When preparing solutions of the 1<sup>st</sup> and the 2<sup>nd</sup> series we used CaNO<sub>3</sub>, (NH<sub>4</sub>)<sub>2</sub>HPO<sub>4</sub> and TiCl<sub>3</sub> (with different order of mixing), of the 3<sup>rd</sup> series – Ca(OH)<sub>2</sub>, H<sub>3</sub>PO<sub>4</sub> and C<sub>12</sub>H<sub>28</sub>O<sub>4</sub>Ti. Ti/Ca ratio varied from 0.01 to 0.60 in all series. Synthesized precipitates were studied with a wide set of methods (X-ray powder diffraction, Raman spectroscopy, SEM, EDX, TEM, diffuse reflection spectroscopy and other) in order to confirm that precipitates are monophasic, make sure that titanium ions entered into apatite and estimate their photocatalytic properties. According to XRD studies, all precipitates consist of hydroxyapatite only. However, Raman spectroscopy revealed presence of anatase in precipitates of 1<sup>st</sup> series (all samples) and 2<sup>nd</sup> series (Ti/Ca in solution ≥0.05). Anatase peaks appear at XRD patterns of the precipitates of 3<sup>rd</sup> series after annealing samples (Ti/Ca>0.03) at 700 °C for 6 hours. This indicates that amorphous TiO<sub>2</sub> which was formed in the synthesis and confirmed by EDX data transformed into anatase.

Unit cell parameters of hydroxyapatite of 1<sup>st</sup> series increase significantly with growth of Ti concentration. However, these changes can be explained by substitution of [OH<sup>-</sup>] by H<sub>2</sub>O and [PO<sub>4</sub><sup>3-</sup>] by [CO<sub>3</sub><sup>2-</sup>], confirmed by IR spectra.

In 2<sup>nd</sup> series parameter a of hydroxyapatite decreases slightly with growth of Ti/Ca ratio, and rises sharply at Ti/Ca = 0.40 – 0.60, while parameter c does not change significantly. Along with that H<sub>2</sub>O and CO<sub>3</sub><sup>2-</sup> IR bands strengthen, which should have brought to increase of both parameters. This confirms incorporation of Ti ions into hydroxyapatite (basically, at Ca site).

In 3<sup>rd</sup> series parameter a increases, while parameter c does not change significantly. As H<sub>2</sub>O IR band does not strengthen, this change is probably linked to incorporation of Ti into P site.

As Ti/Ca ratio increase, diffuse reflectance spectra of received precipitates change, becoming more similar to anatase spectra. The value of band gap decreases, becoming closer to anatase band gap (3.2 eV). Ti-modified apatite of 3<sup>rd</sup> series (Ti/Ca = 0.01 – 0.03) decomposes phenol under Hg-Xe irradiation slightly faster, than non-modified apatite, but much slower than TiO<sub>2</sub> photocatalyst.

The obtained data confirm that Ti incorporates into hydroxyapatite. This process is usually accompanied by formation of nano-particles of TiO<sub>2</sub>, and/or other Ti-compounds that significantly boosts photocatalytic properties of precipitates and hardens estimation of photocatalytic properties of Ti-bearing apatite itself. According to our data, photocatalytic activity of Ti-bearing hydroxyapatite is much weaker than activity of TiO<sub>2</sub>-based commercial photocatalysts.

1. Wakamura, M., Hashimoto, K., Watanabe, T. Photocatalysis by Calcium Hydroxyapatite Modified with Ti(IV): Albumin Decomposition and Bactericidal Effect. *Langmuir*, 2003, 19, 3428-3431.

2. Tsukada, M., Wakamura M., Yoshida, N., Watanabe, T. Band gap and photocatalytic properties of Ti-substituted hydroxyapatite: Comparison with anatase-TiO<sub>2</sub>, *J. Mol. Catal. A: Chem.*, 2011, 338, 18–23.

3. Ribeiro C.C., Gibson I., Barbosa, M.A. The uptake of titanium ions by hydroxyapatite particles structural changes and possible mechanisms // *Biomaterials*, 2006. 27, 1749-1761

**Synthesis and structural study of the new modular uranyl selenite-selenate with melamine**  
**[(UO<sub>2</sub>)(SeO<sub>4</sub>)(H<sub>2</sub>SeO<sub>3</sub>)][(SeO<sub>4</sub>)(C<sub>3</sub>H<sub>8</sub>N<sub>6</sub>)]**

Kuporev I.V.<sup>1\*</sup>, Gurzhiy V.V.<sup>1</sup>, Krivovichev S.V.<sup>1,2</sup>

<sup>1</sup>Department of Crystallography, St. Petersburg State University, University Emb. 7/9, St. Petersburg, 199034, Russia

<sup>2</sup>Kola Science Centre, Fersmana Str. 14, 184209 Apatity, Murmansk Region, Russia

\* st054910@student.spbu.ru

Crystals of the new uranyl selenite(IV)—selenate(VI), (UO<sub>2</sub>)(SeO<sub>4</sub>)(H<sub>2</sub>SeO<sub>3</sub>)[(SeO<sub>4</sub>)(C<sub>3</sub>H<sub>8</sub>N<sub>6</sub>)] (**1**), were obtained by isothermal evaporation at room temperature from aqueous solution of uranyl nitrate, selenic acid and melamine.

X-ray diffraction experiment was performed using a Bruker Smart diffractometer equipped with an Apex II CCD detector. The unit cell parameters were determined and refined by the least-squares method on the basis of 26413 reflections with  $2\theta$  in the range  $5.32^\circ$ – $65.00^\circ$ . Compound crystallizes in the monoclinic system,  $a = 16.247(4)$  Å,  $b = 8.680(2)$  Å,  $c = 13.347(3)$  Å,  $\beta = 90.615(5)^\circ$ ,  $V = 1882.1(8)$  Å<sup>3</sup>. From the systematic absence laws and statistics of reflection distribution,  $P2_1/c$  space group was determined. The absorption correction was introduced taking into account the shape of the crystal. The structure was solved by the direct methods and refined to  $R_1 = 0.0317$  ( $wR_2 = 0.0388$ ) for 4068 reflections with  $|F_o| \geq 4\sigma_F$ . The crystal structure of **1** contains one symmetrically independent U<sup>6+</sup> cation that forms two short (1.749(4) and 1.752(4) Å) U<sup>6+</sup>—O<sup>2-</sup> bonds resulting in a linear uranyl cation, [UO<sub>2</sub>]<sup>2+</sup>. This basic uranyl entity with 5 longer (2.348(3) – 2.476(3) Å) bonds in the equatorial plane forms a pentagonal bipyramid. Compound **1** contains 2 crystallographically unique Se<sup>4+</sup> and Se<sup>6+</sup> cations. Hexavalent selenium atoms are tetrahedrally coordinated by four O<sup>2-</sup> atoms each [ $\langle \text{Se-O} \rangle = 1.609(4) - 1.649(3)$  and  $1.623(3) - 1.639(3)$  Å for Se1 and Se4, respectively]. The Se(IV) positions have a trigonal pyramidal coordination with the apex occupied by the Se(IV) atom. These trigonal pyramids are heavily distorted: one short bond [1.711(4) Å and 1.648(3) Å for Se2 and Se3, respectively], and two longer bonds [1.711(4) Å, 1.739(4) Å and 1.713(4) Å, 1.742(4) Å для Se2 and Se3, respectively]. The observed elongation is the result of the presence of OH groups at these positions.

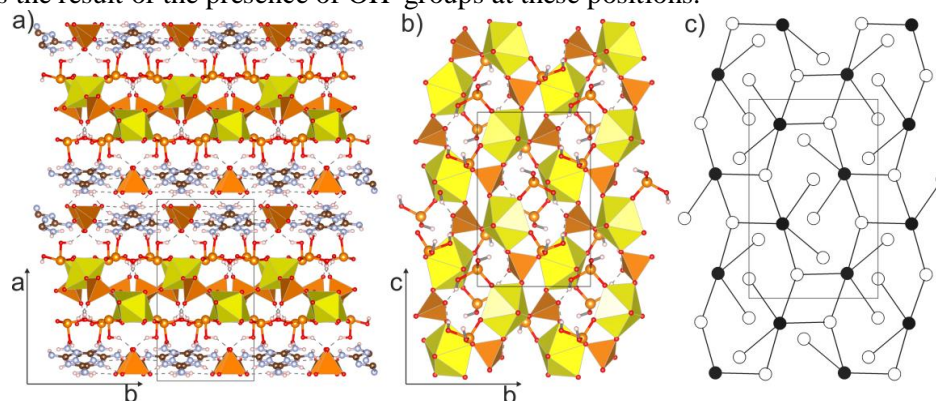


Figure 1. U-Se layer (b) of the structure **1** (a) and its corresponding graph (c)

The structure of **1** is formed by the modular principle, which can be described as follows. The structure of **1** is based on electro-neutral layers [(UO<sub>2</sub>)(SeO<sub>4</sub>)(H<sub>2</sub>SeO<sub>3</sub>)]<sup>0</sup> arranged parallel to the plane [100]. These layers in turn are separated by another electro-neutral organic-inorganic complexes [(SeO<sub>4</sub>)(C<sub>3</sub>H<sub>8</sub>N<sub>6</sub>)]<sup>0</sup>, in which selenate tetrahedra connected to melamine molecules via hydrogen bonds with protonated amino groups of organic molecules. Analysis of the uranyl selenate layers in the structure of **1** (Fig. 1c) using black-and-white graphical approach indicates that it's topology is new not only for uranyl compounds, but also for oxysalts in general (cc2-1:2-22).

This work was supported by St. Petersburg State University and Russian Science Foundation (grant 18-17-00018). X-ray studies were carried out at the Research Center for X-ray structural studies of St. Petersburg State University.

## Термические свойства D, L-аспарагиновой кислоты

Кусуткина А.М., Князев А.В., Князева С.С., Гусарова Е.В., Амосов А.А., Шипилова А.С.

Нижегородский государственный университет им. Н.И. Лобачевского, 603950 Нижний Новгород, Россия

\*Correspondence email: kotovasya2017@gmail.com

Важную роль в любом живом организме играют аминокислоты. Аспарагиновая кислота является одним из основных сырьевых материалов для получения подсластителя аспартама и промежуточного L-аспарагин моногидрата в фармацевтике [1]. Она выполняет роль нейромедиатора в центральной нервной системе и оказывает прямое воздействие на естественную конфигурацию и функциональность белков, что было продемонстрировано на примере нескольких невральных патологий [2]. Используя метод низкотемпературной рентгенографии, оценили тепловое расширение исследуемого вещества вдоль различных кристаллографических направлений. Определили коэффициент теплового расширения исследуемого соединения, что является количественной характеристикой теплового расширения. Рентгенограммы образца записывали на дифрактометре XRD-6000 Shimadzu (CuK $\alpha$ -излучение, геометрия съемки на отражение) с шагом 0.02°, в интервале 2 $\theta$ : 10÷60° при температуре от 150 К до 450 К (шаг 25К). После обработки результатов эксперимента были получены коэффициенты теплового расширения трех изученных азотистых оснований, представленные в таблице 1.

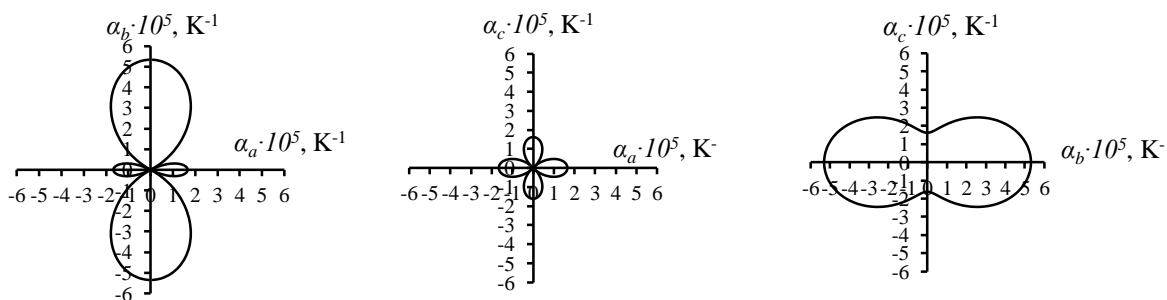
Таблица 1. Коэффициенты теплового расширения исследуемой D, L-аспарагиновой кислоты.

Соединение	К	T, 10 <sup>5</sup> , К <sup>-1</sup>	$\alpha_a \cdot 10^5$ , К <sup>-1</sup>	$\alpha_b \cdot 10^5$ , К <sup>-1</sup>	$\alpha_c \cdot 10^5$ , К <sup>-1</sup>	$\alpha_v \cdot 10^5$ , К <sup>-1</sup>
D, L-аспарагиновой кислоты		300	- 1.66	5.3 5	1.6 2	5.4 1

Было обнаружено, что анизотропия теплового расширения возрастает с повышением температуры (рис.1), наибольшие тепловые деформации наблюдаются по оси b, что обусловлено наличием низкоэнергетических водородных связей вдоль этого кристаллографического направления, по оси a происходит сжатие структуры.

На основании полученных данных были построены двумерные фигуры коэффициентов теплового расширения при различных температурах для исследуемого соединения, демонстрирующие приоритетные направления при тепловом расширении [3].

Рис. 1. 2 D фигуры коэффициентов теплового расширения аспарагиновой кислоты.



1. Wang J. Solubility of d-Aspartic Acid and l-Aspartic Acid in Aqueous Salt Solutions from (293 to 343) K. / J. Wang, J. Liu, S. Wang, J. Pei // Journal of Chemical & Engineering Data. – 2010. – V. 55(4). – P. 1735–1738.

2. Fisher G.H. Free D-aspartate and D-alanine in normal and Alzheimer brain / G.H. Fisher, A. D'Aniello, A. Vetere, L. Padula, G.P. Cusano, E.H. Man // Brain Res. Bull., –1991. – V. 26(6). –P. 983–985.

3. Белоусов, Р.И. Алгоритм расчета тензора и построения фигур коэффициентов теплового расширения в кристаллах / Р.И. Белоусов, С.К. Филатов // Физика и химия стекла. – 2007. – Т. 33. – №3. – С. 377–382.

## Ribbon structure of the wide-gap semiconductor $\text{Sb}_2\text{S}_3$ in the channels of SWCNT

Zakalyukin R.M.<sup>1,2</sup>, Levkevich E.A.<sup>1\*</sup>, Kumskov A.S.<sup>2</sup>

<sup>1</sup> MIREA - Russian Technological University, 119454, Vernadskogo ave., 78, Moscow, Russia.

<sup>2</sup> Shubnikov Institute of Crystallography of Federal Scientific Research Centre «Crystallography and Photonics» of Russian Academy of Sciences, 119333, Leninsky ave., 59, Moscow, Russia.

\*Correspondence email: katya.levkevich@mail.ru

At present time, the creation of new functional materials based on nanocomposites is a perspective and important scientific task. Single-walled carbon nanotubes (SWCNT) are one of such perspective materials because of their extraordinary physical, electrical and chemical properties.

One can get a material with unique characteristics by embedding substances with different properties inside the carbon nanotube channel because compounds incorporated can behave as electron donors or acceptors and also change nanotube properties. One of the most widespread methods of nanocomposites of incorporation synthesis is filling from the melt due to its simplicity and the large number of substances that can be introduced by this method. The essence of this method is the exposure of SWCNTs in a melt of the compound to be incorporated at temperatures exceeding the melting temperature of the introduced compound by 30–50°C, with the subsequent cooling, which leads to the crystallization.

At the same time it is interesting that geometric limitations of the carbon nanotube channel (its diameter is usually in a range 6-25 Å) distort the three-dimensional crystal structure of the inserted compound at the atomic level.

There are many works dedicated to investigation of nanocomposites, which contain narrow-gap semiconductors, but not many works about wide-gap semiconductors. It is interesting to synthesize a nanocomposite, which consists of the nanotube and a wide-gap semiconductor. One such compound is antimony sulfide  $\text{Sb}_2\text{S}_3$ , whose bandgap value is approximately ~1.7 eV. Antimony sulfide has promising optical, photoelectronic and electrochemical characteristics. It is unique semiconductor material with a wide range of practical applications, such as solar cells, lithium-ion and sodium-ion batteries, optical arrays, etc.

In this work we synthesized a nanocomposite  $\text{Sb}_2\text{S}_3@\text{SWCNT}$ . Nanotubes were filled by capillary method. We used  $\text{Sb}_2\text{S}_3$  (chemically pure grade) and carbon nanotubes (IS090626, China). During the synthesis, needle crystals of  $\text{Sb}_2\text{S}_3$  were formed in the ampoule. According to the results of the X-Ray diffraction and Energy-dispersive X-ray spectroscopy analyses there weren't found foreign impurities in the sample. Micrographs of transmission electron microscopy in the channels of the nanotubes revealed the presence of crystalline matter.

To construct the structural model of the  $\text{Sb}_2\text{S}_3@\text{SWCNT}$  we used the structural data for the  $\text{Sb}_2\text{S}_3$  (space group  $Pbnm$ ,  $a = 11.23(9)$  Å;  $b = 11.32(0)$  Å;  $c = 3.834(7)$  Å). The structure of antimony sulfide is represented by ribbons of  $(\text{Sb}_4\text{S}_6)_n$  along the crystallographic direction  $b$ . The ribbons have a distorted structure under the influence of the dimensional factor of the internal channel SWCNT. Due to the high charge of the atomic nucleus, Sb atoms have a high contrast in the microscopic image, while S atoms are practically indistinguishable. Depending on the diameter of the carbon nanotube, a fragment of the ribbon of the initial  $\text{Sb}_2\text{S}_3$  structure enters its channel. Thus, a ribbon with the composition  $(\text{Sb}_2\text{S}_3)_n$  enters the nanotube with a channel diameter of ~ 1 nm. This structural fragment of the ribbon is obtained by turning its axis 30 degrees from the original direction. At the same time a ribbon of composition  $(\text{Sb}_6\text{S}_9)_n$  is included in a wide CNT with a channel diameter of ~1.3 nm. The structure of  $(\text{Sb}_6\text{S}_9)_n$  is obtained by adding an extra number of antimony atoms to the composition  $(\text{Sb}_2\text{S}_3)_n$  ribbon. It is likely that the entry of an antimony sulfide ribbon into the channel of a SWCNT changes its channel shape from an ideal cylindrical one; therefore, the diameter of a carbon nanotube is not determined correctly. To place the initial  $\text{Sb}_2\text{S}_3$  structural tape in the channel of a carbon nanotube, its diameter should be more than 1.4 nm. In this sample, SWCNTs of this diameter were practically not contained.

Thus,  $\text{Sb}_2\text{S}_3@\text{SWCNT}$  nanocomposite was synthesized for the first time by a capillary wetting technique. Antimony sulfide particles almost completely filled the channels of carbon nanotubes, which was confirmed by XRD, EDX analyzes and electron microscopy. The structural model of the nanocomposite was constructed in full accordance with electron microscopic images.



## Formation process of the Bi-Fe-W-O pyrochlore nanoparticles via microwave synthesis

Lomakin M.S.<sup>1</sup>, Proskurina O.V.<sup>1,2</sup>

<sup>1</sup> Ioffe Institute, 26, Politekhnicheskaya St., 194021, St. Petersburg, Russia

<sup>2</sup> St. Petersburg State Institute of Technology, 26, Moskovsky Ave., 190013, St. Petersburg, Russia

\*Correspondence email: lomakinmakariy@gmail.com

The pyrochlore structure  $(A_2)B_2O_6(O^l)$  forms in many oxide systems; it is renowned for a number of interesting electrophysical properties. The pyrochlore-structured compounds can be ferroelectrics, ferromagnets, antiferromagnets, multiferroics, dielectrics, semiconductors and ionic conductors. Often, pyrochlores are the phases of variable composition and have a flexible crystal structure, which makes it possible not only to vary the  $A$  and  $B$  cations ratio in the structure, but also to perform their isomorphic substitution with other elements. The nature of the elements from which the pyrochlore structure is formed, as well as their relative content and position in the structure, determine properties of the compound.

In our previous work [1] the hydrothermal synthesis method application has for the first time resulted in producing and characterizing a pyrochlore-structured phase with the variable composition  $Bi_{y+0.67\delta}Fe_yW_{2-y}O_6O^l_\delta$  in two-phase mixtures. The preparation of BFWO-based single-phase samples with a specified composition has encountered a number of synthesizing difficulties that require a systematic study of the influence of phase formation conditions on the composition and structure of the target product [2].

The present study is devoted to the investigation of the formation process of the Bi-Fe-W-O pyrochlore nanoparticles via microwave synthesis. A series of samples has been successfully synthesized via microwave technique. At a temperature of 180 degrees centigrade the time of isothermal exposure changed as follows: 0 (cooling immediately after heating), 15, 30, 45 sec., 1, 2, 3, 4 and 5 min. The obtained samples were examined by a variety of methods of physical-chemical analysis. Among them powder X-ray diffraction technique, transmission and scanning electron microscopy, local energy dispersive X-ray microanalysis and Mossbauer spectroscopy.

The work was financially supported by the Russian Science Foundation (Project No. 16-13-10252).

1. Lomakin M.S., Proskurina O.V., Danilovich D.P., Panchuk V.V., Semenov V.G., Gusarov V.V., Hydrothermal Synthesis, Phase Formation and Crystal Chemistry of the pyrochlore/ $Bi_2WO_6$  and pyrochlore/ $\alpha$ - $Fe_2O_3$  Composites in the  $Bi_2O_3$ - $Fe_2O_3$ - $WO_3$  System. *J. Solid State Chem.*, 2020, 282, 121064 DOI: 10.1016/j.jssc.2019.121064

2. Lomakin M.S., Proskurina O.V., Gusarov V.V. Influence of hydrothermal synthesis conditions on the composition of the pyrochlore phase in the  $Bi_2O_3$ - $Fe_2O_3$ - $WO_3$  system, *Nanosyst.: Phys. Chem. Math.*, 2020, 11 (2), P. 246–251. DOI: 10.17586/2220-8054-2020-11-2-246-251

## The study of periodic multilayer systems NiMo/Ti and FeCo/TiZr by X-ray diffraction and reflectometry

Matveev V.A. <sup>1</sup>

<sup>1</sup> Petersburg Nuclear Physics Institute named by B.P. Konstantinov of National Research Centre «Kurchatov Institute», 188300, Leningradskaya oblast, Gatchina, mkr. Orlova roshcha 1, Russia.

\*Correspondence email: matveev\_va@pnpi.nrcki.ru

The multilayer systems FeCo/TiZr and NiMo/Ti used as elements of polarizing and non-polarizing neutron-optical devices [see eg. 1-3]. These elements multilayer systems by magnetron deposition of multilayer structures on glass or silicon substrates. An important parameter of these elements is the coefficient of reflectivity of neutrons, what depends on the interlayer roughness of multilayer systems [4]. The sizes and orientation of crystallites determine the interlayer roughness of multilayer structures.

In this work, we studied of interfacial roughness and sizes of crystals in periodic multilayers coatings NiMo/Ti and FeCo/TiZr. The samples were prepared by magnetron sputtering on float-glass (the surface roughness  $\sigma_s = 0.5 \pm 0.2$  nm, as measured by XRR before deposition). The interfacial roughness were measured by X-ray reflectometry, the sizes of crystals were examined by grazing incidents X-ray diffraction. The interlayer roughness increases from the lower layer to the upper layer, while the crystallite size in the metal layers remains practically unchanged.

1. Ul'yanov V.A., Böni P., Khamov V.N., Orlov S.P., Peskov B.G., Pleshanov N.K., Pusenkov V.M., Schebetov A.F., Serebrov A.P., Sushkov P.A. and Syromyatnikov V. G., The Effect of Large Irradiation Doses on Polarizing and Non-polarizing Supermirrors. *Physica B*. 2001. V. 297. P. 136-139.

2. Syromyatnikov V.G., Schebetov A.F., Lott D., Bulkin A.P., Pleshanov N.K., Pusenkov V.M. PNPI wide-aperture fan neutron supermirror analyzer of polarization. *Nuclear Instruments and Methods in Physics Research Section A. Accelerators Spectrometers Detectors and Associated Equipment*. 2011. V. 634. P. 126-129.

3. Syromyatnikov V., Ulyanov V., Lauter V., Pusenkov V. Ambaye H., Goyette R., Hoffmann M., Bulkin A., Kuznetsov I., Medvedev E. A new type of wide-angle supermirror analyzer of neutron polarization. *Journal of Physics: Conference Series*. 2014. V. 528. P. 012021.

4. Pleshanov N.K., Kolyvanova N.G., Metelev S.V., Peskov B.G., Pusenkov V.M., Syromyatnikov V.G. Ul'yanov V.A., Schebetov A.F. Interfacial roughness growth and its account in designing CoFeV/TiZr neutron supermirror with  $m=2.5$ . *Physica B Condensed Matter*. 2005. V. 369. P. 234-242.

## The effect of shock waves on the structure of Bi-2223 superconductors after plasma treatment

Mikhailova A.<sup>1</sup>, Mikhailov B.<sup>1</sup>, Nikulin V.<sup>2</sup>, Silin P.<sup>2</sup>, Borovitskaya I.<sup>1</sup>

<sup>1</sup>Baykov Institute of Metallurgy and Materials Science, RAS, Leninskii pr. 49, Moscow, 119334  
Russia

<sup>2</sup>Lebedev Physical Institute of RAS, Leninskii pr. 53, Moscow, 119333 Russia

\*Correspondence email: sasham1@mail.ru

The report presents the results of the action of shock waves (SW) generated by the Plasma Focus setup on the structure and critical current  $J_c(B)$  of Bi-2223. The studies showed the possibility of an increasing the critical currents ( $J_c$ ) up to 15-25% in transverse and longitudinal magnetic fields to 2-3 T after plasma impact due to changes in the microstructure of the superconducting phase, including: grain refinement, interlayer compaction, microdeformations and appearing of additional crystal lattice defects.

The change in the microstructure of the superconducting core after SW is also consistent with the XRD data. For samples after SW, compared with the peaks in the X-ray diffraction patterns obtained before exposure, broadening of the X-ray peaks was established, and in some cases, with an increase of SW intensity, the formation of an amorphous phase has been found (5-10 wt.%). The lattice constants for initial samples and samples after treatment were calculated by Rietveld method, the sizes of the CSR ( $D$ ) and microstresses ( $\varepsilon$ ) were specified by Winfit program.

The formation of additional defects can contribute to an increase of the pinning force of magnetic vortices, which, according to the accepted theory of superconductivity begin to attach to them and, as a result, prevent the penetration of an external magnetic field into the bulk of the superconductor.

This work was supported by the Russian Science Foundation, grant No. 16-12-10351 in the part of processing samples at the Plasma Focus installation and in the framework of the State task No. 075-00947-20-00 in the part of conducting structural studies.

## Thermal expansion of Cd- and Sr-containing NZP-related solid solutions

Perova E.R. , Mayorov P.A.

Lobachevsky University, 603950, Gagarina Avenue 23, Nizhny Novgorod, Russia

\*Correspondence email: perovakatharina@gmail.com

Framework phosphates with crystal structure related to  $\text{NaZr}_2(\text{PO}_4)_3$  (NZP) are characterized by resistance to high temperatures, aggressive media and radiation. One of practically important properties of the NZP-materials is their controlled thermal expansion. The behavior of the NZP-structure as a whole under thermal effects depends on the nature, the ratio of the sizes and the number of cations filling the crystallographic positions of various types, as well as the number of vacant positions and the symmetry of the unit cell.

In the present study, thermal expansion of Cd- and Sr-containing systems was studied on a Shimadzu XRD-6000 X-ray diffractometer ( $\text{CuK}_\alpha$ -radiation,  $\lambda = 1.54178 \text{ \AA}$ ). X-ray diffraction patterns were obtained within  $2\theta = 10 - 60^\circ$  in the temperature range 173 – 473 K. The unit cell  $a$  and  $c$  parameters were calculated at different temperatures, and their temperature dependences were approximated as linear functions.

The studied phosphates  $\text{Cd}_{0.5+x}\text{Mg}_x\text{Zr}_{2-x}(\text{PO}_4)_3$  were characterized by low average linear thermal expansion coefficients, but their expansion anisotropy was quite large (figure 1a). Temperature dependence of thermal expansion coefficients for the phosphates  $\text{Sr}_{0.5+x}\text{Mg}_x\text{Zr}_{2-x}(\text{PO}_4)_3$  allowed us to predict the composition of the solid solution ( $x = 0.18$ ) with near-zero anisotropy, keeping small average expansion coefficient (figure 1b). The thermal expansion coefficients of the phosphate  $\text{Sr}_{0.7}\text{Mg}_{0.2}\text{Zr}_{1.8}(\text{PO}_4)_3$  ( $x = 0.2$ ) of the nearest composition were  $\alpha_a = 3.73 \cdot 10^{-6}$ ,  $\alpha_c = 4.28 \cdot 10^{-6}$ ,  $\alpha_{av} = 3.92 \cdot 10^{-6}$ ,  $|\alpha_a - \alpha_c| = 0.55 \cdot 10^{-6} \text{ K}^{-1}$ .

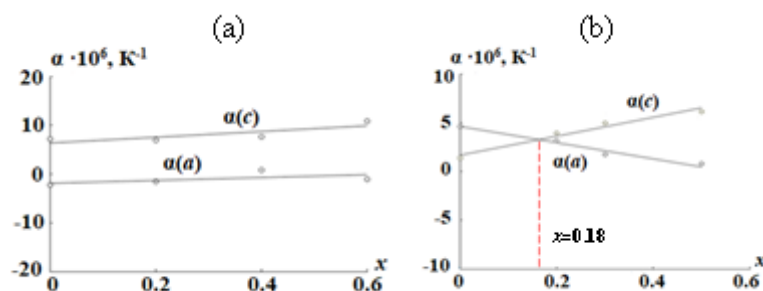


Figure 1. Linear thermal expansion coefficients vs. composition for the phosphates:  $\text{Cd}_{0.5+x}\text{Mg}_x\text{Zr}_{2-x}(\text{PO}_4)_3$  (a) and  $\text{Sr}_{0.5+x}\text{Mg}_x\text{Zr}_{2-x}(\text{PO}_4)_3$  (b).

Thus, the studied phosphates  $\text{M}_{0.5+x}\text{Mg}_x\text{Zr}_{2-x}(\text{PO}_4)_3$  ( $\text{M} - \text{Cd}, \text{Sr}$ ) are characterized by low values of the average coefficients of thermal expansion, which allow us to hope for success in the development of ceramics based on them that are resistant to thermal shock.

Acknowledgments: The reported study was funded by RFBR, project number 19-33-90075.

## Structure and thermal expansion of new high-temperature compounds $\text{Ln}_2\text{CrTaO}_7$ ( $\text{Ln}=\text{Sm}, \text{Gd}, \text{Y}$ )

Popova E.F. \*, Veselova V.O., Egorysheva A.V.

Kurnakov Institute of General and Inorganic Chemistry, Russian Academy of Sciences, 119991, Leninsky pr. 31, Moscow, Russia.

\*Correspondence email: lenapopova11a@yandex.ru

Cubic pyrochlores  $\text{A}_2\text{B}_2\text{O}_7$ , in which A and B cations form infinite interpenetrating sublattices of tetrahedra connected by vertices, have been the subject of persistent interest for many decades for several important reasons. If A or B site is occupied by magnetic ions competing spin interactions within and between different magnetic sublattices can cause important physical properties to appear, such as large magnetoresistance, negative thermal expansion, and magnetoelastic effects. Such properties are observed, for example, in Cr-based spinels, but there are no published works concerning the chromium-containing pyrochlores. In this work, we studied the effect of magnetic properties on thermal expansion of new complex Cr-containing pyrochlores  $\text{Ln}_2\text{CrTaO}_7$ ,  $\text{Ln} = \text{Y}, \text{Sm}, \text{Gd}$ .

Pyrochlores  $\text{Ln}_2\text{CrTaO}_7$  were synthesized by the coprecipitation method with subsequent annealing. The Rietveld refinement showed that all synthesized  $\text{Ln}_2\text{CrTaO}_7$  compounds relate to the spatial group  $Fd\bar{3}m$  and have a cubic structure of pyrochlore. The lattice parameter  $a$  increases along with the RE ionic radius increase in compounds of different composition. The refined Ta- and Cr- site occupancy is very close to the stoichiometric one. It should be noted, that there is no ordering in the distribution of Ta and Cr by their B-site. The analysis of the  $\text{Sm}_2\text{CrTaO}_7$  XANES spectrum at the Cr K-edge showed that chromium oxidation state is +3. Study of the temperature dependence of the lattice parameter revealed presence of negative thermal expansion region in  $\text{Y}_2\text{CrTaO}_7$  (Fig.1a). Upon cooling from 300 K up to  $\sim 150$  K the lattice parameter  $a$  decreases. However, the lattice expansion is negative in the range from 150 to 100 K. Temperature dependence of the thermal expansion coefficient is a flat curve. This indicates that the observed effect is most likely related to second-order transition. In addition, X-ray patterns registered in this temperature range were characterized by broadening of the Bragg peaks, which is due to the development of microstrain upon cooling. No negative thermal expansion regions were detected in the temperature dependences of the  $\text{Sm}_2\text{CrTaO}_7$  and  $\text{Gd}_2\text{CrTaO}_7$  lattice parameters (Fig.1b). At the same time the temperature dependence of the parameter  $a$  of  $\text{Gd}_2\text{CrTaO}_7$  has a subtle inflection in the region of 160-170 K. The detailed study of  $\text{Ln}_2\text{CrTaO}_7$  magnetic properties allows us to conclude that magnetic behavior is caused by the ferromagnetic (FM) interactions of the  $\text{Cr}^{3+}$  sublattice, which is characterized by the presence of FM transition in the 150 K region. So a negative coefficient of thermal expansion in  $\text{Y}_2\text{CrTaO}_7$  is detected due to magnetoelastic effects in the lattice. The appending of a RE magnetic cation (along with chromium) into the pyrochlore lattice gives rise to a competition between AFM and FM interactions of the two sublattices, which significantly changes the magnetic behavior of pyrochlores. As a result, additional magnetic phase transitions appear in  $\text{Sm}_2\text{CrTaO}_7$  and  $\text{Gd}_2\text{CrTaO}_7$ . At the same time, the probability of lattice deformation associated with spontaneous magnetization in the FM transition region, as well as the appearance of negative thermal expansion, is reduced. Thus, -the important role of the Cr-sublattice in the formation of low-temperature thermal expansion was shown.

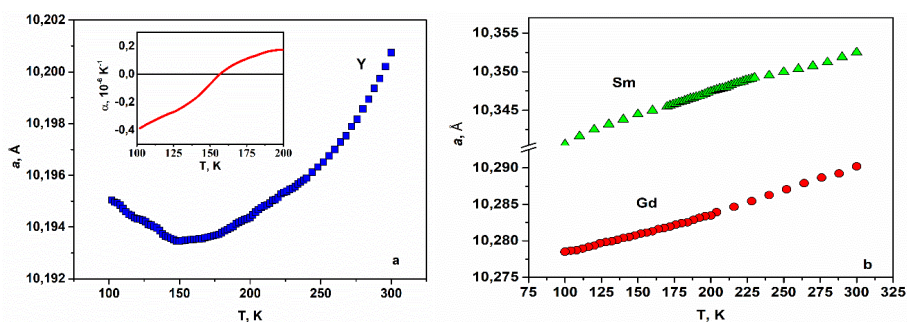


Fig. 1. Variation of the cell parameter  $a$  with  $T$  and the thermal expansion coefficients  $\alpha$  (the inset) for  $\text{Y}_2\text{CrTaO}_7$  (a), and for  $\text{Sm}_2\text{CrTaO}_7$  and  $\text{Gd}_2\text{CrTaO}_7$  (b).

Acknowledgements: This study was supported by the Russian Scientific Foundation (18-13-00025).

## Theoretical study of magnesium and calcium orthocarbonate at *PT* conditions of the Earth's lower mantle

Sagatova D.N.<sup>1,2\*</sup>, Gavryushkin P.N.<sup>1,2</sup>

<sup>1</sup> Sobolev Institute of Geology and Mineralogy, Siberian Branch of the Russian Academy of Science, 630090, prosp. acad. Koptuyuga 3, Novosibirsk, Russia.

<sup>2</sup> Department of Geology and Geophysics, Novosibirsk State University, 630090, Pirogov str. 2, Novosibirsk Russia.

\*Correspondence email: d.sagatova1729@gmail.com, sagatovadn@igm.nsc.ru

The discovery of the carbon transition to an unconventional fourfold coordinate state in high-pressure phases of magnesium and calcium carbonates [1] served us as the motivation for the search for a new class of compounds – orthocarbonates. The aim of this study is to determine the stable phases of magnesium and calcium orthocarbonates and to calculate their *PT* stability fields.

Density functional theory calculations for new stable phases of  $\text{Mg}_3\text{CO}_5$ ,  $\text{Mg}_2\text{CO}_4$ ,  $\text{Mg}_3\text{C}_2\text{O}_7$ ,  $\text{Ca}_3\text{CO}_5$ ,  $\text{Ca}_2\text{CO}_4$ , and  $\text{Ca}_3\text{C}_2\text{O}_7$  were performed at pressures of 10, 25, and 50 GPa using the *ab initio* random structure searching (AIRSS) technique. In the MgO-MgCO<sub>3</sub> system, all the most favorable predicted structures turned out to be thermodynamically unstable with respect to decomposition. In a similar system with calcium, we found a new structure of calcium orthocarbonate  $\text{Ca}_2\text{CO}_4$ -*Pnma* which energetically favorable with respect to decomposition above 13 GPa. The result of the search for the stable phase  $\text{Ca}_3\text{CO}_5$ -*Cmcm* is in agreement with the results of [2]. The predicted structure of the  $\text{Ca}_3\text{C}_2\text{O}_7$ -*P2<sub>1</sub>/c* is unfavorable over the entire pressure range.

The basis of the calcium orthocarbonate structure  $\text{Ca}_2\text{CO}_4$ -*Pnma* is a heteropolyhedral framework of interconnected Ca polyhedra and isolated [CO<sub>4</sub>] tetrahedra. There are two structurally distinct calcium positions in the phase: the Ca(1) is surrounded by nine oxygen atoms and formed a distorted three-cap trigonal prism, while the Ca(2) atoms is located in a distorted five-cap trigonal prism coordinated by oxygen. The average Ca–O distances in both of the calcium polyhedra in  $\text{Ca}_2\text{CO}_4$  smoothly varies from 2.25 Å to 2.86 Å at 25 GPa. Each carbon atom is surrounded by four oxygen atoms (C–O distances 1.38 – 1.40 Å at 25 GPa), and polyhedron – almost regular tetrahedron.

The calculated phase diagram of  $\text{Ca}_2\text{CO}_4$  is shown in Fig.1. We determined that the stability region of calcium orthocarbonate covers the thermodynamic parameters of the transition zone and the lower mantle of the Earth.

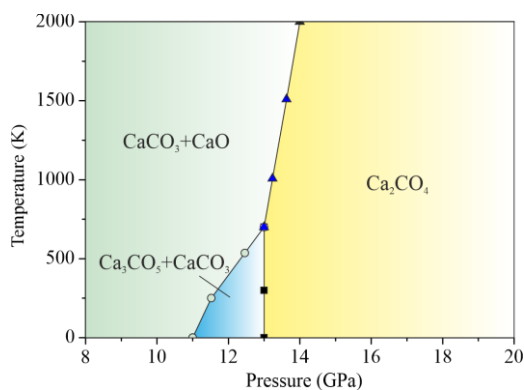


Fig.1. Phase relations in  $\text{Ca}_2\text{CO}_4$  phase.

This work was supported by the Russian Foundation for Basic Research (project No 20-03-00774).

1. Lobanov S. S., Dong X., Martirosyan N. S., Samtsevich A. I., Stevanovic V., Gavryushkin P. N., Litasov K. D., Greenberg E., Prakapenka V. B., Oganov A. R., Goncharov A. F. Raman spectroscopy and x-ray diffraction of  $sp^3$  CaCO<sub>3</sub> at lower mantle pressures. *Physical Review B*. 2017. V. 96. P. 104101.

2. Yao X., Xie C., Dong X., Oganov A. R., Zeng Q. Novel high-pressure calcium carbonates. *Physical Review B*. 2018. V. 98. P. 014108.

## Thermal deformations of the amino acid enantiomers L-serine and L-alanine

Sadovnichii R.V.<sup>1\*</sup>, Lorenz H.<sup>2</sup>, Kotelnikova E.N.<sup>1</sup>

<sup>1</sup>Department of Crystallography, Saint Petersburg State University, 199034 Saint Petersburg, Russia

<sup>2</sup>Max Planck Institute for Dynamics of Complex Technical Systems, 39106 Magdeburg, Germany

\*Correspondence email: rsadovnichii@gmail.com

Amino acids are one of the most actively synthesized organic compounds. They are widely used in pharmaceuticals and food industries. Currently, much attention is paid to the study of chiral binary systems in which the components are the enantiomers of different amino acids [1–3]. This work presents results of studying 1) solid phases relations in the system L-serine—L-alanine and 2) thermal deformations of L-serine (L-ser)  $C_3H_7NO_3$  (S.G.  $P2_12_12_1$ ) and L-alanine (L-ala)  $C_3H_7NO_2$  (S.G.  $P2_12_12_1$ ).

The initial reactants L-ser and L-ala having 99% purity were obtained from Sigma-Aldrich Chemie GmbH (Buchs, Switzerland) and were used to prepare mixtures with various proportions of the components (mol. %): L-ser/L-ala = 0/100, 7/93, 10/90, 15/85, 25/75, 35/65, 50/50, 65/35, 75/25, 85/15, 90/10, 93/7 and 100/0. To obtain samples, the mixture was first dissolved in distilled water and then crystallized via the isothermal evaporation method. The 13 samples were studied by the PXRD method (Rigaku MiniFlex II diffractometer,  $Co_{K\alpha}$ ,  $2\theta = 5-60^\circ$ ). In addition, L-ser, L-ala and the sample of composition L-ser/L-ala = 90/10 mol. % were studied by the TRPXRD method (Rigaku Ultima IV diffractometer,  $Co_{K\alpha}$ ,  $2\theta = 5-60^\circ$ ); temperature range 23–200 °C, with steps of 10 °C. The X-ray diffraction patterns obtained were processed and unit cell parameters were calculated using the programs PDXL and Topas respectively. Calculation of the thermal deformation tensor was carried out using the program TEV. According to the results of the PXRD study, solid solutions in the L-ser—L-ala system are not formed. All samples are physical mixtures of L-ser and L-ala with different quantitative proportions. Peaks of both phases are present in all PXRD patterns. According to TRPXRD data, no polymorphic transformations were detected for L-ser and L-ala in the range 23–200 °C. Both components undergo thermal deformations only. During the heating the parameter  $a$  decreases while the values of the  $b$  and  $c$  parameters and the volume  $V$  of orthorhombic cells increase. These data were used to calculate the thermal deformation tensor for L-ser and L-ala. The crystal structure of L-ser undergoes the greatest thermal expansion along the directions of the crystallographic axes  $b$  and  $c$ . A negative (anomalous) thermal expansion is observed in the direction of the  $a$  axis; this is due to the location of strong N–H...O and O–H...O hydrogen bonds along this direction. In the  $bc$  plane, in addition to N–H...O hydrogen bonds, van der Waals contacts are present between methylene groups  $CH_2$ . These groups are directed towards each other in neighboring molecules.

Thermal deformations of the L-ala crystal structure are similar to those of L-ser, but for L-ala the anisotropy of thermal expansion is also observed in the  $bc$  plane. In the crystal structure of L-ala, only one system of hydrogen bonds N–H...O is present in the direction of the  $a$  axis. N–H...O hydrogen bonds and van der Waals contacts in the  $bc$  plane are the same as in the  $bc$  plane of L-ser. Strong compression in the direction of the  $a$  axis up to negative thermal expansion was observed in the similar study of L-threonine (S.G.  $P2_12_12_1$ ) and L-allo-threonine (S.G.  $P2_12_12_1$ ) [4]. The composition L-ser/L-ala = 90/10 mol. % is a physical mixture of L-ser and L-ala up to a temperature of 200 °C. When this temperature is reached, the L-ala peaks disappear in the X-ray diffraction pattern, but the L-ser peaks remain. This occurs despite the fact that the sublimation temperature of L-ala (315 °C) is significantly higher than that of L-ser (228 °C). This suggests that near a temperature of 200 °C, L-ser and L-ala form a solid solution.

This work was supported by the Russian Foundation for Basic Research (16-05-00837).

1. Dalhus B., Görbitz C.H. Molecular aggregation in selected crystalline 1:1 complexes of hydrophobic D- and L-amino acids. III. The L-leucine and L-valine.

2. Kotelnikova E.N., Isakov A.I., Lorenz H. Non-equimolar discrete compounds in binary chiral systems of organic substances (Highlight). CrystEngComm. 2017, 19, 1851-1869.

3. Isakov A.I., Lorenz H., Zolotarev A.A. Jr., Kotelnikova E.N. Heteromolecular compounds in binary systems of amino acids with opposite and same chiralities. CrystEngComm. 2020, 22, 986-997.

4. Taratin N., Lorenz H., Binev D., Seidel-Morgenstern A., Kotelnikova E. Solubility equilibria and crystallographic characterization of the L-threonine/L-allo-threonine system. Part 2: crystallographic characterization of solid solutions in the threonine diastereomeric system. Cryst. Growth Des. 2015, 15, 137-144.

## Study of phase composition homogeneity of hard alloys based on WC – Co

Smetanina K.E.<sup>1\*</sup>, Andreev P.V.<sup>1,2</sup>, Lantsev E.A.<sup>1</sup>, Vostokov M.M.<sup>1</sup>

<sup>1</sup> Nizhny Novgorod State University named after N.I. Lobachevsky, 603950, Gagarin ave. 23, Nizhny Novgorod, Russia.

<sup>2</sup> Institute of Chemistry of High-Purity Substances of the Russian Academy of Sciences, 603137, Tropinin str. 49, Nizhny Novgorod, Russia.

\*Correspondence email: smetanina-ksenia@mail.ru

Hard alloys based on WC – Co are characterized by high resilience and wear resistance, which allows them to be used as metal cutting tool. Increasing physical and mechanical properties of these materials is associated with the problem of their phase composition homogeneity.

Spark plasma sintering (SPS) is promising method of hard alloys' manufacturing [1]. The surface of the WC powder particles is always oxidized, so that carbon deficiency can occur in the sintering volume at heating due to CO and CO<sub>2</sub> formation. Violation of stoichiometry leads to the formation of brittle  $\eta$ -phases (Co<sub>x</sub>W<sub>y</sub>C<sub>z</sub>) [2]. Carbon diffusion from the graphite mold in which the powder is poured reduces this effect: the surface layer of the sample will not contain  $\eta$ -phases, but at some distance from the surface these phases may exist.

The objects of this study were 3 hard alloy samples sintered from plasma chemical WC powder and cobalt (10% wt.) applied to the surface of WC particles by deposition method [3]. SPS of powder compositions was performed at "Dr. Sinter model SPS-625" in a vacuum (heating speed was 50°C/min, pressure was 70 MPa, sintering temperature was 1050°C). Degassing exposure at 850°C for 10 minutes was conducted during the sintering process of two samples. The surface of the samples was subjected to consecutive mechanical grinding with diamond discs and mechanical polishing with diamond paste to a particle dispersion of 1/0  $\mu$ m. The sample height was controlled by a micrometer.

X-ray diffraction experiments were performed on a powder diffractometer "Shimadzu XRD-7000" (CuK $\alpha$ ,  $\lambda = 1.54 \text{ \AA}$ ). Qualitative phase analysis demonstrated the presence of  $\alpha$ -WC,  $\beta$ -Co and  $\eta$ -phase – Co<sub>3</sub>W<sub>3</sub>C in studied samples. The dependencies  $I_{\eta(511)}/I_{WC(111)}$  on the total value of the remote layer were constructed to determine the carbon diffusion depth (fig. 1).

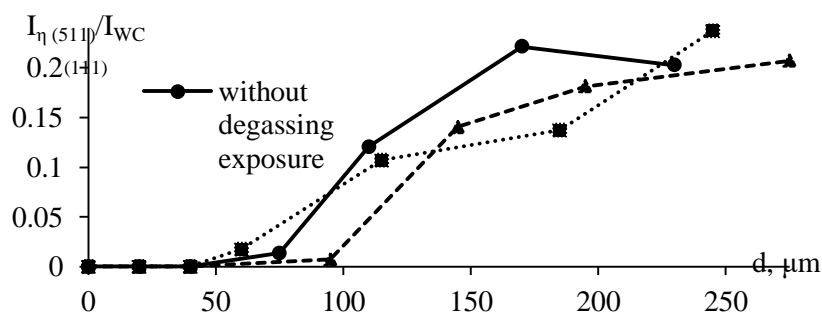


Fig. 1. Distribution of ratio  $I_{\eta(511)}/I_{WC(111)}$  by depth of hard alloy samples sintered at 1050°C

$\eta$ -phase (Co<sub>3</sub>W<sub>3</sub>C) is not detected in the surface layer which thickness does not exceed 100  $\mu$ m. It should also be noted that the degassing exposure during the sintering process had no significant impact on the formation rate of  $\eta$ -phase (Co<sub>3</sub>W<sub>3</sub>C).

The work was financial supported by Russian Science Foundation, grant №18-73-10177.

1. Panov V.S., Chuvilin A.M. Technology and properties of sintered hard alloys and products from them. MISiS, Moscow. 2001. (In Russ.)

2. Kurlov A.S., Gusev A.I. Physics and chemistry of tungsten carbide. M.: FIZMATLIT. 2013. (In Russ.)

3. Isaeva N.V., Blagoveshchensky Yu.V., Blagoveshchenskaya N.V. et al. Obtaining of carbide nanopowders and hard alloy compositions using a low-temperature plasma. Universities' proceedings. Powder metallurgy and functional coatings. 2013. V. 3. P. 7–14. (In Russ.)



## High-temperature XRD studies of some new compounds of Dion – Jacobson series

Syrov E.V.<sup>1\*</sup>, Krasheninnikova O.V.<sup>1</sup>, Knyazev A.V.<sup>1</sup>, Tereshin A.I.<sup>1</sup>

<sup>1</sup> Lobachevsky State University of Nizhni Novgorod, Gagarin Prospekt 23/2, 603950 Nizhni Novgorod, Russia

\*Correspondence email: syrov\_ev@mail.ru

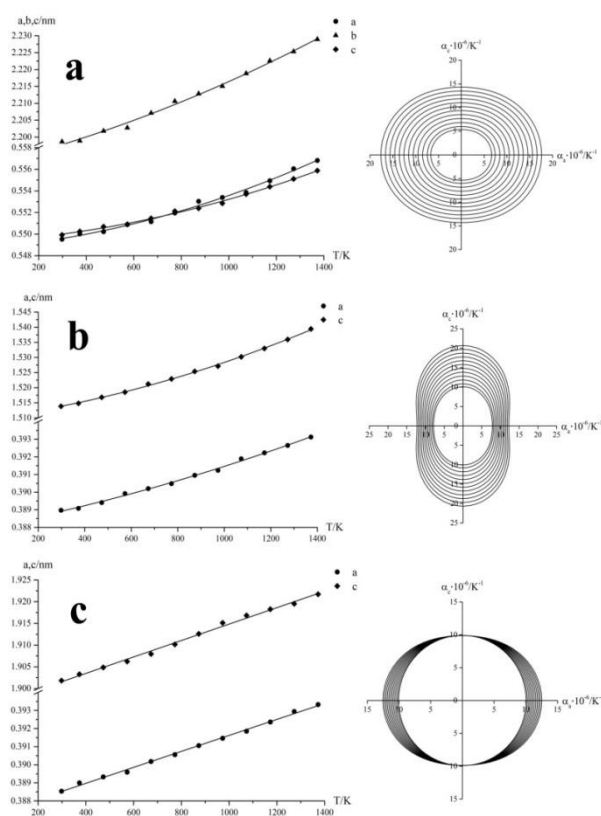


Fig. 1 Unit cell parameters vs. temperature and a-c figures of thermal expansion for a)  $\text{RbLaNb}_2\text{O}_7$  ( $n=2$ ), b)  $\text{RbLaNaNb}_3\text{O}_{10}$  ( $n=3$ ), c)  $\text{RbLaNa}_2\text{Nb}_4\text{O}_{13}$

$\text{RbLaNb}_2\text{O}_7$  crystallizes in orthorhombic  $\text{Imma}$  space group with unit cell parameters  $a = 0.54952$  nm,  $b = 2.1986$  nm and  $c = 0.54992$  nm. However, the next two members are tetragonal with  $P4/mmm$  space group: for  $\text{RbLaNaNb}_3\text{O}_{10}$   $a = 0.38897$  nm,  $c = 1.5138$  nm; for  $\text{RbLaNa}_2\text{Nb}_4\text{O}_{13}$   $a = 0.38853$  nm,  $c = 1.9018$  nm. High-temperature X-ray diffraction measurements were carried out using PANalytical Empyrean diffractometer with Anton Paar HTK 1200 high-temperature camera attachment. The radiation was  $\text{CuK}\alpha_{1,2}$  (1 kW),  $2\theta$  range –  $5\text{--}60^\circ$  at scan speed  $2^\circ/\text{min}$  with  $0.02^\circ$  step, temperature range –  $298\text{--}1373$  K with 100 K step. Thermal expansion plots and 2D figures are presented on Fig. 1. All phases show close to linear expansion in the examined range and no signs of phase transitions. While it's common for tetragonal perovskites, polar orthorhombic layered perovskite structures usually undergo a high-temperature phase transition to non-polar one [1]. It's not happening in the case of  $\text{RbLaNb}_2\text{O}_7$  probably due to the high stability of the two-layer structure. The other noteworthy feature is low expansion coefficients along the c axis of  $\text{RbLaNa}_2\text{Nb}_4\text{O}_{13}$  (Fig. 1 c). This could be explained by the resistance of stacking non-tilting octahedra layers to expand along the densest direction in the anisotropic crystal structure.

1. Knyazev A.V., Krasheninnikova O.V., Syrov E.V., Kyashkin V.M., Lelet M.I., Smirnova N.N. Thermodynamic and X-ray studies of layered perovskite  $\text{KCa}_2\text{NaNb}_4\text{O}_{13}$ , Journal of Chemical Thermodynamics, 2019, V. 138, P. 255-261

Dion – Jacobson family of layered perovskites phases, first described by Dion et al. and Jacobson et al., is drawing much attention recently, mostly because of their abilities for photocatalytic water splitting under UV and visible light irradiation. General chemical formula for such compounds can be written as  $\text{A}'[\text{A}_{n-1}\text{B}_n\text{O}_{3n+1}]$ , where  $\text{A}' = (\text{Li}^+, \text{Na}^+, \text{K}^+, \text{Rb}^+, \text{Cs}^+, \text{H}^+, \text{Ag}^+, \text{NH}_4^+, \text{CuCl}^+, \text{FeCl}^+)$ ,  $\text{A} = (\text{Ca}^{2+}, \text{Sr}^{2+}, \text{Ba}^{2+}, \text{Bi}^{3+}, \text{Ln}^{3+})$  and  $\text{B} = (\text{Nb}^{5+}, \text{Ta}^{5+}, \text{Ti}^{4+}, \text{Mn}^{4+})$ . The crystal structure of such phases consists of  $n$  stacking octahedral perovskite-like layers alternating with  $\text{A}'$  (usually alkali) cation in the interlayer space. Ion – exchange *soft chemistry* reactions to replace  $\text{A}'$  ion are used to obtain metastable Dion – Jacobson phases that can't be synthesized directly.

Dion – Jacobson homologous series of phases  $\text{RbLaNa}_{n-2}\text{Nb}_n\text{O}_{3n+1}$  consisted of only  $n=2$  phase for a long time,  $n=3$  and  $n=4$  members were discovered quite recently and their properties have not been properly studied yet. To fill this gap,  $\text{RbLaNb}_2\text{O}_7$  ( $n=2$ ),  $\text{RbLaNaNb}_3\text{O}_{10}$  ( $n=3$ ) and  $\text{RbLaNa}_2\text{Nb}_4\text{O}_{13}$  ( $n=4$ ) were synthesized using conventional solid-state reaction between  $\text{RbNO}_3$ ,  $\text{La}_2\text{O}_3$ ,  $\text{NaNO}_3$  and  $\text{Nb}_2\text{O}_5$  with 50% molar excess of  $\text{RbNO}_3$  to compensate its volatility at high temperatures. The phase purity of the obtained compounds was determined by qualitative XRD analysis and chemical purity was determined using quantitative XRF analysis.

## Nucleation of tin pyrophosphate crystals under the influence of x-ray radiation

Sycheva G.A., Kostyreva T.G.

Grebenshchikov Institute of Silicate Chemistry, Russian Academy of Sciences, 199034, Makarov Emb. 2, St.Petersburg, Russia.

\*Correspondence email: sycheva\_galina@mail.ru

Glasses in the SnO-ZnO-P<sub>2</sub>O<sub>5</sub> system with different contents of WO<sub>3</sub>, MoO<sub>3</sub> and H<sub>2</sub>O were synthesized. The chemical composition of glass was determined using wet chemistry using complexometric, gravimetric and redox methods. The nucleation of tin pyrophosphate crystals in tin-zinc-phosphate glass was studied by the development method. The parameters of the origin of tin pyrophosphate crystals are determined: the stationary rate of crystal nucleation and the time of non-stationary nucleation. The influence of x-ray radiation on the parameters of nucleation was established. Glasses were synthesized from phosphoric acid (H<sub>3</sub>PO<sub>4</sub>), zinc carbon dioxide and tin dioxide. MoO<sub>3</sub> was added to the charge as molybdenum acid, and WO<sub>3</sub> as monovolframic acid. All the reagents were of the brand "analytical grade". The charge was dried and then mixed in a ball mill for 10 hours. The glass was cooked in a platinum crucible at a temperature of 1170 °C for 2 hours with automatic stirring for 30 minutes. Glass was produced by rapidly cooling the melt on a massive metal mold.

When performing chemical analysis, classical methods of analysis were used: complexometric, gravimetric and redox methods. Previously, it was found that these glasses are easily dissolved in hydrochloric acid when heated, and tin is completely oxidized to Sn (IV). To determine the content of the components, the sample suspension was dissolved in 10 ml of HCl and the resulting solution was carefully (to avoid tin polymerization) diluted in a 250 ml measuring flask with 0.5 n. HCl solution. In aliquot portions of this solution, the gross content of tin, phosphorus, and zinc was determined. A complexometric titration method was used to determine tin.

When studying the effect of reducing the degree of crystallization from the time of isothermal exposure at a temperature of 500 °C, it was found that this effect was more strongly manifested for a sample of glass subjected to x-ray irradiation. Visual inspection of the samples revealed that the areas of glass that were not exposed to radiation crystallized, while the irradiated part of the samples remained transparent after holding the samples at 400 °C for 2300 hours and developing at 420 °C for 10 minutes. The estimated rate of crystal generation in the trained zone is one order of magnitude lower compared to the rate in the non-irradiated zone. In this case, we should talk about the suppression of crystallization centers by radiation. A similar phenomenon was discovered by us when studying the origin of crystals in sodium-zinc phosphate glass in the Na<sub>2</sub>O-ZnO-P<sub>2</sub>O<sub>5</sub> system [1].

1. Sycheva G.A., Golubkov V.V. Reduction of the crystallization ability of sodium-zinc-phosphate glass under the action of x-ray radiation. Journal of the Physics and chemistry of glass. 2012. V. 38. No. 3. P. 350-362.

## Влияние кислотности и поверхностно-активных веществ на фазообразование $\text{BiVO}_4$ при постоянной температуре

Тимчук А.В. <sup>1,2</sup>

<sup>1</sup>Санкт-Петербургский государственный технологический институт (технический университет), 190013, Московский пр. д. 26, Санкт-Петербург, Россия.

<sup>2</sup>Физико-технический институт имени А.Ф. Иоффе РАН, 194021, ул. Политехническая, 26, Санкт-Петербург, Россия.

\*Correspondence email: [tricktimy@yandex.ru](mailto:tricktimy@yandex.ru)

Материалы на основе  $\text{BiVO}_4$  находят применение в таких областях, как катализ, фотокатализ, аккумулярование энергии. Ванадат висмута является полупроводником n-типа, обладает сегнетоэластичностью и химической стабильностью, нетоксичен.

Наиболее широко изучены три полиморфные модификации ванадата висмута: моноклинная фаза со структурой шеелита, тетрагональная со структурой шеелита и тетрагональная со структурой циркона. Перспективной для фотокатализа является моноклинная фаза со структурой шеелита благодаря возможности электронно-дырочной проводимости под действием видимого спектра электромагнитного излучения.

Обратимый переход между двумя фазами моноклинной сингонии происходит при 255 °С; необратимый переход из тетрагональной фазы со структурой циркона в моноклинную фазу со структурой шеелита достигается выдержкой при 400-500 °С [1].

В работе рассматривается возможность гидротермального синтеза моноклинной фазы со структурой шеелита (далее s-m) и тетрагональной фазы со структурой циркона (далее z-t), а также взаимные переходы между ними.

Как указано выше, для получения моноклинной фазы со структурой шеелита необходима высокотемпературная обработка порошка тетрагональной фазы со структурой циркона. При осаждении  $\text{BiVO}_4$  из сильноокислого раствора (pH=0.5, 25 °С) происходит образование (z-t) фазы со средним размером кристаллитов 40 нм. При осаждении в тех же условиях, но в присутствии этилового спирта, как поверхностно-активного вещества, формируются две фазы – моноклинная фаза со структурой шеелита (s-m) и тетрагональная со структурой шеелита (s-t) – в соотношении 48 масс.% и 52 масс.% соответственно. Средний размер кристаллитов составляет по 30 нм для каждой фазы.

При 140 °С в присутствии маточного сильноокислого раствора в гидротермальном флюиде из (z-t) фазы наблюдается переход в (s-m) со средним размером кристаллитов 60 нм. При гидротермальной обработке образца, полученного в присутствии поверхностно-активного вещества, наблюдается переход из смеси (s-m) и (s-t) фаз в (z-t) фазу со средним размером кристаллитов 100 нм.

Таким образом, в гидротермальных условиях становится возможен переход из тетрагональной фазы со структурой циркона (z-t) в моноклинную фазу со структурой шеелита (s-m) при относительно низкой температуре. Применение поверхностно-активного вещества (этилового спирта) позволяет получить из моноклинной фазы тетрагональную фазу со структурой циркона (z-t). Осуществление данных фазовых переходов дает возможность синтеза перспективных гетеропереходных нанокомпозитов с повышенной фотокаталитической активностью на основе (z-t) и (s-m) фаз *in-situ* без применения микроволнового облучения [2]. Средние размеры кристаллитов определялись методом Халдера-Вагнера с помощью программного обеспечения SmartLab Studio II от Rigaku.

Работа выполнена при поддержке РФФИ, проект № 18-29-12119.

Tokunaga S., Kato H., Kudo A. Selective preparation of monoclinic and tetragonal  $\text{BiVO}_4$  with scheelite structure and their photocatalytic properties // *Chemistry of Materials*. – 2001. – Т. 13. – №. 12. – С. 4624-4628.

Yan M. et al. Microwave-assisted synthesis of monoclinic–tetragonal  $\text{BiVO}_4$  heterojunctions with enhanced visible-light-driven photocatalytic degradation of tetracycline // *RSC Advances*. – 2015. – Т. 5. – №. 110. – С. 90255-90264.

## KTm[B<sub>4</sub>O<sub>6</sub>(OH)<sub>4</sub>] $\cdot$ 3H<sub>2</sub>O, a new member of the layered borate family with a high degree of disorder

Topnikova A.P.<sup>1\*</sup>, Belokoneva E.L.<sup>1</sup>, Dimitrova O.V.<sup>1</sup>, Volkov A.S.<sup>1</sup>, Zorina L.V.<sup>2</sup>

<sup>1</sup> Lomonosov Moscow State University, Faculty of Geology, Department of Crystallography, 119991, Leninskie Gory str. 1, Moscow, Russia.

<sup>2</sup> Institute of Solid State Physics RAS, 142432, Akademica Osipyana str. 2, Chernogolovka, Moscow Region, Russia.

\*Correspondence email: nastya\_zorina@rambler.ru

Crystals of the new borate KTm[B<sub>4</sub>O<sub>6</sub>(OH)<sub>4</sub>] $\cdot$ 3H<sub>2</sub>O ( $a = 4.5472(7)$ ,  $c = 12.151(3)$  Å, sp. gr. is  $P\bar{3}1m$ ) was synthesized hydrothermally at the  $T = 280^\circ\text{C}$  and  $P = 100$  atm. in a system  $\text{Tm}_2\text{O}_3\text{:B}_2\text{O}_3=1:1$ .  $\text{K}^+$ ,  $\text{Cl}^-$  and  $\text{CO}_3^{2-}$  ions were added to the solution as mineralizers,  $\text{pH}=10$ . Crystal structure consists of polar mica-like tetrahedral layers  $[\text{B}_4\text{O}_6(\text{OH})_4]_\infty$  parallel  $ab$  (Fig. 1a, b). Two layers of different orientations are connected by isolated  $\text{TmO}_6$  octahedra into the packet. K atoms and water molecules in two positions have statistic occupancy and fill inter-packet space. The Tm position is also characterized by disordering in the direction of  $c$  axis and split into several with less occupancy (Fig. 1b).

The same layers were observed in  $\text{KTa}[\text{B}_4\text{O}_6(\text{OH})_4](\text{OH})_2\cdot 1.33\text{H}_2\text{O}$  (np. rp.  $P\bar{6}2m$ ) [1], pepposite and its synthetic analogue  $\text{NdAl}_{2.07}[\text{B}_4\text{O}_{10}]\text{O}_{0.6}$  (np. rp.  $P\bar{6}2m$ ) [2]. In these borates, heavy atoms are in the trigonal prisms. The inter-packet space is filled by K atoms, OH-groups and water molecules in K,Ta-borate, and by Al and O atoms in Nd,Al-borate. In  $\text{KGd}[\text{B}_6\text{O}_{10}(\text{OH})_2]$  (np. rp.  $P\bar{6}2m$ ) and  $\text{KHo}[\text{B}_6\text{O}_{10}(\text{OH})_2]$  (np. rp.  $P\bar{3}1m$ ) [3], additional  $\text{BO}_2(\text{OH})$  triangles join to the polar tetrahedral layer to form a polyborate layer  $[\text{B}_6\text{O}_{10}(\text{OH})_2]_\infty$ . Ho atom in K,Ho-borate is located in the octahedron as in the new structure. In the K,Gd-borate, a variant of the trigonal prism is realized. In new compound is realized a novel variant of the packet with octahedra as in K,Ho-borate, but without additional triangles in the layers.

For all these structures, the most stable part is a packet from octahedra (prisms) and tetrahedral layers, however K,Tm-borate also has disordering in octahedral position. Perfect cleavage and poor quality of the crystals are typical for layered structures and connected with disordering in the inter-packet space.

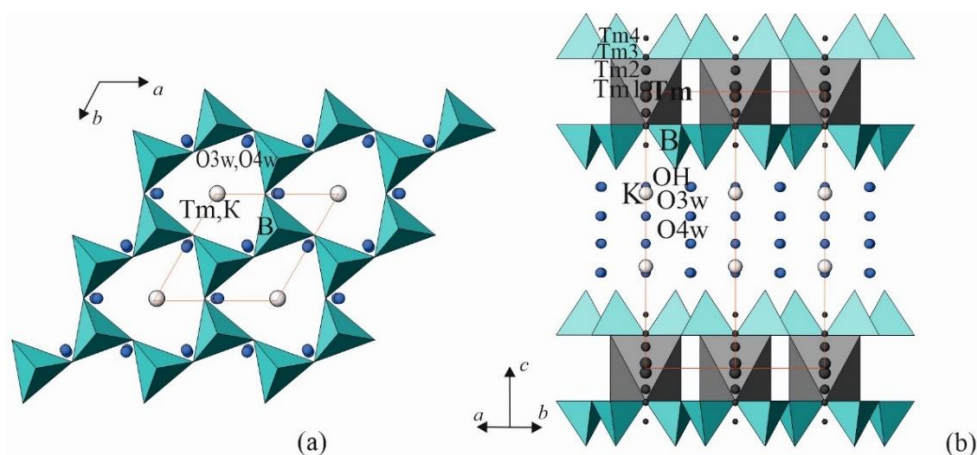


Figure 1.  $\text{KTm}[\text{B}_4\text{O}_6(\text{OH})_4]\cdot 3\text{H}_2\text{O}$ : mica-like layer in  $ab$ -projection (a), crystal structure in side projection (b).

Belokoneva E.L., Stefanovich S.Yu., Dimitrova O.V. New nonlinear optical potassium iodate  $\text{K}[\text{IO}_3]$  and borates  $\text{K}_3[\text{B}_6\text{O}_{10}]\text{Br}$ ,  $\text{KTa}[\text{B}_4\text{O}_6(\text{OH})_4](\text{OH})_2\cdot 1.33\text{H}_2\text{O}$  – synthesis, structures and relation to the properties. *J. Solid State Chem.* 2002. V. 195. P. 79-85.

Pushcharovskii, D.Yu., Karpov, O.G., Leonyuk, N.I., Belov, N.V. Crystal structure of nonstoichiometric Nd,Al-dimetaborate  $\text{NdAl}_{2.07}(\text{B}_4\text{O}_{10})\text{O}_{0.6}$ . *Dokl. AN SSSR.* 1978. V. 241. P. 91-94.

Belokoneva E.L., Topnikova A.P., Stefanovich S.Yu., Dobretsova E.A., Volkov A.S., Dimitrova O.V. New isoformula borates with similar structures and different properties – acentric nonlinear optical  $\text{KGd}[\text{B}_6\text{O}_{10}(\text{OH})_2]$  and centrosymmetric  $\text{KHo}[\text{B}_6\text{O}_{10}(\text{OH})_2]$ . *Solid State Sci.* 2015. V. 46. P. 43-48.

## Non-covalent interactions in layered compounds of MoS<sub>2</sub> with guanidinium cations

Ushakov I. E.<sup>1\*</sup>, Goloveshkin A.S.<sup>1</sup>, Lenenko N.D.<sup>1</sup>, Korlyukov A.A.<sup>1</sup>, Golub A.S.<sup>1</sup>

<sup>1</sup> A.N. Nesmeyanov Institute of Organoelement Compounds, Russia

\*Correspondence email: f0rbmen@gmail.com

Nanostructured heterolayered organic-inorganic compounds based on molybdenum disulfide show promise for many applications ranging from electronics to nanosensors and catalysis. They are obtained by self-assembly of the negatively charged single MoS<sub>2</sub> layers and guest organic cations in liquid medium [1] and are characterized by turbostratic disorder in layer stacking. Attractive properties of such systems stimulate the profound studies of their structure, which necessitate application of specific methods intended for structural studying of low-ordered materials.

In the present communication, we report the structure and binding interaction pattern for new layered nanocrystals, containing protonated forms of guanidine (GUA), and 1,1,3,3-tetramethylguanidine (TMG) in-between the MoS<sub>2</sub> layers. Atomic structure of the host and guest layers was determined from powder X-ray diffraction data, using an original approach previously developed for related compounds, which implies PXRD pattern modeling (Fig. 1) coupled with DFT calculations [1,2]. The structural results confirmed by FTIR and TEM data showed that the organic-inorganic hydrogen bonding is an important structure-forming factor in the present compounds. In the compound with GUA, the main contribution to structure stabilization is provided by the strong NH...S contacts, while in the structure with TMG (Fig. 1), the weaker but more numerous CH...S interactions contribute mainly to stabilization, accounting for 75% of the total cation-MoS<sub>2</sub> binding energy. The geometry of MoS<sub>2</sub> layers in both studied layered compounds was found to be modified by the charge transfer to the sheets of initial 2H-MoS<sub>2</sub>, resulting in its transformation to 1T structure type with Mo atoms arranged in zigzag chains. The obtained results are hoped to be useful for structural design of other MoS<sub>2</sub>-organic compounds.

The funding of the work by the Russian Science Foundation (grant № 20-13-00241) is gratefully acknowledged.

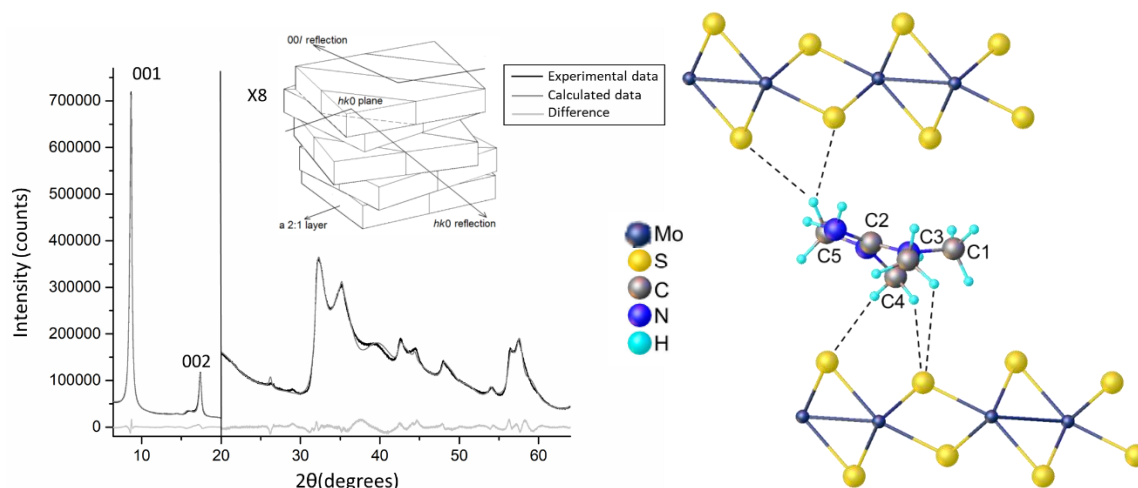


Fig. 1. Fitted XRD pattern (left) and structure of TMG-MoS<sub>2</sub> with indication of the shortest CH...S contacts (right).

1. Goloveshkin A.S., Lenenko N.D., Zaikovskii V.I., Golub A.S., Korlyukov A.A., Bushmarinov I.S. RSC Adv, 2015, V. 5. P. 19206–19212.

2. Goloveshkin A.S., Bushmarinov I.S., Korlyukov A.A., Buzin M.I., Zaikovskii V.I., Lenenko N.D., Golub A.S. Langmuir. 2015. V. 31. P. 8953–8960.

## The influence of temperature on crystal structure and pyroelectric properties of Ni- and Cu-bearing tourmalines

Chernyshova I.A.<sup>1\*</sup>, Frank-Kamenetskaya O.V.<sup>1</sup>, Vereshchagin O.S.<sup>1</sup>, Malyschkina O.V.<sup>2</sup>

<sup>1</sup>St Petersburg State University, 199034, 13B Universitetskaya Emb.6 Saint-Petersburg, Russia.

<sup>2</sup>Tver State University, 170100, 33 Zhelyabova st., Tver, Russia.

\*Correspondence email: i.a.chernyshova@yandex.ru

Tourmaline is the most widespread boratosilicate with the general formula  $XY_3Z_6T_6O_{18}(BO_3)_3V_3W$  and great variety of ionic substitutions in all structural sites. It belongs to the polar symmetry class (space group  $R3m$ ). The search for linear pyroelectrics with spontaneous polarization in the entire temperature range of the existence of the crystalline state, and stable to the effects of electrical fields is relevant. The prospect of using synthetic tourmalines for these purposes is associated with the possibility of targeted synthesis of tourmalines of the required composition. The aim of this work is to study the influence of temperature to the crystal structure and pyroelectric properties of synthetic Ni- and Cu-bearing tourmalines [3,4]. The crystal structure of Ni (1) - and Cu (2) -bearing tourmalines (Table 1) was refined at temperatures of -170, 20, and 120 °C by single crystal X-ray diffraction analysis.

Table 1. Crystallochemical formulae of Ni- and Cu-bearing tourmalines

№	Formula
1	$Na_{0.80}(Ni_{0.516}Al_{0.484})_3(Al_{0.866}Ni_{0.134})_6(Si_{5.27}B_{0.73}O_{18})(BO_3)_3(OH)_4$
2	$Na_{0.91}(Cu_{0.565}Al_{0.435})_3(Al_{0.933}Cu_{0.067})_6(Si_6O_{18})(BO_3)_3(OH)_3(O_{0.813}[OH]_{0.187})$

The value of pyroelectric coefficient of the investigated tourmalines ( $\gamma$ ) in the temperature range of 25-100 °C was determined by the dynamic method [1], which allows obtaining the value of the primary pyroelectric coefficient. The results of the study showed that an increase in temperature significantly affects the unit cell parameters (especially parameter  $c$ ) of tourmalines. In addition, oxygen O1, located on the threefold axis, is displaced, which leads to a significant lengthening of the X-O1 bond (Table 2). The pyroelectric coefficient values of synthetic tourmalines at room temperature are close to those given by Hawkins et al. [2] and increase as the temperature do. Based on the above structural data, it can be assumed that a significant contribution to the pyroelectric coefficient is made by the displacement of oxygen O1, which requires further refinement for samples of other compositions.

Table 2. Structural characteristics of tourmalines at different temperatures

T, °C	Ni-tourmaline			Cu-tourmaline		
	$a$ , Å	$c$ , Å	X-O1, Å	$a$ , Å	$c$ , Å	X-O1, Å
-170	15.868(1)	7.159(1)	3.763(6)	15.868(1)	7.085(1)	3.07(1)
20	15.872(1)	7.169(1)	3.377(7)	15.873(1)	7.097(1)	4.00(1)
120	15.880(1)	7.176(1)	3.785(6)	15.864(1)	7.103(1)	4.01(1)

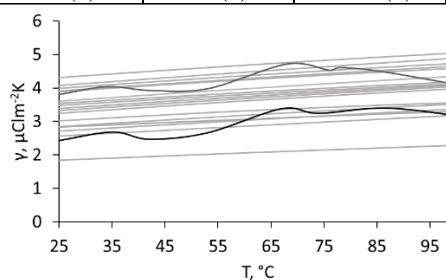


Fig.1. Pyroelectric coefficient ( $\gamma$ ) of natural [2] and Ni-, Cu-bearing tourmalines vs temperature: black – Ni-tourmaline, dark-grey – Cu-tourmaline, light grey – natural tourmalines [2]

The study of the tourmaline crystal structures was carried out at the Centre for X-ray Diffraction Studies (Resource Center of St Petersburg State University).

1. Golovnin B.A. et al. Technosphera Publishers. 2013. p. 271.
2. Hawkins K.D. et al. Am. Min. 1995. V. 80. P. 491-501.
3. Vereshchagin et al. Am. Min. 2013. V. 98. P. 1610-1616.
4. Vereshchagin et al. Min. Mag. 2015. V. 79. P. 997-1006.

## Терморентгенография соединений со структурой минерала пирохлора

Шварева А.Г.<sup>1\*</sup>, Князев А.В.<sup>1</sup>, Кяшкин М.В.<sup>2</sup>, Жакупов Р.М.<sup>1</sup>

<sup>1</sup> Национальный исследовательский Нижегородский государственный университет им. Н.И. Лобачевского, 603950, Нижегородская область, город Нижний Новгород, проспект Гагарина, дом 23, Россия

<sup>2</sup> Национальный исследовательский Мордовский государственный университет им. Н. П. Огарёва, 43005, Республика Мордовия, город Саранск, улица Большевикская, дом 68, Россия  
blokhina08ag@gmail.com

Одними из перспективных классов неорганических материалов являются сложные оксиды вольфрама и теллура со структурой минерала пирохлора. Данные соединения отличаются разнообразным составом благодаря значительной емкости к различным изоморфным включениям. Это обстоятельство позволяет в широких пределах варьировать их состав, а, следовательно, и свойства. Материалы со структурой минерала пирохлора находят широкое применение, включая их использование в качестве адсорбентов, ионных проводников, люминесцентных материалов.

В последнее время возрос интерес к соединениям со структурой минерала пирохлора с общей формулой  $A^I B^{III} M^{VI} O_6$  ( $A^I$ -  $K^{+1}$ ;  $B^{III}$ -  $Al^{+3}$ ,  $Cr^{+3}$ ,  $Fe^{+3}$ ,  $Mn^{+3}$ ;  $M^{VI}$ -  $Te^{+6}$ ,  $W^{+6}$ ), которые являются перспективными материалами, для использования в качестве катализаторов для фотокаталитического расщепления воды и органических соединений. Использование материалов со структурой минерала пирохлора в данных аспектах сопряжено с работой в условиях изменения температурного режима. Таким образом, изучение свойств соединений данного класса в условиях высоких температур, является актуальной задачей.

В данной работе приведен результат исследования соединений  $KCr_{1/3}Te_{5/3}O_6$  и  $KFe_{1/3}W_{5/3}O_6$  методом высокотемпературной и низкотемпературной рентгенографии. Соединения были получены с помощью твердофазных реакций при температуре 1803К для  $KFe_{1/3}W_{5/3}O_6$  и 773К для  $KCr_{1/3}Te_{5/3}O_6$ . Кристаллизуются в кубической сингонии с пр. гр.  $Fd\bar{3}m$ , параметры элементарных ячеек  $a = 10,351 \text{ \AA}$  ( $KFe_{1/3}W_{5/3}O_6$ );  $a = 10,311 \text{ \AA}$  ( $KCr_{1/3}Te_{5/3}O_6$ ).

При изучении соединений состава:  $KFe_{1/3}W_{5/3}O_6$  и  $KCr_{1/3}Te_{5/3}O_6$  методом высокотемпературной и низкотемпературной рентгенографии в интервале температур 198- 773 К, удалось установить ряд аномальных явлений, происходящих с соединениями при нагревании. В интервале температур 198-398К ( $KFe_{1/3}W_{5/3}O_6$ ) и 198-498 К ( $KCr_{1/3}Te_{5/3}O_6$ ) наблюдается резкое уменьшение параметров элементарных ячеек с ростом температуры не характерное для кристаллов кубической сингонии, далее при увеличении температуры, соединения  $KFe_{1/3}W_{5/3}O_6$  и  $KCr_{1/3}Te_{5/3}O_6$  демонстрируют классическое поведение в условиях роста температуры характерное для соединений группы пирохлора- постепенное увеличение параметров элементарных ячеек в интервале 398-773К для  $KFe_{1/3}W_{5/3}O_6$  и 498-773 К для  $KCr_{1/3}Te_{5/3}O_6$ .

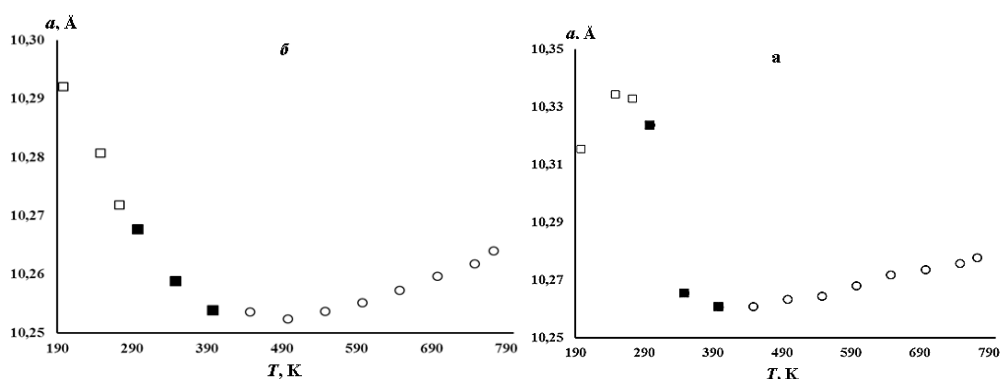


Рисунок 1- Температурная зависимость параметров элементарных ячеек от температуры соединений а-  $KFe_{1/3}W_{5/3}O_6$  и б-  $KCr_{1/3}Te_{5/3}O_6$  в интервале температур 198-773 К.

Рассчитанные в программном комплексе DTC коэффициенты теплового расширения свидетельствуют о наличии отрицательного теплового расширения в интервале 198-398К для  $KFe_{1/3}W_{5/3}O_6$  и 198-498 К для  $KCr_{1/3}Te_{5/3}O_6$ .

## Низкотемпературная рентгенография азотистых оснований

Шипилова А.С., Князев А.В., Князева С.С., Гусарова Е.В., Амосов А.А., Кусуткина А.М.

Нижегородский государственный университет им. Н.И. Лобачевского, 603950 Нижний Новгород, Россия

\*Correspondence email: 28\_stasy@bk.ru

Очень важную роль в любом живом организме играют азотистые основания. Особый интерес представляют не столько пиримидин и пурин, сколько вещества с их характерной структурой – пиримидиновые и пуриновые основания, которые входят в состав природных высокомолекулярных веществ – нуклеиновых кислот, которые осуществляют синтез белков в организмах.

Терморентгенография в широком диапазоне температур дает возможность оценить тепловое расширение исследуемого вещества вдоль различных кристаллографических направлений. Количественной характеристикой теплового расширения является коэффициент теплового расширения. Для изучения термических свойств пурина, теофиллина и теобромина использовали низкотемпературную порошковую рентгенографию. Рентгенограммы поликристаллического образца записывали на дифрактометре XRD-6000 фирмы Shimadzu ( $\text{CuK}\alpha$ -излучение, геометрия съемки на отражение) с шагом сканирования  $0.02^\circ$ , в интервале  $2\theta$ :  $10\div 60^\circ$  в температурном интервале от 150 К до 450 К с шагом в 25 К. После обработки результатов эксперимента были получены коэффициенты теплового расширения трех изученных азотистых оснований, представленные в таблице 1.

**Таблица 1.** Коэффициенты теплового расширения исследуемых азотистых оснований.

Соединение	, К	$\alpha_a$	$\alpha_b$	$\alpha_c$	$\alpha_v$
		$\cdot 10^5, \text{K}^{-1}$	$\cdot 10^5, \text{K}^{-1}$	$\cdot 10^5, \text{K}^{-1}$	$\cdot 10^5, \text{K}^{-1}$
Пурин [1]	00	0.	-	1.	0.
	06	0.63	00	43	
Теофиллин	00	3.	7.	-	8.
	75	16	2.05	84	
Теобромин	00	1.	1.	-	2.
	12	80	0.08	81	

Тепловое расширение всех исследуемых соединений анизотропно. Для пурина наибольшее тепловое расширение наблюдается вдоль оси  $c$ , для теофиллина вдоль оси  $a$ , теобромин –  $b$ .

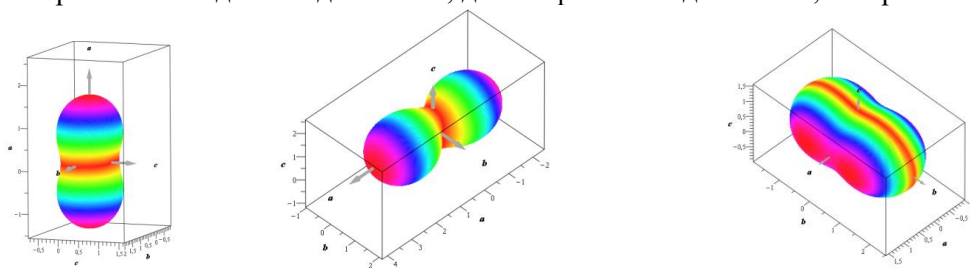


Рис. 1. 3 D фигуры коэффициентов теплового расширения:  $a$  – пурина,  $b$  – теофиллина,  $c$  – теобромин.

На основании полученных данных были построены двух- и трёхмерные фигуры коэффициентов теплового расширения при различных температурах для исследуемых соединений, демонстрирующие приоритетные направления при тепловом расширении [2, 3]. На рисунке 1. приведены 3D фигуры теплового расширения всех трех исследуемых веществ.

1. Amosov A.A. X-ray studies of purine in a wide range of temperatures. A /A. Amosov, A.V. Knyazev, A.S. Shipilova, S.S. Knyazeva, E.V. Gusarova, V.N. Emel'yanenko // Applied solid state chemistry. – 2019. – V. 1(6). – P. 49-52.

2. Белоусов, Р.И. Алгоритм расчета тензора и построения фигур коэффициентов теплового расширения в кристаллах / Р.И. Белоусов, С.К. Филатов // Физика и химия стекла. – 2007. – Т. 33. – №3. – С. 377–382.

3. Maple 2016.0. Maplesoft, a division of Waterloo Maple Inc., Waterloo, Ontario, 2016.



## Thermal stability of the Cu-ZrTe<sub>2</sub> intercalation compounds

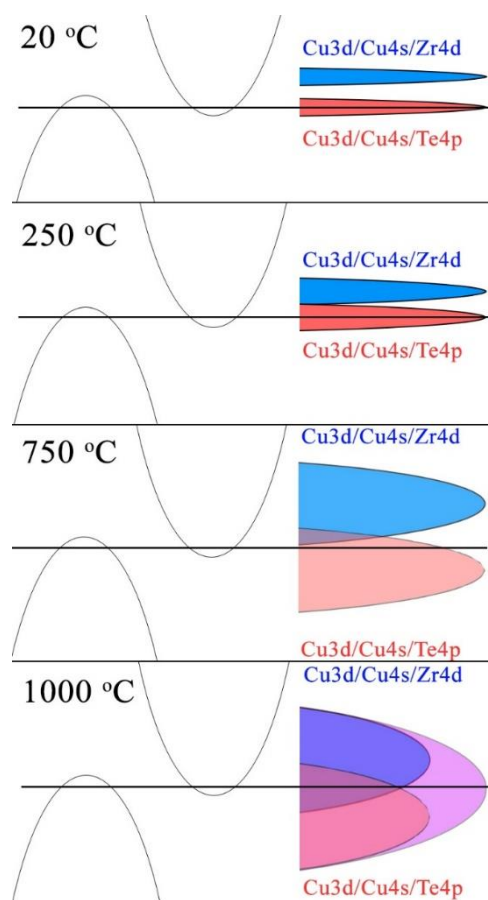
Shkvarin A.S., Titov A.A., Postnikov M.S., Titov A.N., Shkvarina E.G.\*

<sup>1</sup>Institute of Metal Physics, Russian Academy of Sciences-Ural Division, 620990 Yekaterinburg, Russia.

\*Correspondence email: shkvarina@imp.uran.ru

The M-TiX<sub>2</sub> (M = Ag, Cu, Fe etc.; X = S, Se, Te) intercalation compounds have been widely studied in the past [1]; it has been shown that the type of phase diagrams of these systems is determined by the nature of the chemical bond of the intercalated metal within the host lattice [2]. A change in the density of states near the Fermi level can cause a shift of the Fermi level, stabilizing or, conversely, destabilizing the single-phase state. This feature is likely most pronounced in the ZrTe<sub>2</sub>, as the most polarizable lattice of this homologous series. The Cu atoms can occupy crystallographic sites with different coordination by chalcogen [3] which leads to the possibility of the formation of different covalent complexes.

The Cu<sub>x</sub>ZrTe<sub>2</sub> polycrystalline samples were synthesized in the range of  $0 \leq x \leq 0.4$  using previously prepared ZrTe<sub>2</sub> and metallic copper. The Cu<sub>x</sub>ZrTe<sub>2</sub> samples were obtained by usual thermal intercalation procedure. The structure and phase composition of obtained samples were studied by the quenching method — polycrystalline samples of Cu<sub>x</sub>ZrTe<sub>2</sub> ( $0 \leq x \leq 0.4$ ) were annealed at a given temperature (250 °C, 400 °C, 600 °C, 750 °C, 900 °C, 1000 °C, 1050 °C), quenched and studied using the X-ray diffraction. The in situ time-resolved (temperature dependent) SR-XRPD experiments of Cu<sub>0.2</sub>ZrTe<sub>2</sub> were performed at the MCX beamline of Elettra Sincrotrone Trieste (Italy) [4] in transmission mode, with a monochromatic wavelength of 0.827 Å (15 KeV) and 1x0.3 mm<sup>2</sup> spot size. The crystal structure refinement was performed using GSAS (General Structure Analysis System) [5] with space group P-3m1. It is shown that in the temperature range of 250 – 750 °C the Cu atoms predominantly occupy tetrahedral sites in the interlayer space. In this temperature range composition of main layered Cu<sub>x</sub>ZrTe<sub>2</sub> phase are various from x=0.25 to x=0.33 (from 250 and 750 °C respectively). At the temperatures above 900 °C, octahedral sites are predominantly occupied. At the high temperature Cu<sub>0.5</sub>ZrTe<sub>2</sub> phase are observed. A scheme for the band structure formation is proposed, which explains the temperature dependence of the copper solubility in Cu<sub>x</sub>ZrTe<sub>2</sub> intercalation compounds.



Funding for this research was provided by: Russian Science Foundation (project No. 17-73-10219)

1 Enyashin A.N. et al. Interatomic interactions and electronic structure of NbSe<sub>2</sub> and Nb<sub>1.25</sub>Se<sub>2</sub> nanotubes // J. Struct. Chem. 2004. Vol. 45, № 4. P. 547–556.

2. Chemical Physics of Intercalation / ed. Legrand A.P., Flandrois S. Boston, MA: Springer US, 1987. Vol. 172.

3. Guilmeau E., Bréard Y., Maignan A. Transport and thermoelectric properties in Copper intercalated TiS<sub>2</sub> chalcogenide // Appl. Phys. Lett. 2011. Vol. 99, № 5. P. 052107.

4. Rebuffi L. et al. MCX: a Synchrotron Radiation Beamline for X-ray Diffraction Line Profile Analysis // Zeitschrift für Anorg. und Allg. Chemie. 2014. Vol. 640, № 15. P. 3100–3106.

5. Larson A.C., Von Dreele R.B. GSAS: generalized structure analysis system // Doc. LAUR. 1994. P. 86–748.

## Author index

Abdulina V.R.	80	Galafutnik L.G.	72
Abramovich A.I.	81	Gavrilkin S.Yu.	49
Akkuratov V.I.	83	Gavryushkin P.N.	38, 39, 109
Akramov D.F.	58	Golosova N.O.	37
Aksenov S.M.	92	Golovanova O.A.	73, 89
Albert B.	22	Goloveshkin A. S.	116
Alekseeva L.S.	44	Golub A. S.	116
Amosov A.A.	28	Grebenev V.V.	47
Andreev P.V.	44, 91, 111	Gudz D.A.	91
Asensio M.	32	Gurbanova O.A.	92
Avdeev G.	37	Gurianov K.E.	66
Avdontseva E.Yu.	77	Gurzhiy V.V.	62, 74, 96, 101
Avdontseva M.S.	63, 82	Gusarova E.V.	28
Avila J.	32	Heck F.	22
Bakaev S.E.	81	Hixon A.E.	92
Balabanov S.S.	44	Hofmann K.	22
Balakumar S.	53	Huppertz H.	13
Banaev M.V.	38, 39	Ismagilova R.M.	64
Baran V.	20	Izatulina A.R.	74
Baranov N.V.	58	Kalashnikova S.A.	96
Belokoneva E.L.	115	Kalinkin A.M.	87
Belozeroва N.M.	37, 53	Kalinkina E.V.	87
Belskaya N.A.	49	Karazanov K.O.	44
Bezmaternykh L.N.	49	Kazak N.V.	49
Biryukov Y.P.	50, 52	Kazantseva N.V.	32
Blagov A.E.	83	Khamova T.V.	46
Bogdan T.V.	84	Kichanov S.E.	37, 53, 54
Bogdan V.I.	84	Kiriukhina G.V.	97
Boldin M.S.	44	Knyazev A.V.	28, 112
Boldyreva E.V.	15	Knyazev Yu.V.	49
Bolotina N.B.	21	Knyazeva S.S.	28
Borisov A.	59	Koklin A.E.	84
Borovikova E.Yu.	92	Kolesnikov I.E.	69, 99
Borovitskaya I.	106	Kolobov A.Yu.	98
Bubnova R.S.	27, 50, 68, 69, 70, 72, 77	Komornikov V.A.	47
Bulanov E.N.	61	Kopitsa G.P.	46
Bushkova O.V.	32	Kopylova Y.O.	99
Busurin S.M.	85	Korlyukov A. A.	116
Charkin D.O.	66	Korneev A.V.	100
Chernyshova I.A.	117	Kornyakov I.V.	96
Dang T.N.	94	Kostyreva T.G.	113
Depmeier W.	59	Kotelnikova E.N.	110
Deyneko D.V.	92	Kovalenko A.S.	46
Dimitrov V.M.	86	Kozlenko D.P.	37, 54, 94
Dimitrova O.V.	92, 115	Krashennikova O.V.	112
Dinnebier R.E.	26	Krikunova P.V.	56
Dovgaliuk I.N.	97	Krivovichev S.V.	24, 62, 63, 64, 65, 76, 77, 82, 92, 101
Drozhilkin P.D.	44	Krzhozhanovskaya M.G.	29, 63, 70, 72, 74, 82, 99
Dubrovinskaya N.	16	Kumskov A.S.	103
Dubrovinsky L.	14	Kuporev I.V.	101
Egorysheva A.V.	108	Kusutkina A.M.	28
Eliovich I.A.	83	Kuz'mina M.A.	74, 100
Fedorova O.M.	86	Lantsev E.A.	111
Filatov S.K.	27, 50, 68, 69, 70, 76, 77		
Frank-Kamenetskaya O.V.	74, 100, 117		

Le Thao P.T.....	94	Shkvarina E.G.....	67, 120
Lenenko N. D. ....	116	Shorets O.U.....	68
Levkevich E.A.....	85, 103	Shvanskaya L.V. ....	56
Lis O.N.....	53	Siidra O.I.....	33, 59, 80, 88
Lomakin M.S.....	104	Silin P. ....	106
Lorenz H.....	110	Simonov S.V.....	97
Lukin E. V. ....	37, 53	Smetanina K.E. ....	44, 91, 111
Makarova I.P. ....	47	Smirnov A.V. ....	84
Malyshkina O.V.....	117	Solovyov L.A. ....	49
Marchenko A.A. ....	85	Stasenko K.S. ....	61
Matveev V.A. ....	105	Stefanovich S.Yu.....	92
Mayorov P.A. ....	107	Steffan J. ....	22
Merentsov A.I.....	32	Sterkhov E.V.....	31, 55, 75
Mikhailov B.....	106	Sumnikov S.V. ....	75
Mikhailova A.....	106	Sycheva G.A. ....	98, 113
Mishanin I.I. ....	84	Syrov E.V. ....	112
Moshkina E.M. ....	49	Targonskiy A.V.....	83
Moskaleva S.V.....	76, 77	Tereshin A.I. ....	112
Mühlbauer M.J.....	20	Timakov I.S. ....	47
Nicheva D.....	37	Titov A.A. ....	32, 67, 120
Nikolaev A.M. ....	46	Titov A.N.....	32, 67, 120
Nikulin V.....	106	Titova S.G.....	31, 55, 75
Ovchinnikov S.G. ....	49	Topnikova A.P. ....	115
Panikorovskii T.L. ....	65	Totzauer L.....	22
Patrina Zh.G. ....	85	Tsybulya S.V.....	30
Perova E.R.....	107	Ushakov I. E.....	116
Petkov P. ....	37	Vagizov F.G.....	50, 52
Petkova T. ....	37	Valeeva A.A.....	43
Pisarevsky Yu. V. ....	83	Vedmid' L.B. ....	86
Platonova N. ....	59	Veligzhanin A.A. ....	49
Platunov M.S. ....	49	Vereshchagin O.S.....	117
Plokhikh I.V. ....	66	Vergasova L.P.....	76, 77
Popova E.F. ....	108	Veselova V.O.....	108
Postnikov M.S. ....	32, 67, 120	Vinogradov V. Yu. ....	87
Povolotskiy A.V. ....	69	Vladimirova V.A.....	88
Proskurina O. V. ....	104	Volkov A.S. ....	92, 115
Protsenko A.I.....	83	Volkov S.N. ....	72
Pryanichnikov S.V.....	55, 75	Vostokov M.M. ....	111
Radzivonchik D.I.....	67	Yakubovich O.V. ....	34, 97
Rempel A.A.....	17, 19, 43	Yamnova N.A. ....	92
Rotermel M.V.....	75	Yarmoshenko Yu.M. ....	32
Rutkauskas A.V.....	54	Yukhno V.A.....	70
Ryltsev R.E.....	31	Yuriev A.A.....	69
Sadovnichii R.V.....	110	Zainullin O.B. ....	47
Sagatov N. ....	38, 39	Zakalyukin R.M. ....	85, 103
Sagatova D. ....	38, 39, 109	Zakharov B.A. ....	41
Sala A. ....	32	Zel I.Yu.....	94
Savenko B.N.....	37, 53, 54	Zhitova E.S. ....	63, 64
Selezneva E.V.....	47	Zimina G.V. ....	85
Selezneva N.V. ....	58	Zinnatullin A.L.....	50, 52
Senyshyn A.....	20	Zolotarev A.A. ....	64
Shablinskii A.P. ....	69, 76, 77	Zolotarev A.A. Jr.....	63, 82
Shefer K.I. ....	78	Zorina L.V. ....	115
Shilova O.A.....	46	Адамович С.Н.....	95
Shilovskih V.V. ....	64, 99	Амосов А.А.....	102, 119
Shipilova A.S.....	28	Антипов Е.В.....	18
Shkvarin A.S.....	32, 67, 120	Архипов С.Г.....	40

Бирюков Я.П. ....	60	Князева С.С.....	102, 119
Болдырев К.Н. ....	93	Кржижановская М.Г.....	51
Болдырева Е.В.....	40	Кусуткина А.М. ....	102, 119
Бубнова Р.С. ....	60	Кяшкин М.В.....	118
Гайдамака А.А. ....	40	Матвеев В.А.....	90
Губанова Н.Н. ....	90	Моисеев А.А. ....	95
Гусарова Е.В. ....	102, 119	Оборина Е.Н. ....	95
Дейнеко Д.В. ....	93	Проскурина О.В.....	45
Демина С.В.....	60	Сереткин Ю.В.....	40
Дихтяр Ю.Ю. ....	93	Тимчук А.В. ....	114
Еникеева М.О.....	45	Федоров П.П. ....	35
Еремин Н.Н. ....	23	Филатов С.К.....	60
Жакупов Р.М. ....	118	Чупрунов Е.В.....	25
Житова Е.С.....	51	Шаблинский А.П. ....	60
Захаров Б.А. ....	40	Шварева А.Г. ....	118
Зельбст Э.А. ....	95	Шилова О.А. ....	90
Князев А.В.....	102, 118, 119	Шипилова А.С. ....	102, 119



### Настольный рентгеновский дифрактометр D2 PHASER

- Качественный и количественный фазовый анализ
- Определение степени кристалличности
- Характеристики фазы (параметры ячейки, размер кристаллитов, микронапряжения)
- Определение кристаллических структур
- Широкий спектр прободержателей стандартного промышленного размера ( $\varnothing$  51.5 мм) для различных задач

### Рентгеновский дифрактометр D8 ADVANCE

- Качественный и количественный анализ кристаллических фаз
- Определение размеров кристаллитов
- Анализ фазовых переходов при изменении температуры, влажности и давления с использованием соответствующих камер
- Определение остаточных напряжений
- Быстрая съемка при помощи позиционно-чувствительного детектора
- Автоматический режим сбора данных и дальнейшая обработка результатов программным пакетом **DIFFRAC<sup>plus</sup>**



### Рентгенофлуоресцентный волнодисперсионный спектрометр S8 TIGER

- Определение химического состава сырьевых материалов, огнеупоров
- Простая и быстрая пробоподготовка твердых и порошкообразных материалов
- Анализ элементов от бериллия до урана
- Диапазон измеряемых концентраций от долей ppm до 100%
- Воспроизводимость 0,05 % отн.
- Быстрый обзорный анализ и получение полуколичественных результатов без использования стандартных образцов
- Современное программное обеспечение **SPECTRA<sup>plus</sup>**



[xray.ru@bruker.com](mailto:xray.ru@bruker.com)

[www.bruker.com](http://www.bruker.com)

ООО «Брукер»

Москва, ул. Пятницкая 50/2, стр. 1



12 Campus Boulevard • Newtown Square, PA 19073  
 (610) 325-9814  
 sales@icdd.com  
 www.icdd.com

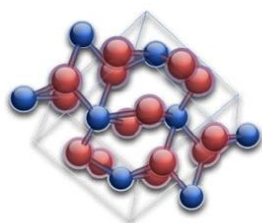


## WORKING TOGETHER FOR YOU

With over 1,000,000 patterns available at your fingertips, ICDD's PDF databases and MDI's JADE software work together to make your life easier. Let the software work for the science and take your results further.

### ABOUT US

For over 30 years, The ICDD and MDI have worked together in a complementary manner since MDI began in 1987. The XRD community has trusted MDI to provide unbiased results and help interpret both the everyday and the difficult XRD data. We are proud of our products and the daily effort we put forth towards advancing the science of XRD. Materials Data creates XRD software applications to collect, analyze, and simulate XRD data. These products are here to help solve issues in an enormous array of materials science projects, and may be found in labs around the world with data collected on virtually every brand of XRD equipment.



### OUR PRODUCTS



#### PDF-4+

##### Phase Identification and Quantitation

The world's largest sources of inorganic diffraction data from crystals and powders in a single database featuring 426,000+ entries, including 323,900+ entries with atomic coordinates



#### PDF-4+/Web

##### Data on the Go

Provides portability to the PDF-4+ database via the internet.



#### PDF-4/Axiom

##### Quality Plus Value

Phase identification and quantitation that requires diffraction equipment manufacturer or vendor software.



#### PDF-2

##### Phase Identification + Value

Quality and subfile filters combined with 68 different searches and 53 display fields enable you to target your results for more accurate identification.



#### PDF-4/Organics

##### Solve Difficult Problems, Get Better Results

Designed to solve difficult problems that are analyzed by powder diffraction analysis for a multitude of applications in the pharmaceutical, regulatory, specialty chemical, biomaterial, and forensic fields.



#### PDF-4/Minerals

##### Comprehensive Mineral Collection

Ninety-seven percent of all known mineral types, as defined by the International Mineralogical Association (IMA), are represented in the database, as well as many unclassified minerals.



#### JADE Pro

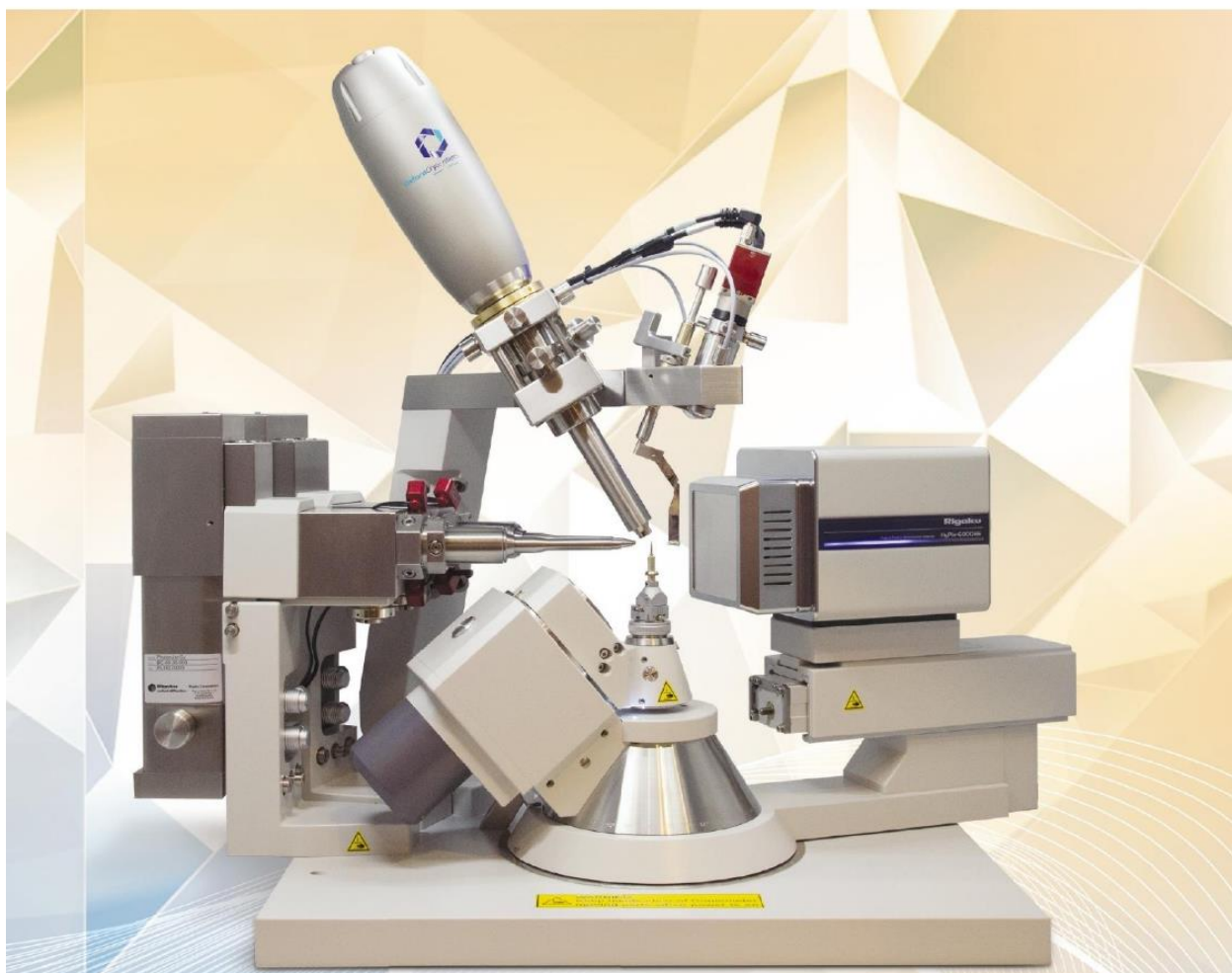
##### JADE Works The Way You Do

Automate your analysis with JADE. In so many cases, it's just one click and you're done. Often these results are better than those an experienced analyst could report and in a more timely manner.

For more information contact ICDD at [marketing@icdd.com](mailto:marketing@icdd.com)

@TheICDD  
 @TheICDD  
 @ICDDICDD  
 @TheICDD

ICDD, the ICDD logo, PDF and JADE are registered in the U.S. Patent and Trademark Office. Powder Diffraction File, Materials Data, Materials Data-JADE logo, and Denver X-ray Conference logo are trademarks of the ICPDS-International Centre for Diffraction Data. ©2020 ICPDS-International Centre for Diffraction Data 09/20



**XtaLAB Synergy** – удобная и производительная платформа для проведения исследований кристаллической и молекулярной структуры монокристаллических соединений. Микрофокусные источники **PhotonJet-S** или **PhotonJet-R** с медным, молибденовым или серебряным анодами, высокопроизводительной оптикой и автоматизированной системой регулировки размера и сходимости пучка обеспечат мощный поток рентгеновского излучения. Детектор **HyPix-6000HE**, созданный на основе технологии НРС, достоверно зафиксирует даже самые сильные или слабые отражения благодаря широкому динамическому диапазону и чрезвычайно низкому уровню шума. Быстрый, точный и надёжный гониометр с каппа-геометрией позволит эффективно собрать необходимый набор данных для любой научной задачи. В свою очередь, мультифункциональный программный пакет **CrysAlis<sup>Pro</sup>** корректно обработает полученные данные при минимальном участии пользователя.

Компания **Техноинфо** основана в 1999 году и является дистрибьютором ведущих производителей аналитического, лабораторного, испытательного и технологического оборудования. **Техноинфо** эксклюзивно представляет **Rigaku Oxford Diffraction** на территории России и обеспечивает сервисное обслуживание и методическую поддержку.



**Олег Корнейчик**  
[o.korneychik@technoinfo.ru](mailto:o.korneychik@technoinfo.ru)  
**Антон Черкасов**  
[a.cherkasov@technoinfo.ru](mailto:a.cherkasov@technoinfo.ru)

## 8. Late abstracts



## Новый политип арсеновагнерита-*Mabc* Mg<sub>2</sub>(AsO<sub>4</sub>)F с вулкана Толбачик, Камчатка

Шаблинский А.П.<sup>1</sup>, Вергасова Л.П.<sup>2</sup>, Филатов С.К.<sup>3</sup>, Москалева С.В.<sup>2</sup>

<sup>1</sup> Институт химии силикатов им. И.В. Гребенщикова РАН, 199053, Набережная Макарова 2, Санкт-Петербург, Россия.

<sup>2</sup> Институт вулканологии и сейсмологии ДВО РАН, 683006, Бульвар Пийпа 9, Петропавловск-Камчатский, Россия.

<sup>3</sup> Санкт-Петербургский государственный университет, 199034, Университетская набережная 7 – 9, Санкт-Петербург, Россия.

\*Correspondence email: shablinskii.andrey@mail.ru

Арсеновагнерит Mg<sub>2</sub>(AsO<sub>4</sub>)F был впервые обнаружен в 2014 году в Арсенатной fumarole, и опубликован в [1]. Политип арсеновагнерита-*Mabc* найден на втором конусе Большого трещинного Толбачинского извержения. Проба была отобрана в 1983 г. при температуре 600 °С). В минералогической ассоциации преобладают пономаревит, пийпит и сильвин, а арсенаты представлены филатовитом [2], райтитом [3] и озероваитом [4]. Данный политип арсеновагнерита образует пластинчатые прозрачные бесцветные кристаллы со стеклянным блеском.

Минерал полностью изоструктурен триплиту: моноклинная сингония, пр. гр. *C2/c*,  $a = 12.9943(10)$ ,  $b = 6.4817(10)$ ,  $c = 9.8428(10)$  Å,  $\beta = 116.63(2)^\circ$ ,  $V = 741.1(2)$  Å<sup>3</sup>,  $Z = 8$ . Химический состав был определен по данным рентгеноспектрального анализа (масс. %): MgO 41.12, CaO 0.15, As<sub>2</sub>O<sub>5</sub> 52.03, V<sub>2</sub>O<sub>5</sub> 0.93, P<sub>2</sub>O<sub>5</sub> 0.20, SO<sub>3</sub> 0.18, сумма 103.61%. Эмпирическая формула, рассчитанная на 9 отрицательных зарядов (Mg<sub>2.05</sub>Ca<sub>0.01</sub>) $\Sigma$ 2.06(As<sub>0.91</sub>V<sub>0.02</sub>P<sub>0.01</sub>S<sub>0.01</sub>) $\Sigma$ 0.95O<sub>4</sub>F<sub>0.95</sub>, идеализированная Mg<sub>2</sub>AsO<sub>4</sub>F. Кристаллическая структура арсеновагнерита-*Mabc* уточнена до *R*-фактора 5.5 %. Кристаллическая структура арсеновагнерита-*Mabc* содержит две симметрично независимые позиции для атомов магния, одну для атома мышьяка, четыре для атомов кислорода и две для атомов фтора с частичной заселенностью, которые формируют MgO<sub>4</sub>F<sub>2</sub> полиэдры, и AsO<sub>4</sub> тетраэдр.

Работа выполнена при поддержке РФФИ (проект № 18-29-12106). Рентгенография выполнена в Ресурсном центре СПбГУ «Рентгенодифракционные методы исследования».

1. Pekov I.V., Zubkova, N.V., Agakhanov, A.A., Yapaskurt, V.O., Chukanov, N.V., Belakovskiy, D.I., Sidorov E.G., Pushcharovsky, D.Yu. New arsenate minerals from the Arsenatnaya fumarole, Tolbachik volcano, Kamchatka, Russia. VIII. Arsenowagnerite, Mg<sub>2</sub>(AsO<sub>4</sub>)F // Mineralogical Magazine. 2018. V. 82(4). P. 877-888.

2. Vergasova L.P., Krivovichev S.V., Britwin S.N., Burns P.N., Ananiev V.V. Filatovite, K(Al, Zn)<sub>2</sub>(As, Si)<sub>2</sub>O<sub>8</sub>, a new mineral species from the Tolbachik volcano, Kamchatka peninsula, Russia // European Journal of Mineralogy. 2004. V. 16(3). P. 533-536.

3. Shablinskii A.P., Filatov S.K., Vergasova L.P., Avdontseva E.Yu., Moskaleva S.V. Wrightite, K<sub>2</sub>Al<sub>2</sub>O(AsO<sub>4</sub>)<sub>2</sub>, a new oxo-orthoarsenate from the Second scoria cone, Northern Breakthrough, Great Fissure eruption, Tolbachik volcano, Kamchatka peninsula, Russia // Mineralogical Magazine. 2018. V. 82(6). P. 1243-1251.

4. Shablinskii A.P., Filatov S.K., Vergasova L.P., Avdontseva E.Yu., Moskaleva S.V., Povolotskiy A.V. Ozerovaitite, Na<sub>2</sub>KAl<sub>3</sub>(AsO<sub>4</sub>)<sub>4</sub>, new mineral species from Tolbachik volcano, Kamchatka peninsula, Russia // European Journal of Mineralogy. 2019. V. 31(1). P. 159-166.

## Homogenization of a mechanical mixture of lithium, sodium, and potassium sulfate's during heating and subsequent cooling

Shorets O.U.<sup>1,2</sup>, Filatov S.K.<sup>2\*</sup>, Bubnova R.S.<sup>1</sup>

<sup>1</sup> Grebenshchikov Institute of Silicate Chemistry, Russian Academy of Sciences, 199053, Makarov Emb. 2, St.Petersburg, Russia.

<sup>2</sup> Department of Crystallography, Institute of Earth Sciences, Saint Petersburg State University, University Emb. 7/9, 199034, Saint Petersburg, Russia.

\*Correspondence email: filatov.stanislav@gmail.com

Lithium sulfates are widely used in the manufacture of various materials, used for the manufacture of detector heads in ultrasonic flaw detection and as a component of phosphors. Several phase transitions are described in LiNaSO<sub>4</sub> and LiKSO<sub>4</sub> sulfates [1, 2] that occur with temperature changes.

To study thermal phase transformations and expansion for LiNaSO<sub>4</sub>, samples obtained by mechanical mixing of Li<sub>2</sub>(SO<sub>4</sub>) and Na<sub>2</sub>(SO<sub>4</sub>) in a ratio of 1:1 were used; for LiKSO<sub>4</sub>, samples obtained by mechanical mixing of Li<sub>2</sub>(SO<sub>4</sub>) and K<sub>2</sub>(SO<sub>4</sub>) in a ratio of 1:1 were used.

The unit cell parameters of various phases, including in heterogeneous mixtures, were refined at different temperatures by the Rietveld method, the temperature dependences of these parameters were approximated by 2nd-degree polynomials, and the coefficients of thermal expansion were calculated using the RietTensor [3] and ThetaToTensor-TTT [4] software complexes.

The LiNaSO<sub>4</sub> sample at room temperature and up to 240 °C contains a mechanical mixture of lithium and sodium sulfates. Then there is a phase transition of the low-temperature modification of sodium sulfate to the high-temperature one. And already at 480 °C, the sample is homogenized into the LiNaSO<sub>4</sub> modification (*P3<sub>1</sub>c*).

The LiKSO<sub>4</sub> sample at room temperature and up to 400 °C contains a mechanical mixture of lithium and potassium sulfates. Then there is a phase transition of the low-temperature modification of lithium sulfate to the high-temperature one. And already at 550 °C, the sample is homogenized in the high-temperature modification of LiKSO<sub>4</sub>.

In the course of the work, the main values of the thermal expansion tensor of all polymorphs were obtained for all the studied lithium sulfates. The  $\alpha_V$  values for the high-temperature LiKSO<sub>4</sub> modification and LiNaSO<sub>4</sub> modification increase sharply with increasing temperature.

The investigations were performed using the equipment of the Saint-Petersburg State University Resource Center «X-ray diffraction studies». The authors appreciate the financial support provided by the Russian Fund for Basic Research (project 18-29-12106).

1. Nilsson L., Hessel A.N. and Lunden A. The structure of the solid electrolyte LiKSO<sub>4</sub> at 803 K and of LiNaSO<sub>4</sub> at 848 K // Solid State Ionics. 1989. V. 34. P. 111-119.

2. Schulz H., Zucker U. and Frech R. Crystal structure of KLiSO<sub>4</sub> as a function of temperature // Acta Cryst. 1985. B41. P. 21-26.

3. Bubnova R.S., Firsova V.A., Volkov S.N., Filatov S.K. Rietveld To Tensor: Program for Processing Powder X-Ray Diffraction Data under Variable Conditions // Glass Physics and Chemistry. 2018. V. 44. P. 33-40.

4. Bubnova R.S., Firsova V.A., Filatov S.K. Software for Determining the Thermal Expansion Tensor and the Graphic Representation of Its Characteristic Surface (ThetaToTensor-TTT) // Glass Physics and Chemistry. 2013. V. 39. P. 347-350.